ISSN (1230-0322)

2022, Vol. 72, No. 1

Food

Polish Journal of Food and Nutrition Sciences

formerly Acta Alimentaria Polonica

Published

by Institute of Animal Reproduction and Food Research of the Polish Academy of Sciences, Olsztyn

ISSN (1230–0322)
2 0 2 2 , Vol. 72, No. 1

Polish Journal of Food and Nutrition Sciences

formerly Acta Alimentaria Polonica

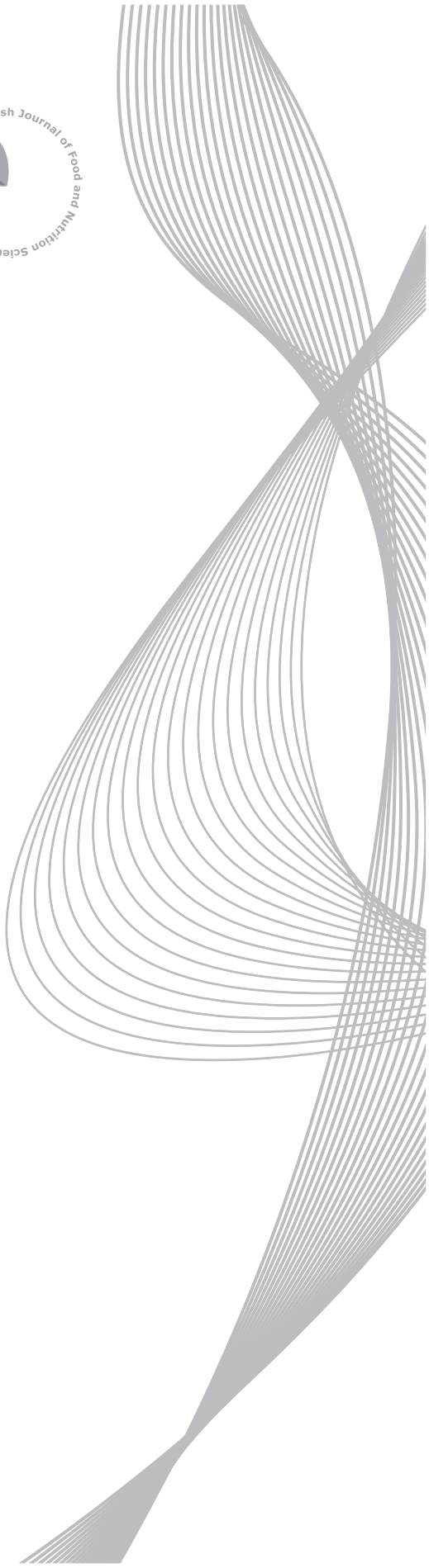

Published

by Institute of Animal Reproduction and Food Research of the Polish Academy of Sciences, Olsztyn

Pol. J. Food Nutr. Sci. 2022, Vol. 72, No. 1

Advisory Board of PJFNS 2019–2022

Pol. J. Food Nutr. Sci. 2022, Vol. 72, No. 1

POLISH JOURNAL OF FOOD AND NUTRITION SCIENCES
covered by CURRENT CONTENTS/AGRICULTURE, BIOLOGY & ENVIRONMENTAL SCIENCES, JOURNAL CITATION REPORTS AND SCIENCE CITATION INDEX EXPANDED, BIOSIS, SCOPUS, IFIS Publishing and CAS abstracts, and AGRO-Librex, FROSTI, PSJC, AGRIS and Index Copernicus data bases
2022, VOL. 72, NO. 1

ORIGINAL PAPERS

Subscription

2022 – One volume, four issues per volume. Annual subscription rates are: Poland 150 PLN, all other countries 80 EUR. Prices are subject to exchange rate fluctuation. Subscription payments should be made by direct bank transfer to Bank Gospodarki Żywnościowej, Olsztyn, Poland, account No 17203000451110000000452110 SWIFT code: GOPZPLWOLA with corresponding banks preferably. Subscription and advertising offices at the Institute of Animal Reproduction and Food Research of Polish Academy of Sciences, ul. J. Tuwima 10, 10-747 Olsztyn, Poland, tel./fax (48 89) 5234670, fax (48 89) 5240124, e-mail: pjfns@pan.olsztyn.pl; http://journal.pan.olsztyn.pl

Zamówienia prenumeraty: Joanna Molga (e-mail: pjfns@pan.olsztyn.pl)

Wersja pierwotna (referencyjna) kwartalnika PJFNS: wersja papierowa (ISSN 1230–0322)
Nakład: 70 egz.; Ark. wyd. 18,7; Ark. druk. 18,7
Skład i druk: Mercurius, www.mercurius.com.pl

Pol. J. Food Nutr. Sci., 2022, Vol. 72, No. 1, pp. 5–15
On-line ISSN: 2083-6007
Print ISSN: 1230-0322
DOI: 10.31883/pjfns/144223
http://journal.pan.olsztyn.pl

Original article
Section: Food Quality and Functionality

Characterisation of Selected Emulsion Phase Parameters in Milk, Cream and Buttermilk

Oskar Brożek, Katarzyna Kiełczewska, Krzysztof Bohdziewicz*

Department of Dairy Science and Quality Management, Faculty of Food Sciences, University of Warmia and Mazury in Olsztyn, Oczapowskiego Str. 7, 10–719 Olsztyn, Poland

Key words: milk products, size of fat globules, fatty acid profile, differential scanning calorimetry curves, differential scanning calorimetry parameters

Milk fat undergoes modification during butter production, which can alter its parameters and suitability for processing. The aim of this study was to compare selected milk fat parameters, including the size of milk fat globules, fatty acid profile and thermal properties, based on the thermal history of milk, cream and sweet buttermilk obtained during continuous churning in butter production. The size of milk fat globules was measured by the laser diffraction method; the fatty acid profile of milk fat was determined by gas chromatography; and the thermal properties of freeze-dried samples were determined by differential scanning calorimetry. The analysed products were arranged in the following descending order based on the size of milk fat globules, expressed by the Sauter mean diameter: cream > raw milk > buttermilk. Buttermilk was characterised by the greatest variations in the size of milk fat globules. A microscopic analysis revealed that an increase in fat content intensified the agglomeration of milk fat globules in cream relative to milk. Chains of milk fat globules were observed in buttermilk. Buttermilk was more abundant in monoenoic and polyenoic fatty acids than raw milk and cream. A thermal analysis demonstrated significant ($p \leq 0.05$) differences in the parameters of fat crystallisation and melting peaks between raw milk, buttermilk and cream. The thermal history of the samples influenced the results. Cream was characterised by significantly greater changes in the melting and crystallisation enthalpy of milk fat and significantly higher peaks than milk and buttermilk.

INTRODUCTION

Many food products can be considered oil-in-water (o/w) or water-in-oil (w/o) emulsions. Dairy products such as milk, cream and buttermilk are examples of natural o/w emulsions in which the dispersed phase is fat in the form of globules. Milk fat globules comprise a lipid core surrounded by a stabilizing membrane with a thickness of 10–20 nm. The membrane acts as an emulsifier and promotes the dispersion of fat globules in milk. The membrane also protects fat globules against flocculation, coalescence, oxidation and hydrolysis, which improves the processing suitability of milk fat [El-Loly, 2011; Singh & Gallier, 2017; Smoczyński *et al*., 2012]. In their native form, milk fat globule membranes are complex structures with numerous components. The mass of the membrane accounts for 2–6% of the total mass of fat globules, and membrane proteins and lipids represent more than 90% of its dry mass [Jukkola & Rojas, 2017; Singh, 2006; Singh & Gallier, 2017; Smoczyński *et al*., 2012]. Polar lipids, mainly phosphatidylcholine, phosphatidylethanolamine and sphingomyelin, and – in smaller amounts – phosphatidylinositol, phosphatidylserine and lysophosphatidylcholine, make up 25% of the milk fat globule membrane [Conway *et al*., 2014; Dewettinck *et al*., 2008; El-Loly, 2011; Singh, 2006; Smoczyński *et al*., 2012].

Processing operations in dairy plants, including butter production, can affect the parameters of emulsions and modify the composition and properties of milk fat globule membranes [Jukkola & Rojas, 2017]. During churning, fragments of fat globule membranes are released into the hydrophilic phase of milk, which increases the content of polar lipids in the dry matter of buttermilk [Dewetinck *et al*., 2008; Lambert *et al*., 2016; Lopez *et al*., 2015].

Milk fat is characterised by a high content of palmitic acid which is a saturated fatty acid. Oleic acid is the predominant unsaturated fatty acid. The fatty acid composition of phospholipids differs from that of triacylglycerols [Jhanwar & Ward, 2014]. Phospholipids contain mainly unsaturated fatty acids whose contents are higher in the membrane than in the lipid core of milk fat globules [Fauquant *et al*., 2005; Sanchez-Juanes *et al*., 2009]. Briard *et al*. [2003] demonstrated that the composition of fatty acids was influenced by the size of milk fat globules. Small fat globules contain more lauric, myristic, palmitic and palmitoleic acids than large fat globules. In turn, larger fat globules are more abundant in oleic and linoleic acid than fat globules with a small diameter. These differences can be attributed to a relatively higher content of membrane components in fat composed of smaller globules, and a smaller content of membrane

* Corresponding Author:
Tel.: +48 89 523 32 11; Fax: +48 89 523 34 02;
E-mail: kaka@uwm.edu.pl (K. Kiełczewska)

Submitted: 16 May 2021
Accepted: 24 November 2021
Published on-line: 13 December 2021

components in fat composed of larger globules. According to Fauquant *et al*. [2005], the size of fat globules determines the fatty acid composition of the membrane and the lipid core of a fat globule, which is consistent with the previous findings of Briard *et al*. [2003].

The melting point of milk fat ranges from -40°C to 40°C, and crystallisation occurs between 20°C and -20°C. The melting and crystallisation of milk fat are influenced by the size of milk fat globules, the composition of the emulsion and the structure of triacylglycerols, including their fatty acid profile and crystal polymorphism. These parameters of the emulsion phase are reflected in differential scanning calorimetry (DSC) curves, including the number of peaks, peak temperature and overlapping peaks, which are also affected by scan rate (heating/cooling rate) and thermal history [Hokkanen *et al*., 2021, Michalski *et al*., 2004; Tomaszewska-Gras, 2013; Truong *et al*., 2014]. The DSC peaks do not represent the crystallisation or melting of individual fatty acids, but the entire milk fat mixture. Therefore, peak temperature is determined by several factors, including the overlap between peaks (mainly simultaneous phase transitions of different fatty acids), and triacylglycerol polymorphism [Tomaszewska–Gras, 2013]. In DSC analyses, fat crystallisation is usually represented by two exothermic peaks during cooling. Melting is visualised by three endothermic peaks corresponding to low- (LMPF), middle- (MMPF) and high-melting point fractions (HMPF). Truong *et al.* [2014] observed that the fatty acid profile contributes to differences in the crystallisation curves of anhydrous milk fat, and stearin (hard fraction with a higher content of saturated fatty acids) and olein fractions (soft fraction with a higher content of monounsaturated and polyunsaturated fatty acids). The cited authors also found that a decrease in crystallisation onset temperature (T_{onset}) and enthalpy change (ΔH) was associated with a decrease in the size of fat droplets. Similar relationships were reported for milk fat globules [Bugeat *et al*., 2011; Lopez *et al*., 2001, 2007].

The size of milk fat globules influences their fatty acid profile, which is partly associated with the content of fat globule membranes in the product. Processing operations during butter production, including milk centrifugation and churning, modify the fatty acid profile of skim milk, cream and buttermilk. The composition of fatty acids differs subject to their origin. Buttermilk contains fragments of milk fat globule membranes that are released during churning, which can induce changes in fatty acid composition regardless of the size of fat globules. The fatty acid profile of polar lipids in milk fat globule membranes derived from buttermilk differs from the fatty acid profile of lipids derived from whole milk [Jhanwar & Ward, 2014; Singh & Gallier, 2017]. Truong *et al*. [2014] observed that the crystallisation temperature of emulsified fats decreased with the decrease in droplet size.

Berton *et al*. [2012] analysed the digestion of native and homogenised milk fat globules *in vitro* and evaluated the benefits of replacing homogenisation with other fractioning methods based on the size of milk fat globules, including membrane filtration [Michalski *et al.*, 2006] and centrifugation [Dhungana *et al.*, 2017]. Therefore, the applicability of milk fat with differently sized milk fat globules and different fatty acid profiles should be analysed to maximise the functional and bioactive attributes of the end product. For example, the application of milk fat derived from buttermilk increases phospholipid levels and improves the health-promoting properties of dairy products containing buttermilk [Gassi *et al.,* 2016; Hickey *et al.*, 2017].

Differential scanning calorimetry is a technique that enables the identification of phase transitions, and the obtained results deliver new knowledge and can be effectively used in dairy practice. Thermal analyses investigate the effects of temperature on milk, cream and buttermilk, and the results can be used to select the optimal process parameters and to modify the production technology of dairy products. Sweet buttermilk has attracted considerable interest as a product that is abundant in milk fat globule membrane components. The thermal properties of buttermilk can be effectively harnessed in the process of developing new dairy products and new production technologies.

The comprehensive comparison of the emulsion phase parameters, such as the size of fat globules, fatty acid profile and thermal properties of milk, cream and sweet buttermilk is insufficient in the literature. The aim of this study was to select the parameters of phase transition peaks differentiating milk, cream and sweet buttermilk, and to determine the influence of thermal history on the characteristics of DSC curves, considering the significant importance of the size of fat globules and fatty acid profile on the milk fat phase transitions.

MATERIALS AND METHODS

Materials

The experimental material comprised pooled samples of cow's milk produced in the Bałdy Educational and Research Station of the University of Warmia and Mazury (UWM) in Olsztyn. Milk was cooled and transported in a refrigeration unit to the laboratory of the Faculty of Food Sciences of the UWM in Olsztyn. The raw milk, matured cream (obtained by centrifuging raw milk) and buttermilk (obtained by continuous churning of cream) were analysed. The experiment was performed in three replications.

Proximate composition of milk, cream and buttermilk

The dry matter content [AOAC International, method 990.20; 33.2.44, 2007], total nitrogen (TN) content (Kjeldahl method) [AOAC International, method 991.20; 33.2.11, 2007] and fat content (butyrometric method) [ISO 19662, 2018; ISO 19660, 2018] of the liquid samples of milk, cream and buttermilk were determined. Total protein content was calculated by multiplying the TN content of the samples by a conversion factor of 6.38.

Size of milk fat globules

The size of milk fat globules was determined in liquid samples of milk, cream and buttermilk by the laser diffraction method in the Mastersizer 3000 particle size analyser and the Hydro EV sample dispersion unit (Malvern Instrument, Malvern, United Kingdom). The refractive index of milk was determined at 1.46, and the refractive index of Milli-Q deionised water (Millipore, Molsheim, France) was 1.33.

The following parameters were determined: the diameter below which lies 10% of globules volume (d_v10); median diameter, 50% of the volume distribution is above, and 50% is below observed diameter (d_v50); the diameter below which lies 90% of globules volume (d_v90); uniformity of particles (SPAN), SPAN=$(d_v90-d_v10)/d_v50$; a volume-surface mean diameter of fat globules, Sauter Mean Diameter (d_{32}), $d_{32}=\Sigma Sd_i^3n_i/Sd_i^2n_i$; a volume-weighted mean diameter, De Brouckere Mean Diameter (d_{43}), $d_{43}=\Sigma Sd_i^4n_i/Sd_i^3n_i$, where n_i is the number of particles with diameter d_i.

Microscopic analysis

The liquid samples of milk, cream and buttermilk were analysed under the Nikon Eclipse TieC 1 microscope (Nikon, Düsseldorf, Germany) at 60× magnification.

Fatty acid profile

Fat was extracted from milk, cream and buttermilk by the Rose-Gottlieb method [ISO, 2010]. Fatty acid esters were prepared according to a standard ISO 15884 method [ISO, 2002]. The fatty acid profile was determined by gas chromatography with a flame ionisation detector using the 7890 A Agilent Technologies system (Santa Clara, CA, USA). Separation was performed on the CP-Sil 88 column (100 m, 0.25 mm, 0.20 μm) (Agilent Technologies) with a temperature gradient of 60°C (1 min) to 180°C; time gradient of 5°C/min; injector temperature, 225°C; detector temperature, 250°C; carrier gas, helium; flow rate, 0.8 mL/min; split ratio, 1:100; sample volume, 1 μL; and liner, 0.4 mm. The reference material was BCR-164 anhydrous milk fat (LGC Standards, Kiełpin, Poland). The proportions of saturated fatty acids (SFAs), monounsaturated fatty acids (MUFAs), polyunsaturated fatty acids (PUFAs), short-chain fatty acids (SCFAs), medium-chain fatty acids (MCFAs), long-chain fatty acids (LCFAs) and branched-chain fatty acids (BCFAs) were calculated. The proportions of SCFAs, MCFAs and LCFAs in total fatty acids were determined according to the method proposed by Jensen [2002]. The content of fatty acids was expressed in g/100 g of total fatty acids in a product and in g/100 g of the product. The following abbreviations were used in the description of fatty acid isomers: ai – *anteiso*, i – *iso*, c – *cis*, t – *trans*.

Freeze drying

Milk, cream and buttermilk samples were freeze-dried in the Alpha 1–2 LD plus freeze-dryer (Martin Christ Gefriertrocknungsanlagen GmbH, Osterode am Harz, Germany) at a pressure of 0.34 mbar and a temperature of –32°C.

Analysis of freeze-dried samples

Water activity (a_w) of freeze-dried milk, cream and buttermilk was determined using the AquaLab 4TEV analyser (Meter Group AG, München, Germany). The analysis was carried out at a temperature of 25°C. Water activity was measured with an accuracy of ±0.003, and temperature was measured with an accuracy of ±0.3°C. The dry matter, fat and protein contents of freeze-dried samples were determined with the NIRS™ DS2500 analyser (FOSS, Hilleroed, Denmark).

Differential scanning calorimetry

Freeze-dried milk, cream and buttermilk (10±1 mg) were weighed on the Mettler Toledo XS205 Dual Range analytical balance (Mettler Toledo, Columbus, OH, USA), placed in airtight aluminium pans, and subjected to a thermal analysis with the use of the DSC Q10 instrument with a refrigerated cooling system (TA Instruments, New Castle, DE, USA). The cell was purged with dry nitrogen at 50 mL/min and calibrated for baseline in an empty oven and for temperature using standard pure indium. An empty sealed aluminium pan was used as a reference in every test. Samples were cooled or heated at a rate of 10°C/min and were held for 1 min at the endset temperature after each stage. They were analysed in triplicate in a DSC sequence composed of two cycles. Cycle I involved the following stages: 1) sample cooling from 30°C to –40°C; 2) sample heating from –40°C to 95°C. Cycle II commenced immediately after cycle I and involved sample cooling from 95°C to –40°C and sample heating from –40°C to 95°C in the following sequence: 1) cooling, 2) heating, 3) cooling, 4) heating, 5) cooling, 6) heating. Cycle II was applied to determine the effect of a sample's thermal history on the DSC curve, and to calculate the parameters of phase transition peaks. The results of the DSC analysis were processed using the Universal Analysis 2000 programme (TA Instruments). The following parameters of the identified phase transition peaks were determined: peak temperature (T_{max}; °C; determined as the peak maximum), phase transition onset temperature (T_{onset}; °C; defined by the intersection of a line tangent to the steepest section of the leading edge and the baseline of the thermogram), peak width at half height ($\Delta T_{1/2}$; °C; temperature range of the transition as peak width at half height), enthalpy change (ΔH; J/g; determined as the area limited by the curve, *i.e.* the peak and the baseline), peak height at maximum (P_{height}; W/g; determined as the heat flow range limited by T_{max} and P_s), peak onset temperature (P_s; °C; a point where a peak is formed) and peak endset temperature (P_e; °C; a point where a peak ends).

Statistical analysis

The results were analysed by one-way ANOVA, and the significance of differences between means was determined in Duncan's test at $p \leq 0.05$. The percentage content of individual fatty acids in total fatty acids in different samples was subjected to principal component analysis (PCA). Data were processed statistically in StatSoft Inc. Statistica v. 13.1 software (Tulsa, OK, USA).

RESULTS AND DISCUSSION

Proximate composition of raw milk, cream and buttermilk

Raw milk contained 13.34±0.17 g/100 g dry matter, 3.99±0.05 g/100 g fat and 3.21±0.03 g/100 g protein. Cream contained 53.59±4.40 g/100 g dry matter, 46.38±2.55 g/100 g fat and 2.77±0.11 g/100 g protein. The content of dry matter, fat and protein in buttermilk was determined at 9.02±0.60 g/100 g, 0.56±0.01 g/100 g and 3.02±0.08 g/100 g, respectively. The composition of milk, cream and buttermilk was similar to that described by other authors [Vanderghem *et al*., 2010].

TABLE 1. Size of fat globules in milk, cream and buttermilk.

Product	d_v10 (μm)	d_v50 (μm)	d_v90 (μm)	SPAN	d_{43} (μm)	d_{32} (μm)
Milk	0.56±0.01[b]	3.69±0.18[a]	7.75±0.05	1.95±0.09[b]	3.89±0.18	1.70±0.02[b]
Cream	0.93±0.08[a]	3.87±0.19[a]	8.35±0.55	1.92±0.17[b]	5.15±0.85	2.22±0.10[a]
Buttermilk	0.38±0.01[c]	1.72±0.06[b]	8.55±2.31	4.74±1.22[a]	5.42±1.25	0.97±0.03[c]

The presented values are means ± standard deviations (n=3). Values with different superscripts (a–c) in columns differ significantly at $p \leq 0.05$. d_v10 – diameter below which lies 10% of globules volume; d_v50 – diameter below which lies 50% of globules volume; d_v90 – diameter below which lies 90% of globules volume; SPAN – uniformity of particles; d_{32} – volume-surface mean diameter of fat globules; d_{43} – volume-weighted mean diameter.

Size of milk fat globules

The size of fat globules was determined in the samples of liquid milk, cream and buttercream. The products were arranged in the following order based on the decreasing diameter of the fat globules (d_v10) and the Sauter mean diameter (d_{32}): cream > raw milk > buttermilk ($p \leq 0.05$) (Table 1). The values of d_v50 did not differ significantly between milk and cream ($p > 0.05$), but they were significantly higher than in buttermilk ($p \leq 0.05$). Buttermilk contained large fat globules or aggregates characterised by high values of d_v90 and d_{43}. The size of fat globules was comparable in buttermilk and cream, but greater variations in d_v90 and d_{43} were noted in buttermilk. Due to high standard deviation values, no significant differences in d_v90 or d_{43} values were found between the analysed samples ($p > 0.05$). Buttermilk was characterised by the highest values of SPAN ($p \leq 0.05$) denoting the size distribution of fat globules in the sample (Table 1). The microscopic analysis revealed the presence of fat globule agglomerates in cream and chains of very small fat globules in buttermilk (Figure 1).

Fatty acid profile

The fatty acid profiles of fats extracted from milk, cream and buttermilk are shown in Table 2. The percentage content of individual fatty acids in the examined samples demonstrated that their fatty acid composition was characteristic of milk fat and similar to these reported in the literature [Briard *et al*., 2003; Fauquant *et al*., 2005]. In our study, the milk, cream and buttermilk fatty acid profiles differed significantly ($p \leq 0.05$) in the content of C6:0, C12:0, C15:0 ai, C14:1, C16:0, C16:1, C17:0, C18:0, C18:1 Σt, C18:1 c9, C18:1 c11, C18:1 Σc, C18:2 Σt, and C18:2 c9 t11. The percentage content of most of the above fatty acids was highest in buttermilk and lowest in milk. The only exceptions were C6:0, C16:0 and C18:0 whose proportions were highest in milk and lowest in buttermilk. The percentage content of C12:0 and C16:1 was highest in buttermilk and lowest in cream, whereas the content of C17:0 was highest in cream and lowest in milk. Milk and cream were characterised by lower proportions of C10:0, C10:1, C13:0 ai, C13:0, C14:0, C15:0, C18:1 c12 and C18:2 than buttermilk. In turn, buttermilk was less abundant in C4:0 than the remaining products.

The variations in the fatty acid composition of the compared products could be attributed to differences in the fatty acid profile of phospholipids in buttermilk and milk. Buttermilk phospholipids have a lower content of C16:0 and a higher content of C18:0 and PUFAs that are found in larger quantities in membranes than inside milk fat globules [Fauquant *et al*., 2005; Garczewska-Murzyn *et al.*, 2021; Jhanwar & Ward, 2014]. The churning process induces a greater increase in phospholipid levels in buttermilk than in cream. Churning also increases the content of C18:1 and C18:2 in buttermilk relative to cream, and decreases the content of C16:0 in buttermilk phospholipids relative to cream phospholipids [Hokkanen *et al.*, 2021].

The potential relationship between the proportions of the analysed fatty acids and product type (milk, cream and buttermilk) was determined by PCA. The first two principal components (PC1 and PC2), presented in Figure 2, explained 92.45% of the total variance in input data. The first principal component (PC1) explained 71.81% of the variance in input data. A large positive score (0.60) was observed for buttermilk in the first principal direction, on the opposite side of the PC1 axis relative to milk and cream. The score for cream was very small at 0.18, whereas milk had

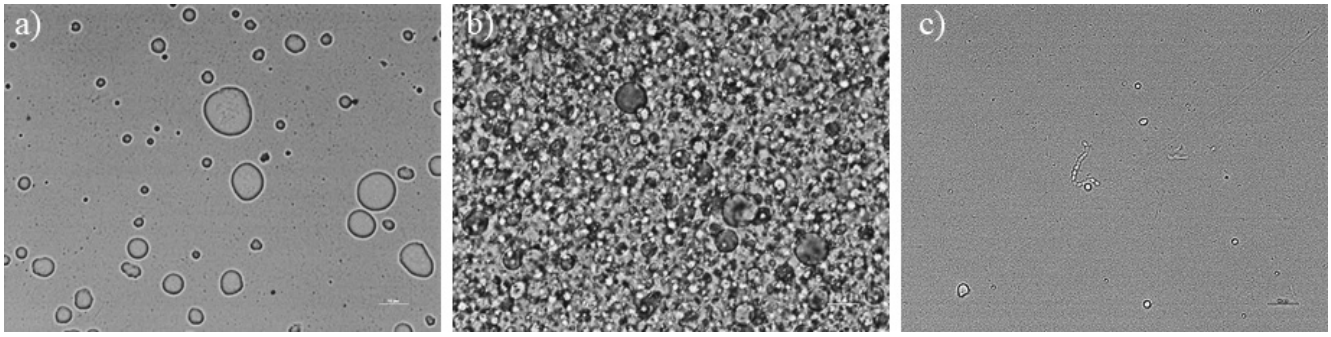

FIGURE 1. Microstructure of milk (a), cream (b) and buttermilk (c), 60× magnification.

a larger score of 0.42. Therefore, in milk and buttermilk, product type was highly related with the scalar projections for PC1. At the same time, the larger the loading for a given variable (fatty acid) relative to PC1, the greater the influence of product type (milk and buttermilk) on the percentage content of a given fatty acid. The points representing individual fatty acids and the sum of fatty acids of a given type were clustered in two groups at the opposite ends of the PC1 axis. The cluster on the left side of the plot grouped fatty acids with negative loadings in the range of -0.99 to -0.79 relative to the scalar projections for PC1. In this group, fatty acids were arranged in the following descending order based on the absolute value of the loadings relative to PC1: C16:0 i, C14:0 i, C16:0, C4:0, C6:0 and C18:0. The second group on the right side of the PC1 axis contained fatty acids with very large loadings in the range of 0.77 to 0.99. These fatty acids were arranged in the following ascending order based on the values of the loadings relative to PC1: C18:2 Σt, C18:1 c9, C15:0 i, C10:0, C12:0, C18:1 Σc, C13:0 ai, C14:0, C13:0, C10:1, C18:1 c12, C18:2, C15:0, C18:1 c11, C18:1 Σt, C15:0 ai, C14:1 and C18:2 c9 t11. The second principal component (PC2) explained 20.37% of the variance in input data. Cream had a score of 0.29, and it was represented by a point at the top of the plot. Milk had a negative loading of -0.22, and it was represented by a point in the bottom part of the plot. Therefore, in milk and cream, the relationship between the proportions of fatty acids and product type was stronger in relation to the scalar projections for PC2 than PC1. The larger the loading for a given variable (fatty acid) relative to PC2, the greater the influence of product type (milk and cream) on the percentage content of a given fatty acid. In relation to PC2, very large loadings were observed for C17:0 (0.94) at the top of the plot and C8:0 (-0.83) in the bottom part of the plot.

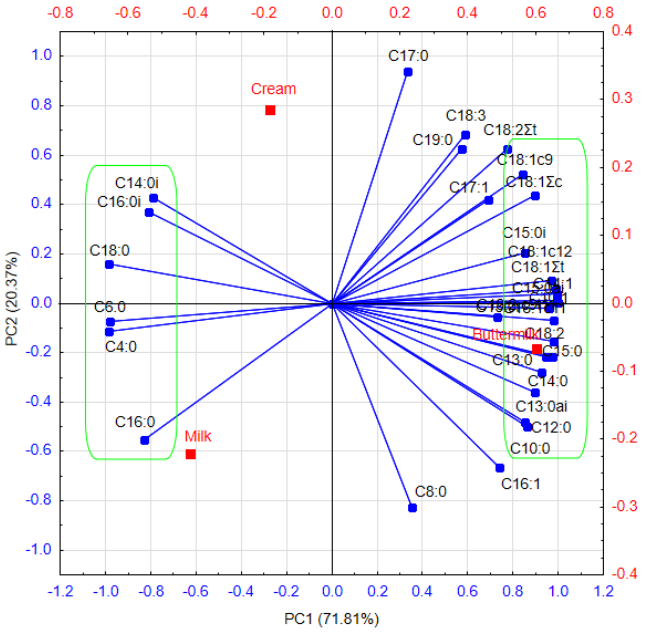

FIGURE 2. Principal component analysis (PCA) biplot of the milk, cream and buttermilk and relative content of their fatty acid to principal component 1 (PC1) and principal component 2 (PC2).

TABLE 2. Relative content of fatty acids of milk, cream and buttermilk (g/100 g total fatty acids).

Fatty acid	Milk	Cream	Buttermilk
C4:0	2.67±0.05^{a}	2.60±0.01^{a}	2.44±0.01^{b}
C6:0	1.80±0.00^{a}	1.78±0.00^{b}	1.72±0.01^{c}
C8:0	1.11±0.01	1.10±0.00	1.11±0.01
C10:0	2.60±0.02^{b}	2.56±0.00^{b}	2.69±0.02^{a}
C10:1	0.25±0.00^{b}	0.26±0.00^{b}	0.27±0.00^{a}
C12:0	3.12±0.00^{b}	3.06±0.00^{c}	3.27±0.02^{a}
C13:0 i	0.07±0.00	0.07±0.00	0.07±0.00
C13:0 ai	0.08±0.00^{b}	0.08±0.00^{b}	0.09±0.00^{a}
C13:0	0.09±0.00^{b}	0.09±0.00^{b}	0.10±0.00^{a}
C14:0 i	0.12±0.00	0.13±0.00	0.12±0.00
C14:0	11.07±0.02^{b}	11.06±0.00^{b}	11.20±0.03^{a}
C15:0 i	0.23±0.00^{b}	0.23±0.00^{ab}	0.24±0.00^{a}
C15:0 ai	0.38±0.00^{c}	0.41±0.00^{b}	0.47±0.00^{a}
C14:1	0.89±0.00^{c}	0.91±0.00^{b}	1.01±0.01^{a}
C15:0	1.02±0.00^{b}	1.03±0.00^{b}	1.11±0.01^{a}
C16:0 i	0.29±0.00	0.30±0.00	0.28±0.00
C16:0	32.84±0.09^{a}	31.80±0.01^{b}	31.48±0.06^{c}
C16:1	1.51±0.01^{b}	1.47±0.01^{c}	1.55±0.00^{a}
C17:0	0.40±0.00^{c}	0.55±0.00^{a}	0.49±0.00^{b}
C17:1	0.28±0.10	0.37±0.00	0.40±0.01
C18:0	12.66±0.04^{a}	12.54±0.00^{b}	10.93±0.00^{c}
C18:1 Σt	1.57±0.03^{c}	1.68±0.04^{b}	1.95±0.02^{a}
C18:1 c9	22.03±0.14^{c}	22.76±0.01^{b}	23.03±0.03^{a}
C18:1 c11	0.55±0.01^{c}	0.57±0.01^{b}	0.71±0.03^{a}
C18:1 c12	0.19±0.01^{b}	0.21±0.00^{b}	0.25±0.01^{a}
C18:1 Σc[1]	22.77±0.13^{c}	23.54±0.00^{b}	23.99±0.06^{a}
C19:0	0.28±0.01	0.30±0.01	0.30±0.00
C18:2 Σt[2]	0.00±0.00^{c}	0.14±0.01^{b}	0.17±0.00^{a}
C18:2	1.19±0.00^{b}	1.19±0.00^{b}	1.64±0.00^{a}
C18:3	0.31±0.01^{b}	0.35±0.00^{a}	0.34±0.00^{ab}
C18:2 c9 t11	0.38±0.00^{c}	0.42±0.00^{b}	0.55±0.00^{a}
SFAs	70.85±0.19^{a}	69.68±0.03^{b}	68.13±0.09^{c}
MUFAs	27.26±0.19^{c}	28.22±0.04^{b}	29.18±0.10^{a}
PUFAs	1.88±0.01^{c}	2.10±0.01^{b}	2.69±0.00^{a}
SCFAs	5.58±0.05^{a}	5.47±0.02^{b}	5.28±0.01^{c}
MCFAs	54.57±0.10^{a}	53.45±0.02^{c}	53.96±0.09^{b}
LCFAs	39.84±0.15^{b}	41.08±0.03^{a}	40.76±0.10^{a}
BSFAs	1.17±0.01^{c}	1.21±0.00^{b}	1.28±0.00^{a}

The presented values are means ± standard deviations (n=3). Values with different superscripts (a–c) in rows differ significantly at $p \leq 0.05$. n.d. – not detected; i – *iso*; ai – *anteiso*; c – *cis*; t – *trans*; SFAs – saturated fatty acids; MUFAs – monounsaturated fatty acids; PUFAs – polyunsaturated fatty acids; SCFAs – short-chain fatty acids, (C4–C8); MCFAs – – medium-chain fatty acids, (C10–C16); LCFAs – long-chain fatty acids, (C17–C19); BSFAs – branched-chain fatty acids (C13:0 i, C13:0 ai, C14:0 i, C15:0 i, C15:0 ai, C16:0 i).
[1]C18:1 Σc (c9, c11, c12).
[2]C18:2 Σt (t9 c12, t11 c15, c9 t12, c9 t13).

A comparison of the fatty acid groups located on opposite sides of the PC1 axis with the results of Duncan's test demonstrated that the proportions of these fatty acids (excluding C16:0 and C14:0 with loadings of 0.79 and -0.81, respectively) were significantly ($p \leq 0.05$) affected by product type. It can be assumed that the proportions of the remaining fatty acids also differed between the examined products (milk, cream and buttermilk).

The share of the main fatty acid groups, *i.e.* SFAs, MUFAs, PUFAs, SCFAs, MCFAs and BCFAs, in the total fatty acids differed significantly ($p \leq 0.05$) between the analysed products (Table 2). Whole milk fat was most abundant in SFAs and least abundant in MUFAs, PUFAs and BCFAs. The proportion of SFAs was lowest, whereas the proportions of MUFAs, PUFAs and BCFAs were highest in buttermilk fat. In terms of the length of the fatty acid chain, MCFAs (mostly C16:0 and C14:0) were the predominant fatty acids. The content of MCFAs was lowest in cream fat and highest in milk fat. Buttermilk was least abundant in SCFAs relative to the remaining products. The content of LCFAs was highest in cream, lower in buttermilk, and lowest in milk. The LCFA values in cream and buttermilk fat formed a homogeneous group ($p > 0.05$) and differed significantly ($p \leq 0.05$) from the values noted in milk. A similar content of MCFAs and LCFAs was reported by Jensen [2002]. The content of fatty acids per 100 g of the analysed product was approximately 15 times higher in cream than in buttermilk, and approximately 3 times higher in cream than in milk (Table 3).

TABLE 3. Fatty acid content of milk, cream and buttermilk (g/100 g of the product).

Fatty acids	Milk	Cream	Buttermilk
SFAs	21.00±0.23[b]	58.79±0.21[a]	3.88±0.12[c]
MUFAs	8.08±0.09[b]	23.81±0.08[a]	1.66±0.05[c]
PUFAs	0.56±0.01[b]	1.77±0.01[a]	0.15±0.01[c]
SCFAs	1.65±0.02[b]	4.62±0.02[a]	0.30±0.01[c]
MCFAs	16.17±0.18[b]	45.10±0.16[a]	3.08±0.09[c]
LCFAs	11.81±0.13[b]	34.66±0.12[a]	2.32±0.07[c]
BSFAs	0.35±0.01[b]	1.02±0.01[a]	0.07±0.01[c]

The presented values are means ± standard deviations (n=3). Values with different superscripts (a–c) in rows differ significantly at $p \leq 0.05$. SFAs – saturated fatty acids; MUFAs – monounsaturated fatty acids; PUFAs – polyunsaturated fatty acids; SCFAs – short-chain fatty acids, (C4–C8); MCFAs – medium-chain fatty acids, (C10–C16); LCFAs – – long-chain fatty acids, (C17–C19); BSFAs – branched-chain fatty acids (C13:0 i, C13:0 ai, C14:0 i, C15:0 i, C15:0 ai, C16:0 i).

Differential scanning calorimetry

DSC involved freeze-dried samples of milk, cream and buttermilk because the presence of water could lead to the formation of unclear peaks, in particular lipid phase transition peaks. During DSC analysis, the phase transition peaks of water can overlap with the peaks of the remaining milk components, which could prevent the identification of differences between the DSC curves of milk, cream and buttermilk. Water was removed from the samples by freeze-drying which is the least invasive dehydration technique with minimum effects on milk components [Pugliese *et al.,* 2019].

Freeze-dried samples of buttermilk, milk and cream were characterised by water activity (a_w) of 0.05–0.08, dry matter content of 97.83±0.47 g/100 g, 97.73±0.69 g/100 g and 97.89±0.24 g/100 g; fat content of 5.70±0.17 g/100 g, 29.64±0.33 g/100 g and 84.37±0.30 g/100 g; and protein content of 34.72±0.12 g/100 g, 24.79±0.25 g/100 g and 5.08±0.20 g/100 g, respectively.

Differential scanning calorimetry supported the identification of exothermic (Figure 3) and endothermic (Figure 4) peaks that occurred in all samples and differed between the analysed products. Exothermic peaks were noted during cooling, and they were identified as: A – peaks that occurred in all samples within a temperature range of around 11°C to around -40°C; B – peaks that were not clearly separated from peaks A and were observed in milk and cream within a temperature range of around 15°C to around 11°C; C – peak noted only in cream within a temperature range of around 20–22°C to around 15°C. Peaks (A-C) denoting the crystallisation of the entire milk fat were not completely separated at a cooling rate of 10°C/min. Milk fat was crystallised within a temperature range of 20°C to -40°C, but clear zones denoting the crystallisation of selected milk fat fractions were also observed. The first zone ranged from 20°C to 15°C (peak C), and the second zone ranged from 10°C to -40°C (peak A). These peaks were separated by a zone where the crystallisation of selected milk fat fractions was accompanied by less pronounced thermal effects (peak B). The partial overlap between peaks A and B resulted from similar phase transition characteristics of milk fat components [Tomaszewska-Gras, 2013].

The peaks on the DSC curves of milk, cream and buttermilk in the present study (Figure 3), had similar characteristics to those reported by Truong *et al*. [2014]. A review of the literature indicates that exothermic peaks (A-C) were associated with crystallisation [Hokkanen *et al*., 2021; Michalski *et al.*, 2004; Tomaszewska-Gras, 2013; Truong *et al*., 2014]. Therefore, exothermic peaks A were probably associated with the proportions of MUFAs and PUFAs (mostly C18:1), whereas peaks B and C were influenced by the percentage content of SFAs (mostly C14:0, C16:0 and C18:0).

Endothermic peaks associated with milk fat melting were observed in the DSC curves of all samples (Figure 4) during heating within a temperature range of -40°C to 95°C. The first peak (D) did not have a clear onset temperature, and its endset temperature was determined at 18–24°C. Peak D was associated with LMPF and MMPF that were not clearly separated (they were separated at a temperature of around 14°C in the DSC curves of cream and milk). The second peak (E) began at approximately 18–24°C and ended at 34–42°C, and it was identified as HMPF.

In a study by Szulc *et al*. [2016], endothermic melting peaks in whole milk powder were identified in the temperature range of -10°C to 50°C. Endothermic peaks D and E associated with milk fat melting were reported by Hokkanen *et al*. [2021] and Michalski *et al.* [2004]. In the DSC curves of milk, cream and buttermilk, peak D representing the overlap between LMPF and MMPF was highly related with the scan rate.

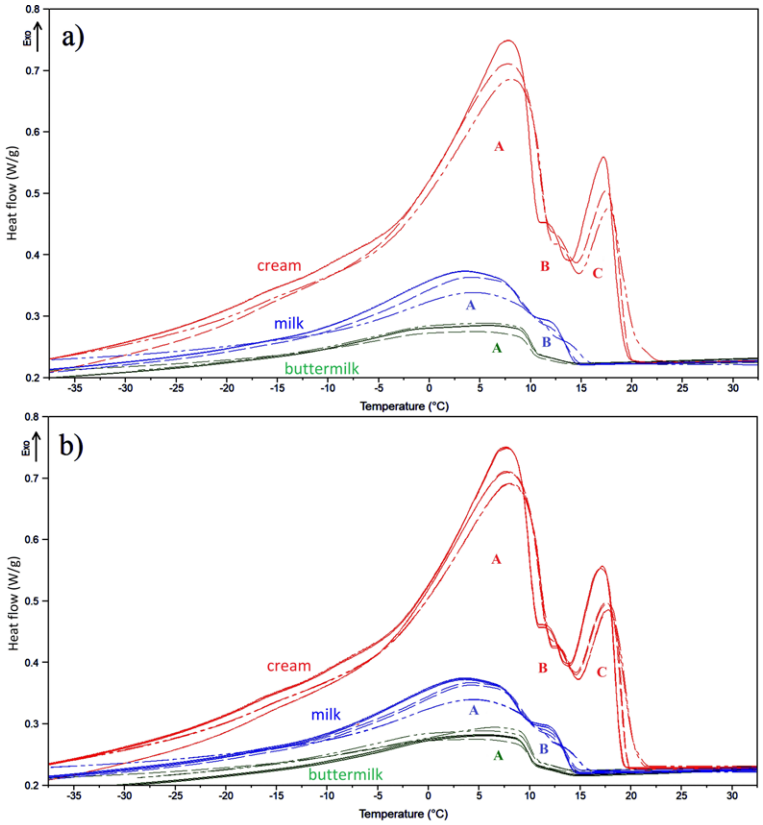

FIGURE 3. Exothermic peaks in differential scanning calorimetry (DSC) curves during freeze-dried milk, cream and buttermilk cooling in cycle I (a) and cycle II (b). Long-dash, short-dash and broken-dash lines represent replicate measurements in the same product. Different types of peaks are marked with letters A–C.

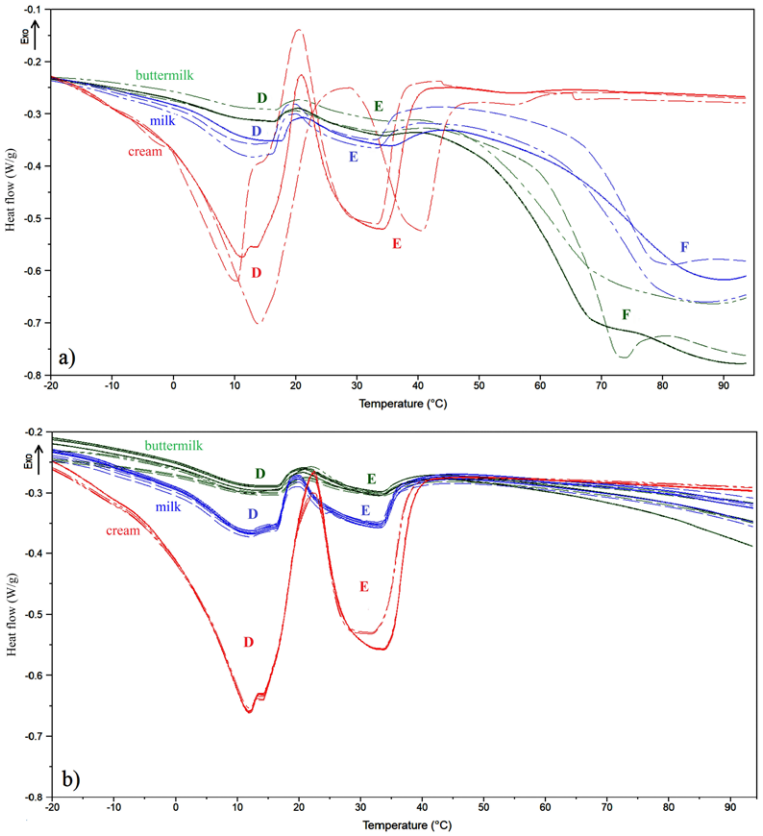

FIGURE 4. Endothermic peaks in differential scanning calorimetry (DSC) curves during freeze-dried milk, cream and buttermilk heating in cycle I (a) and cycle II (b). Long-dash, short-dash and broken-dash lines represent replicate measurements in the same product). Different types of peaks are marked with letters D–F.

TABLE 4. Parameters of exothermic phase transition peaks of freeze-dried milk, cream and buttermilk in cycle I and cycle II of the differential scanning calorimetry (DSC) sequence.

Peak	Cycle	Product	T_{max} (°C)	P_{height} (W/g)	$\Delta T_{1/2}$ (°C)	T_{onset} (°C)	ΔH (J/g)	P_s (°C)	P_e (°C)
A[1]	I	Milk	3.95±0.44^{b}	0.14±0.02^{b}	18.90±0.44^{b}	14.46±0.14^{a}	18.19±2.50^{b}	16.36±0.84^{a}	n.d.*
		Cream	7.19±0.19^{a}	0.36±0.02^{a}	10.67±1.11^{c}	11.64±0.68^{b}	37.24±0.71^{a}	14.38±0.47^{b}	n.d.*
		Buttermilk	4.58±0.62^{b}	0.06±0.01^{c}	21.97±1.71^{aA}	11.47±0.88^{b}	8.93±0.98^{c}	15.56±0.24^{a}	n.d.*
	II	Milk	4.01±0.45^{c}	0.14±0.02^{b}	19.09±0.59^{b}	14.81±0.65^{a}	18.49±2.23^{b}	16.33±0.69^{a}	n.d.*
		Cream	7.30±0.37^{a}	0.36±0.02^{a}	10.65±0.97^{c}	11.64±0.65^{b}	34.21±4.49^{a}	14.33±0.45^{b}	n.d.*
		Buttermilk	4.69±0.36^{b}	0.06±0.01^{c}	19.88±0.33^{aB}	10.94±0.07^{c}	8.42±0.74^{c}	15.48±0.20^{a}	n.d.*
C	I	Cream	17.79±0.30	0.21±0.05	2.76±0.05^{B}	19.64±0.66	3.53±0.56	21.96±1.64	14.38±0.47
	II	Cream	17.99±0.33	0.22±0.04	3.01±0.09^{A}	19.50±0.53	3.71±0.57	20.79±1.11	14.33±0.45

The presented values are means ± standard deviations (n=3). Values in columns, marked with lowercase letters (a–c) in the superscript differ significantly at $p \leq 0.05$; experimental factor – three products in the same cycle. Values in columns, marked with uppercase letters (A, B) in the superscript differ significantly at $p \leq 0.05$; experimental factor – two cycles in the same product. T_{max} – peak temperature; T_{onset} – phase transition onset temperature; $\Delta T_{1/2}$ – peak width at half height, ΔH – enthalpy change; P_{height} – peak height at maximum; P_s – peak onset temperature; P_e – peak endset temperature. The peaks A and C are related to DSC curves in Figure 3.
[1]Undifferentiated peaks A and B (milk and cream) and peak A (buttermilk).
*no clear endset temperature.

Tomaszewska-Gras [2013] observed a peak corresponding to the overlap between LMPF and MMPF (-30°C to around 18°C) and a clearly separated second peak corresponding to HMPF (from around 18°C to 35°C) at the heating rate of 20°C/min. At the heating rate of 10°C/min, the peaks corresponding to LMPF and MMPF were clearly separated at a temperature of around 10°C.

Milk and buttermilk samples were also characterised by endothermic peaks F which began to form at around 40°C and extended beyond the heating threshold of 95°C (Figure 4). However, these peaks were not fully formed within the temperature range set in the experiment, and their parameters were not determined. Peaks F were associated with irreversible reactions, which is why they were not noted in cycle II of the DSC sequence. The characteristics of peaks F differed in the DSC curves of the analysed products (buttermilk, milk) (Figure 4). Taller peaks were noted in buttermilk than in milk due to differences in the protein content of these products. Therefore, peaks F were probably related to protein transitions, including denaturation or evaporation of water. In the experiments conducted by Szulc *et al*. [2016] and Ostrowska-Ligęza *et al*. [2012], peaks associated with protein denaturation in milk powders occurred within a temperature range of around 40°C to nearly 140°C, with a maximum at around 105°C.

In both cycles of the DSC sequence, peaks A-E were tallest and most clearly differentiated in cream. The peaks in the DSC curves of milk were much smaller, and the smallest peaks were observed in buttermilk. Peaks became clearly separated, and the value of ΔH and the absolute value of P_{height} increased with a rise in fat content (Table 4 and Table 5). These findings suggest that both exothermic and endothermic phase transitions promoted greater heat exchange in cream fat than in milk and buttermilk fat. The DSC curves (Figure 3 and Figure 4) and the chemical composition of milk, cream and buttermilk samples indicate that the presence of peaks in the analysed DSC sequence was influenced mainly by fat content. Higher fat content was also associated with a higher content of fatty acids in the examined samples (Table 3), and this factor played a role in the formation of peaks on DSC curves (Figure 3 and Figure 4). The effect of fat content on the DSC curves of milk, cream and buttermilk within the analysed temperature range was reported by Pugliese *et al*. [2019] who did not observe phase transition peaks in freeze-dried skim milk between -50°C and 100°C.

The parameters of phase transition peaks differed between milk, cream and buttermilk samples (Table 4 and Table 5). In most peaks, $\Delta T_{1/2}$ values were lowest in cream relative to the remaining samples ($p \leq 0.05$). The only exception was the value of $\Delta T_{1/2}$ in peak D in cycle I, which did not differ significantly between cream and the remaining products ($p > 0.05$). The lowest value of $\Delta T_{1/2}$ was noted in cycle II of the endothermic phase transition of cream ($p \leq 0.05$) (Table 5). The values of $\Delta T_{1/2}$ indicate that cream was characterised by the highest rates of crystallisation and melting. Exothermic peaks A and B in the DSC curves of cream were analysed jointly, and they were characterised by the highest maximum phase transition temperature ($p \leq 0.05$). In milk and buttermilk samples, T_{max} values were lower and did not differ significantly in cycle I ($p > 0.05$), but differed in cycle II ($p \leq 0.05$) (Table 4). In cycle II, T_{max} was lowest in peak D in the DSC curve of cream ($p \leq 0.05$). The T_{max} value of peak E did not differ between the examined products ($p > 0.05$) (Table 5). The highest value of T_{onset} denoting the beginning of a given phase transition was observed in exothermic peak A of milk in cycles I and II ($p \leq 0.05$) (Table 4) and in endothermic peak D of milk in cycle II ($p \leq 0.05$) (Table 5). The T_{onset} value of peak E was highest in cream ($p \leq 0.05$) (Table 5). An analysis of the overlap between peaks A and B in cycles I and II revealed the highest value of P_s in milk ($p \leq 0.05$) (Table 4), whereas in endothermic peaks in cycle II, the value of P_s was highest in cream ($p \leq 0.05$) (Table 5). The values

TABLE 5. Parameters of endothermic phase transition peaks of freeze-dried milk, cream and buttermilk in cycle I and cycle II of the differential scanning calorimetry (DSC) sequence.

Peak	Cycle	Product	T_{max} (°C)	P_{height} (W/g)	$\Delta T_{1/2}$ (°C)	T_{onset} (°C)	ΔH (J/g)	P_s (°C)	P_e (°C)
D	I	Milk	12.94±0.47^{A}	-0.08±0.02^{b}	13.70±0.44^{B}	-1.88±1.07	7.51±1.93^{b}	n.d.*	20.16±0.90
		Cream	11.85±1.79	-0.42±0.06^{a}	14.76±1.28	-4.33±2.41	42.03±4.19^{a}	n.d.*	23.36±4.54
		Buttermilk	11.73±0.24	-0.03±0.00^{c}	14.55±0.45^{B}	-2.93±0.87^{A}	2.78±0.54^{cB}	n.d.*	20.22±0.33^{B}
	II	Milk	12.09±0.30^{aB}	-0.09±0.02^{b}	14.63±0.26^{abA}	-2.90±1.02^{a}	8.64±1.76^{b}	n.d.*	20.21±0.64^{c}
		Cream	11.62±0.49^{b}	-0.40±0.03^{c}	13.61±1.11^{b}	-3.80±0.88^{b}	38.84±1.88^{a}	n.d.*	22.58±0.36^{a}
		Buttermilk	12.07±0.37^{a}	-0.04±0.01^{a}	15.51±0.29^{aA}	-4.35±0.64^{bB}	3.81±0.72^{cA}	n.d.*	21.19±0.44^{bA}
E	I	Milk	33.46±1.20	-0.05±0.01^{b}	12.66±0.71^{A}	20.97±0.97	3.86±0.77^{b}	20.26±0.83	42.79±2.04^{B}
		Cream	34.37±5.58	-0.29±0.04^{c}	11.34±2.45	24.73±5.80	19.63±5.08^{a}	23.36±4.54	45.17±4.12
		Buttermilk	32.50±0.26	-0.02±0.00^{aA}	12.69±0.36^{A}	21.61±0.48	1.26±0.28^{cB}	20.25±0.29^{B}	40.05±0.87^{B}
	II	Milk	33.36±0.87	-0.07±0.01^{b}	11.73±0.30^{aB}	20.88±0.70^{c}	4.68±0.89^{b}	20.22±0.74^{c}	45.58±0.60^{aA}
		Cream	32.74±0.68	-0.28±0.02^{c}	10.69±1.09^{b}	23.32±0.45^{a}	17.31±2.02^{a}	22.62±0.46^{a}	43.66±0.39^{b}
		Buttermilk	32.96±0.43	-0.03±0.00^{aB}	10.98±0.14^{bB}	21.85±0.41^{b}	1.88±0.28^{cA}	21.23±0.40^{bA}	42.64±0.37^{cA}

The presented values are means ± standard deviations (n=3). Values in columns, marked with lowercase letters (a–c) in the superscript differ significantly at $p \leq 0.05$; experimental factor – three products in the same cycle. Values in columns, marked with uppercase letters (A, B) in the superscript differ significantly at $p \leq 0.05$; experimental factor – two cycles in the same product. T_{max} – peak temperature; T_{onset} – phase transition onset temperature; $\Delta T_{1/2}$ – peak width at half height, ΔH – enthalpy change; P_{height} – peak height at maximum; P_s – peak onset temperature; P_e – peak endset temperature. The peaks D and E are related to DSC curves in Figure 4.
*no clear onset temperature.

of P_e differed significantly between the samples ($p \leq 0.05$) only in endothermic peaks D and E in cycle II (Table 5).

The DSC sequence was divided into two cycles to analyse the impact of thermal history on the characteristics of DSC curves and the parameters of phase transition peaks in milk, buttermilk and cream samples. A comparison of cycle I and cycle II revealed minor differences in the exothermic crystallisation peaks of milk fat (Figure 3). Significant differences ($p \leq 0.05$) in $\Delta T_{1/2}$ values were found between peak A of buttermilk and peak C of cream (Table 4), which suggests that buttermilk fat was crystallised more rapidly, whereas cream fat was crystallised at a slower rate in cycle II. An analysis of endothermic peaks revealed greater differences in curve characteristics and the parameters of phase transition peaks between cycle I and cycle II (Figure 4, Table 5). The most notable difference was the absence of peaks F in milk and buttermilk samples in cycle II, which are probably associated with irreversible phase transitions of proteins in cycle I. Only endothermic peaks relating to reversible fat melting reactions were noted in cycle II. Significant differences ($p \leq 0.05$) in the parameters of melting peaks were observed between cycle I and cycle II, including in the values of T_{max} in peak D, $\Delta T_{1/2}$ and ΔH in peaks D and E, P_e in peak E in milk samples, T_{onset} and P_e in peak D, $\Delta T_{1/2}$ and ΔH in peaks D and E, and P_s and P_e in peak E in buttermilk samples (Table 5). The remaining parameters of exothermic and endothermic processes did not differ significantly ($p > 0.05$) between cycle I and cycle II (Table 4 and Table 5). In repeated analyses of the same product, greater differences in peak parameters (higher standard deviation) and curve characteristics were observed in cycle I than in cycle II, in particular in endothermic peaks in cream (Table 5, Figure 4). In endothermic peaks, significant differences ($p \leq 0.05$) in the values of $\Delta T_{1/2}$, P_s and P_e were determined only in cycle II (Table 5). The differences between DSC cycles indicate that the thermal history of the examined samples influenced curve characteristics, crystallisation rate, onset temperature, melting rate and changes in melting enthalpy. Other authors also observed that thermal history affects the shape of the DSC curves, the parameters of crystallisation and melting of milk fat, as well as microcrystal structure and nucleation rate which determine crystal polymorphism and size [Lopez *et al*., 2007; ten Grotenhuis, 1999; Tomaszewska-Gras, 2013]. Changes in temperature promote the conversion of unstable polymorphic α forms of milk fat crystals into stable β and β' forms due to thermal memory effects [Wiking *et al*., 2009]. These factors were probably responsible for the differences between cycle I and cycle II of the analysed DSC sequence, in particular in melting parameters, as well as the similarities in DSC curves representing repeated heating and cooling stages in cycle II (Figure 4).

CONCLUSIONS

The research results provide a comprehensive overview of the properties of the milk, cream and sweet buttermilk emulsion phase. The fat globules were largest in cream and smallest in buttermilk. The microscopic analysis revealed the presence of fat globule agglomerates in cream and chains of small fat globules in buttermilk. The size of fat globules was related with the fatty acid content of the examined products. The proportion of LCFAs was highest in cream and lowest in milk, whereas the reverse was noted in an

analysis of MCFAs. The content of monoenoic and polyenoic fatty acids was highest in buttermilk and lowest in milk, and it was related with the content of fat globule membrane components. The analysed products differed in the shape of DSC curves and the parameters of phase transition peaks. Unlike milk and buttermilk, cream was characterised by an additional peak on the DSC curve, as well as much higher values of crystallisation and greater changes in melting enthalpy. These differences were probably induced by fat content which was related with the fatty acid composition of each product. The study demonstrated that parameters T_{max}, P_{height} and $\Delta T_{1/2}$ of exothermic crystallisation peaks and parameters P_{height}, $\Delta T_{1/2}$ and ΔH of endothermic melting peaks were reliable indicators for comparing the thermal properties of milk, cream and buttermilk. The thermal history of the examined products, which was shaped during repeated heating and cooling stages within a temperature range of -40°C to 95°C, influenced the crystallisation and melting characteristics of milk, cream and buttermilk fat. The thermal phase transitions should be characterised in greater detail and linked with the fatty acid profile and the size of milk fat globules, which may be used to optimise the production and storage processes of dairy products and to improve and control their quality. Milk, buttermilk and cream should also be compared in terms of the contents of components other than milk fat.

ACKNOWLEDGEMENTS

The authors would like to thank Justyna Ziajka and Waldemar Brandt for technical assistance during the study.

RESEARCH FUNDING

Project financially supported by the Minister of Education and Science under the program entitled “Regional Initiative of Excellence” for the years 2019–2022, Project No. 010/RID/2018/19, amount of funding 12.000.000 PLN.

CONFLICT OF INTERESTS

Authors declare no conflict of interests.

ORCID IDs

K. Bohdziewicz https://orcid.org/0000-0003-2394-0495
O. Brożek https://orcid.org/0000-0002-0133-3224
K. Kiełczewska https://orcid.org/0000-0002-5267-925X

REFERENCES

1. AOAC. 2007. Official Methods of Analysis of AOAC International. 18th ed. Gaithersburg, MD, AOAC International.
2. Berton, A., Rouvellac, S., Robert, B., Rousseau, F., Lopez, C., Crenon, I. (2012). Effect of the size and interface composition of milk fat globules on their *in vitro* digestion by the human pancreatic lipase: Native *versus* homogenized milk fat globules. *Food Hydrocolloids, 29*(1), 123–134. https://doi.org/10.1016/j.foodhyd.2012.02.016
3. Briard, V., Leconte, N., Michel, F., Michalski, M.-C. (2003). The fatty acid composition of small and large naturally occurring milk fat globules. *European Journal of Lipid Science and Technology, 105*(11), 677–682. https://doi.org/10.1002/ejlt.200300812
4. Bugeat, S., Briard-Bion, V., Pérez, J., Pradel, P., Martin, B., Lesieur, S., Lopez, C. (2011). Enrichment in unsaturated fatty acids and emulsion droplet size affect the crystallization behaviour of milk triacylglycerols upon storage at 4°C. *Food Research International, 44*(5), 1314–1330. https://doi.org/10.1016/j.foodres.2011.01.003
5. Conway, V., Gauthier, S.F., Pouliot, Y. (2014). Buttermilk: Much more than a source of milk phospholipids. *Animal Frontiers, 4*(2), 44–51. https://doi.org/10.2527/af.2014-0014
6. Dewettinck, K., Rombaut, R., Thienpont, N., Le, T.T., Messens, K., Van Camp, J. (2008). Nutritional and technological aspects of milk fat globule membrane material. *International Dairy Journal, 18*, 436–457. https://doi.org/10.1016/j.idairyj.2007.10.014
7. Dhungana, P., Truong, T., Palmer, M., Bansal, N., Bhandari, B. (2017). Size-based fractionation of native milk fat globules by two-stage centrifugal separation. *Innovative Food Science & Emerging Technologies, 41*, 235–243. https://doi.org/10.1016/j.ifset.2017.03.011
8. El-Loly, M.M. (2011). Composition, properties and nutritional aspects of milk fat globule membrane: a review. *Polish Journal of Food and Nutrition Sciences, 61*(1), 7–32. https://doi.org/10.2478/v10222-011-0001-0
9. Fauquant, C., Briard, V., Leconte, N., Michalski, C. (2005). Differently sized native milk fat globules separated by microfiltration: fatty acid composition of the milk fat globule membrane and triglyceride core. *European Journal of Lipid Science and Technology, 107*(2), 80–86. https://doi.org/10.1002/ejlt.200401063
10. Garczewska-Murzyn, A., Smoczyński, M., Kotowska, N., Kiełczewska K. (2021). Effect of buttermilk and skimmed milk powder on the properties of low-fat yoghurt. *Journal of Food Science and Technology*. https://doi.org/10.1007/s13197-021-05227-w
11. Gassi, J.Y., Blot, M., Beaucher, E., Robert, B., Leconte, N., Camier, B., Rousseau, F., Bourlieu, C., Jardin, J., Briard-Bion, V., Lambert, S., Gesan-Guiziou, G., Lopez, C., Gaucheron, F. (2016). Preparation and characterisation of a milk polar lipids enriched ingredient from fresh industrial liquid butter serum: Combination of physico-chemical modifications and technological treatments. *International Dairy Journal, 52*, 26–34. https://doi.org/10.1016/j.idairyj.2015.08.012
12. Hickey, C.D., Diehl, B.W.K., Nuzzo, M., Millqvist-Feurby, A., Wilkinson, M.G., Sheehan, J.J. (2017). Influence of buttermilk powder or buttermilk addition on phospholipid content, chemical and bio-chemical composition and bacterial viability in Cheddar style-cheese. *Food Research International, 102*, 748–758. https://doi.org/10.1016/j.foodres.2017.09.067
13. Hokkanen, S.P., Partanen, R., Jukkola, A., Frey, A.D., Rojas, O.J. (2021). Partitioning of the milk fat globule membrane between buttermilk and butter serum is determined by the thermal behaviour of the fat globules. *International Dairy Journal, 112*, art. no. 104863. https://doi.org/10.1016/j.idairyj.2020.104863

14. ISO (2002). Milk fat – Preparation of fatty acid methyl esters. ISO standard 15884/IDF 182:2002.
15. ISO (2010). Milk – Determination of fat content – Gravimetric method (Reference method). ISO standard 1211/IDF 1:2010.
16. ISO (2018). Cream – Determination of fat content – Acido-butyrometric (Gerber method). ISO standard 19660/IDF 237:2018.
17. ISO (2018). Milk – Determination of fat content – Acido-butyrometric (Gerber method). ISO standard 19662/IDF 238:2018.
18. Jensen, R.G. (2002). The composition of bovine milk lipids: January 1995 to December 2000. *Journal of Dairy Science, 85*(2), 295–350. https://doi.org/10.3168/jds.S0022-0302(02)74079-4
19. Jhanwar, A., Ward, R.E. (2014). Particle size distribution and lipid composition of skim milk lipid material. *International Dairy Journal, 36*(2), 110–117. https://doi.org/10.1016/j.idairyj.2014.01.010
20. Jukkola, A., Rojas, O.J. (2017). Milk fat globules and associated membranes: Colloidal properties and processing effects. *Advances in Colloid and Interface Science, 245*, 92–101. https://doi.org/10.1016/j.cis.2017.04.010
21. Lambert, S., Leconte, N., Blot, M., Rousseau, F., Robert, B., Camier, B., Gassi, J-Y., Cauty, C., Lopez, Ch., Gésan-Guiziou, G. (2016). The lipid content and microstructure of industrial whole buttermilk and butter serum affect the efficiency of skimming. *Food Research International, 83*, 121–130. https://doi.org/10.1016/j.foodres.2016.03.002
22. Lopez, C., Bourgaux, C., Lesieur, P., Ollivon, M. (2007). Coupling of time-resolved synchrotron X-ray diffraction and DSC to elucidate the crystallisation properties and polymorphism of triglycerides in milk fat globules. *Le Lait, 87*(4–5), 459–480. https://doi.org/10.1051/lait:2007018
23. Lopez, C., Cauty, C., Guyomarc'h, F. (2015). Organization of lipids in milks, infant milk formulas and various dairy products: role of technological processes and potential impacts. *Dairy Science & Technology, 95*(6), 863–893. https://doi.org/10.1007/s13594-015-0263-0
24. Lopez, C., Lesieur, P., Bourgaux, C., Keller, G., Ollivon, M. (2001). Thermal and structural behavior of milk fat: 2. Crystalline forms obtained by slow cooling of cream. *Journal of Colloid and Interface Science, 240*(1), 150–161. https://doi.org/10.1006/jcis.2001.7664
25. Michalski, M.-C., Leconte, N., Briard-Bion, V., Fauquant, J., Maubois, J., Goudédranche, H. (2006). Microfiltration of raw whole milk to select fractions with different fat globule size distributions: Process optimization and analysis. *Journal of Dairy Science, 89*(10), 3778–3790. https://doi.org/10.3168/jds.S0022-0302(06)72419-5
26. Michalski, M.-C., Ollivon, M., Briard, V., Leconte, N., Lopez, C. (2004). Native fat globules of different sizes selected from raw milk: thermal and structural behavior. *Chemistry and Physics of Lipids, 132*(2), 247–261. https://doi.org/10.1016/j.chemphyslip.2004.08.007
27. Ostrowska-Ligęza, E., Górska, A., Wirkowska, M., Koczoń, P. (2012). An assessment of various powdered baby formulas by conventional methods (DSC) or FT-IR spectroscopy. *Journal of Thermal Analysis and Calorimetry, 110*(1), 465–471. https://doi.org/10.1007/s10973-011-2158-5
28. Pugliese, A., Paciulli, M., Chiavaro, E., Mucchetti, G. (2019). Application of differential scanning calorimetry to freeze-dried milk and milk fractions. *Journal of Thermal Analysis and Calorimetry, 137*(2), 703–709. https://doi.org/10.1007/s10973-018-7971-7
29. Sanchez-Juanes, F., Alonso, J.M., Zancada, L., Hueso, P. (2009). Distribution and fatty acid content of phospholipids from bovine milk and bovine milk fat globule membranes. *International Dairy Journal, 19*(5), 273–278. https://doi.org/10.1016/j.idairyj.2008.11.006
30. Singh, H. (2006). The milk fat globule membrane – A biophysical system for food applications. *Current Opinion in Colloid and Interface Science, 11*(2–3), 154–163. https://doi.org/10.1016/j.cocis.2005.11.002
31. Singh, H., Gallier, S. (2017). Nature's complex emulsion: The fat globules of milk. *Food Hydrocolloids, 68*, 81–89. https://doi.org/10.1016/j.foodhyd.2016.10.011
32. Smoczyński, M., Staniewski, B., Kiełczewska, K. (2012). Composition and structure of the bovine milk fat globule membrane – some nutritional and technological implications. *Food Review International, 28*(2), 188–202. https://doi.org/10.1080/87559129.2011.595024
33. Szulc, K., Nazarko, J., Ostrowska-Ligęza, E., Lenart, A. (2016). Effect of fat replacement on flow and thermal properties of dairy powders. *LWT – Food Science and Technology, 68*, 653–658. https://doi.org/10.1016/j.lwt.2015.12.060
34. ten Grotenhuis, E., van Aken, G.A., van Malssen, K.F., Schenk, H. (1999). Polymorphism of milk fat studied by differential scanning calorimetry and real-time X-ray powder diffraction. *Journal of the American Oil Chemists' Society, 76*(9), 1031–1039. https://doi.org/10.1007/s11746-999-0201-5
35. Tomaszewska-Gras, J. (2013) Melting and crystallization DSC profiles of milk fat depending on selected factors. *Journal of Thermal Analysis and Calorimetry, 113*(1), 199–208. https://doi.org/10.1007/s10973-013-3087-2
36. Truong, T., Bansal, N., Sharma, R., Palmer, M., Bhandari, B. (2014). Effects of emulsion droplet sizes on the crystallisation of milk fat. *Food Chemistry, 145*, 725–735. https://doi.org/10.1016/j.foodchem.2013.08.072
37. Vanderghem, C., Bodson, P., Danthine, S., Paquot, M., Deroanne, C., Blecker, C. (2010). Milk fat globule membrane and buttermilks: from composition to valorization. *Biotechnology, Agronomy, Society and Environment, 14*(3), 485–500.
38. Wiking, L., De Graef, V., Rasmussen, M., Dewettinck, K. (2009). Relations between crystallisation mechanisms and microstructure of milk fat. *International Dairy Journal, 19*(8), 424–430. https://doi.org/10.1016/j.idairyj.2009.03.003

Pol. J. Food Nutr. Sci., 2022, Vol. 72, No. 1, pp. 17–26
On-line ISSN: 2083-6007
Print ISSN: 1230-0322
DOI: 10.31883/pjfns/144836
http://journal.pan.olsztyn.pl

Original article
Section: Food Quality and Functionality

A Step Forward Towards Exploring Nutritional and Biological Potential of Mushrooms: A Case Study of *Calocybe gambosa* (Fr.) Donk Wild Growing in Serbia

Jovana Petrović[1], Ângela Fernandes[2], Dejan Stojković[1], Marina Soković[1], Lillian Barros[2], Isabel C.F.R. Ferreira[2], Aditya Shekhar[3], Jasmina Glamočlija[1]*

[1]*Institute for Biological Research "Siniša Stanković", National Institute of Republic of Serbia, University of Belgrade, Bulevar despota Stefana 142, 11000 Belgrade, Serbia*
[2]*Centro de Investigação de Montanha (CIMO), Instituto Politécnico de Bragança, Campus de Santa Apolónia, 5300-253, Bragança, Portugal*
[3]*Helmholtz Centre for Infection Research, Inhoffenstraße 7, 38124 Braunschweig, Germany*

Key words: *C. gambosa*, nutritional value, biological activity, chemical characterization, food ingredient

Edible mushrooms have been appreciated globally for their organoleptic, nutritional and chemical properties. In the present study, fruiting body of *Calocybe gambosa*, wild growing in Serbia, has been chemically characterized (content of macronutrients, soluble sugars, tocopherols, fatty and organic acids) and its bioactive (antimicrobial and antioxidant) properties were evaluated. The results obtained suggest that this mushroom is a source of carbohydrates and proteins (72 g/100 g dry weight (dw) and 16 g/100 g dw, respectively), with a low fat content (1.5 g/100 g dw). Sugar analysis revealed the presence of trehalose (3.82 g/100 g dw) and mannitol (0.22 g/100 g dw). Tocopherol composition revealed the presence of α-tocopherol (7.8 μg/100 g dw), while fatty acid analysis revealed the presence of 24 fatty acids with the prevalence of polyunsaturated fatty acids. Amongst organic acids, oxalic, quinic, malic, citric and fumaric acid were detected (2.8 g/100 g dw, 1.45 g/100 g dw, 11.3 g/100 g dw, 1.3 g/100 g dw, 0.08 g/100 g dw, respectively). Comprehensive antioxidant activity analysis (reducing power, DPPH radical scavenging activity, β-carotene/linoleate and TBARS assays) indicate that the mushroom is a perspective antioxidant source, whereas its antimicrobial potential turned out to be moderate. Nevertheless, at a sub-inhibitory level, the methanolic extract disrupted cell-to-cell communication using *Pseudomonas aeruginosa* PAO1 as a model system. Finally, enrichment of oatmeal cookies with *C. gambosa* flakes not only improved their nutritional value, but was praised among the participants in sensory evaluation test, indicating that along with results of chemical composition and biological activity, this mushroom has a potential to be regarded as functional food.

INTRODUCTION

Wild edible mushrooms have been appreciated worldwide for their unique odor, taste and texture, as well as their beneficial nutritional and chemical properties [Barroetaveña & Toledo, 2017]. They have been used as food by Chilean tribes 13,000 years ago, whereas the most comprehensive data on their medicinal use are 3,000 years old and come from traditional Chinese medicine.

Until recently, use of mushrooms for medicinal purposes has been marginalized in Western countries, while only their organoleptic properties have been appreciated. Nowadays, the situation has changed significantly, as is indicated by extensive research studies in the field of medical mycology [Valverde *et al.,* 2015]. Furthermore, a favorable nutritional profile (including high contents of carbohydrates and proteins, and a low lipid level) along with the presence of biologically active compounds, including phenolics, terpenoids, steroids, lectins, *etc*., highlight the potential of mushrooms to be regarded as functional food [Barroetaveña & Toledo, 2017; Rathee *et al*., 2012].

The discovery of therapeutics with antimicrobial activity at the beginning of the XXth century significantly improved treatment of infections caused by pathogenic microorganisms, reduced the mortality rate, and contributed to the prolongation of human life. Nevertheless, due to their unreasonable and excessive use, a number of bacterial strains resistant to certain types of antibiotics has significantly risen [Zhong, 2009]. As to resolve this problem, the quest for new antimicrobial products has been reevaluated, with edible mushrooms emerging as an important source of compounds with this activity [Alves *et al*., 2012, 2013]. Over the last decade and more so, a large number of mushrooms have been tested with the aim of finding substances with antimicrobial potential [Alves *et al*., 2012, 2013; Barros *et al*., 2007]. Results of studies have shown that mushrooms are rich in polysaccharides,

* Corresponding Author:
Tel.: +381 11 2078 419;
E-mail: jovana0303@ibiss.bg.ac.rs (J. Petrović)

Submitted: 27 September 2021
Accepted: 13 December 2021
Published on-line: 19 January 2022

phenolics, terpenoids, sterols, organic acids, anthraquinone derivatives, peptides, proteins, and ribonucleases, and as such may be used for the development of new antimicrobial, antitumor, antineurodegenerative, and antidiabetic therapeutics; and finally that they are a source of prophylactic antioxidants *etc*. [Alves *et al*., 2013; Petrović *et al*., 2020]. This has been substantiated with literature data which imply that as much as 130 different bioactivities may be attributed to various species of mushrooms [Wasser, 2014]. Therefore, this study was performed to determine the detailed nutritional value and chemical composition of wild *Calocybe gambosa* (Fr.) Donk collected in Serbia, as well as to assess the biological activities of the methanolic extract prepared. To check its potential to be incorporated in food products, a recipe for oatmeal cookies enriched with *C. gambosa* flakes was developed and cookies were subjected to sensory evaluation.

MATERIALS AND METHODS

Mushroom collection and identification

Fruiting bodies of wild growing mushroom *C. gambosa* (Fr.) Donk (Lyophyllaceae) were collected in Bežanija, near Belgrade, Serbia, and authenticated by Jasmina Glamočlija, PhD, Institute for Biological Research "Siniša Stanković", National Institute of Republic of Serbia, University of Belgrade, Serbia. A voucher specimen has been deposited at the Fungal Collection Unit of the Mycological Laboratory, Department for Plant Physiology, Institute for Biological Research "Siniša Stanković", Belgrade, Serbia. The samples were freeze-dried (LH Leybold, Lyovac GT2, Frankendorf, Switzerland), reduced to a fine dried powder (20 mesh), mixed to obtain homogenous samples and stored at 4°C, protected from light, until further analysis.

Standards and reagents

Acetonitrile 99.9%, *n*-hexane 95% and ethyl acetate 99.8% were of HPLC grade and purchased from Fisher Scientific (Lisbon, Portugal). The fatty acid methyl ester (FAME) reference standard mixture 37 (standard 47885-U) was purchased from Sigma (St. Louis, MO, USA), as well as other individual fatty acid isomers and standards of tocopherols, sugars, organic acids and 6-hydroxy-2,5,7,8-tetramethylchroman-2-carboxylic acid (Trolox). Racemic tocol, 50 mg/mL, was purchased from Matreya (State College, PA, USA), while 2,2-diphenyl-1-picrylhydrazyl (DPPH) radical was obtained from Alfa Aesar (Ward Hill, MA, USA). Mueller-Hinton agar (MH) and malt agar (MA) were obtained from the Institute of Immunology and Virology, Torlak (Belgrade, Serbia). Methanol and other chemicals/solvents were of analytical grade and purchased from common sources. Water was treated in a Milli-Q water purification system (TGI Pure Water Systems, Greenville, SC, USA).

Chemical composition analysis

Nutritional value and energy

Fat, protein, and ash contents were determined acc. to the Association of Official Analytical Chemists (AOAC) procedures [AOAC, 2016]. The crude fat content was determined by Soxhlet extraction of the samples with petroleum ether. The ash content was determined by sample incineration at 550±15°C. The crude protein content was analyzed using an automatic distillation and titration unit (Pro-Nitro-A model, JP Selecta, Barcelona, Spain) by the macro-Kjeldahl method (N×correction factor, namely 4.38). The results were expressed in g per 100 g of dry weight (dw). Total carbohydrates (g/100 g dw) and energy (kcal/100 g dw) were calculated according to the following equations: [100 – (g protein + g fat + g ash)] and [4×(g protein + g carbohydrates) + 9×(g fat)], respectively.

Hydrophilic compounds

Soluble sugars were analyzed using a high performance liquid chromatography (HPLC) system coupled to a refraction index (RI) detector as previously described by Reis *et al*. [2012a]. Briefly, the samples (1 g) were spiked with melezitose (internal standard, IS, 5 mg/mL) and extracted with 80% (*v/v*) ethanol at 80°C. The mixture was centrifuged and the supernatant was concentrated and defatted with ethyl ether. After concentration at 40°C, the residues were dissolved in 5 mL of water and filtered through 0.2 μm nylon filters. Identification was achieved by comparing the peak retention times with those of the authentic standards, while quantification was based on the internal standard (IS) method, with calibration curves constructed with commercial standards. The results were expressed in g per 100 g dw.

The organic acids profile was analyzed by ultra-fast liquid chromatography (UFLC; Shimadzu 20A series, Kyoto, Japan) following a procedure previously described and optimized by the authors [Barros *et al*., 2013]. Briefly, the samples (1 g) were stirred with 25 mL of metaphosphoric acid for 45 min and filtered, first through Whatman No. 4 filter paper and then through 0.2 μm nylon filters. Chromatographic separation was achieved in reverse phase on a C18 column (5 μm particle size, 250×4.6 mm; Phenomenex, Torrance, CA, USA). Detection was performed in a photo-diode array detector (PDA), at 215 nm. The detected compounds were identified and then quantified by chromatographic comparison of the peak area with calibration curves obtained from commercial standards. The results were expressed in g per 100 g dw.

Lipophilic compounds

After transesterification of the lipid fraction obtained by Soxhlet extraction [Reis *et al*., 2012a], the fatty acid methyl ester (FAME) mixture was analyzed by gas-liquid chromatography (GC) with flame ionization detection, using a YOUNG IN Chromass 6500 GC system (Anyang, South Korea) apparatus equipped with a split/splitless injector, a flame ionization detector (FID), and a Zebron-Fame column (Phenomenex). Identification was made by chromatographic comparison of the retention times of the FAME peaks with those of the standard 47885-U. The results were recorded and processed using Clarity DataApex 4.0 software (Prague, Czech Republic) and the content of each fatty acid was expressed as percentage of total fatty acids.

Tocopherols were analyzed according to a procedure described by Heleno *et al*. [2010], using the HPLC system coupled to a fluorescence detector (FP-2020; Jasco, Tokyo, Japan), programmed for excitation at 290 nm and emission at 330 nm. Briefly, the samples (500 mg) were spiked with

a butylated hydroxytoluene solution (10 mg/mL) and tocol (IS, 2 μg/mL), and homogenized first with 4 mL of methanol and then with 4 mL of *n*-hexane. Then, 2 mL of a saturated NaCl aqueous solution were added, the mixture was homogenized and centrifuged, and the upper layer was collected. The extraction was repeated twice with *n*-hexane. The extracts were dried under a nitrogen stream, redissolved in 1 mL of *n*-hexane, dehydrated, and filtered through 0.22 μm syringe filters. Chromatographic separation was performed in normal phase on a Polyamide II column (5 μm particle size, 250×4.6 mm; YMC, Kyoto, Japan). Identification was made by chromatographic comparison with authentic standards, and quantification was based on the fluorescence signal response of each standard, using the IS (tocol) method and calibration curves constructed from commercial standards. The results were expressed in μg per 100 g of dw.

Preparation of extract

Extract was prepared from lyophilized mushroom powder using methanol (Merck, Darmstadt, Germany) as a solvent according to a procedure earlier published by Vaz *et al*. [2010]. Briefly, 10 g of mushroom powder was used for the extraction with 240 mL of methanol overnight at -20°C. The extract was then sonicated for 15 min in an ultrasonic bath (Bandelin sonorex, Berlin, Germany) and centrifuged for 10 min at 4,000×*g* and 4°C (Heraeus Biofuge Stratos centrifuge, Thermo Electron Corporation, Waltham, MA, USA). The extract was filtered through Whatman No. 4 filter paper, and the precipitate was re-extracted in an ultrasonic bath three times with 100 mL of methanol each. The combined supernatant was evaporated to dryness at 40°C using a rotary vacuum evaporator (Büchi R-210, Flawil, Germany). The extract was stored at 4°C until further use.

Antioxidant activity determination

Five assays were used for the evaluation of *in vitro* antioxidant activity: ferricyanide/Prussian blue assay, DPPH radical scavenging activity assay, β-carotene/linoleate assay and thiobarbituric acid reactive substances (TBARS) assay. Moreover, the Folin-Ciocalteu assay was used to evaluate the total phenolic content. For the assays, a stock solution was used to make successive dilutions [Reis *et al*., 2012b]. The concentrations of the samples that provided 50% of antioxidant activity or 0.5 of absorbance (EC_{50} and $EC_{0.5}$, respectively) were calculated from the obtained graphical results (DPPH, β-carotene/linoleate and TBARS assays) or absorbance at 690 nm (ferricyanide/Prussian blue assay) against sample concentrations. Trolox was used as a standard.

Total phenolic content (Folin-Ciocalteu assay) was determined according to the procedure described by Reis *et al*. [2012b], with gallic acid used to obtain the standard curve. Results were expressed as mg of gallic acid equivalents (GAE) per g of extract.

Antimicrobial activity determination

Antibacterial assay

The Gram-positive bacteria *Staphylococcus aureus* (ATCC 6538), *Bacillus cereus* (clinical isolate), *Micrococcus luteus* (ATCC 10240) and *Listeria monocytogenes* (NCTC 7973), as well as Gram-negative bacteria *Pseudomonas aeruginosa* (ATCC 27853), *Salmonella* Typhimurium (ATCC 13311), *Escherichia coli* (ATCC 35210), and *Enterobacter cloacae* (human isolate), were used. The microorganisms were obtained from the Mycological Laboratory, Department of Plant Physiology, Institute for Biological Research "Siniša Stanković", University of Belgrade, National Institute of Republic of Serbia. The antibacterial assay was carried out by a modified microdilution method [CLSI, 2009]. The lowest concentrations that showed a distinct reduction in color intensity – light red in comparison to the intensive red in the control well (with no added extract), or an absence of color (clear yellow solution of the well), were defined as minimal inhibitory concentration (MICs). The minimal bactericidal concentrations (MBCs) were determined by serial sub-cultivation of 2 μL into the wells already containing 100 μL of broth and further incubation for 24 h at 37°C. The lowest concentration with no visible growth was defined as the MBC, indicating 99.5% killing of the original inoculum.

Antifungal assay

The following micromycetes were used for the evaluation of antifungal activity: *Aspergillus fumigatus* (ATCC 1022), *Aspergillus versicolor* (ATCC 11730), *Aspergillus ochraceus* (ATCC 12066), *Aspergillus niger* (ATCC 6275), *Trichoderma viride* (IAM 5061), *Penicillium funiculosum* (ATCC 36839), *Penicillium ochrochloron* (ATCC 9112) and *Penicillium verrucosum* var. *cyclopium* (food isolate). The lowest concentrations with significant reduction in mycelial growth (at the binocular microscope) were defined as MICs. The minimal fungicidal concentrations (MFCs) were determined by serial sub-cultivation of a 2 μL of the tested sample dissolved in medium and further incubated for 72 h at 25°C. The lowest concentration with no visible growth was defined as MFC indicating 99.5% killing of the original inoculum.

Anti-quorum sensing (QS) activity determination

Bacterial strains, growth media and culture conditions

P. aeruginosa PA01 (ATCC 27853) was cultured overnight in Lysogeny broth (LB) medium (1% *w/v* NaCl, 1% *w/v* Tryptone, 0.5% *w*/v yeast extract) with shaking (220 rpm) at 37°C.

Twitching and flagella motility

These features were determined following a procedure described by Yeo & Tham [2012] to estimate the potential of the mushroom extract to alter structures type IV pili (TIVP) necessary for *P. aeruginosa* PAO1 motility (which consequently leads to colony dispersion and colonization of the host). The experiment was done in triplicate. Length of TIVP was estimated under the binocular microscope (type 020-518.500 DM LS, Leica, Wetzlar, Germany). Streptomycin and ampicillin used as positive controls were purchased from Zorka Pharma (Šabac, Serbia). The extract was tested at 0.5 MIC value – 21.9 mg/mL, while the positive controls were tested at 0.10 mg/mL.

Pyocyanin production inhibition

The potential inhibitory effect of the mushroom extract towards the production of pyocyanin (virulence factor

of PAO1) was evaluated using the method described by El Fouly *et al*. [2015]. Antibiotics: streptomycin and ampicillin (Zorka Pharma), were used as positive controls in the concentration 0.10 mg/mL, while the concentration of the extract was 0.5 MIC value – 21.9 mg/mL. The results were calculated according to equation: $I\ (\%) = [(OD_c\text{-}OD_s)/OD_c] \times 100$ with optical density (OD) measured on spectra from 520 nm to 600 nm, reaching its maximum at 520 nm (OD_c – optical density of the control pyocyanin, OD_s – optical density of the extract/antibiotics).

Preparation of the oatmeal cookies enriched with *C. gambosa* flakes

For the preparation of oatmeal cookies, 60 g of softened butter was mixed with 170 g of castor sugar, 1 large egg (~ 50 g), 120 g of self-rising flour, 50 g of rolled oats and 25 g of *C. gambosa* flakes. As for the seasoning, 2.50 g of salt, 2.50 g of vanilla extract, 2.50 g of grounded cinnamon and 75 g of chocolate chips (70% cocoa) were added to the mixture. The mixture was poured with ice cream scoop onto the pane and baked at 180°C for 20 min, or until golden brown. In total, with this recipe, we obtained 24 cookies which after the baking weighed approximately 25 g each.

Sensory evaluation and nutritional value determination of cookies

The sensory evaluation of the freshly baked product was attended by 24 untrained participants. Oatmeal cookies without *C. gambosa* flakes were used as a positive control, and were evaluated by the participants in relation to the mushroom-enriched product. Participants were asked to evaluate overall acceptability, appearance, aroma, taste and consistency of oatmeal cookies alone and those enriched with *C. gambosa* flakes on a scale 1–5 (1 – extremely dislike, 2 – dislike, 3 – neither like nor dislike, 4 – like, 5 – extremely like). Results were averaged by number of participants. The nutritional value of oatmeal cookies was determined, based on the nutritional value of the ingredients. Furthermore, the nutritional value (the content of fat, proteins and carbohydrates) of the mushroom-enriched cookies was calculated taking into account the nutritional value of the cookie ingredients as well as the nutritional value of *C. gambosa* flakes, determined in our study.

Statistical analysis

All the performed assays were carried out in triplicate, and their results were expressed as mean values and standard deviation.

RESULTS AND DISCUSSION

Chemical composition of *C. gambosa*

Nutritional value and hydrophilic compounds

Nutritional value analysis (Table 1) revealed that the wild growing *C. gambosa* collected in Serbia is rich in carbohydrates (72 g/100 g dw), followed by proteins (16 g/100 g dw), and has a low total fat content (1.5 g/100 g dw), resulting in energy value of 365 kcal/100 g dw. A few studies exploring the nutritional potential of *C. gambosa* (commonly known as St. George mushroom) indicate that the level of macronutrients may vary greatly, depending on the origin of the tested sample [Barroetaveña & Toledo, 2017].

TABLE 1. Nutritional value and contents of hydrophilic compounds (g/100 g dw) of *Calocybe gambosa*.

	Component/compound	Content
Nutritional value	Ash	10.6±0.9
	Proteins	16±2
	Fat	1.5±0.3
	Carbohydrates	72±1
	Energy (kcal/100 g dw)	365±2
Soluble sugars	Mannitol	0.22±0.01
	Trehalose	3.82±0.04
	Total sugars	4.04±0.04
Organic acids	Oxalic acid	2.8±0.2
	Quinic acid	1.45±0.04
	Malic acid	11.3±0.7
	Citric acid	1.3±0.2
	Fumaric acid	0.08±0.01
	Total	16.9±0.6

Data represent mean ± standard deviation; dw: dry weight.

Comparative analysis of the samples originating from Serbia and Croatia suggested the following: a sample from Croatia [Beluhan & Ranogajec, 2011] had almost twice the value of protein content (36.65 g/100 g dw) than Serbian sample obtained in this study (16 g/100 g dw), but rather similar fat content (1.34 g/100 g dw and 1.5 g/100 g dw for the Croatian and Serbian sample, respectively). The main difference among the two samples was in the carbohydrate content (72 g/100 g dw in Serbian, 42.65 g/100 g dw in Croatian), which eventually determined a higher energy value of the sample collected in Serbia. This leads to the conclusion that the nutritional value may show strong discrepancy even though climatic and geographic conditions are similar. Furthermore, according to Vaz *et al*. [2011], the Portuguese sample was rather rich in proteins (15.46 g/100 g of dw), ash (13.89 g/100 g of dw), while the contents of fat (0.83 g/100 g of dw), carbohydrates (69.83 g/100 g of dw) and energy (348.58 kcal/100 g dw) were rather lower than the values determined in the present study. Moreover, a sample collected in India was rather rich in proteins (20.22 g/100 g dw) with somewhat lower total carbohydrate content than the previously mentioned samples – 65.61 g/100 g dw [Mridu & Atri, 2017]. Altogether, *C. gambosa* may be considered a desirable food in several dietary regimens used to achieve blood lipid level homeostasis, as well as to obtain all the necessary nutrients. Regarding soluble sugar composition (Table 1), the results obtained did not diverge from the values usually observed for wild growing mushrooms; trehalose was the most abundant sugar with 3.82 g/100 g dw, followed by mannitol which was present in rather low amount (0.22 g/100 g dw). As for the soluble sugar content in samples of different origin,

compared to the Serbian sample (Table 1), a sample collected in Croatia [Beluhan & Ranogajec, 2011] had approximately similar mannitol content (0.34 g/100 g dw), while the trehalose content (7.69 g/100 g dw) was almost twice the level determined for the sample collected in Serbia. Furthermore, mannose and glucose were identified only in the Croatian sample, which resulted in its significantly higher total sugar content (36.39 g/100 g dw) in comparison to 4.04 g/100 g dw determined for the Serbian sample. A similar content of mannitol was identified in a study conducted by Vaz *et al*. [2011], while the trehalose level (7.96 g/100 g dw) was significantly higher than the value obtained in this study. In the present study, among the identified organic acids, malic and oxalic acid were the most abundant (11.3 g/100 g dw and 2.8 g/100 g dw, respectively), whereas contents of the other identified organic acids were significantly lower (Table 1).

Lipophilic compounds

Among identified tocopherols, α-tocopherol (7.8 μg/100 g dw) was the only identified tocopherol isomer (Table 2). Regarding fatty acid analysis (Table 2), 24 acids were identified in total, with polyunsaturated ω-6 linoleic acid as the most abundant among the identified (75.1% of the total fatty acids). Additionaly, polyunsaturated fatty acids (PUFA) predominated over saturated (SFA) and monounsaturated (MUFA) fatty acids, 75.8% over 20.2% and 3.98% respectively. Compared to the other published results of *C. gambosa* fatty acid profile, Vaz *et al*. [2011] reported a high proportion of linoleic acid in a Portuguese wild growing sample, while data regarding samples collected from other geographic regions are not available. Even though a fair amount of SFA was determined as well (palmitic acid, 13.2%), the prevalence of PUFA over SFA and MUFA, along with a total low fat content indicates that the *C. gambosa* is a desirable food in dietary regimens, when controlled intake of fat is required. According to Barroetaveña & Toledo [2017], the prevalence of PUFA over MUFA and SFA was also recorded in other species, with rather high values of linoleic acid measured in *Coprinus comatus* (74.86%), *Calvatia utriformis* (70.29%) and *Agaricus campestris* (68.97%), with the exception is *Lactarius deliciosus* whose fruiting body contains a significant amount of stearic acid [Ferreira *et al*., 2017]. In terms of mushroom metabolism, fatty acids are important as precursors of aromatic compounds; for example, linoleic acid is a precursor of the alcoholic compound 1-octen-3-ol, which gives mushrooms a specific aroma [Ribeiro *et al*., 2009].

Furthermore, according to Ribeiro *et al*. [2009], fatty acids may also exert anti-inflammatory, hypolipidemic and vasodilatory activities and may act preventively in cardiovascular diseases and hypertension, while Su *et al*. [2013] revealed that unsaturated fatty acids can delay the breakdown of carbohydrates in the intestine, thus preventing an increase in postprandial glucose levels and, possibly, managing symptoms of diabetes.

TABLE 2. Chemical composition with regard to lipophilic compounds of *Calocybe gambosa*.

Group	Compound	Content
Tocopherols (μg/100 g dw)	α-Tocopherol	7.8±0.4
Fatty acids (% total fatty acids)	Caproic acid (C6:0)	0.11±0.01
	Caprylic acid (C8:0)	0.07±0.01
	Capric acid (C10:0)	0.06±0.01
	Lauric acid (C12:0)	0.12±0.01
	Myristic acid (C14:0)	0.28±0.01
	Myristoleic acid (C14:1)	0.03±0.03
	Pentadecanoic acid (C15:0)	0.67±0.01
	Palmitic acid (C16:0)	13.2±0.2
	Palmitoleic acid (C16:1)	0.40±0.01
	Heptadecanoic acid (C17:0)	0.29±0.01
	Stearic acid (C18:0)	2.51±0.01
	Oleic acid (C18:1*n*9)	3.43±0.01
	Linoleic acid (C18:2*n*6)	75.1±0.1
	α-Linoleic acid (C18:3*n*3)	0.26±0.02
	Arachidic acid (C20:0)	0.14±0.01
	Eicosenoic acid (C20:1)	0.03±0.01
	cis-11,14-Eicosatienoic acid (C20:2)	0.08±0.01
	cis-11,14,17-Eicosatrienoic acid and heneicosanoic acid (C20:3*n*3+C21:0)	0.29±0.04
	cis-5,8,11,14,17-Eicosapentaenoic acid (C20:5*n*3)	0.05±0.01
	Behenic acid (C22:0)	0.63±0.02
	Behenic acid (C22:1*n*9)	0.04±0.02
	Tricosanoic acid (C23:0)	0.70±0.01
	Lignoceric acid (C24:0)	1.41±0.09
	Nervonic acid (C24:1)	0.05±0.01
	Total SFA	20.2±0.1
	Total MUFA	3.98±0.03
	Total PUFA	75.8±0.1

Data represent mean ± standard deviation; SFA: saturated fatty acids; MUFA: monounsaturated fatty acids; PUFA: polyunsaturated fatty acids; dw: dry weight.

Antioxidant activity of *C. gambosa* extract

Regarding antioxidant properties, the *C. gambosa* extract has been evaluated *via* several *in vitro* assays. A comprehensive analysis of antioxidant activity (Table 3) included the following assays: ferricyanide/Prussian blue assay, DPPH radical scavenging activity, β–carotene/linoleate assay and TBARS assay, which engage different mechanisms of action, implying the presence of more than one group of compounds with antioxidant potential. The results obtained indicate that the reducing power of the sample was significant ($EC_{0.5}$=0.89 mg/mL). Results of the other employed assays (β–carotene/linoleate, DPPH radical scavenging activity and TBARS) indicate that the extract possessed antioxidant activity which varied

TABLE 3. *In vitro* antioxidant activity of the *Calocybe gambosa* extract.

Action mode	Antioxidant activity assay	*C. gambosa*	Trolox
Reducing power	Folin-Ciocalteu assay (mg GAE/g extract)	29.9±0.1	–
	Ferricyanide/Prussian blue assay ($EC_{0.5}$; mg/mL)	0.89±0.02	0.04±0.01
Scavenging activity	DPPH radical scavenging activity (EC_{50}; mg/mL)	2.22±0.03	0.04±0.01
Lipid peroxidation inhibition	β-Carotene/linoleate assay (EC_{50}; mg/mL)	1.3±0.2	0.02±0.01
	TBARS assay (EC_{50}; mg/mL)	2.4±0.3	0.02±0.01

Data represent mean ± standard deviation. Concerning the Folin-Ciocalteu assay, higher values correspond to higher reducing power; for the other assays, the results are presented in $EC_{0.5}$ or EC_{50}, which means that higher values correspond to lower reducing power or antioxidant activity. $EC_{0.5}$: extract concentration corresponding to 0.5 of absorbance for the ferricyanide/Prussian blue assay; EC_{50}: extract concentration corresponding to 50% of antioxidant activity; GAE: gallic acid equivalent.

depending on the method used, but was lower in comparison to the positive control – Trolox (Table 3). Antioxidant activity may be correlated to the relatively high content of total phenolics in the extract determined with the Folin-Ciocalteu assay – 29.9 mg GAE/g extract. Even though the data obtained on the antioxidant activity of *C. gambosa* extract are not exclusive, they are the most comprehensive, since they encompass four assays with different mechanisms of achieving antioxidant activity. This may eventually indicate the overall antioxidant potential of St. George mushroom. Previously, several authors reported the antioxidant potential of *C. gambosa* [Angelini *et al*., 2012; Barroetaveña & Toledo, 2017; Vaz *et al*., 2011], though results of their investigations indicate its lower antioxidant potential compared to the sample analyzed in this study. Furthermore, a comparative antioxidant activity analysis of ethanolic and water extract with soluble polysaccharides conducted by Vaz *et al*. [2011], revealed that the extent of antioxidant activity depends not only on the type of the assay utilized for evaluation, but on the type of extract as well. For instance, the ethanolic extract exerted better DPPH radical scavenging activity than the water extract with soluble polysaccharides (EC_{50}=7.08 mg/mL and 34.60 mg/mL, respectively); whereas regarding the reducing power, the ethanolic extract showed $EC_{0.5}$ of 11.46 mg/mL while the water extract showed $EC_{0.5}$ of 0.18 mg/mL. This implies that the antioxidant potential may be achieved through compounds other than the phenolics, such as high-molecular-weight polysaccharides identified in the water extract.

Given all the data, it may be concluded that the antioxidant potential depends on several factors: complex chemical environment, chemical constituents of the sample itself, but also on the type of the antioxidant assay employed. Even though it seems quite unrealistic to evaluate individual antioxidant potential of all the present components, it is known that the antioxidant activity of individual compounds does not necessarily reflect their overall antioxidant capacity (due to the possibility of synergistic/antagonistic interactions). In more details, since a number of diseases (atherosclerosis, cancer, diabetes, rheumatoid arthritis, post-ischemic perfusion injury, myocardial infarction, cardiovascular diseases, chronic inflammation *etc*.) have been associated to increased oxidative stress and overproduction of free radicals, the possibility of their mitigation and homeostasis maintenance with natural products seems to be a matter with high priority [Ferreira *et al*., 2009; Carocho & Ferreira, 2013]. Given this data, the assumption that a substance with antioxidant potential can be used as a prophylactic agent towards diseases whose etiology and progression are considered to be a consequence of oxidative stress, must be critically contemplated [Soobrattee *et al*., 2005].

Antimicrobial activity of *C. gambosa* extract

The results presented in Table 4 indicate that the *C. gambosa* extract exerts moderate to low antimicrobial activity. Among the tested bacterial and fungal strains, the best antimicrobial activity of extract was observed for the *S. aureus* (MIC 9.30 mg/mL, MBC 18.60 mg/mL) among bacteria, and *T. viride* and *A. versicolor* among micromycetes (MIC 10.94 mg/mL, MFC 43.75 mg/mL, for both species). The lowest antimicrobial potential was observed for *M. luteus*, *L. monocytogenes*, *P. aeruginosa* and *E. coli* (MIC 43.75 mg/mL, MBC 87.50 mg/mL) among bacteria and *P. verrucosum* var. *cyclopium* (MIC 29.12 mg/mL, MFC 58.25 mg/mL) among micromycetes.

Since its beginning, human society has been faced with the problem of diseases caused by pathogenic microorganisms. Although the discovery of antibiotics almost a century ago revolutionized the treatment of infectious diseases, today we once again face numerous multidrug-resistant strains that are very difficult to treat with available antimicrobial agents [Alves *et al*., 2013]. Many Gram-positive and Gram-negative bacteria have acquired mechanisms of resistance to antimicrobial agents including: *Shigella* sp., *Salmonella* sp., *Escherichia coli*, *Enterococcus faecium*, as well as respiratory pathogens *Klebsiella pneumoniae* and *P. aeruginosa*. Experimental data indicate that exposure of bacteria to low concentrations of tetracycline leads to a 100-fold increase in gene transfer whose products increase resistance [Wilson *et al*., 2002]. Furthermore, infections caused by micromycetes have been particularly expanding in recent years, due to an increased number of immunocompromised patients, with selective and toxic antifungal drugs used in clinical practice, indicating desperate need for new effective agents among which mushrooms turned out to be very perspective. As for the literature data on the antimicrobial potential of *C. gambosa*, they indicate antibacterial activity towards *E. coli* and *Bacillus subtilis* [Vaz *et al*., 2011] and antifungal activity of an ethyl acetate extract prepared from broth, against 33 (5 yeasts and 28 filamentous fungi) clinically relevant

TABLE 4. Antibacterial and antifungal activity of the *Calocybe gambosa* methanolic extract.

Bacteria	MIC (mg/mL)	MBC (mg/mL)
Staphylococcus aureus (ATCC 6538)	9.30±0.01	18.60±0.01
Bacilus cereus (clinical isolate)	10.94±0.01	21.88±0.01
Micrococcus luteus (ATCC 10240)	43.75±0.01	87.50±0.01
Listeria monocytogenes (NCTC 7973)	43.75±0.01	87.50±0.01
Pseudomonas aeruginosa (ATCC 27853)	43.75±0.01	87.50±0.01
Enterobacter cloacae (human isolate)	10.94±0.01	21.88±0.01
Salmonella Typhimurium (ATCC 13311)	10.94±0.01	21.88±0.01
Escherichia coli (ATCC 35210)	43.75±0.01	87.50±0.01
Fungi	**MIC (mg/mL)**	**MFC (mg/mL)**
Aspergillus ochraceus (ATCC 12066)	21.88±0.01	43.75±0.01
Aspergillus fumigatus (ATCC 1022)	21.88±0.01	43.75±0.01
Aspergillus niger (ATCC 6275)	21.88±0.01	43.75±0.01
Aspergillus versicolor (ATCC 11730)	10.94±0.01	43.75±0.01
Penicillium funiculosum (ATCC 36839)	21.88±0.01	43.75±0.01
Penicillium ochrochloron (ATCC 9112)	21.88±0.01	43.75±0.01
Penicillium verrucosum var. *cyclopium* (food isolate)	29.12±0.01	58.25±0.01
Trichoderma viride (IAM 5061)	10.94±0.01	43.75± 0.01

Data represent mean ± standard deviation; MIC: minimal inhibitory concentration; MBC: minimal bactericidal concentration; MFC: minimal fungicidal concentration.

fungal strains [Angelini *et al*., 2012]. Among the tested strains, *C. albicans* (DBVPG 4268) strain turned out to be the most susceptible to the activity of the extract. MIC values were significantly lower than those obtained in our study and ranged from 1.56 to 12.5 μg/mL, with better observed activity in comparison to fungicide amphotericin B (positive control). Altogether, the obtained data imply that *C. gambosa* may be a source of bioactive compounds important in the food industry, pharmacy and drug development.

Anti-quorum sensing activity of *C. gambosa* extract

A more detailed assessment of possible mechanisms underlying the determined antibacterial activity towards *P. aeruginosa* PAO1 revealed that the *C. gambosa* extract efficiently interfered within bacterial cell-to-cell communication. This was measured on the morphological (motility changes) and physiological (changes in the production of pigment – pyocyanin) level. Speaking of the colony appearance, the results obtained indicate that the control colony of *P. aeruginosa* PAO1 appeared with rough edges due to the presence of a series of TIVP needed for colony dispersal (Figure 1C). *P. aeruginosa* PAO1 colony incubated with the *C. gambosa* methanolic extract (0.5 MIC – 21.9 mg/mL) strongly inhibited the formation of TIVP as was indicated by the complete reduction of these structures (Figure 1D). Moreover, commercial antibiotics: streptomycin and ampicillin, selectively inhibited the dispersion of *P. aeruginosa* PAO1 colony: streptomycin completely reduced motility structures, whereas ampicillin was less efficient (Figure 1A and Figure 1B). Production of pyocyanin was lower (Figure 2) in the presence of the *C. gambosa* methanolic extract compared to level of this virulence factor in the control pyocyanin sample (indicating the extract may alter the pathway of its production, making it the perspective anti-QS agent.

Results of anti-QS activity – a decrease in colony diameter, along with a change in TIVP number and colony color, may indicate that the extract effectively affects the QS-regulated functions in *P. aeruginosa* PAO1, since it limits the colony dispersion which is crucial for the expansion of the pathogen. Furthermore, a change measured in the production of pyocyanin, which is a known virulence factor, may also indicate interference of molecules present in the extract with the physiology of *P. aeruginosa* PAO1. A decrease in pyocyanin production (Figure 2) in the presence of subMIC of the *C. gambosa* methanolic extract strongly supports this fact.

Numerous compounds identified in mushroom extracts turned out to be efficient inhibitors of QS-regulated functions. For example, Soković *et al*. [2014] reported that the aqueous extract of *Agaricus blazei* reduced pyocyanin production, motility, and biofilm formation of *P. aeruginosa* PAO1, while Zhu *et al*. [2011] demonstrated that pigments extracted from the basidiocarp of *Auricularia auricular*, inhibited production

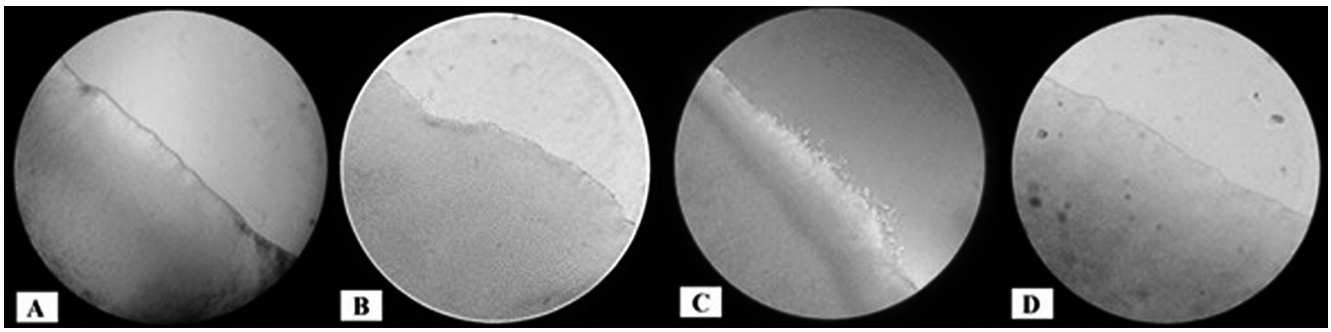

FIGURE 1. Light microscopic images of colony edges of *Pseudomonas aeruginosa* PAO1 twitching motibility plates, grown in the presence of antibiotics (0.10 mg/mL) or 0.5 MIC *Calocybe gambosa* extract (21.9 mg/mL). The colonies of bacteria grown in the presence of streptomycin (A) and ampicillin (B) show flat edges and slight reduction in the number and diameter of type IV pili (TIVP) structures for colony dispersal, respectively. Image (C) shows edge of colony with fully grown pili (control without inhibitors), whereas image (D) reveals flat surface indicating their complete reduction with *C. gambosa* extract. Magnification (A-D) × 100.

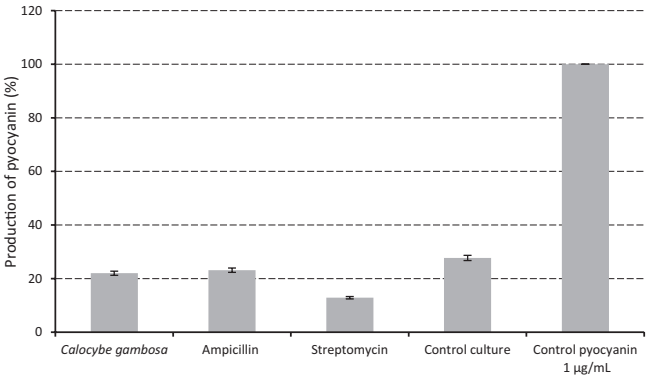

FIGURE 2. Production of pyocyanin by *Pseudomonas aeruginosa* PAO1 in the presence of 0.5 MIC *Calocybe gambosa* extract (21.9 mg/mL), positive controls: ampicillin and streptomycin (0.10 mg/mL) and without inhibitors (control).

of a pigment – violacein (also a virulence factor). The anti-QS activity of compounds of natural origin, as demonstrated in this study, is, in fact, a potentially new pathway to control the diseased caused by *P. aeruginosa* PAO1.

Sensory and nutritional evaluation of cookies with *C. gambosa*

Results of the determination of the nutritional value of oatmeal cookies enriched with *C. gambosa* flakes and their sensory evaluation are presented in Table 5. In general, the newly designed product was positively assessed by the evaluation group. Our attempt to harness various aspects of science and food industry into designing cookies was accepted by the respondents. The score that the enriched product gained was higher than the one obtained for the oatmeal cookie alone, pointing out that participants liked a bit more the new product enriched with mushroom flakes in comparison to the cookies without them – at least in terms of their appearance, aroma, taste and consistency (Table 5). Development of new food products enriched with ingredients of natural origin (in this case mushrooms) with biological activity has been a trend in both science and food industry for quite some time [Soković *et al*., 2017]. For example, previously published results indicate that the chestnut mushroom (*Agrocybe aegerita*) fits very-well with cream cheese, or that button mushroom (*Agaricus bisporus*) may be used as a natural preservative in yoghurt [Petrović *et al*., 2015; Stojković *et al*., 2014]. Having in mind that the results obtained point out that *C. gambosa* has a desirable nutrient profile and bioactive compound contents (Tables 1–3), the mushroom may be considered a candidate for nutraceutical or functional food ingredient. However, for future reference, the consumption of both nutritive and non-nutritive compounds through food has to be observed within the context of their bioavailability in the gastro-intestinal system, which is related to the gut microbiota [Vamanu & Gatea, 2020]. Possible changes in the bioactivity of the compounds, which stem from the gut microbiota activity or chemical modifications due to their metabolic pathway, are potential key limiting factors in using the bioactive compounds for health-beneficial purposes.

An up-to-date literature survey showed that there is a growing interest in investigating the influence of the bioactive compounds onto the gut microbiota – hence the future research should focus on this aspect. This is supported by a recent study by Li *et al*. [2021], which indicates that the application of different mushrooms, such as *Lentinula edodes*, *Hericium erinaceus*, *Grifola frondosa*, *Ganoderma lucidum,* positively affects gut microbiota. This has been validated by using experimental animals fed with *Bulgaria inquinans*; after a course of treatment, the status of their gut microbiota has been significantly improved [Sang *et al*., 2020]. Among the identified compounds from mushrooms, non-digestable carbohydrates had a profound impact on the gut microbiota, leading to its restoration in individuals suffering from dysbiosis [Ma *et al*., 2021]. Aside from carbohydrates, phenolic compounds are also considered valuable ingredients which improve the gut microbiota status [Mithul Aravind *et al*., 2021].

TABLE 5. Nutritional value and sensory evaluation of oatmeal cookies enriched with *Calocybe gambosa* flakes.

	Cookie enriched with *C. gambosa* flakes	Cookie without *C. gambosa* (control)
Fat (g/100 g dw)	3.40	3.37
Proteins (g/100 g dw)	1.82	1.47
Carbohydrates (g/100 g dw)	14.95	13.47
Energy (kcal/100 g dw)	98.57	90.98
Appearance	4.66±0.48	4.25±0.74
Aroma	4.25±0.74	4.25±0.74
Taste	4.66±0.48	4.25±0.74
Consistency	4.83±0.38	4.54±0.51
Overall acceptability	4.68±0.64	4.24±0.68

The results of sensory evaluation are expressed as mean of grades given by the untrained participants ± standard deviation (n=24). Grading scale: 1 – extremely dislike; 2 – dislike; 3 – neither like nor dislike; 4 – like; 5 – extremely like.

CONCLUSION

This study took a step forward towards assessing mushroom's potential to be regarded as functional food, using cookie as a food matrix. The developed cookie product was praised among the participants in sensory evaluation, in terms of appearance, aroma, taste, consistency and overall acceptability. In the long run, this data may be of interest for the market, hence further research should be directed towards this. To summarize, the results obtained in this study provide fresh perspective on using wild growing mushrooms as a valuable source of both nutritive and bioactive compounds, which may confer beneficial health effects as well. The favorable profile of macronutrients, coupled with the presence of α-tocopherol, free sugars, organic and fatty acids indicate that *C. gambosa* is a desirable food in several dietary regimens. Results of determinations of bioactive properties suggest that some of the identified compounds may be responsible for antioxidant, antimicrobial and anti-QS potentials. Moreover,

they point to the fact that mushrooms have a great potential in both pharmaceutical and food industry, due to the presence of several groups of compounds. Unique and versatile organoleptic properties of mushrooms allow them to fit very well with both sweet and savory ingredients, which was the basic presumption of this study after all. As a result, the developed cookie enriched with mushroom flakes was perceived by sensory assessment participants as delicious.

RESEARCH FUNDING

This research was funded by the Ministry of Education, Science and Technological Development of the Republic of Serbia, grant number 451-03-9/2021-14/ 200007. The authors acknowledge the Foundation for Science and Technology (FCT, Portugal) for financial support by national funds FCT/MCTES to CIMO (UIDB/00690/2020).

CONFLICT OF INTERESTS

Authors declare no conflict of interests.

ORCID IDs

L. Barros https://orcid.org/0000-0002-9050-5189
Â. Fernandes https://orcid.org/0000-0002-0157-9873
I.C.F.R. Ferreira https://orcid.org/0000-0003-4910-4882
J. Glamočlija https://orcid.org/0000-0001-6823-1137
J. Petrović https://orcid.org/0000-0002-9016-9971
A. Shekhar https://orcid.org/0000-0001-7383-6050
M. Soković https://orcid.org/0000-0002-7381-756X
D. Stojković https://orcid.org/0000-0002-4159-1471

REFERENCES

1. Alves, M., Ferreira, I.F.R., Dias, J., Teixeira, V., Martins, A. Pintado, M. (2012). A review on antimicrobial activity of mushroom (Basidiomycetes) extracts and isolated compounds. *Planta Medica*, *78*, 1707–1718. https://doi.org/10.1055/s-0032-1315370
2. Alves, M.J., Ferreira, I.C.F.R., Froufe, H.J.C., Abreu, R.M.V, Martins, A., Pintado, M. (2013). Antimicrobial activity of phenolic compounds identified in wild mushrooms, SAR analysis and docking studies. *Journal of Applied Microbiology*, *115*, 346–357. https://doi.org/10.1111/jam.12196
3. Angelini, P., Tirillini, B., Venanzoni, R., (2012). *In vitro* antifungal activity of *Calocybe gambosa* extracts against yeasts and filamentous fungi. *African Journal of Microbiology Research*, *6*, 1810–1814. https://doi.org/10.5897/AJMR11.1384
4. AOAC (2016). Official Methods of Analysis of AOAC International. Official Methods of Analysis of AOAC International; AOAC International: Gaithersburg, MD, USA.
5. Barroetaveña, C., Toledo, C.V. (2017). The nutritional benefits of mushrooms. Chapter 3, In: I.C.F.R. Ferreira, P. Morales, L. Barros (Eds)., *Wild Plants, Mushroom and Nuts. Functional Food Properties and Applications*. Wiley Blackwell, pp. 65–81. https://doi.org/10.1002/9781118944653.ch3
6. Barros, L., Calhelha, R.C., Vaz, J.A., Ferreira, I.C.F.R., Baptista, P., Estevinho, L.M. (2007). Antimicrobial activity and bioactive compounds of Portuguese wild edible mushrooms methanolic extracts. *European Food Research and Technology*, *225*, 151–156. https://doi.org/10.1007/s00217-006-0394-x
7. Barros, L., Pereira, C., Ferreira, I.C.F.R. (2013). Optimized analysis of organic acids in edible mushrooms from Portugal by ultrafast liquid chromatography and photodiode array detection. *Food Analytical Methods*, *6*, 309–316. https://doi.org/10.1007/s12161-012-9443-1
8. Beluhan, S., Ranogajec, A. (2011). Chemical composition and non-volatile components of Croatian wild edible mushrooms. *Food Chemistry*, *124*, 1076–1082. https://doi.org/10.1016/j.foodchem.2010.07.081
9. Carocho, M., Ferreira, I.C.F.R. (2013). A review on antioxidants, prooxidants and related controversy: Natural and synthetic compounds, screening and analysis methodologies and future perspectives. *Food & Chemical Toxicology*, *51*, 15–25. https://doi.org/10.1016/j.fct.2012.09.021
10. CLSI (2009). Clinical and Laboratory Standards Institute Methods for dilution antimicrobial susceptibility tests for bacteria that grow aerobically. In: Approved standard, 8th ed. CLSI publication M07-A8. Clinical and Laboratory Standards Institute, Wayne, PA, USA.
11. El Fouly, M.Z., Sharaf, A.M., Shahin, A.A.M., El-Bialy, H.A., Omara, A.M.A. (2015). Biosynthesis of pyocyanin pigment by *Pseudomonas aeruginosa*. *Journal of Radiation Research and Applied Sciences*, *8*, 36–48. https://doi.org/10.1016/j.jrras.2014.10.007
12. Ferreira, I.C.F.R., Barros, L., Abreu, R. (2009). Antioxidants in wild mushrooms. *Current Medicinal Chemistry, 16*(12), 1543–1560. https://doi.org/10.2174/092986709787909587
13. Heleno, S., Barros, L., Sousa, M., Martins, A., Ferreira, I.C.F.R. (2010). Tocopherols composition of Portuguese wild mushrooms with antioxidant capacity. *Food Chemistry*, *119*(4), 1443–1450. https://doi.org/10.1016/j.foodchem.2009.09.025
14. Li, M., Leilei, Y., Zhao, J., Zhang, H., Chen, W., Zhai, Q., Fengwei, T. (2021). Role of dietary edible mushrooms in the modulation of gut microbiota. *Journal of Functional Foods*, *83*, art. no. 104538. https://doi.org/10.1016/j.jff.2021.104538
15. Ma, G.X., Du, H.J., Hu, Q.H., Yang, W.J., Pei, F., Xiao, H. (2021). Health benefits of edible mushroom polysaccharides and associated gut microbiota regulation. *Critical Reviews in Food Science and Nutrition*. https://doi.org/10.1080/10408398.2021.1903385
16. Mithul Aravind, S., Wichienchot, S., Tsao, S., Ramakrishnan, S., Chakkaravarthi, S. (2021). Role of dietary polyphenols on gut microbiota, their metabolites and health benefits. *Food Research International*, *142*, art. no. 110189. https://doi.org/10.1016/j.foodres.2021.110189
17. Mridu, C., Atri, N.S. (2017). Nutritional and nutraceutical characterization of three wild edible mushrooms from Haryana, India. *Mycosphere, 8*(8), 1035–1043. https://doi.org/10.5943/mycosphere/8/8/4
18. Petrović, J., Glamoclija, J., Stojković, D., Ciric, A., Barros, L., Ferreira, I., Soković, M. (2015). Nutritional value, chemical composition, antioxidant activity and enrichment of cream cheese with chestnut mushroom *Agrocybe aegerita* (Brig.) Sing. *Journal of Food Science and Technology Mysore*, *52*, 6711–6718. https://doi.org/10.1007/s13197-015-1783-6

19. Petrović, J., Glamočlija, J., Ilić-Tomić, T., Soković, M., Robajac, D., Nedić, O., Pavić, A. (2020). Lectin from *Laetiporus sulphureus* effectively inhibits angiogenesis and tumor development in the zebrafish xenograft models of colorectal carcinoma and melanoma. *International Journal of Biological Macromolecules*, *148*, 129–139. https://doi.org/10.1016/j.ijbiomac.2020.01.033
20. Rathee, S., Rathee, D., Rathee, D., Kumar, V., Rathee, P. (2012). Mushrooms as therapeutic agents. *Revista Brasileira de Farmacognosia*, *22*, 459–474. https://doi.org/10.1590/S0102-695X2011005000195
21. Reis, F.S., Barros, L., Martins, A., Ferreira, I.C.F.R. (2012a). Chemical composition and nutritional value of the most widely appreciated mushrooms: an inter-species comparative study. *Food & Chemical Toxicology*, *50*, 191–197. https://doi.org/10.1016/j.fct.2011.10.056
22. Reis, F.S., Martins, A., Barros, L., Ferreira, I.C.F.R. (2012b). Antioxidant properties and phenolics profile of the most widely appreciated cultivated mushrooms: a comparative study between *in vivo* and *in vitro* samples. *Food & Chemical Toxicology*, *50*, 1201–1207. https://doi.org/10.1016/j.fct.2012.02.013
23. Ribeiro, B., Guedes de Pinho, P., Andrade, P.B., Baptista, P., Valentão, P. (2009). Fatty acid composition of wild edible mushrooms species: A comparative study. *Microchemical Journal*, *93,* 29–35. https://doi.org/10.1016/j.microc.2009.04.005
24. Sang, H., Xie, Y., Su, X., Zhang, M., Zhang, Y., Liu, K., Wang, J. (2020). Mushroom *Bulgaria inquinans* modulates host immunological response and gut microbiota in mice. *Frontiers in Nutrition*, 7, art. no. 144. https://doi.org/10.3389/fnut.2020.00144
25. Soković, M., Ćirić, A., Glamočlija, J., Nikolić, M., Griensven, L.J.L.D. (2014). *Agaricus blazei* hot water extract shows anti quorum sensing activity in the nosocomial human pathogen *Pseudomonas aeruginosa*. *Molecules*, *19*(4), 4189–4199. https://doi.org/10.3390/molecules19044189
26. Soković, M., Ćirić, A., Glamočlija, J., Stojković, D. (2017). The bioactive properties of mushrooms. Chapter 4, In: I.C.F.R. Ferreira, P. Morales, L. Barros (Eds)., *Wild Plants, Mushroom and Nuts. Functional Food Properties and Applications*. Wiley Blackwell, pp. 83–122. https://doi.org/10.1002/9781118944653.ch4
27. Soobrattee, M.A., Neergheen, V.S., Luximon-Ramma, A., Aruoma, O.I., Bahorun, T. (2005). Phenolics as potential antioxidant therapeutic agents: mechanism and actions. *Mutation Research/Fundamental and Molecular Mechanisms of Mutagenesis, 579*(1–2), 200–213. https://doi.org/10.1016/j.mrfmmm.2005.03.023
28. Stojković, D., Reis, F., Glamoclija, J., Ciric, A., Barros, L., Van Griensven, L., Ferreira, I., Soković, M. (2014). Cultivated strains of *Agaricus bisporus* and *A. brasiliensis*: Chemical characterization and evaluation of antioxidant and antimicrobial properties for the final healthy product-natural preservatives in yoghurt. *Food & Function*, *5*, 1602–1612. https://doi.org/10.1039/c4fo00054d
29. Su, C.H., Laib, M.N., Ng, L.T. (2013). Inhibitory effects of medicinal mushrooms on α-amylase and α-glucosidase – enzymes related to hyperglycemia. *Food & Function*, *4*, 644–649. https://doi.org/10.1039/c3fo30376d
30. Valverde, M.E., Hernández-Pérez, T., Paredes-López, O. (2015). Edible mushrooms: improving human health and promoting quality life. *International Journal of Microbiology*, *2015*, art. no. 376387. https://doi.org/10.1155/2015/376387
31. Vamanu, E., Gatea, F. (2020). Correlations between microbiota bioactivity and bioavailability of functional vompounds: A miniteview. *Biomedicines*, *8*(2), art. no. 39. https://doi.org/10.3390/biomedicines8020039
32. Vaz, A.J., Heleno, S.A., Martins, A., Almeida, M.G., Vasconcelos, M.H., Ferreira, I.C.F.R. (2010). Wild mushrooms *Clitocybe alexandri* and *Lepista inversa*: *In vitro* tumor cell lines. *Food & Chemical Toxicology*, *48*(10), 2881–2884. https://doi.org/10.1016/j.fct.2010.07.021
33. Vaz, J., Barros, L., Martins, A., Santos-Buelga, C., Vasconcelos, H.M., Ferreira, I.C.F.R. (2011). Chemical composition of wild edible mushrooms and antioxidant properties of their water soluble polysaccharidic and ethanolic fractions. *Food Chemistry*, *126*(2), 610–616. https://doi.org/10.1016/j.foodchem.2010.11.063
34. Wasser, S. (2014). Medicinal mushroom science: Current perspectives, advances, evidences, and challenges. *Biomedicinal Journal*, *37*(6), 345–356. https://doi.org/10.4103/2319-4170.138318
35. Wilson, J.W., Schurr, M.J., LeBlanc, C.L., Ramamurthy, R., Buchanan, K.L., Nickerson, C.A. (2002). Mechanisms of bacterial pathogenicity. *Postgraduate Medical Journal*, *78*, 216–224. https://doi.org/10.1136/pmj.78.918.216
36. Yeo, S.S.M., Tham, F.Y. (2012). Anti-quorum sensing and antimicrobial activities of some traditional Chinese medicinal plants commonly used in South-East Asia. *Malaysian Journal of Microbiology, 8,* 11–20. https://doi.org/10.21161/mjm.34911
37. Zhong, J.H.X. (2009). Secondary metabolites from higher fungi: Discovery, bioactivity and bioproduction. *Advances in Biochemical Engineering/Biotechnology*, *113*, 79–150. https://doi.org/10.1007/10_2008_2
38. Zhu, H, He, C.C., Chu, Q.H., (2011). Inhibition of quorum-sensing in *Chromobacterium violaceum* by pigments from *Auricularia auricular*. *Letters in Applied Microbiology*, *52*, 269–274. https://doi.org/10.1111/j.1472-765X.2010.02993.x

Pol. J. Food Nutr. Sci., 2022, Vol. 72, No. 1, pp. 27–38
On-line ISSN: 2083-6007
Print ISSN: 1230-0322
DOI: 10.31883/pjfns/144835
http://journal.pan.olsztyn.pl

Original article
Section: Food Technology

Drying Kinetics and Changes of Total Phenolic Content, Antioxidant Activity and Color Parameters of Mango and Avocado Pulp in Refractance Window Drying

Thi-Van-Linh Nguyen[1,], Quoc-Duy Nguyen[1], Phuoc-Bao-Duy Nguyen[2,3]*

[1]*Faculty of Environmental and Food Engineering, Nguyen Tat Thanh University, 300A Nguyen Tat Thanh Street, District 4, Ho Chi Minh City, Vietnam*
[2]*Faculty of Electrical and Electronics Engineering, Ho Chi Minh University of Technology (HCMUT), 268 Ly Thuong Kiet Street, District 10, Ho Chi Minh City, Vietnam*
[3]*Vietnam National University Ho Chi Minh City, Linh Trung Ward, Thu Duc District, Ho Chi Minh City, Vietnam*

Key words: avocado pulp, mango pulp, refractance window drying, drying kinetics, phenolics, color parameters

Refractance window drying is an innovative technology belonging to the fourth generation of drying technologies that could enhance the quality of the dried product and improve the drying process. In this study, two factors with the type of fruit pulps (avocado and mango) and drying temperature (ranging from 80 to 95°C) were investigated. Results showed that in refractance window drying, the evaporation process rapidly occurred, mainly in the falling-rate period with undetectable constant-rate period. The Weibull was the best fit model among eight investigated mathematical models that could determine the drying behavior. The effective diffusivity was found to be from 4.25×10^{-10} m^2/s to 7.24×10^{-10} m^2/s for avocado pulp, and from 4.50×10^{-10} m^2/s to 10.67×10^{-10} m^2/s for mango pulp when the drying temperature was changed from 80 to 95°C. Moreover, the corresponding activation energy was 32.06 and 66.03 kJ/mol for avocado and mango pulp moisture evaporation, respectively, and the highest quality of powders of both dried pulps was obtained after processing at 90°C. The refractance window drying revealed a high potential in the production of fruit powders from avocado and mango due to the high retention of more than 80% of total phenolic content (TPC) and antioxidant activity. TPC could be used as a useful criterion for the evaluation of the drying process in terms of dried product quality.

INTRODUCTION

Drying technology is a traditional unit operation that is most popular and important in food processing and preservation. During the drying process, moisture is removed from the material to enhance the stability of the product, reduce unexpected reactions, extend shelf-life, and produce dried products. Among dried products, powder from fruits and vegetables has been shown to offer exciting benefits as very convenient in developing industrial products such as beverages, baby foods, sauces, confectionery, yogurt, ice cream, nutritional bars, bakery products, and cereals [Ramaswamy & Marcotte, 2005]. Besides, the use of fruit powders entails lower costs of distribution and storage [Zotarelli *et al.*, 2017]. In the literature, some drying methods, such as spray-, drum-, freeze-drying, have been studied in respect of fruit powder production. However, each drying method had still some significant drawbacks related to the quality of powder (spray- and drum drying) or costs of system maintenance and implementation (freeze-drying). Recently, the fourth generation of drying technologies has been developed to enhance the quality of the dried product and improve the drying process, among which the refractance window (RW) drying is an innovative technology designed to remove moisture from fruit purees to produce powder, dried sheets, or concentrated products [Vega-Mercado *et al.*, 2001]. During the RW drying, the heat conduction from hot water to film interface is dominant and the drying material would absorb energy due to heat conduction from plastic film to force moisture diffusion and evaporation. While heat conduction, convection, and radiation also happen at the hot-water interface and convection occurs at the air-film interface [Raghavi *et al.*, 2018].

In RW drying, the nutritional and sensory values were proved to be preserved effectively, bringing health benefits to consumers [Nindo & Tang, 2007]. In the literature, the RW drying was successfully applied to fruits and vegetables such as carrot, strawberry [Nindo & Tang, 2007], and tomato [Abul-Fadl & Ghanem, 2011]. As a consequence, the nutritional quality (especially vitamin contents) and the sensory values (color, flavor) could be highly retained [Nindo &

* Corresponding Author:
E-mail: ntvlinh@ntt.edu.vn (Thi-Van-Linh Nguyen)

Submitted: 30 October 2021
Accepted: 8 December 2021
Published on-line: 27 January 2022

Tang, 2007]. For example, the bright green color of asparagus puree after the RW drying was retained similarly to freeze--drying [Abonyi *et al*., 2002]. Additionally, thermal efficiency in RW drying was also higher than using convective drying equipment, as illustrated by the reduction of 50–70% in costs and 50% in energy consumption compared to freeze-drying in the same material capacity [Nindo & Tang, 2007].

Among food materials, avocado and mango are fascinating objects of study. Avocado fruits are superfoods rich in nutrients and phytochemicals [Comerford *et al*., 2016]. Mango possesses high nutritional value [Abbasi *et al.*, 2015; Haytowitz *et al.*, 2018; Shariful *et al.*, 2015]. It belongs to the group of tropical fruits with the top increased consumption with high economic value [Fitzpatrick & Ahrné, 2005; Occena-Po, 2006]. Although both avocado and mango have great nutritional and economic values, they have considerable limitations when it comes to moisture removal. In the literature, some drying methods were applied to dehydrate avocado, such as freeze-drying [Castañeda-Saucedo *et al.*, 2014; Rafidah *et al.*, 2014; Souza *et al.*, 2015], hot-air drying [Temu, 2013], heat--pump drying [Ceylan *et al.*, 2007], or superheated-steam drying [Rafidah *et al.*, 2014]. The most critical drawback in these studies is the long operating time (varying from 3 to more than 20 h), because the higher the temperature or the longer the time of avocado thermal treatment, the more bitter--tasting molecules are produced [Degenhardt & Hofmann, 2010]. However, Degenhardt & Hofmann [2010] found that the thermal processing of avocado within 30 min (at temperatures ranging from 80 to 120°C) or 60 min (at 80°C) only slightly increased bitter taste in comparison with untreated avocado. Thus, the higher quality of dried avocado will be obtained if the temperature and duration of drying are well controlled. In the case of mango, the reported drying methods included freeze- [Caparino *et al.*, 2012], drum- [Caparino *et al.*, 2012; Germer *et al.*, 2018], spray- [Cano-Chauca *et al.*, 2005; Caparino *et al.*, 2012; Zotarelli *et al.*, 2017], spout fluidized bed- [da Cunha *et al.*, 2006], vacuum- [Jaya *et al.*, 2006], hot air- [Yao *et al.*, 2020], infrared- [Yao *et al.*, 2020], foam mat- [Chaux-Gutiérrez *et al.*, 2017], and RW drying [Caparino *et al.,* 2012, 2017; Zotarelli *et al.*, 2015, 2017]. Most of these studies were focused on drying kinetics and physicochemical analysis. A few publications reported about the effect of drying on the quality of dried mango, including the determination of ascorbic acid and β-carotene contents without the analysis of total phenolic content (TPC) and antioxidant activity. Caparino *et al*. [2017] studied mango powder obtained using RW drying, but the results they achieved showed the physical and chemical stability of mango powder during storage [Caparino *et al.*, 2017]. Mango powder obtained using RW drying had a better physical quality than that produced using drum-drying and spray-drying [Caparino *et al.*, 2012; Zotarelli *et al.*, 2017].

In the literature, the RW drying was conducted for mango pulp [Caparino *et al.*, 2012] and low-fat avocado paste [Da Silva & Da Silva, 2018]. However, there is still a limited number of studies on drying kinetics of RW drying of avocado and mango. Only the change of physicochemical properties under the effects of drying conditions was reported. In the field of the drying process, studies on drying kinetics and the change of quality upon drying are always essential to evaluate the drying process and choose its suitable conditions [Onwude *et al.*, 2016]. The application of innovative drying, such as the RW drying, was expected to produce high-quality dried avocado and mango.

Therefore, this study aimed to investigate the drying kinetics and the changes of TPC, antioxidant activity and color parameters of avocado and mango pulp exposed to RW drying at different drying temperatures. The experimental data was used to determine the drying behavior, the effective diffusivity coefficients, activation energy and quality of dried products. These results would support the identification of suitable conditions of avocado and mango pulp drying.

MATERIALS AND METHODS

Material preparation

Fresh avocado (*Persea americana*) and mango (*Mangifera indica*) were received from a local farm in DakLak and Ben Tre, Vietnam. The fully-ripe avocado and mango without the physical damages were chosen. Then, materials were washed, peeled, and sliced using a fruit knife (Royal VKB, China). Slices were pretreated with steam for 3 min to inactivate enzymes responsible for the browning phenomena, such as polyphenol oxidase and peroxidase. After steaming, slices were cooled promptly in cold water at 5.0±0.5°C. Fruit pulp was then produced using a Berjaya commercial blender (BJY-CB2L60-A, Kuala Lumpur, Malaysia) and passed through 16-mesh sieves to remove large particles and fibers. Before drying, 9% (*w/w*) maltodextrin was added to pulps to act as a coating material, creating a physical barrier to oxygen and light to protect against chemical and enzymatic degradation [Wang *et al.*, 2009]. Our previous study demonstrated that the addition of maltodextrin (9%, *w/w*) improved the quality of dried products and facilitated the grinding to produce fruit powder (data not shown).

Refractance window drying apparatus

A custom-built refractance window drying equipment was set up with a similar principle in previous researches [Parisotto *et al.*, 2020; Rajoriya *et al.*, 2019] with some modifications. The drying apparatus was operated in batch laboratory-scale configuration and consisted of a hot water reservoir (0.42 m×0.28 m×0.10 m) and a thermostatic water bath (DH.WB000106, Daihan-Scientific, Wonju-si, South Korea). A polyester film (Mylar™, Jiangsu, China) with a 0.25-mm thickness was used to conduct heat from hot water to fruit pulp spread into 2-mm-thick layers on the films.

Experimental design and refractance window drying operation

In this study, the experiments were conducted with two factors, including the pulp types (avocado pulp – AP and mango pulp – MP) and 4-level drying temperature (from 80 to 95°C at an interval of 5°C) with three replications.

Each pulp sample was dried using the RW drying system and moisture content was analyzed at 5-min intervals. The drying process was stopped when the moisture content reached of 0.04 g/g on the dry basis (d.b.). The moisture

content was determined by the moisture analyzer with infrared heating (MB23, Ohaus, Parsippany, NJ, USA). Experiment data was used to determine the mathematical model and kinetic parameters in the RW drying of AP and MP.

To determine the quality of AP and MP after drying, each pulp sample (100 g) was dried to a moisture content of 0.040±0.005 g/g d.b., and dried products were collected. Then, these products were ground to powder for future determination of TPC, antioxidant activity, and color parameters.

Mathematical models for thin-layer drying curves

The moisture ratio (MR) was determined using the following equation [Pala *et al*., 1996]:

$$MR = \frac{M_t}{M_0} \quad (1)$$

where: M_t is moisture content at t drying time (g water/g d.b.) and M_0 is the initial moisture content (g water/g d.b.).

Of the many mathematical models suggested to determine the drying characteristics of food products [Onwude *et al.*, 2016], this study fitted drying curves to the eight semi-theoretical and empirical models including Newton, Page, Modified Page (II), Modified Page (IV), Henderson & Pabis, Logarithmic, Midilli, and Weibull models. Statistical parameters, including the determination coefficient (R^2) and the root mean square error (RMSE), were determined to identify the ability to predict the tested models:

$$R^2 = 1 - \frac{\sum_{i=1}^{N}\left(M_{exp,i} - M_{pre,i}\right)^2}{\sum_{i=1}^{N}\left(\overline{MR_{exp}} - MR_{pre,i}\right)^2} \quad (2)$$

$$RMSE = \sqrt{\frac{1}{N}\sum_{i=1}^{N}\left(M_{exp,i} - M_{pre,i}\right)^2} \quad (3)$$

where: $M_{exp,i}$ is the experimental dimensionless moisture ratio, $M_{pre,i}$ is the predicted dimensionless moisture ratio, $\overline{MR_{exp}}$ is the mean value of the experimental dimensionless moisture ratio, and N is the number of observations.

Determination of the effective diffusivity

Fick's second law of diffusion was chosen to determine moisture movement within the mango and avocado pulp, considered an infinite flat plate. The diffusion equation is as follows:

$$\frac{\partial M}{\partial t} = D_{eff}\nabla^2 M \quad (4)$$

where: M is the moisture content (g water/g d.b.), D_{eff} is the effective moisture diffusivity (m^2/s), and t is the time (s).

Crank [1975] gave a general analytical solution for thin-layer drying case with some assumptions such as the product with homogeneous, isotropic sizes, and constant characteristics; negligible shrinkage, negligible external resistance to heat and mass transfer; evaporation only at product surface; uniform initial moisture distribution; constant of the moisture diffusivity. The solution was given as:

$$MR = \frac{8}{\pi^2}\sum_{n=0}^{\infty}\frac{1}{(2n+1)^2}\exp\left(-(2n+1)^2\pi^2\frac{D_{eff}}{L^2}t\right) \quad (5)$$

where: MR is the dimensionless moisture ratio, L is the layer thickness (m), n is the term in series expansion, and t is time (s).

For long drying times, the first term in the above series expansion (n=0) was considered as an approximate solution:

$$MR = \frac{8}{\pi^2}\exp\left(-\pi^2\frac{D_{eff}}{L^2}t\right) \quad (6)$$

The effective diffusivity (D_{eff}) was found on the basis of Eq. 6 by the non-linear least square method using the Levenberg-Marquardt algorithm [Marquardt, 1963].

Determination of activation energy

The activation energy (E_a) of moisture removal was estimated from an Arrhenius equation, and it was given as:

$$D_{eff} = D_0\exp\left(-\frac{E_a}{RT}\right) \quad (7)$$

where: E_a is the activation energy (kJ/mol), R is the ideal gas constant (8.3143 kJ/mol), T is the absolute temperature (K), and D_0 is the pre-exponential factor (m^2/s).

Preparation of extracts

The preparation of extracts from avocado and mango pulps was performed according to Wang *et al.* [2010] and Bloor [2001] procedures, respectively, with some modifications. The AP (0.2 g) was mixed with 10 mL of the solvent (7 mL acetone + 0.03 mL glacial acetic acid + 2.97 mL water), and the MP (0.5 g) was mixed with 10 mL of the solvent (6 mL methanol + 4 mL water). The suspensions were vortexed for 30 s at 2,000 rpm using the VELP ZX4 advanced IR vortex mixer (VELP Scientifica, Milan, Italy). Then, after sonication (40 KHz, 240 W, 5 min) in the Pro 100 ultrasonic cleaner (Asonic, Ljubljana, Slovenia), the samples were again vortexed for 10 s and cooled for 20 min at 10°C. The cooled samples were then sonicated for a second time at the previous conditions and centrifuged in the PLC-05 centrifuge (Gemmy Industrial Corp., Taipei, Taiwan) at 1,220×*g* for 10 min. The supernatant was collected and diluted to 25 mL to analyze TPC and DPPH radical scavenging activity.

Determination of total phenolic content

The total phenolic content of the extract was determined according to ISO 14502-1:2005 [2005] method. Briefly, 0.6 mL of the extract was mixed with 1.5 mL of the Folin-Ciocalteu reagent (10-fold dilution) and allowed to stand for

5 min at room temperature. Then, 1.2 mL of 7.5% Na_2CO_3 solution was added, and the mixture was incubated for 1 h in the dark. Finally, the absorbance of the mixture was measured at 765 nm using the UV-9000 spectrometer (Metash, Shanghai, China). TPC was determined through the gallic acid standard curve and expressed as mg gallic acid equivalent per g of pulp on the dried basis (mg GAE/g d.b.). For the dried powders, the retention percentage of TPC was calculated on the basis of the ratio of TPC of powdered pulp to TPC of pulp before drying.

Determination of antioxidant activity

The 2,2-diphenyl-1-picrylhydrazyl (DPPH) radical scavenging activity of the extract was determined according to Brand-Williams *et al.* [1995] with minor changes. To prepare the radical stock solution, 24 mg of solid DPPH• were dissolved in 100 mL of methanol and stored at 4°C in the dark for 24 h. The DPPH• working solution was prepared by diluting the DPPH• stock solution to the absorbance of 1.1 units at 515 nm using methanol. Then, 150 mL of the extract was reacted with 2850 mL of DPPH• working solution for 30 min under dark conditions. Finally, the absorbance of the mixture was measured at 515 nm over methanol blank. In parallel, the standard curve for Trolox was prepared and DPPH radical scavenging activity was expressed as mg Trolox equivalent per g of pulp on the dried basis (mg TE/g d.b.). For the dried powders, the retention percentage of antioxidant activity was calculated on the basis of the ratio of DPPH• scavenging activity of powdered pulp to DPPH• scavenging activity of pulp before drying.

Determination of color attributes

The values of L^*, a^*, and b^* color parameters were measured with the NR110 precision colorimeter (Shenzhen 3nh Technology Co., Guangdong, China) using the Hunter CIELAB color system. L^* indicates lightness, with a scale ranging from 0 (black) to 100 (white). Positives and negatives in a^* represent red and green, whereas positives and negatives in b^* represent yellow and blue, respectively.

Statistical analysis

All experiments were conducted in triplicate. The mean and standard deviation were calculated in WPS Spreadsheets software (Microsoft Inc., Redmond, WA, USA). The coefficients of mathematical models were found by the non-linear least square method based on the Levenberg-Marquardt algorithm. One-way analysis of variance (ANOVA) was used to determine the differences between samples, and Tukey's multiple range test was applied to determine significant differences between mean values at the significance level of 5%. Pearson correlation was also calculated to determine the coefficients between TPC, antioxidant activity and color parameters of avocado and mango powders.

RESULTS AND DISCUSSION

Quality of avocado and mango pulp

Before performing the drying experiments, the materials were standardized and analyzed for the physicochemical properties. Table 1 shows the chemical composition of fresh avocado and mango pulp. The moisture content in avocado pulp (82.4±0.5 g/100 g) and mango pulp (90.03±0.68 g/100 g) were significantly different from these shown in previous studies for avocado [Kassim *et al*., 2013; Lye *et al.*, 2020] and mango [Jaya & Das, 2003; Pu & Sun, 2017]. Differences in variety, culture, soil properties, ripeness stage, harvest time, and post-harvest handling could all contribute to this variation. Table 1 shows that the mango pulp had a higher content of total phenolics and antioxidant activity than avocado pulp.

TABLE 1. The physicochemical properties of avocado and mango pulp.

Properties		Avocado pulp	Mango pulp
Moisture (g/100 g fresh pulp)		82.4±0.5	90.03±0.68
Total phenolic content (mg GAE/g d.b.)		5.33±0.06	23.18±0.45
Antioxidant activity (mg TE/g d.b.)		1.60±0.05	6.31±0.66
Color parameters	L^*	61.05±1.02	66.63±0.52
	a^*	-23.77±1.17	3.41±0.94
	b^*	55.05±1.09	62.51±0.80

GAE – gallic acid equivalents; TE – Trolox equivalents; d.b. – dry basis.

Drying curves and drying rate

The changes of moisture content during RW drying of AP and MP at different drying temperatures are shown in Figure 1 and Figure 2, respectively. The results revealed that the higher the RW temperature was, the shorter was the drying time. Specifically, when the temperature increased from 80 to 95°C, it would consume from 70 to 40 min for AP and from 85 to 45 min for MP to remove moisture from the initial moisture content to 0.040 g/g d.b., respectively. Figure 1b and Figure 2b present the drying rate *versus* moisture content during RW drying of AP and MP at different temperatures. The results showed that the higher the RW drying temperature was, the higher was the drying rate. It was clear that the higher RW drying temperature could increase the absorbed heat energy transferred from hot water to materials [Raghavi *et al*., 2018]. Then, the more considerable heat rising in the material was, the faster was internal and external moisture diffusion. Therefore, the higher RW drying temperature would increase the drying rate and significantly reduce drying time.

For RW drying of AP, it was observed that the drying process only happened in the falling-rate period with the undetectable constant-rate period (Figure 1b). Meanwhile, there are two periods, including (i) the pre-heating period in the first 5 min of the drying process, and (ii) the falling-rate period for RW drying of MP (Figure 2b). Therefore, the RW drying of AP and MP mainly occurred in the falling-rate period. This phenomenon is because the conditions required for constant rate drying are seldom met [Berk, 2018], leading to all of the practical dryings of biological products taking place in the falling-rate period [Madamba *et al*., 1996]. Also, most of the studies on drying have supported this conclusion [Onwude *et al*., 2016]. Besides, the evaporation process happened rapidly in drying, causing the drying to occur only in the falling-rate period. In this study, the material grinding could release free

water from the vacuole and the xylem, so it was easy to evaporate when the pulp was spread into thin layers and quickly heated. That caused the moisture removal in RW drying of AP and MP to happen very fast. Similar observations were reported in the literature for RW drying of tomato [Abul-Fadl & Ghanem, 2011], murta berry leather [Gómez-Pérez *et al.*, 2020], and mango slices [Ochoa-Martínez *et al.*, 2012].

The drying rates were found to be positively correlated with moisture content. At the beginning of the drying process, it was observed that all samples had a higher drying rate (Figure 1 and Figure 2). Continuing the drying process, the drying rate decreased during moisture removal. Initially, the moisture content in the material was high; the heat energy from hot water transferred to materials would force water evaporation faster. Subsequently, the driving force of moisture removal was reduced. Because of the rubbery-glassy phase transition of the material, the critical phenomenon during drying would change the material from soft and rubbery to hard and glassy [Gulati & Datta, 2015]. Plus, when most of the free water escaped, heat energy was mainly responsible for breaking the water bonding, then diffusing moisture to evaporate. Therefore, the smaller moisture content was, the slower was the drying rate in the RW drying of AP and MP.

Mathematical model for RW drying of AP and MP

Changes in moisture ratio during RW drying of AP and MP were used to evaluate the fitting of mathematical models, and then to figure out the best model describing the behavior of RW drying of AP and MP. The selection was based on statistical parameters, including the coefficient of determination (R^2) and root-mean-square error (RMSE) (Table 2).

The thin-layer model, which has the highest R^2 value and smallest RMSE, was the best in this study. The average R^2 and RMSE were calculated to be convenient to compare the predicted power of mathematical models. The results showed that the higher the R^2 value was, the smaller was the RMSE. Among eight investigated models, the order of decreasing the average value of R^2 was as follows: (i) for RW drying of AP: Weibull > Midilli > Logarithmic > Modified Page (IV), Modified Page (II) and Page > Henderson & Pabis > Newton, and (ii) for RW drying of MP: Weibull > Midilli > Modified Page (IV) > Modified Page (II) and Page > Logarithmic > Henderson & Pabis > Newton.

The Newton model is the simplest model for determining the behavior of the drying process and the Henderson & Pabis model was developed from the first term in the numerical solution of Fick's second law of diffusion equation [Onwude

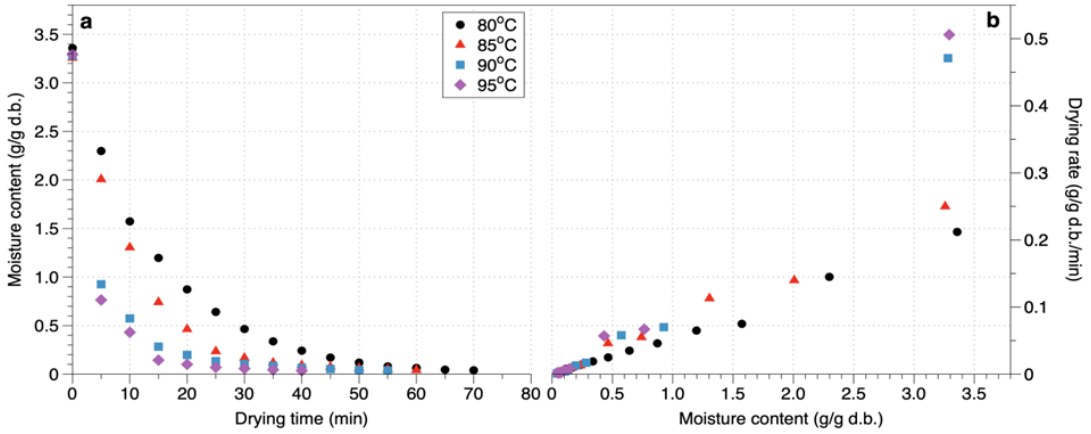

FIGURE 1. The changes of moisture content (a) and the drying rate curves (b) in refractance window drying of avocado pulp at different temperatures.

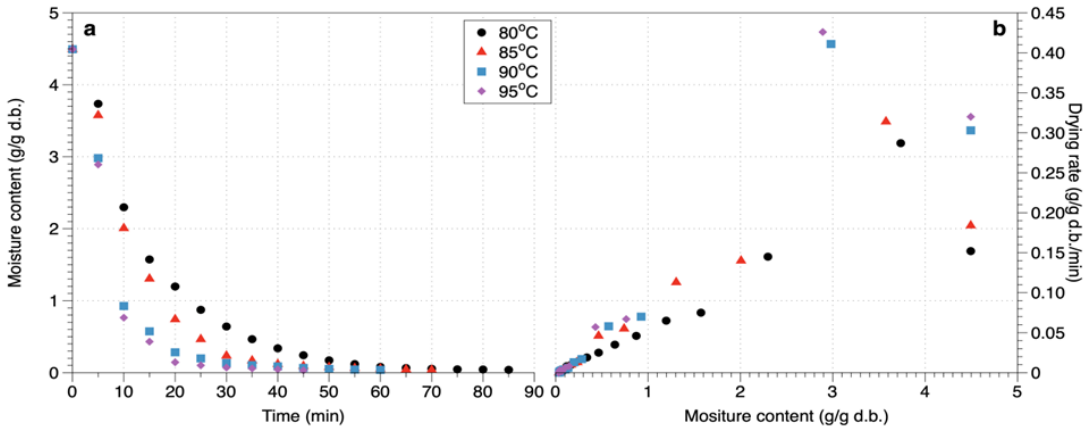

FIGURE 2. The changes of moisture content (a) and the drying rate curves (b) in refractance window drying of mango pulp at different temperatures.

TABLE 2. Equation parameters of drying models and statistical parameters of non-linear regression analysis for refractance window drying of avocado pulp and mango pulp at different temperatures.

Model and equation	Temperature (°C)	Avocado pulp			Mango pulp		
		Equation parameters	R^2	RMSE	Equation parameters	R^2	RMSE
Newton model MR = exp(–kt)	80	k=0.0639	0.9952	0.02147	k=0.0643	0.9915	0.02720
	85	k=0.0962	0.9988	0.01025	k=0.0839	0.9962	0.01840
	90	k=0.1525	0.9966	0.01725	k=0.1345	0.9934	0.02390
	95	k=0.2196	0.9976	0.01576	k=0.1568	0.9966	0.01879
		Average	**0.9971**	**0.01618**	**Average**	**0.9944**	**0.02207**
Page MR = exp(–kt^n)	80	k=0.0451; n=1.119	0.9978	0.01516	k=0.0469; n=1.108	0.9935	0.02459
	85	k=0.0926; n=1.015	0.9989	0.01055	k=0.0557; n=1.153	0.9994	0.00793
	90	k=0.1516; n=1.003	0.9966	0.01809	k=0.1007; n=1.132	0.9946	0.02263
	95	k=0.2798; n=0.872	0.9982	0.01459	k=0.1158; n=1.145	0.9979	0.01566
		Average	**0.9979**	**0.01460**	**Average**	**0.9964**	**0.01770**
Modified Page (II) MR = exp(–(kt)^n)	80	k=0.0627; n=1.119	0.9978	0.01516	k=0.0614; n=1.108	0.9935	0.02459
	85	k=0.0959; n=1.015	0.9989	0.01055	k=0.0816; n=1.153	0.9994	0.00793
	90	k=0.1524; n=1.003	0.9966	0.01809	k=0.1316; n=1.132	0.9946	0.02263
	95	k=0.2321; n=0.872	0.9982	0.01459	k=0.1521; n=1.145	0.9979	0.01566
		Average	**0.9979**	**0.01460**	**Average**	**0.9964**	**0.01770**
Modified Page (IV) MR = a exp(–kt^n)	80	a=1.0100; k=0.0472; n=1.107	0.9978	0.01516	a=1.021; k=0.0513; n=1.085	0.9938	0.02474
	85	a=0.9997; k=0.0925; n=1.015	0.9989	0.01055	a=1.002; k=0.0561; n=1.150	0.9994	0.00824
	90	a=1.0020; k=0.1525; n=1.001	0.9966	0.01809	a=1.004; k=0.1021; n=1.128	0.9946	0.02369
	95	a=1.0010; k=0.2801; n=0.872	0.9982	0.01459	a=1.002; k=0.1163; n=1.143	0.9979	0.01673
		Average	**0.9979**	**0.01460**	**Average**	**0.9964**	**0.01835**
Henderson & Pabis MR = a exp(–kt)	80	a=1.0310; k=0.0658	0.9962	0.01985	a=1.037; k=0.0665	0.9928	0.02588
	85	a=1.0020; k=0.0964	0.9988	0.01069	a=1.024; k=0.0857	0.9968	0.01760
	90	a=1.0020; k=0.1528	0.9966	0.01808	a=1.012; k=0.1359	0.9935	0.02469
	95	a=0.9985; k=0.2194	0.9977	0.01683	a=1.008; k=0.1578	0.9967	0.01972
		Average	**0.9973**	**0.01636**	**Average**	**0.9950**	**0.02197**
Logarithmic MR = a exp(–kt) + c	80	a=1.0350; k=0.0646; c=-0.0062	0.9963	0.02037	a=1.037; k=0.0668; c=0.0016	0.9928	0.02671
	85	a=0.9976; k=0.0984; c=-0.0063	0.9990	0.01030	a=1.027; k=0.0845; c=-0.0046	0.9969	0.01804
	90	a=0.9894; k=0.1610; c=-0.0162	0.9984	0.01295	a=1.004; k=0.1401; c=-0.0099	0.9942	0.02454
	95	a=0.9830; k=0.2327; c=-0.0175	0.9995	0.00841	a=1.006; k=0.1592; c=-0.0029	0.9967	0.02095
		Average	**0.9983**	**0.01301**	**Average**	**0.9952**	**0.02256**
Midilli MR = a exp(–kt) + bt	80	a=1.0070; k=0.0430; n=1.146; b=-2.1E-04	0.9983	0.01446	a=1.019; k=0.0473; n=1.118; b=1.7E-04	0.9943	0.02445
	85	a=0.9981; k=0.0861; n=1.049; b=-2.2E-04	0.9994	0.00885	a=1.000; k=0.0529; n=1.177; b=1.7E-04	0.9980	0.00512
	90	a=1.0010; k=0.1343; n=1.071; b=-4.3E-04	0.9986	0.01289	a=1.004; k=0.0926; n=1.181; b=3.5E-04	0.9963	0.02077
	95	a=1.0000; k=0.2423; n=0.958; b=-4.8E-04	0.9992	0.01139	a=1.001; k=0.1080; n=1.184; b=3.3E-04	0.9986	0.01475
		Average	**0.9989**	**0.01190**	**Average**	**0.9968**	**0.01627**
Weibull MR = α – b exp(–kt^n)	80	a=0.0162; b=-0.9903; k=0.0417; n=1.164	0.9984	0.01391	a=0.0151; b=-1.0030; k=0.0455; n=1.14	0.9946	0.02392
	85	a=0.0117; b=-0.9862; k=0.0854; n=1.059	0.9993	0.00909	a=0.0992; b=-0.9898; k=0.0521; n=1.189	0.9998	0.00501
	90	a=0.0218; b=-0.9789; k=0.1227; n=1.137	0.9992	0.00950	a=0.0201; b=-0.9826; k=0.0836; n=1.249	0.9971	0.01836
	95	a=0.0186; b=-0.9816; k=0.2212; n=1.029	0.9995	0.00906	a=0.0141; b=-0.9869; k=0.1032; n=1.222	0.9988	0.01358
		Average	**0.9991**	**0.01039**	**Average**	**0.9976**	**0.01522**

R^2 – determination coefficient; RMSE – root mean square error; MR – moisture ratio; k – drying constant, n, a, b, c, α – empirical parameters.

et al., 2016]. Both the Newton and Henderson & Pabis models had the lowest power of prediction in the change of moisture ratio during RW drying of AP and MP (Table 2). From Newton and Henderson & Pabis model, the Logarithmic, Page, Modified Page (II), Modified Page (IV) were developed by either addition of the constant "c" or a dimensionless empirical constant "n". The experimental data from this study showed the ability in prediction was higher in developed models (higher R^2 and lower RMSE values) (Table 2). Midilli and Weibull models were inserted both a dimensionless empirical constant "n" or linear term "bt" and the constant "a", respectively. That was the reason why Midilli and Weibull models had the highest power of prediction.

In the literature review, Onwude *et al*. [2016] pointed to many studies in which it was concluded that the Midilli model was the most suitable in determining the thin-layer drying characteristics of fruits and vegetables. However, these studies were carried out without analyzing the Weibull model. Only a few publications conducted evaluations of both the Midilli and Weibull models. They confirmed that both of them were suitable to represent the behavior of the thin-layer drying of persimmon slices [Doymaz, 2012] and lemongrass [Nguyen *et al*., 2019]. However, in our study, the Weibull model was the best fit model among the investigated models with the highest value of R^2 and lowest RMSE values. Some previous studies showed that the Weibull model could characterize the drying behavior of mango slices [Corzo *et al*., 2010], pepino fruit [Uribe *et al*., 2011], quince slices [Tzempelikos *et al.*, 2015] and yam slices [Ju *et al.*, 2018].

Effective diffusivity and activation energy

During the drying process, the mechanism of moisture transport is not known precisely. Therefore, numerous studies used effective diffusivity as a valid value to determine the ability of moisture removal from different materials using different drying methods. In this study, the effective diffusivity (with R^2 values) for RW drying of AP and MP was found and presented in Table 3, which also shows the activation energy for moisture removal (with R^2 values) for AP and MP in RW drying.

The result revealed that when the RW drying temperature was increased from 80 to 95°C, D_{eff} would increase from 4.25×10^{-10} m^2/s to 7.24×10^{-10} m^2/s for AP, and from 4.50×10^{-10} m^2/s to 10.67×10^{-10} m^2/s for MP. The range of these D_{eff} values was from 10^{-11} to 10^{-8} m^2/s when dealing with thin-layer food drying [Onwude *et al*., 2016]. It seems that the increase in D_{eff} with the temperature was mainly due to a higher hot water temperature in which a more significant amount of thermal energy was transferred into materials leading to faster movement of the water molecules from inside to the surface to evaporate. Some studies in RW drying showed similar results [Rajoriya *et al.*, 2019, 2021]. In the literature, the D_{eff} values in drying of AP are still limited. For mango, Corzo *et al.* [2008] obtained values of D_{eff} changing from 1.74×10^{-10} to 3.15×10^{-10} m^2/s and from 2.30×10^{-10} to 3.28×10^{-10} m^2/s for green and half-ripe mango, respectively, when the air-drying temperature varied from 50 to 80°C [Corzo *et al*., 2008].

The activation energy for AP and MP moisture evaporation was 32.06 and 66.03 kJ/mol in RW drying, respectively.

TABLE 3. The effective diffusivity (D_{eff}) and the activation energy (E_a) in refractance window drying of avocado pulp and mango pulp

Material	Temperature (°C)	D_{eff} (m^2/s)	R^2	E_a (kJ/mol)	R^2
Avocado pulp	80	4.45×10^{-10}	0.9978	32.06	0.8363
	85	5.02×10^{-10}	0.9610		
	90	5.15×10^{-10}	0.9083		
	95	7.24×10^{-10}	0.9138		
Mango pulp	80	4.50×10^{-10}	0.9928	66.03	0.9678
	85	5.79×10^{-10}	0.9968		
	90	9.19×10^{-10}	0.9935		
	95	10.67×10^{-10}	0.9967		

R^2 – coefficient of determination.

In the literature review of Onwude *et al.* [2016], most publications found E_a values for thin-layer drying of fruits and vegetables ranging from 14.42 to 43.26 kJ/mol; however, few reports obtained E_a values varying from 78.93 to 130.61 kJ/mol. The results clearly showed that MP required more energy for removing moisture than AP. It showed that the drying material's composition, type, and characteristics would directly affect the activation energy values.

Changes of polyphenol content, antioxidant activity and color in RW drying of AP and MP

Figure 3 shows the percentage retention of TPC and antioxidant activity in dried AP and MP at different RW drying conditions. For AP, the retention of TPC decreased when the drying temperature was increased from 80 to 85°C ($p<0.05$) but the TPC tended to reach highest retention at the drying temperature of 90°C (85.4%). For MP, when drying temperature varied from 80 to 95°C, the TPC retention increased gradually to get highest values at 90°C (85.6%) ($p<0.05$) and then insignificantly dropped at 95°C ($p\geq0.05$). The changes of antioxidant activity were similar to the trend of TPC retention (Figure 3).

Figure 3 also indicated that, generally, the loss of TPC and antioxidant activity occurred in the drying process. During drying, the degradation of TPC was mainly due to the action of enzymes, such as polyphenol oxidases (PPOs) and peroxidase (POD) [McSweeney & Seetharaman, 2015]. The activities of PPOs and POD were previously reported in avocado and mango [Korbel *et al*., 2013]. The PPOs in avocado pulp were more heat-resistant than those in other fruits and vegetables [Zhou *et al.*, 2016]. However, under heat inactivation at 84°C for 15 min, only around 0.2% of the relative activity of PPOs was maintained in avocado flesh [Gómez-López, 2002]. Vanini *et al*. [2010] found that fruit maturation, as well as changes in temperature and time, can reduce POD activity. For mango fruit, PPO and POD were most active at temperatures of 50–60°C [Korbel *et al*., 2013] and could be inactivated at high temperatures of 70–90°C [Queiroz *et al.*, 2008]. Thus, the PPO and POD could have a significant impact on the degradation of phenolics in avocado and mango. In this study, the results indicated that high temperature (90–95°C)

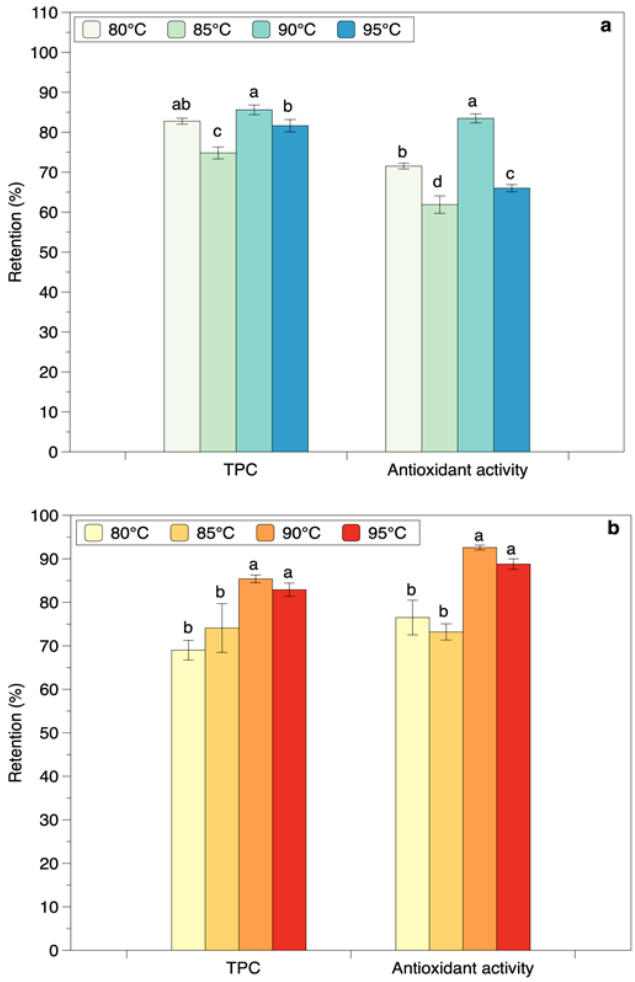

FIGURE 3. The total phenolic content (TPC) and antioxidant activity of powders of avocado pulp (a) and mango pulp (b) obtained by refractance window drying at different temperatures. The same letters above bars within a group indicated that the values are not significantly different ($p \geq 0.05$).

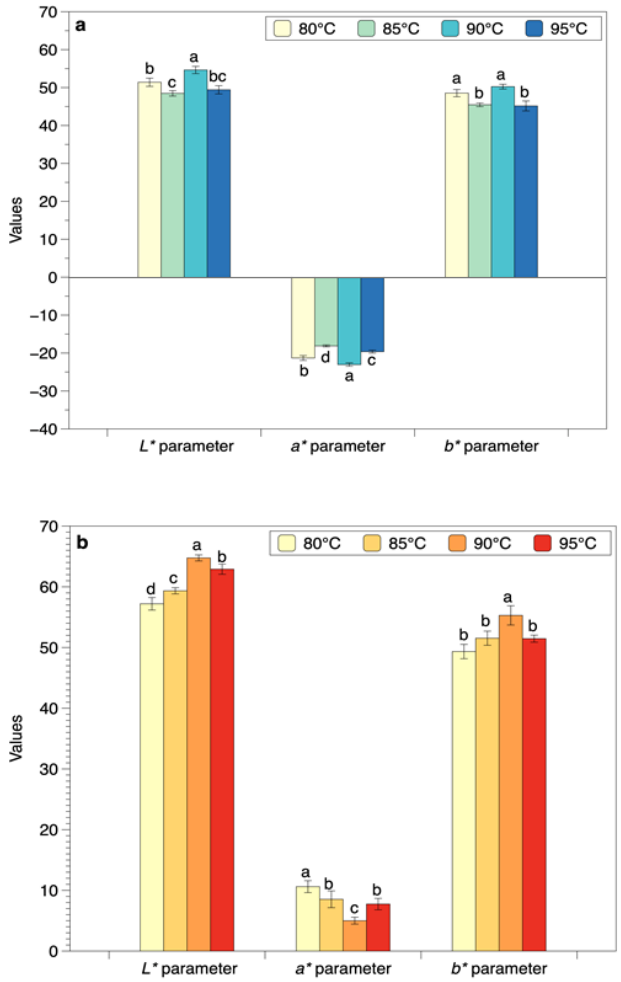

FIGURE 4. The color parameters of powders avocado pulp (a) and mango pulp (b) obtained by refractance window drying at different temperatures. The same letters above bars within a group indicated that the values are not significantly different ($p \geq 0.05$).

represented the good control of enzyme activity leading to the highest retention of TPC. Besides, drying at lower temperatures (80–85°C) consumed more time to complete operation, which could increase the levels of phenolic degradation. In the drying process, the change of moisture content also contributed to the enzyme activity because of the positive correlation between moisture content and water activity [Chen, 2019]. Therefore, in the initial drying process, the high amount of water could accelerate enzymatic reactions, thereby enhacing degradation of phenolics. The higher temperature resulted in higher rate of reactions, causing more loss at drying temperature of 95°C than 90°C. As a consequence, the drying of AP and MP by the RW technique at 90°C allowed retaining the highest TPC.

Phenolics and phytopigments, such as carotenoids, could act as antioxidants [Huyut *et al.,* 2017; Lanfer-Marquez *et al.*, 2005] based on their structure ideal for acting as free radical scavengers, reducing agents or inhibitors of the formation of free radicals under the catalysis of transition metals. As expected, in this study, the correlations between the antioxidant activity and TPC were very strong, with correlation coefficients of 0.825 and 0.881 for avocado and mango powders, respectively, obtained by RW drying at different temperatures (Table 4 and Table 5). The correlation between TPC and antioxidant activity measured as DPPH$^{\bullet}$ scavenging activity was also found for dried Thai red curry powder [Inchuen *et al.*, 2010] and dried fruits, such as apples, mulberries, apricots, and black mulberries [Bushra Sultana, 2012]. It was noted that beyond TPC, other antioxidants found in avocado and mango also contributed to the antioxidant activity, such as vitamins, natural pigments, *etc*. [Lye *et al.*, 2020; Schieber *et al.*, 2000]. However, the high correlation coefficients between TPC and antioxidant activity (more than 0.8) indicated that the phenolics played an important role in the total antioxidant activity.

Figure 4 shows values of the color parameters L^*, a^* and b^* of AP and MP dried using RW at different temperatures. Compared to pulp before drying, the L^* and b^* values of the color of the powders were lower and a^* values was higher. It is implied that, in this study, the color of the dried samples became darker (decrease in L^* value), less green (increase in a^* value), and more yellow (increase of b^* value). Besides, the color parameters (L^* and a^*) had strong correlations with TPC (Table 4 and Table 5).

TABLE 4. Coefficients of Pearson correlation between total phenolic content (TPC), antioxidant activity, and color parameters (L^*, a^*, and b^*) of avocado powders obtained by refractance window drying at different temperatures.

	TPC	Antioxidant activity	L^*	a^*
Antioxidant activity	**0.825** (0.001)	1		
L^*	**0.815** (0.001)	**0.926** (0.000)	1	
a^*	**-0.893** (0.000)	**-0.957** (0.000)	**-0.889** (0.000)	1
b^*	**0.760** (0.004)	**0.879** (0.000)	**0.937** (0.000)	**-0.867** (0.000)

The p values are shown in parentheses. Correlations are considered statistically significant at $p<0.05$ (in bold).

TABLE 5. Coefficients of Pearson correlation between total phenolic content (TPC), antioxidant activity, and color parameters (L^*, a^*, and b^*) of mango powders obtained by refractance window drying at different temperatures.

	TPC	Antioxidant activity	L^*	a^*
Antioxidant activity	**0.881** (0.000)	1		
L^*	**0.905** (0.000)	**0.888** (0.000)	1	
a^*	**-0.748** (0.005)	**-0.672** (0.017)	**-0.883** (0.000)	1
b^*	0.514 (0.087)	0.529 (0.077)	**0.705** (0.010)	**-0.805** (0.002)

The p values are shown in parentheses. Correlations are considered statistically significant at $p<0.05$ (in bold).

During thermal processing, the discoloration of the product happened, related to pigment destruction and oxidation, enzymatic and non-enzymatic browning, and phenolic polymerization [Bahloul *et al.*, 2009]. For the green-pigmented foods, such as avocado, the less green color was mainly due to the biotransformation of chlorophylls to pheophytins by replacing magnesium ion with hydrogen ions in the center of the porphyrin ring [Rudra *et al.*, 2008]. For foods with the high sugar content, like mango, the browning phenomena were associated with Maillard reaction and caramelization [Potter & Hotchkiss, 1995]. For fruits containing phenolics, it was reported that the browning phenomena were linked to the enzymatic breakdown of these compounds, producing brown pigments [Dorantes-Alvarez *et al.*, 1998; Hershkovitz *et al*., 2005]. That explained why the correlation was very strong between TPC and color parameters (L^* value and a^* value).

CONCLUSIONS

This study aimed to determine the RW drying behavior of AP and MP. It was found that the drying process mainly occurred in the falling-rate period. Among the investigated mathematical models, the Weibull model showed the best-predicted power of moisture ratio change during RW drying of AP and MP. The effective diffusivity and activation energy for moisture removal in RW drying of AP and MP were in previously reported ranges of thin-layer drying of food. The RW drying had significant effects on the quality of dried avocado and mango and drying at 90°C could retain the highest quality of dried products. It was observed that the RW drying had a high potential in the production of fruit powder from avocado and mango due to the ability to retain more than 80% of TPC and antioxidant activity. This study found that TPC could be used as a useful criterion for evaluating drying process in terms of dried product quality because TPC was strongly correlated with the antioxidant activity and color parameters.

ACKNOWLEDGEMENTS

The authors would like to thank Nguyen Tat Thanh University, Ho Chi Minh Univeristy of Technology (HCMUT), VNU-HCM, The Youth Development Science and Technology Center – Ho Chi Minh Communist Youth Union and Department of Science and Technology of Ho Chi Minh City for permission and for providing facilities, DAKADO Group and Ms. Dao Hai Nguyen for supplying avocado and mango fruits during the research period.

RESEARCH FUNDING

This research is funded by Nguyen Tat Thanh University, Ho Chi Minh city, Vietnam under grant 2021.01.023.

CONFLICT OF INTERESTS

The authors declare no conflict of interest.

ORCID IDs

Quoc-Duy Nguyen https://orcid.org/0000-0001-9097-4471
Thi-Van-Linh Nguyen https://orcid.org/0000-0003-1471-6352

REFERENCES

1. Abbasi, A.M., Guo, X., Fu, X., Zhou, L., Chen, Y., Zhu, Y., Yan, H., Liu, R.H. (2015). Comparative assessment of phenolic content and *in vitro* antioxidant capacity in the pulp and peel of mango cultivars. *International Journal of Molecular Sciences*, *16*(6), 13507–13527. https://doi.org/10.3390/ijms160613507
2. Abonyi, B., Feng, H., Tang, J., Edwards, C., Chew, B., Mattinson, D., Fellman, J. (2002). Quality retention in strawberry and carrot purees dried with Refractance WindowTM system. *Journal of Food Science*, *67*(3), 1051–1056. https://doi.org/10.1111/j.1365-2621.2002.tb09452.x
3. Abul-Fadl, M., Ghanem, T. (2011). Effect of refractance-window (RW) drying method on quality criteria of produced tomato powder as compared to the convection drying method. *World Applied Sciences Journal*, *15*(7), 953–965.
4. Bahloul, N., Boudhrioua, N., Kouhila, M., Kechaou, N. (2009). Effect of convective solar drying on colour, total phenols and radical scavenging activity of olive leaves (*Olea europaea* L.). *International Journal of Food Science & Technology*, *44*(12), 2561–2567. https://doi.org/10.1111/j.1365-2621.2009.02084.x

5. Berk, Z. (2018). Dehydration. Chapter 22, In Z. Berk (Ed.), *Food Process Engineering and Technology* (3rd Edition). Academic Press, pp. 513–566. https://doi.org/10.1016/B978-0-12-812018-7.00022-1
6. Bloor, S.J. (2001). Overview of methods for analysis and identification of flavonoids. *Methods in Enzymology*, *335*, 3–14. https://doi.org/10.1016/S0076-6879(01)35227-8
7. Brand-Williams, W., Cuvelier, M.-E., Berset, C. (1995). Use of a free radical method to evaluate antioxidant activity. *LWT – Food Science and Technology*, *28*(1), 25–30. https://doi.org/10.1016/S0023-6438(95)80008-5
8. Bushra Sultana (2012). Effect of drying techniques on the total phenolic contents and antioxidant activity of selected fruits. *Journal of Medicinal Plants Research*, *6*(1), 161–167. https://doi.org/10.5897/JMPR11.916
9. Cano-Chauca, M., Stringheta, P., Ramos, A., Cal-Vidal, J. (2005). Effect of the carriers on the microstructure of mango powder obtained by spray drying and its functional characterization. *Innovative Food Science & Emerging Technologies*, *6*(4), 420–428. https://doi.org/10.1016/j.ifset.2005.05.003
10. Caparino, O.A., Nindo, C., Tang, J., Sablani, S., Chew, B., Mathison, B., Fellman, J., Powers, J. (2017). Physical and chemical stability of Refractance Window®–dried mango (Philippine 'Carabao' var.) powder during storage. *Drying Technology*, *35*(1), 25–37. https://doi.org/10.1080/07373937.2016.1157601
11. Caparino, O., Tang, J., Nindo, C., Sablani, S., Powers, J., Fellman, J. (2012). Effect of drying methods on the physical properties and microstructures of mango (Philippine 'Carabao' var.) powder. *Journal of Food Engineering*, *111*(1), 135–148. https://doi.org/10.1016/j.jfoodeng.2012.01.010
12. Castañeda-Saucedo, M.C., Valdés-Miramontes, E.H., Tapia-Campos, E., Delgado-Alvarado, A., Bernardino-García, A.C., Rodríguez-Ramírez, M.R., del Pilar Ramirez-Anaya, J. (2014). Effect of freeze-drying and production process on the chemical composition and fatty acids profile of avocado pulp. *Revista Chilena de Nutrición*, *41*(4), 404–411. https://doi.org/10.4067/S0717-75182014000400009
13. Ceylan, İ., Aktaş, M., Doğan, H. (2007). Mathematical modeling of drying characteristics of tropical fruits. *Applied Thermal Engineering*, *27*(11–12), 1931–1936. https://doi.org/10.1016/j.applthermaleng.2006.12.020
14. Chaux-Gutiérrez, A.M., Santos, A.B., Granda-Restrepo, D.M., Mauro, M.A. (2017). Foam mat drying of mango: Effect of processing parameters on the drying kinetic and product quality. *Drying Technology*, *35*(5), 631–641. https://doi.org/10.1080/07373937.2016.1201486
15. Chen, C. (2019). Relationship between water activity and moisture content in floral honey. *Foods*, *8*(1), art. no. 30. https://doi.org/10.3390/foods8010030
16. Comerford, K.B., Ayoob, K.T., Murray, R.D., Atkinson, S.A. (2016). The role of avocados in complementary and transitional feeding. *Nutrients*, *8*(5), art. no. 316. https://doi.org/10.3390/nu8050316
17. Corzo, O., Bracho, N., Alvarez, C. (2008). Water effective diffusion coefficient of mango slices at different maturity stages during air drying. *Journal of Food Engineering*, *87*(4), 479–484. https://doi.org/10.1016/j.jfoodeng.2007.12.025
18. Corzo, O., Bracho, N., Alvarez, C. (2010). Weibull model for thin-layer drying of mango slices at different maturity stages. *Journal of Food Processing and Preservation*, *34*(6), 993–1008. https://doi.org/10.1111/j.1745-4549.2009.00433.x
19. Crank, J. (1975). *The Mathematics of Diffusion*. Oxford University Press.
20. da Cunha, R.L., de la Cruz, A.G., Menegalli, F.C. (2006). Effects of operating conditions on the quality of mango pulp dried in a spout fluidized bed. *Drying Technology*, *24*(4), 423–432. https://doi.org/10.1080/07373930600611869
21. Da Silva, C., Da Silva, C. (2018). Recovery of avocado paste from avocado oil milling process or guacamole processing. *U.S. Patent,* No. 9,894,908.
22. Degenhardt, A.G., Hofmann, T. (2010). Bitter-tasting and kokumi-enhancing molecules in thermally processed avocado (*Persea americana* Mill.). *Journal of Agricultural and Food Chemistry*, *58*(24), 12906–12915. https://doi.org/10.1021/jf103848p
23. Dorantes-Alvarez, L., Parada-Dorantes, L., Ortiz-Moreno, A., Santiago-Pineda, T., Chiralt-Boix, A., Barbosa-Cánovas, G. (1998). Effect of anti-browning compounds on the quality of minimally processed avocados/Efecto de inhibidores del pardeamiento en la calidad de aguacates mínimamente procesados. *Food Science and Technology International*, *4*(2), 107–113. https://doi.org/10.1177/108201329800400205
24. Doymaz, İ. (2012). Evaluation of some thin-layer drying models of persimmon slices (*Diospyros kaki* L.). *Energy Conversion and Management*, *56*, 199–205. https://doi.org/10.1016/j.enconman.2011.11.027
25. Fitzpatrick, J.J., Ahrné, L. (2005). Food powder handling and processing: Industry problems, knowledge barriers and research opportunities. *Chemical Engineering and Processing: Process Intensification*, *44*(2), 209–214. https://doi.org/10.1016/j.cep.2004.03.014
26. Germer, S.P.M., Tonin, I.P., de Aguirre, J.M., Alvim, I.D., Ferrari, C.C. (2018). Influence of process variables on the drum drying of mango pulp. *Drying Technology*, *36*(12), 1488–1500. https://doi.org/10.1080/07373937.2017.1410707
27. Gómez-López, V.M. (2002). Some biochemical properties of polyphenol oxidase from two varieties of avocado. *Food Chemistry*, *77*(2), 163–169. https://doi.org/10.1016/S0308-8146(01)00331-4
28. Gómez-Pérez, L.S., Navarrete, C., Moraga, N., Rodríguez, A., Vega-Gálvez, A. (2020). Evaluation of different hydrocolloids and drying temperatures in the drying kinetics, modeling, color, and texture profile of murta (*Ugni molinae* Turcz) berry leather. *Journal of Food Process Engineering*, *43*(2), art. no. e13316. https://doi.org/10.1111/jfpe.13316
29. Gulati, T., Datta, A.K. (2015). Mechanistic understanding of case-hardening and texture development during drying of food materials. *Journal of Food Engineering*, *166*, 119–138. https://doi.org/10.1016/j.jfoodeng.2015.05.031
30. Haytowitz, D.B., Wu, X., Bhagwat, S. (2018). USDA Database for the Flavonoid Content of Selected Foods, Release 3.3. *US Department of Agriculture, Agricultural Research Service, Nutrient Data Laboratory*.
31. Hershkovitz, V., Saguy, S.I., Pesis, E. (2005). Postharvest application of 1-MCP to improve the quality of various avocado cultivars. *Postharvest Biology and Technology*, *37*(3), 252–264. https://doi.org/10.1016/j.postharvbio.2005.05.003

32. Huyut, Z., Beydemir, Ş., Gülçin, İ. (2017). Antioxidant and antiradical properties of selected flavonoids and phenolic compounds. *Biochemistry Research International*, *2017*, art. no. 7616791. https://doi.org/10.1155/2017/7616791
33. Inchuen, S., Narkrugsa, W., Pornchaloempong, P. (2010). Effect of drying methods on chemical composition, color and antioxidant properties of thai red curry powder. *Kasetsart Journal – Natural Science, 44*, 142–151.
34. ISO 14502-1:2005 (2005). International Organization for Standardization. Determination of substances characteristic of green and black tea — Part 1: Content of total polyphenols in tea-colorimetric method using Folin-Ciocalteu reagent, p. 10.
35. Jaya, S., Das, H. (2003). A vacuum drying model for mango pulp. *Drying Technology*, *21*(7), 1215–1234. https://doi.org/10.1081/DRT-120023177
36. Jaya, S., Das, H., Mani, S. (2006). Optimization of maltodextrin and tricalcium phosphate for producing vacuum dried mango powder. *International Journal of Food Properties*, *9*(1), 13–24. https://doi.org/10.1080/10942910500217666
37. Ju, H.Y., Zhao, S.H., Mujumdar, A., Fang, X.M., Gao, Z.J., Zheng, Z.A., Xiao, H.W. (2018). Energy efficient improvements in hot air drying by controlling relative humidity based on Weibull and Bi-Di models. *Food and Bioproducts Processing*, *111*, 20–29. https://doi.org/10.1016/j.fbp.2018.06.002
38. Kassim, A., Workneh, T., Bezuidenhout, C. (2013). A review on postharvest handling of avocado fruit. *African Journal of Agricultural Research*, *8*(21), 2385–2402.
39. Korbel, E., Servent, A., Billaud, C., Brat, P. (2013). Heat inactivation of polyphenol oxidase and peroxidase as a function of water activity: A case study of mango drying. *Drying Technology*, *31*(13––14), 1675–1680. https://doi.org/10.1080/07373937.2013.808659
40. Lanfer-Marquez, U.M., Barros, R.M., Sinnecker, P. (2005). Antioxidant activity of chlorophylls and their derivatives. *Food Research International*, *38*(8–9), 885–891. https://doi.org/10.1016/j.foodres.2005.02.012
41. Lye, H.S., Ong, M.K., Teh, L.K., Chang, C.C., Wei, L.K. (2020). Avocado. Chapter 4, In C.M. Galanakis (Ed.), *Valorization of Fruit Processing By-Products*. Academic Press, pp. 67–93. https://doi.org/10.1016/B978-0-12-817106-6.00004-6
42. Madamba, P.S., Driscoll, R.H., Buckle, K.A. (1996). The thin-layer drying characteristics of garlic slices. *Journal of Food Engineering*, *29*(1), 75–97. https://doi.org/10.1016/0260-8774(95)00062-3
43. Marquardt, D.W. (1963). An algorithm for least-squares estimation of nonlinear parameters. *Journal of the Society for Industrial and Applied Mathematics*, *11*(2), 431–441. https://doi.org/10.1137/0111030
44. McSweeney, M., Seetharaman, K. (2015). State of polyphenols in the drying process of fruits and vegetables. *Critical Reviews in Food Science and Nutrition*, *55*(5), 660–669. https://doi.org/10.1080/10408398.2012.670673
45. Nguyen, T.V., Nguyen, M.D., Nguyen, D.C., Bach, L.G., Lam, T.D. (2019). Model for thin layer drying of lemongrass (*Cymbopogon citratus*) by hot air. *Processes*, *7*(1), art. no. 21. https://doi.org/10.3390/pr7010021
46. Nindo, C.I., Tang, J. (2007). Refractance window dehydration technology: A novel contact drying method. *Drying Technology*, *25*(1), 37–48. https://doi.org/10.1080/07373930601152673
47. Occena-Po, L.G. (2006). Banana, mango, and passion fruit. Chapter 33, In Y.H. Hui (Ed.), *Handbook of Fruits and Fruit Processing*. Wiley Online Library, p. 635. https://doi.org/10.1002/9780470277737.ch33
48. Ochoa-Martínez, C., Quintero, P., Ayala, A., Ortiz, M. (2012). Drying characteristics of mango slices using the Refractance Window™ technique. *Journal of Food Engineering*, *109*(1), 69–75. https://doi.org/10.1016/j.jfoodeng.2011.09.032
49. Onwude, D.I., Hashim, N., Janius, R.B., Nawi, N.M., Abdan, K. (2016). Modeling the thin-layer drying of fruits and vegetables: A review. *Comprehensive Reviews in Food Science and Food Safety*, *15*(3), 599–618. https://doi.org/10.1111/1541-4337.12196
50. Pala, M., Mahmutoğlu, T., Saygi, B. (1996). Effects of pretreatments on the quality of open-air and solar dried apricots. *Food/Nahrung*, *40*(3), 137–141. https://doi.org/10.1002/food.19960400308
51. Parisotto, E.I.B., Teleken, J.T., Laurindo, J.B., Carciofi, B.A.M. (2020). Mathematical modeling and experimental assessment of the cast-tape drying. *Drying Technology*, *38*(8), 1024–1035. https://doi.org/10.1080/07373937.2019.1610768
52. Potter, N.N., Hotchkiss, J.H. (1995). *Food Science. 5 Edition*. Springer Science+ Business Media, LLC New York. https://doi.org/10.1007/978-1-4615-4985-7
53. Pu, Y.Y., Sun, D.W. (2017). Combined hot-air and microwave-vacuum drying for improving drying uniformity of mango slices based on hyperspectral imaging visualisation of moisture content distribution. *Biosystems Engineering*, *156*, 108–119. https://doi.org/10.1016/j.biosystemseng.2017.01.006
54. Queiroz, C., Mendes Lopes, M.L., Fialho, E., Valente-Mesquita, V.L. (2008). Polyphenol oxidase: Characteristics and mechanisms of browning control. *Food Reviews International*, *24*(4), 361–375. https://doi.org/10.1080/87559120802089332
55. Rafidah, H., Ando, Y., Amin, I., Shirai, Y., Mohd Ali, H. (2014). Enhanced polyphenol content and antioxidant capacity in the edible portion of avocado dried with superheated-steam. *International Journal of Advanced Research*, *8*, 241–248.
56. Raghavi, L., Moses, J., Anandharamakrishnan, C. (2018). Refractance window drying of foods: A review. *Journal of Food Engineering*, *222*, 267–275. https://doi.org/10.1016/j.jfoodeng.2017.11.032
57. Rajoriya, D., Bhavya, M.L., Hebbar, H.U. (2021). Impact of process parameters on drying behaviour, mass transfer and quality profile of refractance window dried banana puree. *LWT – Food Science and Technology*, *145*, art. no. 111330. https://doi.org/10.1016/j.lwt.2021.111330
58. Rajoriya, D., Shewale, S.R., Hebbar, H.U. (2019). Refractance window drying of apple slices: Mass transfer phenomena and quality parameters. *Food and Bioprocess Technology*, *12*(10), 1646–1658. https://doi.org/10.1007/s11947-019-02334-7
59. Ramaswamy, H.S., Marcotte, M. (2005). *Food processing: Principles and applications*. CRC Press, Boca Raton. https://doi.org/10.1201/9780203485248
60. Rudra, S.G., Singh, H., Basu, S., Shivhare, U.S. (2008). Enthalpy entropy compensation during thermal degradation of chlorophyll in mint and coriander puree. *Journal of Food Engineering*, *86*(3), 379–387. https://doi.org/10.1016/j.jfoodeng.2007.10.020

61. Schieber, A., Ullrich, W., Carle, R. (2000). Characterization of polyphenols in mango puree concentrate by HPLC with diode array and mass spectrometric detection. *Innovative Food Science & Emerging Technologies*, *1*(2), 161–166. https://doi.org/10.1016/S1466-8564(00)00015-1
62. Shariful, H., Parveen, B., Maksuda, K., Islam, S.N. (2015). Total carotenoid content in some mango (*Mangifera indica*) varieties of Bangladesh. *International Journal of Pharmaceutical Sciences and Research*, *6*(11), 4875–4878.
63. Souza, D.S., Marques, L.G., Gomes, E., Narain, N. (2015). Lyophilization of avocado (*Persea americana* Mill.): Effect of freezing and lyophilization pressure on antioxidant activity, texture, and browning of pulp. *Drying Technology*, *33*(2), 194–204. https://doi.org/10.1080/07373937.2014.943766
64. Temu, A.T. (2013). Effect of temperature and slice size on avocado pulp drying rate and oil yield. *Tanzania Journal of Engineering and Technology*, *34*(2), 116–124. https://doi.org/10.52339/tjet.v34i2.464
65. Tzempelikos, D.A., Vouros, A.P., Bardakas, A.V., Filios, A.E., Margaris, D.P. (2015). Experimental study on convective drying of quince slices and evaluation of thin-layer drying models. *Engineering in Agriculture, Environment and Food*, *8*(3), 169–177. https://doi.org/10.1016/j.eaef.2014.12.002
66. Uribe, E., Vega-Gálvez, A., Di Scala, K., Oyanadel, R., Saavedra Torrico, J., Miranda, M. (2011). characteristics of convective drying of pepino fruit (*Solanum muricatum* Ait.): application of Weibull distribution. *Food and Bioprocess Technology*, *4*(8), 1349–1356. https://doi.org/10.1007/s11947-009-0230-y
67. Vanini, L.S., Kwiatkowski, A., Clemente, E. (2010). Polyphenoloxidase and peroxidase in avocado pulp (*Persea americana* Mill.). *Food Science and Technology*, *30*, 525–531. https://doi.org/10.1590/S0101-20612010000200036
68. Vega-Mercado, H., Góngora-Nieto, M.M., Barbosa-Cánovas, G.V. (2001). Advances in dehydration of foods. *Journal of Food Engineering*, *49*(4), 271–289. https://doi.org/10.1016/S0260-8774(00)00224-7
69. Wang, W., Bostic, T.R., Gu, L. (2010). Antioxidant capacities, procyanidins and pigments in avocados of different strains and cultivars. *Food Chemistry*, *122*(4), 1193–1198. https://doi.org/10.1016/j.foodchem.2010.03.114
70. Wang, Y., Lu, Z., Lv, F., Bie, X. (2009). Study on microencapsulation of curcumin pigments by spray drying. *European Food Research and Technology*, *229*(3), 391–396. https://doi.org/10.1007/s00217-009-1064-6
71. Yao, L., Fan, L., Duan, Z. (2020). Effect of different pretreatments followed by hot-air and far-infrared drying on the bioactive compounds, physicochemical property and microstructure of mango slices. *Food Chemistry*, *305*, art. no. 125477. https://doi.org/10.1016/j.foodchem.2019.125477
72. Zhou, L., Tey, C.Y., Bingol, G., Bi, J. (2016). Effect of microwave treatment on enzyme inactivation and quality change of defatted avocado puree during storage. *Innovative Food Science & Emerging Technologies*, *37*, 61–67. https://doi.org/10.1016/j.ifset.2016.08.002
73. Zotarelli, M.F., Carciofi, B.A.M., Laurindo, J.B. (2015). Effect of process variables on the drying rate of mango pulp by Refractance Window. *Food Research International*, *69*, 410–417. https://doi.org/10.1016/j.foodres.2015.01.013
74. Zotarelli, M.F., da Silva, V.M., Durigon, A., Hubinger, M.D., Laurindo, J.B. (2017). Production of mango powder by spray drying and cast-tape drying. *Powder Technology*, *305*, 447–454. https://doi.org/10.1016/j.powtec.2016.10.027

Pol. J. Food Nutr. Sci., 2022, Vol. 72, No. 1, pp. 39–55
On-line ISSN: 2083-6007
Print ISSN: 1230-0322
DOI: 10.31883/pjfns/145665
http://journal.pan.olsztyn.pl

Original article
Section: Food Quality and Functionality

Impact of Grape Variety, Yeast and Malolactic Fermentation on Volatile Compounds and Fourier Transform Infrared Spectra in Red Wines

Anna Stój[1], Tomasz Czernecki[1], Bożena Sosnowska[1], Agnieszka Niemczynowicz[2], Arkadiusz Matwijczuk[3]*

[1]Department of Biotechnology, Microbiology and Human Nutrition, Faculty of Food Science and Biotechnology, University of Life Sciences in Lublin, Skromna 8, 20-704 Lublin, Poland
[2]Faculty of Mathematics and Computer Science, University of Warmia and Mazury in Olsztyn, Słoneczna 54, 10-710 Olsztyn
[3]Department of Biophysics, University of Life Sciences in Lublin, Akademicka 13, 20-950 Lublin

Key words: fermentation, *Saccharomyces cerevisiae, Saccharomyces bayanus, Oenococcus oeni*, aroma compounds, Fourier transform infrared spectroscopy

Volatile compounds are very important to the flavour and quality of the wine. The study aimed to determine the effect of grape variety (Rondo and Zweigelt), yeast, malolactic fermentation (MLF) and yeast×MLF interaction on the content of volatile compounds in red wines. The wines were produced by sequential inoculation with five commercial yeast strains and a commercial lactic acid bacteria (LAB) strain (induced malolactic fermentation) as well as by inoculation with five commercial yeast strains and without LAB inoculation (spontaneous malolactic fermentation). The volatile compounds were determined by headspace solid-phase microextraction/gas chromatography-mass spectrometry (HS-SPME-GC/MS). Forty-six volatile compounds belonging to alcohols, esters, acids, aldehydes, ketones, furan compounds, sulfur compounds and volatile phenols were identified in the wines. The grape variety was the factor with a significant impact on the highest number of volatile compounds, 32 out of 46. Furthermore, 7 compounds were affected by yeast, 10 by MLF and only 3 by yeast×MLF interaction. Characteristic bands in Fourier transform infrared (FTIR) spectra were assigned to the vibrations of functional groups of volatile compounds. The whole FTIR spectra were analysed in detail; three characteristic spectral ranges such as 3650–2700, 1750–1500, and below 1500 cm^{-1} were shown for different classes of volatile compounds. The most remarkable spectral changes were observed for the last two areas.

INTRODUCTION

Volatile compounds (VOCs) largely determine the aroma of the wine. The concentration of VOCs in wines ranges from several mg/L to a few ng/L [Welke *et al.,* 2012; Zhu *et al.,* 2016]. These volatile compounds originate from grapes (varietal aromas) and are secondary products of fermentation processes (fermentation aromas) and aging (post-fermentation aromas) [Callejon *et al*., 2010]. Alcoholic fermentation (AF) and malolactic fermentation (MLF) processes play a fundamental role in creating the taste and aroma of the product [Gammacurta *et al*., 2014, 2017].

Yeasts, responsible for AF, transform sugar into ethanol, carbon dioxide, and minor secondary metabolites, including higher alcohols, esters, fatty acids, aldehydes, ketones, and others [Englezos *et al.*, 2018]. Yeasts also release varietal aromatic compounds from grapes. The ability to synthesize secondary metabolites and to release varietal compounds depends on the yeast species and strain [Blanco *et al*., 2014; Callejon *et al*., 2010; Gammacurta *et al*., 2017]. The primary yeast species responsible for AF is *Saccharomyces cerevisiae* [Azzolini *et al.*, 2012]. A wide range of selected yeast strains are commercially available that guarantee fermentation control and wine quality. However, some wineries are interested in selecting autochthonous (indigenous) yeast starters because of their ability to ensure the sensory characteristic of wines originating from a specific *terroir* [Blanco *et al*., 2014; Tufariello *et al*., 2014].

During MLF, L-malic acid is an enzymatically decarboxylated into L-lactic acid and carbon dioxide by lactic acid bacteria (LAB), mainly *Oenococcus oeni* [Tristezza *et al.*, 2016]. This process is an important step in the production of most red and some white and sparkling wines [Abrahamse & Bartowsky, 2012; Costello *et al*., 2012; Lasik-Kurdyś *et al*., 2018]. MLF reduces the total acidity (by slightly increasing the pH), causes microbiological stability, and modifies wine aroma and taste [Costello *et al*., 2012]. Aroma modification is associated with citric acid catabolism by LAB, resulting in the production of diacetyl, acetic acid, acetoin, and 2,3-butanediol [Malherbe *et al*., 2012]. MLF typically takes place after AF and can occur spontaneously, carried out by indigenous LAB populations, or may be induced by starter culture inoculation to control this step of winemaking. Two types of LAB

* Corresponding Author:
E-mail: anna.stoj@up.lublin.pl (A. Stój)

Submitted: 11 April 2021
Accepted: 10 January 2022
Published on-line: 27 January 2022

inoculation are commonly used: traditional inoculation after AF (sequential) or simultaneous inoculation with the yeast and LAB (co-inoculation) [Abrahamse & Bartowsky, 2012; Antalick *et al*., 2013]. The undoubted advantage of simultaneous inoculation is the reduction of the vinification time. However, this inoculation may slow down the growth and deteriorate the viability of yeast cells, leading to a delay or inhibition of AF, and increase volatile acidity caused by higher acetic acid production [Stój, 2020a].

In recent years, several authors have conducted studies on the influence of grape variety and microorganisms on the content of volatile compounds in red wines [Cañas *et al.*, 2012; Cioch-Skoneczny *et al.*, 2021; Englezos *et al.*, 2018; Tristezza *et al.*, 2016]. The grape variety affects not only varietal aromas (C13-norisoprenoids, lactones, and terpenes) but also other volatile compounds, such as higher alcohols, esters, and fatty acids [Vilanova *et al*., 2007]. Both grape cultivar and yeast species significantly impacted content of ethyl esters in wines. The effect of grape cultivar on the content of higher alcohols seems more significant than the effect of yeast species. Fatty acid (acetic acid, 2-methylpropanoic acid, butanoic acid, 3-methylbutanoic acid and octanoic acid) contents showed significant differences as an effect of yeast species [Liu *et al*., 2017]. A specific volatile profile corresponded to each yeast/LAB combination, wherein the yeast strain had a predominant effect on aromatic compounds [Gammacurta *et al.*, 2017]. The wine matrix, particularly pre-MLF pH, ethanol content, and grape source affected the ability of LAB strains to modulate volatile compounds in wines [Costello *et al*., 2012].

The composition of grapes depends on the varietal and clonal genotype of the grapevine as well as the interaction of the genotype and phenotype with many environmental factors (*terroir*) [Styger *et al*., 2011]. One of the most popular red grape hybrids in Poland is Rondo (non-*Vitis vinifera*). It derives from a cross between two species of *Vitis, Zarya severa* × *Saint Laurent* [Wojdyło *et al*., 2018]. However, noble grape varieties, such as Zweigelt (*Vitis vinifera*), cover a small area of Poland [Stój *et al*., 2020b]. To the best of our knowledge, there have been no studies on the varieties of grapes cultivated in Poland and the wine factors influencing the concentration of different classes of volatile compounds in red wines. The study aimed to determine the effects of Rondo and Zweigelt varieties, yeast, MLF, and yeast×MLF interaction on the content of volatile compounds in wines. The wines were produced by sequential inoculation of grape pulp with five commercial yeast strains (*S. cerevisiae* or *S. cerevisiae* × *S. bayanus*) and a commercial LAB (*O. oeni*) as well as by inoculation with five commercial yeast strains and without LAB inoculation. Moreover, the analysis of Fourier transform infrared (FTIR) spectra used in conjunction with the multivariate analysis allowed for assigning vibration bands to specific functional groups of volatile compounds.

MATERIALS AND METHODS

Winemaking

Details of winemaking are presented in our previous article [Stój *et al*., 2020b]. The grapes of Zweigelt and Rondo varieties were obtained from 'Małe Dobre' and 'Dom Bliskowice' vineyards, respectively. The vineyards are located in the Lublin Province, Poland. The grapes were harvested manually in 2017. The grape pulp was subjected to alcoholic fermentation by using five commercial yeast strains, four *S. cerevisiae*: SafOEno™ SC 22, Essentiale Grand Cru (Lesaffre, Marcq-en-Barœul, France), Siha Active Yeast 8, Siha Rubino Cru (Eaton, Tinton Falls, NJ, USA); and one *S. cerevisiae* × *S. bayanus* – SafOEno™ HD S62 (Lesaffre), the same for the Zweigelt and Rondo varieties. Spontaneous MLF occurred in one part of the wines, *i.e*. that without LAB inoculation, and induced MLF – in the other part of the wines, *i.e.* that with *O. oeni* (Viniflora Oenos, Eaton) inoculation. *O. oeni* starter culture was added after the completion of AF (sequential inoculation) to the wines in which induced malolactic fermentation was carried out. We did not obtain complete reduction of malic acid in any of the wines. The concentrations of malic and lactic acids in the final wines are presented in the supplementary material to the previous article [Stój *et al.*, 2020b]. The experiments were performed in duplicate. The following abbreviations are used for the wines: Z1-Z5 – Zweigelt wines, in which AF was induced using various yeast strains, and the wines were left to undergo spontaneous MLF; Z1 LAB-Z5 LAB – Zweigelt wines, in which AF was induced using various yeast strains (the same strains as in Z1-Z5 wines), and MLF was carried out by inoculation with lactic acid bacteria; R1-R5 – Rondo wines, in which AF was induced using various yeast strains, and the wines were left to undergo spontaneous MLF; R1 LAB-R5 LAB – Rondo wines, in which AF was induced using various yeast strains (the same strains as in R1-R5 wines), and MLF was carried out by inoculation with lactic acid bacteria.

Reagents

Sodium chloride and hydrochloric acid were obtained from POCh (Gliwice, Poland). Sodium chloride was oven-dried at 200°C overnight. Hydrochloric acid was dissolved in water at a concentration of 78 g/L. 4-Hydroxy-4-methyl-2-pentanone (the internal standard of volatile compound analysis) was purchased from Sigma-Aldrich (Saint Louis, MO, USA) and prepared in water at a concentration of 7 mg/L. A mixture of *n*-alkanes (C_7-C_{30}) for the calculations of linear retention indices (RI) was supplied by Supelco (Bellefonte, PA, USA). All chemicals were of analytical grade.

Determination of volatile compounds

The volatile compounds were determined by headspace solid-phase microextraction and gas chromatography-mass spectrometry analysis (HS-SPME-GC/MS) according to our previous method [Stój *et al*., 2017a,b] with slight modification.

A fiber holder and an 85 μm CAR/PDMS fiber were used (Supelco). Before each analysis, the fiber was conditioned by inserting it into the auxiliary GC injection port at 280°C for 5 min. Then, 0.9 g of NaCl, 3 mL of wine, 50 μL of HCl, 100 μL of 4-hydroxy-4-methyl-2-pentanone, and a magnetic stirring bar were placed in a glass vial of 7 mL. The vial was capped with a PTFE-silicone septum (Supelco) on which a screw cap with a hole was placed. The vial was placed in a block on an MS7-H550-S magnetic stirrer with a hotplate (DLAB Scientific Co., Beijing, China). The sample was incubated at 40°C

for 15 min, and then the fiber was exposed to the headspace (HS) at 40°C for 30 min. The incubation and microextraction were carried out with continuous stirring at a minimum speed. The fiber was thermally desorbed in the GC injection port for 2 min at 220°C in the split-less mode.

The samples were analyzed using a gas chromatograph combined with a quadrupole mass spectrometer (GCMS--QP2010, Shimadzu, Kyoto, Japan). All analyses were made in triplicate. Chromatographic separations were carried out using a VF-WAXms capillary column (60 m, 0.25 mm ID, 0.25 μm film thickness, 100% polyethylene glycol, Agilent, Santa Clara, CA, USA). Helium was used as the carrier gas at a flow rate of 1.8 mL/min. The column oven temperature was held at 34°C for 5 min, then raised to 100°C at a rate of 3°C/min and held for 6 min, and finally raised to 220°C at a rate of 5°C/min and held for 15 min. The total run time was 72 min. The specification of the mass spectrometer was as follows: electron ionization source with a temperature of 200°C, 70 eV ionization energy and mass range of 30–300 *m/z* in the full scan mode (scan time 0.4 s). Data were collected using the GCMSsolution software ver. 2 (Shimadzu). The tentative identification of aromatic compounds was performed based on mass spectra and confirmed by linear retention index. The mass spectrum of each peak was compared to data provided in the National Institute of Standards and Technology mass spectral library (NIST 05). The peak was correctly identified when the similarity of the spectra was at least 80%. Chromatographic retention data for C_7-C_{30} *n*-alkanes (Supelco) were used to calculate the RI of each compound. Experimental RI results were compared to the retention indices found in the bibliography for similar GC columns. Data for the volatile compounds were calculated by relating their peak areas to the peak area of the internal standard. The contents of volatiles in wines were expressed as μg/L.

Fourier transform infrared spectroscopy

FTIR spectra were measured on a 670-IR spectrometer from Agilent. FTIR measurements were made five times for each wine. An attenuated total reflection (ATR) trough in the form of a horizontal ATR (HATR) Ge crystal with an appropriate geometry (*i.e.*, truncated at 45°) was used in the measurements. This was to ensure a 20-fold internal reflection of the absorbed beam. Additionally, background correction was applied and 24 scans were recorded at the recording of each spectrum. Then, the program averaged the spectra obtained, before and after each measurement the crystal was thoroughly purified using ultra-pure and clear solvents from Sigma-Aldrich. The apparatus was continuously purged with argon before (1 h) and during the entire spectral measurement. FTIR spectra were recorded with a resolution of 1 cm^{-1} and measured in the range of 4000 to 400 cm^{-1}. In the end, the spectra were analyzed with Grams/AI 8.0 software (Thermo Fisher Scientific, Waltham, MA, USA). All samples were measured at room temperature.

Statistical analysis

The effects of grape variety, yeast, MLF, and yeast×MLF interaction on the content of volatile compounds in wines were tested using one-way and two-way analysis of variance (ANOVA). One- and two-way ANOVA was performed with the Statistica 13.3 software (Statsoft, Krakow, Poland).

Next, hierarchical cluster analysis (HCA) with Euclidean distance was applied as an unsupervised classification technique in order to explore the FTIR data structure. The hierarchical cluster analysis and dendrogram were performed with Statistica 13.3 software. Next, principal component analysis (PCA) was applied to verify the similarities and differences among the wines. The PCA was based on the data array of the fingerprints of FTIR spectra of each considered wine, and carried out using OriginPro software (OriginLab, Northampton, MA, USA).

RESULTS AND DISCUSSION

Forty-six volatile compounds belonging to several groups – alcohols (21 compounds), esters (12 compounds), acids (5 compounds), aldehydes (2 compounds), ketones (2 compounds), furan compounds (2 compounds), sulfur compounds (1 compound) and volatile phenols (1 compound) – were identified in red wines produced from Zweigelt and Rondo grape varieties (Table 1). Figure S1 and Figure S2 in the supplementary materials present the chromatograms of volatile compounds of Zweigelt and Rondo wines, respectively. Table 2 and Table 3 present the concentrations of volatile compounds of Zweigelt and Rondo wines, respectively, produced with different yeast and MLF combinations.

The dominating alcohols in the wines produced from the Zweigelt variety were: 3-methylbutan-1-ol, 2-methylpropan-1-ol, and hexan-1-ol (Table 2). The concentrations of 2-(2-ethoxyethoxy)-ethanol, decan-1-ol and (*Z*)-2-hexen-1-ol were the lowest. The major esters were ethyl 2-hydroxypropanoate (ethyl lactate), ethyl octanoate, and 3-methylbutyl acetate, while minor ones were: 2-phenylethyl acetate, hexyl acetate, and methyl octanoate. Among the acids, acetic acid and hexanoic acid were found at the highest concentrations. Propanoic acid was detected only in Z2 LAB-Z5 LAB wines. Benzaldehyde was the most abundant compound in the two detected aldehydes, 4-methyl-3-penten-2-one was the most abundant compound in the two detected ketones, dihydrofuran-2(3*H*)-one was the most abundant in the two detected furan compounds.

The most abundant alcohols in wines produced from the Rondo variety were: 3-methylbutan-1-ol, 2-methylpropan-1-ol, and 2-phenylethanol (Table 3). Rondo wines had the highest concentration of 3-methylbutan-1-ol, similarly to our previous works [Stój *et al*., 2017a,b] and to the work of Liu *et al*. [2017]. Contrary to our findings, Ruocco *et al*. [2019] reported the highest content of 2,3-butanediol among all alcohols. The minor alcohols of Rondo wines were: 3-ethyl-4-methylpentan-1-ol, phenylmethanol, and decan-1-ol (Table 3). The dominating esters were: ethyl 2-hydroxypropanoate, 3-methylbutyl acetate, and ethyl octanoate, and it is in agreement with our previous works [Stój *et al*., 2017a,b]. According to Liu *et al*. [2017], ethyl octanoate and ethyl acetate were the main esters in wines produced from Rondo variety. In turn, Ruocco *et al*. [2019] stated that ethyl 2-hydroxypropanoate and ethyl acetate were the dominating esters in Rondo wines. The dissimilarities between

TABLE 1. Volatile compounds identified in red wines.

Peak no.	Compound	Similarity (%)	RT (min)	RI exp.	RI lit.	References
	Alcohol					
2	Propanol-1-ol	95	13.50	1051	1044	Mendes *et al.* [2012]
4	2-Methylpropan-1-ol	97	16.31	1122	1100	Mendes *et al.* [2012]
7	Butan-1-ol	96	18.73	1169	1173	Welke *et al.* [2012]
8	3-Methylbutan-1-ol	98	21.79	1228	1210	Mendes *et al.* [2012]
9	Pentan-1-ol	94	23.46	1261	1259	Mallouchos *et al.* [2007]
12	4-Methylpentan-1-ol	95	26.35	1318	1309	Duarte *et al.* [2010]
13	3-Methylpentan-1-ol	97	26.94	1329	1322	Duarte *et al.* [2010]
16	Hexan-1-ol	98	28.20	1353	1361	Mallouchos *et al.* [2007]
17	3-Ethoxypropan-1-ol	93	29.44	1376	1371	Welke *et al.* [2012]
19	(*Z*)-2-Hexen-1-ol	87	31.73	1417	1397	Welke *et al.* [2012]
21	Octen-3-ol	95	33.94	1453	1451	Song *et al.* [2014]
22	Heptan-1-ol	97	34.24	1458	1470	Welke *et al.* [2012]
24	2-Ethylhexan-1-ol	98	36.19	1490	1486	Duarte *et al.* [2010]
25	3-Ethyl-4-methylpentan-1-ol	92	37.14	1508	1509	Welke *et al.* [2012]
27	Butane-2,3-diol	98	38.61	1543	1563	Welke *et al.* [2012]
29	Octan-1-ol	98	39.32	1559	1567	Mallouchos *et al.* [2007]
32	Propane-1,2-diol	90	40.75	1592	1591	Welke *et al.* [2012]
33	2-(2-Ethoxyethoxy)-ethanol	89	41.67	1618	1622	Welke *et al.* [2012]
40	Decan-1-ol	95	46.13	1760	1778	Welke *et al.* [2012]
43	Phenylmethanol	84	49.27	1881	1869	Duarte *et al.* [2010]
44	2-Phenylethanol	97	50.10	1916	1919	Mallouchos *et al.* [2007]
	Ester					
1	Ethyl butanoate	97	13.05	1037	1034	Mallouchos *et al.* [2007]
3	Ethyl 3-methylbutanoate	94	14.43	1078	1066	Duarte *et al*. [2010]
5	3-Methylbutyl acetate	98	16.88	1133	1125	Duarte *et al.* [2010]
10	Hexyl acetate	90	24.16	1275	1272	Mallouchos *et al.* [2007]
14	Ethyl heptanoate	91	27.38	1337	1349	Welke *et al.* [2012]
15	Ethyl 2-hydroxypropanoate	98	27.87	1346	1339	Welke *et al.* [2012]
18	Methyl octanoate	85	30.01	1387	1381	Welke *et al.* [2012]
20	Ethyl octanoate	97	32.85	1435	1429	Welke *et al.* [2012]
30	3-Methylbutyl 2-hydroxypropanoate	97	39.85	1572	1568	Mendes *et al.* [2012]
36	Ethyl decanoate	88	42.38	1639	1643	Welke *et al.* [2012]
38	Diethyl butanedioate	96	43.66	1677	1672	Duarte *et a*l. [2010]
41	2-Phenylethyl acetate	90	47.73	1819	1810	Duarte *et al.* [2010]
	Acid					
23	Acetic acid	98	34.59	1464	1457	Welke *et al.* [2012]
28	Propanoic acid	86	39.02	1552	1536	Welke *et al.* [2012]
31	2-Methylpropanoic acid	97	40.11	1578	1573	Mallouchos *et al.* [2007]

TABLE 1 continued

Peak no.	Compound	Similarity (%)	RT (min)	RI exp.	RI lit.	References
42	Hexanoic acid	96	48.53	1851	1851	Mallouchos *et al*. [2007]
45	Octanoic Acid	95	53.38	2065	2067	Mallouchos *et al.* [2007]
	Aldehyde					
26	Benzaldehyde	91	37.90	1526	1522	Mallouchos *et al.* [2007]
37	4-Methylbenzaldehyde	92	42.78	1651	1638	Duarte *et al.* [2010]
	Ketone					
6	4-Methyl-3-penten-2-one	98	17.56	1146	1139	Jørgensen *et al.* [2000]
11	3-Hydroxybutan-2-one	90	25.39	1299	1289	Mallouchos *et al.* [2007]
	Furan compound					
34	Ethyl 2-furoate	88	41.93	1625	1627	Welke *et al.* [2012]
35	Dihydrofuran-2(3*H*)-one	93	42.22	1634	1627	Mallouchos *et al.* [2007]
	Sulphur compound					
39	3-(Methylsulfanyl)propan-1-ol	96	44.95	1718	1715	Duarte *et al.* [2010]
	Volatile phenol					
46	3,5-Di-*tert*-butylphenol	86	58.08	2305	2310	Shimoda *et al.* [1995]

RT – retention time; RI exp. –retention index experimentally determined; RI lit. –retention index reported in the literature for a CP-Wax columns or equivalent stationary phase. Peak no. correspond to those in the chromatograms in Figures S1 and S2 in the supplementary materials.

concentrations of volatile compounds among studies may have been due to differences in geographical origins of grapes, winemaking, and methods of determination of volatile compounds. Acetic acid was present at the highest concentration among the acids of Rondo wines (Table 3), while propanoic acid was not detected. Similarly, other authors reported that acetic acid was the major acid of wines produced using Rondo grapes [Liu *et al*., 2017; Ruocco *et al.*, 2019] and we also stated this in our previous publications [Stój *et al.*, 2017a,b]. Major volatile compounds within the other classes were: benzaldehyde, 4-methyl-3-penten-2-one, and dihydrofuran-2(3*H*)-one (Table 3).

A one-way ANOVA was used to study the grape variety/yeast/MLF effect on volatile compound profile of wines. Results of this analysis revealed a significant effect of grape variety, yeast, and MLF on the concentrations of 32, 7, and 10 volatile compounds, respectively, belonging to all groups of compounds (Table 4). The grape variety was the factor with a significant impact on the highest number of identified volatile compounds. The two-way ANOVA confirmed the effects of yeast and MLF on volatile compounds in wines (Table 4). The yeast and MLF factors had a significant impact on a greater number of volatile compounds compared to the yeast×MLF interaction, which affected concentrations of only three compounds: 2-phenylethanol, octanoic acid and 3-(methylsulfanyl)propan-1-ol.

In our study, the grape variety effect was significant for most alcohols, including: propanol-1-ol, butan-1-ol, 3-methylbutan-1-ol, pentan-1-ol, 4-methylpentan-1-ol, 3-methylpentan-1-ol, hexan-1-ol, 3-ethoxypropan-1-ol, (*Z*)-2-hexen-1-ol, octen-3-ol, heptan-1-ol, 2-ethylhexan-1-ol, 3-ethyl-4-methylpentan-1-ol, octan-1-ol, decan-1-ol, phenylmethanol, and 2-phenylethanol (Table 4), while Liu *et al.* [2017] reported that the concentration of all determined alcohols was affected by the variety. Higher alcohols are strictly related to yeast metabolism [Blanco *et al*., 2014; Callejon *et al*., 2010]. They could be synthesized by yeast through two mechanisms: the anabolic pathway from glucose or the catabolic pathway from their corresponding amino acids [Liu *et al*., 2017; Stój *et al*., 2017a]. Yeast species and strains (and other factors such as pH, grape juice composition and fermentation temperature) influence the formation of higher alcohols during fermentation [Liu *et al*., 2017]. In our study, concentrations of 3-ethoxypropan-1-ol, (*Z*)-2-hexen-1-ol, phenylmethanol, and 2-phenylethanol were significantly affected by yeast strain used in winemaking. Both Blanco *et al*. [2014] and Tufariello *et al.* [2014] found no differences in phenylmethanol concentration, whereas Callejon *et al*. [2010] and Tufariello *et al.* [2014] found no differences in 2-phenylethanol concentration between red wines produced using different yeast strains. Similarly to our study, Callejon *et al*. [2010] reported a correlation of phenylmethanol concentration with a yeast strain, and Blanco *et al*. [2014] reported a correlation of 2-phenylethanol content with a yeast strain. The yeast strains used in this study did not influence the concentrations of other higher alcohols, such as propanol-1-ol, 2-methylpropan-1-ol, butan-1-ol, 3-methylbutan-1-ol, hexan-1-ol, heptan-1-ol (Table 4). Blanco *et al.* [2014], Callejon *et al.* [2010], and Tufariello *et al.* [2014] observed the effect of yeast strain or no effect on the concentrations of higher alcohols. Finally, the MLF

TABLE 2. Concentrations of volatile compounds in Zweigelt wines (μg/L) produced with different yeast and malolactic fermentation (MLF) combinations.

Compound	Z1	Z2	Z3	Z4	Z5	Mean±SD	Z1 LAB	Z2 LAB	Z3 LAB	Z4 LAB	Z5 LAB	Mean±SD
Alcohol												
Propanol-1-ol	56.41	99.01	34.18	84.46	95.78	73.97±27.86	101.21	146.66	68.96	56.19	103.14	95.23±35.20
2-Methylpropan-1-ol	284.23	192.49	163.93	389.60	672.59	340.57±205.51	321.81	276.36	423.62	420.16	447.18	377.83±74.38
Butan-1-ol	6.45	8.39	4.58	nd	15.26	6.94±5.60	13.73	4.16	6.46	6.16	5.75	7.25±3.73
3-Methylbutan-1-ol	2563.09	2261.99	2188.89	3435.22	5011.19	3092.08±1181.67	5050.42	3215.93	3343.36	3591.01	3576.70	3755.48±741.09
Pentan-1-ol	1.89	1.51	2.06	2.19	2.88	2.11±0.50	3.78	2.50	2.73	2.16	2.10	2.66±0.68
4-Methylpentan-1-ol	4.60	4.23	6.32	5.08	8.21	5.69±1.61	8.68	6.74	7.81	4.93	5.44	6.72±1.57
3-Methylpentan-1-ol	6.30	5.85	7.96	7.45	9.66	7.44±1.50	11.45	9.32	9.71	7.22	6.64	8.87±1.95
Hexan-1-ol	205.80	172.87	241.20	270.36	332.39	244.52±61.31	381.30	268.08	281.05	298.70	199.89	285.80±65.20
3-Ethoxypropan-1-ol	0.22	1.22	1.07	0.82	1.57	0.98±0.50	0.50	1.35	1.40	1.17	1.14	1.11±0.36
(*Z*)-2-Hexen-1-ol	nd	0.05	0.26	0.18	nd	0.10±0.12	0.07	0.25	0.18	0.23	nd	0.15±0.11
Octen-3-ol	1.48	1.50	1.93	1.81	2.98	1.94±0.61	2.81	2.35	2.21	1.44	1.66	2.09±0.55
Heptan-1-ol	2.81	2.48	5.63	4.85	5.93	4.34±1.60	6.35	5.12	6.34	6.98	3.78	5.71±1.27
2-Ethylhexan-1-ol	11.95	11.88	25.79	15.52	25.40	18.11±6.99	24.32	18.84	29.47	18.71	11.42	20.55±6.77
3-Ethyl-4-methylpentan-1-ol	2.37	2.23	3.02	2.99	4.48	3.02±0.89	4.64	3.51	3.43	3.48	2.27	3.47±0.84
Butane-2,3-diol	69.81	60.81	37.13	37.82	108.91	62.90±29.42	80.47	37.14	47.80	63.35	38.49	53.45±18.37
Octan-1-ol	12.15	6.09	13.96	9.82	30.19	14.44±9.28	28.98	11.13	15.83	14.07	14.62	16.93±6.95
Propane-1,2-diol	2.14	3.55	0.82	0.87	5.62	2.60±2.02	3.14	0.51	1.11	1.62	0.30	1.34±1.13
2-(2-Ethoxyethoxy)-ethanol	0.32	0.16	0.32	0.29	0.69	0.36±0.20	0.60	0.21	0.35	0.41	0.36	0.38±0.14
Decan-1-ol	0.14	nd	0.27	0.08	0.48	0.19±0.19	nd	0.03	0.19	0.13	nd	0.07±0.09
Phenylmethanol	1.14	0.66	0.17	0.46	0.28	0.54±0.38	0.54	0.18	0.10	0.18	0.14	0.23±0.18
2-Phenylethanol	165.80	143.58	104.27	133.89	327.69	175.05±88.15	221.62	135.84	118.37	187.75	149.87	162.69±41.68
Ester												
Ethyl butanoate	38.82	23.36	36.50	49.30	83.64	46.32±22.81	60.27	48.58	53.47	34.52	33.10	45.99±11.88
Ethyl 3-methylbutanoate	6.87	5.69	4.36	6.21	12.87	7.20±3.30	8.81	6.82	5.31	3.51	7.07	6.30±2.00
3-Methylbutyl acetate	53.96	7.55	37.56	44.86	nd	28.79±23.71	12.92	93.08	107.50	69.76	109.37	78.52±39.95
Hexyl acetate	nd	nd	0.50	0.22	nd	0.14±0.22	nd	0.33	0.16	nd	0.56	0.21±0.24

TABLE 2 continued

Compound	Z1	Z2	Z3	Z4	Z5	Mean±SD	Z1 LAB	Z2 LAB	Z3 LAB	Z4 LAB	Z5 LAB	Mean±SD
Ethyl heptanoate	3.20	4.87	1.07	3.30	3.08	3.10±1.35	4.15	2.43	2.00	1.09	2.35	2.41±1.11
Ethyl 2-hydroxypropanoate	121.21	154.99	456.41	104.51	196.32	206.69±143.95	889.19	773.57	623.82	532.46	670.39	697.89±137.78
Methyl octanoate	0.56	0.21	nd	0.85	nd	0.32±0.37	nd	0.16	0.09	nd	nd	0.03±0.07
Ethyl octanoate	14.65	43.95	48.91	79.09	136.10	64.54±46.07	89.80	47.53	59.08	82.74	66.90	69.21±17.21
3-Methylbutyl 2-hydroxypropanoate	2.74	3.28	9.66	2.16	6.33	4.83±3.14	22.02	15.50	12.01	15.06	17.14	16.35±3.67
Ethyl decanoate	nd	0.31	nd	0.57	1.48	0.47±0.61	1.03	nd	0.46	nd	nd	0.21±0.46
Diethyl butanedioate	44.27	42.33	42.08	27.72	84.13	48.11±21.20	61.72	38.77	41.85	29.03	40.48	42.37±11.93
2-Phenylethyl acetate	nd	nd	0.29	0.25	0.27	0.16±0.15	0.82	nd	0.35	nd	0.26	0.28±0.34
Acid												
Acetic acid	73.80	74.54	211.19	93.53	195.70	129.75±67.96	222.29	242.45	1232.57	295.25	281.45	254.80±31.82
Propanoic acid	nd	nd	nd	nd	nd	nd	nd	0.43	0.37	0.17	0.62	0.32±0.24
2-Methylpropanoic acid	nd	nd	5.13	4.80	nd	1.99±2.72	nd	nd	4.03	nd	nd	0.81±1.80
Hexanoic acid	29.40	33.71	30.08	40.54	88.85	44.51±25.17	44.59	28.65	27.04	46.90	29.29	35.29±9.61
Octanoic Acid	7.43	6.51	5.42	6.76	25.19	10.26±8.38	11.57	5.32	3.47	6.60	2.80	5.95±3.48
Aldehyde												
Benzaldehyde	nd	nd	49.99	nd	77.06	25.41±36.09	7.37	28.86	15.98	32.97	47.02	26.44±15.37
4-Methylbenzaldehyde	0.71	1.72	0.98	1.15	1.42	1.19±0.39	1.40	0.88	0.91	1.24	1.07	1.10±0.22
Ketone												
4-Methyl-3-penten-2-one	297.66	308.21	231.75	559.12	903.98	460.14±277.69	636.30	676.76	380.98	430.74	512.75	527.50±127.64
3-Hydroxybutan-2-one	0.31	0.15	0.84	1.05	nd	0.47±0.45	0.15	0.54	1.09	0.29	0.84	0.58±0.39
Furan compound												
Ethyl 2-furoate	0.52	0.51	0.47	0.59	1.11	0.64±0.27	0.76	0.46	0.50	0.48	0.47	0.53±0.13
Dihydrofuran-2(3*H*)-one	3.95	3.69	6.93	2.65	7.27	4.90±2.07	8.37	4.02	4.82	5.62	4.85	5.54±1.68
Sulphur compound												
3-(Methylsulfanyl)propan-1-ol	1.52	0.95	0.59	1.09	2.00	1.23±0.54	1.97	0.64	1.07	1.17	0.76	1.12±0.52
Volatile phenol												
3,5-Di-*tert*-butylphenol	4.17	3.25	3.61	4.08	9.39	4.90±2.54	6.51	5.63	3.44	3.27	1.81	4.13±1.90

nd – not detected; SD – standard deviation. Z1-Z5 – Zweigelt wines, in which alcoholic fermentation (AF) was induced using various yeast strains, and the wines were left to undergo spontaneous MLF; Z1 LAB-Z5 LAB – Zweigelt wines, in which AF was induced using various yeast strains (the same strains as in Z1-Z5 wines), and MLF was carried out by inoculation with lactic acid bacteria.

TABLE 3. Concentrations of volatile compounds in Rondo wines (μg/L) produced with different yeast and malolactic fermentation (MLF) combinations.

Compound	R1	R2	R3	R4	R5	Mean±SD	R1 LAB	R2 LAB	R3 LAB	R4 LAB	R5 LAB	Mean±SD
Alcohol												
Propanol-1-ol	49.20	32.97	55.28	24.88	48.32	42.13±12.67	18.26	46.87	39.06	66.87	66.75	47.56±20.45
2-Methylpropan-1-ol	354.16	276.16	457.58	202.60	288.59	315.82±95.78	204.64	215.66	294.11	500.74	379.76	318.98±123.59
Butan-1-ol	4.18	1.24	2.82	nd	5.01	2.65±2.06	0.13	2.47	3.45	5.22	2.57	2.77±1.84
3-Methylbutan-1-ol	2776.85	2577.03	3611.82	1798.22	2165.92	2585.97±686.64	1869.50	1604.25	2381.25	2796.93	2821.31	2294.65±546.48
Pentan-1-ol	nd	0.96	1.66	0.51	0.33	0.69±0.64	nd	0.30	0.77	1.16	1.10	0.67±0.51
4-Methylpentan-1-ol	nd	0.47	4.13	0.60	1.35	1.31±1.65	2.22	1.28	1.90	1.17	1.78	1.67±0.44
3-Methylpentan-1-ol	3.71	0.91	7.01	1.50	1.56	2.94±2.51	4.33	2.43	3.31	3.23	2.07	3.08±0.88
Hexan-1-ol	97.72	87.73	154.02	66.99	71.45	95.58±34.93	83.96	70.51	106.43	125.72	101.75	97.67±21.25
3-Ethoxypropan-1-ol	0.28	0.59	0.88	0.40	0.42	0.51± 0.23	0.09	0.50	0.67	0.59	0.52	0.47±0.23
(*Z*)-2-Hexen-1-ol	nd	nd	nd	nd	nd	nd	nd	nd	nd	nd	nd	nd
Octen-3-ol	1.10	1.27	1.83	0.90	0.93	1.21±0.38	1.17	0.97	1.93	1.94	1.62	1.53±0.44
Heptan-1-ol	1.22	1.05	2.59	0.89	1.32	1.42±0.68	1.31	1.08	2.87	2.32	1.87	1.89±0.73
2-Ethylhexan-1-ol	6.65	6.13	12.12	2.36	7.36	6.92±3.49	8.54	3.64	10.58	4.34	9.56	7.33±3.15
3-Ethyl-4-methylpentan-1-ol	0.23	0.22	0.33	0.15	0.13	0.21±0.08	0.19	0.15	0.25	0.28	0.22	0.22±0.05
Butane-2,3-diol	121.13	74.36	37.61	68.27	75.70	75.42±29.88	51.76	58.62	102.65	113.04	61.57	77.53±28.14
Octan-1-ol	0.70	0.67	3.11	0.79	2.22	1.50±1.11	3.82	1.68	6.65	4.79	5.78	4.54±1.92
Propane-1,2-diol	2.65	1.43	0.11	0.82	1.68	1.34±0.95	nd	0.28	2.13	2.37	1.19	1.19±1.06
2-(2-Ethoxyethoxy)-ethanol	0.34	0.31	0.35	0.22	0.37	0.32±0.06	0.13	0.19	0.35	0.28	0.24	0.24±0.08
Decan-1-ol	nd	nd	nd	nd	nd	nd	nd	nd	0.04	nd	nd	0.01±0.02
Phenylmethanol	0.15	0.06	0.07	0.02	0.04	0.07±0.05	0.04	0.03	0.07	0.03	0.08	0.05±0.01
2-Phenylethanol	144.07	75.36	61.75	116.18	176.69	114.81±47.59	90.11	83.79	141.58	146.74	117.70	115.98±28.77
Ester												
Ethyl butanoate	13.98	14.26	29.45	5.51	16.27	15.89±8.63	10.39	13.67	21.49	27.31	18.65	18.30±6.62
Ethyl 3-methylbutanoate	3.83	2.58	2.65	1.82	3.71	2.92±0.84	2.26	1.81	1.92	2.71	2.80	2.30±0.45
3-Methylbutyl acetate	72.26	66.66	39.94	43.11	89.77	62.35±20.86	85.87	80.32	18.75	48.36	118.89	70.44±38.22
Hexyl acetate	0.25	0.46	0.16	nd	nd	0.17±0.19	0.37	0.09	0.12	0.12	0.19	0.18±0.11

TABLE 3 continued

Compound	R1	R2	R3	R4	R5	Mean±SD	R1 LAB	R2 LAB	R3 LAB	R4 LAB	R5 LAB	Mean±SD
Ethyl heptanoate	9.28	2.67	7.42	1.01	3.51	4.78±3.45	3.13	2.16	4.37	3.89	0.90	2.89±1.39
Ethyl 2-hydroxypropanoate	95.55	95.39	127.08	72.82	54.21	89.01±27.41	507.93	388.00	487.93	535.72	536.76	491.27±61.23
Methyl octanoate	0.14	0.18	nd	0.20	nd	0.10±0.10	0.16	nd	nd	nd	nd	0.03±0.07
Ethyl octanoate	12.59	22.69	39.00	15.39	24.07	22.75±10.29	14.35	12.45	45.26	32.63	32.30	27.40±13.82
3-Methylbutyl 2-hydroxypropanoate	1.47	1.28	1.35	1.29	1.25	1.33±0.09	7.85	6.16	10.05	10.96	10.45	9.09±2.03
Ethyl decanoate	0.10	0.07	0.40	0.12	0.38	0.21±0.16	nd	0.10	0.40	0.25	0.31	0.21±0.16
Diethyl butanedioate	20.99	15.44	22.12	13.61	20.65	18.56±3.78	12.88	10.99	29.31	14.14	17.36	16.94±7.29
2-Phenylethyl acetate	nd	0.47	0.15	0.21	0.39	0.24±0.19	0.74	0.16	0.53	0.54	1.18	0.63±0.37
Acid												
Acetic acid	54.19	84.16	76.34	63.63	87.78	73.22±14.10	159.17	161.58	197.76	269.61	213.71	200.37±45.22
Propanoic acid	nd	nd	nd	nd	nd	nd	nd	nd	nd	nd	nd	nd
2-Methylpropanoic acid	nd	nd	nd	nd	nd	nd	nd	nd	nd	3.71	11.62	3.07±5.04
Hexanoic acid	9.26	5.05	8.42	9.38	15.39	9.50±3.73	4.48	6.94	12.79	12.17	11.97	9.67±3.73
Octanoic Acid	nd	0.12	1.20	0.38	2.04	0.75±0.86	0.16	1.38	3.16	1.29	2.21	1.64±1.12
Aldehyde												
Benzaldehyde	5.56	10.01	14.58	5.37	12.75	9.65±4.15	5.64	8.76	20.43	5.10	9.36	9.86±6.20
4-Methylbenzaldehyde	0.84	0.13	0.35	0.62	0.31	0.45±0.28	0.65	0.19	0.16	0.74	0.90	0.53±0.34
Ketone												
4-Methyl-3-penten-2-one	368.12	229.16	143.72	149.74	272.35	232.62±93.17	179.93	192.16	248.48	305.21	251.76	235.51±50.64
3-Hydroxybutan-2-one	0.15	0.44	0.79	0.19	0.04	0.32±0.30	0.15	nd	0.47	0.61	0.35	0.32±0.24
Furan compound												
Ethyl 2-furoate	0.48	0.45	0.52	0.32	0.53	0.46±0.08	0.27	0.23	0.44	0.33	0.35	0.32±0.08
Dihydrofuran-2(3*H*)-one	6.66	4.13	4.10	3.25	5.29	4.69±1.32	7.57	6.50	12.99	10.44	8.10	9.12±2.60
Sulphur compound												
3-(Methylsulfanyl)propan-1-ol	1.99	0.74	0.90	1.13	1.71	1.30±0.54	1.08	0.82	1.70	1.43	1.09	1.22±0.34
Volatile phenol												
3,5-Di-*tert*-butylphenol	2.23	1.83	1.57	2.00	1.97	1.92±0.24	2.06	1.26	3.95	2.55	2.69	2.50±0.99

nd – not detected; SD – standard deviation. R1-R5 – Rondo wines, in which alcoholic fermentation (AF) was induced using various yeast strains, and the wines were left to undergo spontaneous MLF; R1 LAB-R5 LAB – Rondo wines, in which AF was induced using various yeast strains (the same strains as in R1-R5 wines), and MLF was carried out by inoculation with lactic acid bacteria.

TABLE 4. Results of one-way analysis of variance (ANOVA) and two-way ANOVA of Rondo and Zweigelt wines produced with different yeast and malolactic fermentation (MLF) strategies.

Compound	One-way ANOVA			Two-way ANOVA		
	Grape variety effect	Yeast effect	MLF effect	Yeast effect	MLF effect	Yeast×MLF effect
Alcohol						
Propanol-1-ol	***	NS	NS	NS	NS	NS
2-Methylpropan-1-ol	NS	NS	NS	NS	NS	NS
Butan-1-ol	**	NS	NS	NS	NS	NS
3-Methylbutan-1-ol	**	NS	NS	NS	NS	NS
Pentan-1-ol	***	NS	NS	NS	NS	NS
4-Methylpentan-1-ol	***	NS	NS	NS	NS	NS
3-Methylpentan-1-ol	***	NS	NS	NS	NS	NS
Hexan-1-ol	***	NS	NS	NS	NS	NS
3-Ethoxypropan-1-ol	***	***	NS	***	NS	NS
(*Z*)-2-Hexen-1-ol	***	*	NS	*	NS	NS
Octen-3-ol	*	NS	NS	NS	NS	NS
Heptan-1-ol	***	NS	NS	NS	NS	NS
2-Ethylhexan-1-ol	*	NS	NS	NS	NS	NS
3-Ethyl-4-methylpentan-1-ol	***	NS	NS	NS	NS	NS
Butane-2,3-diol	NS	NS	NS	NS	NS	NS
Octan-1-ol	***	NS	NS	NS	NS	NS
Propane-1,2-diol	NS	NS	NS	NS	NS	NS
2-(2-Ethoxyethoxy)-ethanol	NS	NS	NS	NS	NS	NS
Decan-1-ol	*	NS	NS	NS	NS	NS
Phenylmethanol	***	*	*	**	*	NS
2-Phenylethanol	**	**	NS	**	NS	**
Ester						
Ethyl butanoate	***	NS	NS	NS	NS	NS
Ethyl 3-methylbutanoate	***	NS	NS	NS	NS	NS
3-Methylbutyl acetate	NS	NS	*	NS	*	NS
Hexyl acetate	NS	NS	NS	NS	NS	NS
Ethyl heptanoate	NS	NS	*	NS	*	NS
Ethyl 2-hydroxypropanoate	*	NS	***	NS	***	NS
Methyl octanoate	NS	NS	*	NS	*	NS
Ethyl octanoate	**	NS	NS	NS	NS	NS
3-Methylbutyl 2-hydroxypropanoate	***	NS	***	NS	***	NS
Ethyl decanoate	NS	NS	NS	NS	NS	NS
Diethyl butanedioate	***	NS	NS	NS	NS	NS
2-Phenylethyl acetate	NS	NS	NS	NS	NS	NS

TABLE 4 continued

Compound	One-way ANOVA			Two-way ANOVA		
	Grape variety effect	Yeast effect	MLF effect	Yeast effect	MLF effect	Yeast×MLF effect
Acid						
Acetic acid	*	NS	***	NS	***	NS
Propanoic acid	**	NS	**	NS	**	NS
2-Methylpropanoic acid	NS	NS	NS	NS	NS	NS
Hexanoic acid	***	NS	NS	NS	NS	NS
Octanoic acid	***	NS	NS	NS	NS	*
Aldehyde						
Benzaldehyde	**	***	NS	***	NS	NS
4-Methylbenzaldehyde	***	NS	NS	NS	NS	NS
Ketone						
4-Methyl-3-penten-2-one	***	NS	NS	NS	NS	NS
3-Hydroxybutan-2-one	NS	**	NS	***	NS	NS
Furan compound						
Ethyl 2-furoate	***	NS	*	NS	*	NS
Dihydrofuran-2(3*H*)-one	NS	NS	**	NS	**	NS
Sulphur compound						
3-(Methylsulfanyl)propan-1-ol	NS	**	NS	**	NS	**
Volatile phenol						
3,5-Di-*tert*-butylphenol	**	NS	NS	NS	NS	NS

Statistical significance: *significant at $p<0.05$, **significant at $p<0.01$, *** significant at $p<0.001$, NS – not significant.

and yeast×MLF interaction influenced the concentrations of phenylmethanol and 2-phenylethanol, respectively (Table 4). Regarding yeast×MLF interaction, according to Gammacurta *et al*. [2017], 3-methylbutan-1-ol was the only higher alcohol not affected by yeast/LAB combination, while concentrations of other alcohols, such as propan-1-ol, 2-methylpropan-1-ol, and 2-methylbutan-1-ol, differed significantly depending on yeast/LAB combination.

Concentrations of half of the esters: ethyl butanoate, ethyl 3-methylbutanoate, ethyl 2-hydroxypropanoate, ethyl octanoate, 3-methylbutyl 2-hydroxypropanoate, and diethyl butanedioate differed significantly according to the grape variety (Table 4). However, Liu *et al*. [2017] found that grape variety significantly impacted concentrations of most esters. Ethyl esters are produced enzymatically by yeast from ethanolysis of acetyl-CoA formed during fatty acid synthesis or degradation [Liu *et al*., 2017; Stój *et al*., 2017a]. The concentrations of any esters were not significantly affected by yeast strain nor by yeast×MLF interaction (Table 4). On the contrary, Gammacurta *et al*. [2014] observed a significant effect of yeast strain on all esters in the red wines studied. Blanco *et al*. [2014] found that the concentrations of several esters (ethyl butanoate, hexyl acetate, 2-phenylethyl acetate, diethyl butanedioate) were independent of yeast strain, while other esters (3-methylbutyl acetate and ethyl octanoate) were yeast strain-dependent. Regarding yeast×MLF interaction, Gammacurta *et al*. [2017] reported that among 40 quantified esters, only seven were not affected by the yeast/LAB combination. Among seven esters, the concentrations of hexyl acetate and ethyl octanoate (also identified in our study) did not depend on the combination of microorganisms. MLF significantly influenced the concentrations of almost half of the esters, *i.e.* 3-methylbutyl acetate (isoamyl acetate), ethyl heptanoate, ethyl 2-hydroxypropanoate (ethyl lactate), methyl octanoate, and 3-methylbutyl 2-hydroxypropanoate (isoamyl lactate). Gammacurta *et al*. [2014] considered that the impact of LAB on esters was controversial because results differed between studies. Several reports showed changes in ester concentrations in wines after MLF with *O. oeni* due to its esterase activity [Brizuela *et al.*, 2018; Diez-Ozaeta *et al.*, 2021; Sumby *et al.*, 2013]. However, Gammacurta *et al*. [2014] found that levels of esters were slightly affected by the LAB. In our study, the ethyl lactate concentration was higher in the wines subjected to induced MLF than in those subjected to spontaneous MLF. Ethyl lactate is one

of the most characteristic aromatic compounds produced during MLF and a marker of LAB activity. Its content increased following MLF [Abrahamse & Bartowsky, 2012; Costello *et al*., 2012; Lasik-Kurdyś *et al*., 2018].

We observed a grape variety effect on most acids, *i.e.* acetic acid, propanoic acid, hexanoic acid, and octanoic acid, whereas Liu *et al*. [2017] found significant differences for almost half of the acids. Fatty acids could be produced *via* anabolic pathways by yeast or during β-oxidation of long-chain fatty acids [Stój *et al*., 2017a]. The concentrations of any acids did not vary depending on yeast strain (Table 4). According to Blanco *et al*. [2014], only the hexanoic acid content of red wines depended on the yeast strain. MLF significantly modulated half of the acid (acetic acid and propanoic acid) contents in our study (Table 4). The concentration of acetic acid was higher in the wines subjected to induced MLF than in those subjected to spontaneous MLF (Table 2 and Table 3). The increase in acetic acid content is due to the metabolism of citric acid [Abrahamse & Bartowsky, 2012; Styger *et al*., 2011]. The octanoic acid concentration was significantly impacted by yeast×MLF interaction (Table 4), which agreed with the results obtained by Gammacurta *et al*. [2017]. Concentrations of 2-methylpropanoic acid and hexanoic acid were not significantly modulated by yeast/LAB combinations, while Gammacurta *et al*. [2017] reported significant differences in the contents of these acids between microorganism combinations.

Regarding the two quantified aldehydes, concentrations of benzaldehyde and 4-methylbenzaldehyde differed significantly between grape varieties (Table 4). Yeast strain significantly impacted the concentration of benzaldehyde, similarly to the work of Tufariello *et al*. [2014] and contrary to the work of Blanco *et al*. [2014]. Neither MLF nor yeast×MLF interaction affected aldehyde concentrations.

The concentration of 4-methyl-3-penten-2-one differed significantly between wines produced from different grape varieties (Table 4). Grape variety did not affect 3-hydroxybutan-2-one (acetoin) concentration, contrary to the report of Liu *et al*. [2017]. The concentration of 3-hydroxybutan-2-one was significantly affected by yeast strain, which agreed with results obtained by Blanco *et al*. [2014]. The concentrations of the two identified ketones did not differ significantly upon the influence of either MLF or yeast×MLF interaction (Table 4). Considering the interactions, Gammacurta *et al*. [2017] observed no significant differences in the concentration of 3-hydroxybutan-2-one. Acetoin is produced from the metabolism of citric acid by lactic acid bacteria [Malherbe *et al*., 2012; Styger *et al*., 2011; Tempère *et al*., 2018]. In our study, there was no trend in its concentration in Zweigelt and Rondo wines subjected to spontaneous and induced MLF. Its concentration was higher in a few wines in which MLF was spontaneous and in a few wines in which MLF was induced. According to López *et al*. [2011], spontaneous MLF resulted in a higher content of acetoine in wines, whereas Malherbe *et al*. [2012] found that acetoin concentration was affected by the bacterial strain used for MLF.

Considering the two quantified furan compounds, grape variety significantly impacted the content of ethyl 2-furoate (Table 4). In turn, the concentration of dihydrofuran-2(3*H*)-one was not influenced by the grape variety, and it is in agreement with the results obtained by Liu *et al*. [2017]. The yeast strain and yeast×MLF interaction did not affect ethyl 2-furoate and dihydrofuran-2(3*H*)-one. Similarly, the yeast did not affect ethyl 2-furoate in studies performed by Callejon *et al*. [2010]. Concentrations of both furan compounds, ethyl 2-furoate and dihydrofuran-2(3*H*)-one (butyrolactone), depend on MLF. Butyrolactone is particularly produced during MLF [Tempère *et al*., 2018]. In our study, the concentration of butyrolactone was higher in most wines subjected to induced MLF. According to López *et al*. [2011], spontaneous MLF resulted in wines with a higher butyrolactone concentration.

The concentration of 3-(methylsulfanyl)propan-1-ol (Table 4) was not affected by grape variety and MLF, but changes in its values were determined as affected by yeast strain and yeast×MLF interaction.

Among the analyzed factors, *i.e*. grape variety, yeast, MLF, yeast×MLF interaction, only grape variety significantly affected the concentration of 3,5-di-*tert*-butylphenol (Table 4).

We showed that in the case of Polish wines produced from grape varieties grown in a cold climate, the grape variety was the factor eliciting a significant impact on the highest number of identified volatile compounds, whereas microorganisms used had a lesser effect. In our study, malic acid was not completely reduced during MLF (spontaneous and induced), similarly to the experiment conducted by Lasik-Kurdyś *et al.* [2018]. Lactic acid has an antimicrobial activity, and at a higher concentration, it can also inhibit LAB. In the case of high-acid musts, a total reduction of malic acid can be impossible [Lasik-Kurdyś *et al.*, 2017].

Figure 1 presents the FTIR spectra of the wines. For more straightforward analysis, discussion, and comparison of the tested wines, the spectra were normalized to the maximum at 3327 cm^{-1}. Table 5 presents all the characteristic bands of wine spectra and appropriate vibrations assigned to the functional groups. All spectra of wines (R1-R5, Z1-Z5, R1 LAB-R5 LAB and Z1 LAB-Z5 LAB) had very intense and similar bands (Figure 1). They exhibited bands characteristic of water and ethanol absorption. The broad peak of 3800–3000 cm^{-1} results mainly from stretching vibrations in water molecules, ν(-OH), and in alcohol or phenol molecules [Basalekou *et al*., 2019; Geană *et al*., 2019]. Characteristic bands for vibrations of water molecules are absorption bands with a maximum of about 990 and 1460 cm^{-1} (stretching and deformation – related to the third overtone of these bands) and characteristic deformation bands with a maximum at about 1600 cm^{-1} [Geană *et al*., 2019; Hu *et al*., 2019]. Alcohol-related absorption bands were observed (for all samples) at 2850–3000 cm^{-1} with characteristic peaks at 2937 and 2881 cm^{-1} (Figure 1, Table 5) corresponding to the symmetric and asymmetric stretching vibrations of the CH_2 and CH_3 groups. The build-up of these bands with a broad and noticeably flattened maximum in the range of 2400–2705 cm^{-1} could correspond to a combination of C-H stretching vibrations and overtones of these vibrations originating from molecules of ethanol and partly sugar [Basalekou *et al*., 2019; Geană *et al*., 2019; Hu *et al*., 2019]. Vibrations originating from primary alcohols and glycerol with maximum bands at 1087 and 1050 cm^{-1}, respectively, are related to

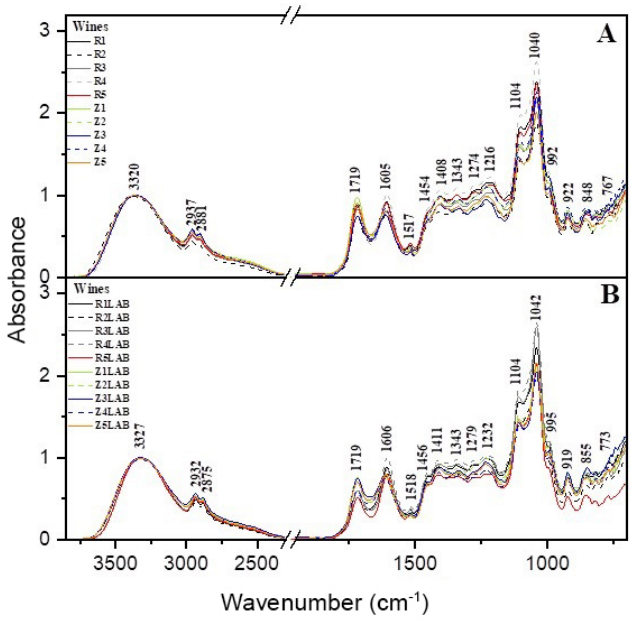

FIGURE 1. Normalized Fourier transform infrared (FTIR) spectra of wines. R1-R5 – Rondo wines, in which alcoholic fermentation (AF) was induced using various yeast strains, and the wines were left to undergo spontaneous malolactic fermentation (MLF); Z1-Z5 – Zweigelt wines, in which AF was induced using various yeast strains, and the wines were left to undergo spontaneous MLF; R1 LAB-R5 LAB – Rondo wines, in which AF was induced using various yeast strains (the same strains as in R1-R5 wines), and MLF was carried out by inoculation with lactic acid bacteria; Z1 LAB-Z5 LAB – Zweigelt wines, in which AF was induced using various yeast strains (the same strains as in Z1-Z5 wines), and MLF was carried out by inoculation with lactic acid bacteria.

strong C-O stretching vibrations [Martelo-Vidal *et al*., 2013]. The bands in the 3000–2800 cm^{-1} region were most likely due to stretching vibrations of C–H bonds of hydrocarbons, O–H bonds of carboxylic acids, and asymmetric stretching vibrations of C–H bonds of methyl ($–CH_3$) groups: polyols (glycerol), free phenolic acids and catechins [Geană *et al*., 2019].

The vibration area between 1800–1000 cm^{-1} was characteristic of C-OH stretching, CH_3 and CH_2 deformation, C=C stretching, and C≡N stretching vibrations (Table 5). This area derives from such components as phenols, alcohols, aldehydes, higher alcohols, polyols, acids, sugars, volatile acids and amino acids [Basalekou *et al*., 2020; Hu *et al*., 2019; Versari *et al*., 2014]. The spectral range of about 1850–1590 cm^{-1} was related to the combination of stretching vibrations -OH, $-CH_3$ (first overtone), $-CH_2$, -CH (first overtone) derived from ethanol [Geană *et al*., 2019; Martelo-Vidal *et al*., 2013].

Very interesting vibrations occured in the spectral region of 1580–950 cm^{-1} (Figure 1). In this area, the vibrations show functional groups characteristic for many wine compounds; therefore, there were more considerable differences between the FTIR spectra obtained in this region. Basically, in the region of 1580–950 cm^{-1}, there were vibrations from phenols of the wines tested. The area between 1460 and 1280 cm^{-1} was very complex and provided information about stretching vibrations of the carbonyl group C=O, stretching vibrations C=C, CH_2, and C-H derived from molecules of aldehydes, carboxylic acids, proteins, and esters [Tarantilis *et al*., 2008].

TABLE 5. The maxima of the Fourier transform infrared absorption bands of wines produced with different yeast and malolactic fermentation (MLF) strategies, with assignment of particular vibrations to the respective wine samples. Spectra registered within the range of 700–3700 cm^{-1}.

R1-R5 Z1-Z5	R1 LAB-R5 LAB Z1 LAB-Z5 LAB	Type and origin of vibrations
Wavenumber (cm^{-1})		
3320	3327	ν(-OH) in carboxylic acids
2937	2932	ν_w(-CH) of hydrocarbons $\nu_m(–CH_3)$
2881	2875	
1719	1719	ν_m(-C=O)
1605	1606	δ(-OH) and ν(C=C)
1517	1518	ν(C=C) and ν(C–N)
1454	1456	ν(C=C), $\delta(–CH_3)$, $\delta_m(–CH_2)$ and δ(–CH)
1408	1411	
1343	1343	ν(C=C), $\delta(–CH_2)$
1274	1279	$\delta(-CH_2-)$
1216	1232	ν_m(-C-O) or $\delta_m(-CH_2-)$
1104	1104	ν_{st}(-C-O) and ν_w(O–H) second overtones
1040	1042	ν_m(-C-O)
992	995	δ_w(-HC=CH-, *trans*-) out-of-plane $\delta(-(CH_2)_n-$ and –HC=CH- (*cis*-) (scissor)
922	919	
848	855	
767	773	

ν – stretching vibrations; δ – deformation vibrations; st – strong; m – medium; w – weak; R1-R5 – Rondo wines, in which alcoholic fermentation (AF) was induced using various yeast strains, and the wines were left to undergo spontaneous MLF; Z1-Z5 – Zweigelt wines, in which AF was induced using various yeast strains, and the wines were left to undergo spontaneous MLF; R1 LAB-R5 LAB – Rondo wines, in which AF was induced using various yeast strains (the same strains as in R1-R5 wines), and MLF was carried out by inoculation with lactic acid bacteria; Z1 LAB-Z5 LAB – Zweigelt wines, in which AF was induced using various yeast strains (the same strains as in Z1-Z5 wines), and MLF was carried out by inoculation with lactic acid bacteria

The ester bands showed very characteristic peaks at about 1460–1400 cm^{-1} [Geană *et al*., 2019; Tarantilis *et al*., 2008]. It is also worth emphasizing the bands with maxima of around 1232, 1110–1100, and 1070–990 cm^{-1}, which correspond to C–O and O–H stretching vibrations (second overtone) derived from sugars and organic acids [Ferreiro-González *et al*., 2019; Hu *et al*., 2019; Martelo-Vidal *et al*., 2013; Tarantilis *et al*., 2008].

Spectral analysis showed differences in the area for groups associated with alcohols, esters, and acids. It was most likely related to the grape varieties used, however, the main constituents formed during fermentation could also explain the difference. The wines marked as LAB (induced MLF) in the area mentioned above differed from the wines which were left to undergo spontaneous MLF.

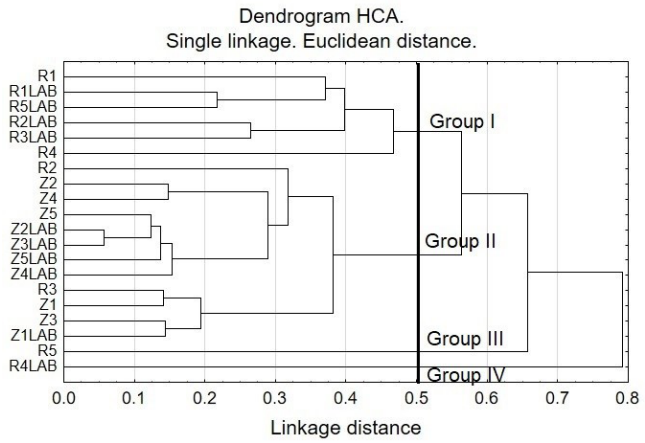

FIGURE 2. Dendrogram of hierarchical cluster analysis (HCA) of wines based on the Fourier transform infrared (FTIR) spectral data for wavenumber range of 1580–950 cm^{-1}. R1-R5 – Rondo wines, in which alcoholic fermentation (AF) was induced using various yeast strains, and the wines were left to undergo spontaneous malolactic fermentation (MLF); Z1-Z5 – Zweigelt wines, in which AF was induced using various yeast strains, and the wines were left to undergo spontaneous MLF; R1 LAB-R5 LAB – Rondo wines, in which AF was induced using various yeast strains (the same strains as in R1-R5 wines), and MLF was carried out by inoculation with lactic acid bacteria; Z1 LAB-Z5 LAB – Zweigelt wines, in which AF was induced using various yeast strains (the same strains as in Z1-Z5 wines), and MLF was carried out by inoculation with lactic acid bacteria.

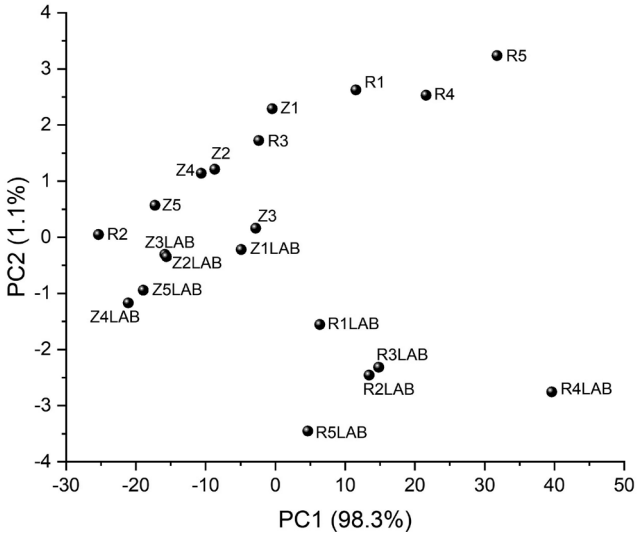

FIGURE 3. The scattered scores plot of principal component analysis (PCA) based on Fourier transform infrared (FTIR) spectra fingerprint of wines. R1-R5 – Rondo wines, in which alcoholic fermentation (AF) was induced using various yeast strains, and the wines were left to undergo spontaneous MLF; Z1-Z5 – Zweigelt wines, in which AF was induced using various yeast strains, and the wines were left to undergo spontaneous malolactic fermentation (MLF); R1 LAB-R5 LAB – Rondo wines, in which AF was induced using various yeast strains (the same strains as in R1-R5 wines), and MLF was carried out by inoculation with lactic acid bacteria; Z1 LAB-Z5 LAB – Zweigelt wines, in which AF was induced using various yeast strains (the same strains as in Z1-Z5 wines), and MLF was carried out by inoculation with lactic acid bacteria.

HCA was performed on FTIR spectra to identify similarities or dissimilarities between the considered samples of wine [Brereton, 2003]. Figure 2 shows the dendrogram obtained from the 20 wine samples. Considering the cut-off of 0.5 dissimilarity units, four clusters were distinguished. The first cluster (Group I) aggregated on the far-left arm of the dendrogram and was formed by six wine samples, while the second cluster (Group II) was the biggest cluster and comprised all samples of Zweigelt wine and two samples of Rondo – R2 and R3. This result suggests these wines have physicochemical properties more similar than the others. The last two Rondo wine samples – R5 and R4 LAB aggregated in third and fourth clusters. The hierarchical cluster analysis showed that the placement of the wine samples on the dendrogram depended on the grape variety and type of MLF (spontaneous or induced).

To more precisely discriminate the relationship between the investigated wines, the 1580–950 cm^{-1} bands were selected as their characteristic spectral fingerprint. The PCA was set as the primary choice for analysis. PCA transforms the original high-dimensional variables into the new low-dimensional variables [Abdi & Williams, 2010; Xu *et al*., 2006]. According to the Scree test criterion, we selected two main components for analysis. Figure 3 shows a two-dimensional scatter plot of the principal components (PC1 and PC2) obtained from the FTIR spectra of different wine samples. The PC1 was the most critical and explained 98.3% of the variance; the second principal component contributed 1.1% to the variance. The first two principal components explained 99.4% of the variance, and only 0.6% of the information was lost. It indicates that the first two principal components expressed 99.4% of all the information. Figure 3 and Figure S3 (supplementary materials) show the relative location of the FTIR spectra in the two-dimensional graph. The location was related to their similarity distance shown by HCA (Figure 2). For example, the close location of Zweigelt wines in the PCA plot was related to their close locations in the HCA graph. Samples R4 LAB and R5, which did not clustered with the other Rondo wines (Figure 2), were obviously distinguished from other samples shown in the two-dimensional PCA graph (Figure 3). Samples of the Zweigelt variety distinguished one another in the same category, as shown on the grouped-scatter plot for all samples (Figure S3). These samples differed only to a slight extent. As it is known, the scatter plot does not classify the objects in every level of distance as accurately as the clustering graph. Still, it can reflect the relationships between the investigated wines. Therefore, the use of complementary analytical methods provides researchers profound knowledge of the wine differences.

CONCLUSIONS

Among the factors studied, the grape variety significantly affected most volatile compounds, most alcohols and acids, and half of the esters. The yeast strains selected in this study had no significant effect on the concentration of either any ester or any acid. MLF significantly influenced the concentration of almost half of esters and acids. Among forty-six quantified compounds, only three were affected by yeast×MLF interaction. Knowledge of the influence of grape, yeast, MLF, and yeast×MLF interaction on wine aroma may help

producers make informed decisions. Further investigations into the effects of the wine matrix on the production of volatile compounds by microorganisms are also required.

The results of FTIR measurements showed differences, most remarkable in the range of 1750–1500 and below 1500 cm^{-1}. These differences are mainly related to various concentrations of volatile compounds, such as alcohols, acids, and esters, in the wines. The results obtained in the experiment may contribute to the expansion of the wine database.

SUPPLEMENTARY MATERIALS

The following are available online at http://journal.pan.olsztyn.pl/Impact-of-Grape-Variety-Yeast-and-Malolactic-Fermentation-on-Volatile-Compounds-and,145665,0,2.html. The concentrations of malic and lactic acids in the final wines; chromatograms of volatile compounds of Zweigelt and Rondo wines, and PCA results.

CONFLICT OF INTERESTS

Authors declare no conflict of interests.

ORCID IDs

T. Czernecki https://orcid.org/0000-0002-3277-2326
A. Matwijczuk https://orcid.org/0000-0003-2630-120X
A. Niemczynowicz https://orcid.org/0000-0002-4370-3326
B. Sosnowska https://orcid.org/0000-0001-9719-9359
A. Stój https://orcid.org/0000-0003-1824-2051

REFERENCES

1. Azzolini, M., Fedrizzi, B., Tosi, E., Finato, F., Vagnoli, P., Scrinzi, C., Zapparoli, G. (2012). Effects of *Torulaspora delbrueckii* and *Saccharomyces cerevisiae* mixed cultures on fermentation and aroma of Amarone wine. *European Food Research and Technology*, *235*, 303–313. https://doi.org/10.1007/s00217-012-1762-3
2. Abdi, H., Williams, L.J. (2010). Principal component analysis. *Wiley Interdisciplinary Reviews: Computational Statistics, 2*(4), 433–459. https://doi.org/10.1002/wics.101
3. Abrahamse, C.E., Bartowsky, E.J. (2012). Timing of malolactic fermentation inoculation in Shiraz grape must and wine: influence on chemical composition. *World Journal of Microbiology and Biotechnology, 28*(1), 255–265. https://doi.org/10.1007/s11274-011-0814-3
4. Antalick, G., Perello, M.C., de Revel, G. (2013). Co-inoculation with yeast and LAB under winery conditions: modification of the aromatic profile of Merlot wines. *South African Journal of Enology and Viticulture, 34*(2), 223–232. https://doi.org/10.21548/34-2-1098
5. Basalekou, M., Kallithraka, S., Tarantilis, P.A., Kotseridis, Y., Pappas, C. (2019). Ellagitannins in wines: Future prospects in methods of analysis using FT-IR spectroscopy. *LWT – Food Science and Technology, 101*, 48–53. https://doi.org/10.1016/j.lwt.2018.11.017
6. Basalekou, M., Pappas, C., Tarantilis, P.A., Kallithraka, S. (2020). Wine authenticity and traceability with the use of FT-IR. *Beverages, 6*(2), art. no. 30. https://doi.org/10.3390/beverages6020030
7. Blanco, P., Mirás-Avalos, J.M., Pereira, E., Fornos, D., Orriols, I. (2014). Modulation of chemical and sensory characteristics of red wine from Mencía by using indigenous *Saccharomyces cerevisiae* yeast strains. *Journal International des Sciences de la Vigne et du Vin, 48*(1), 63–74. https://doi.org/10.20870/oeno-one.2014.48.1.1659
8. Brizuela, N.S., Bravo-Ferrada, B.M., Pozo-Bayón, M.Á., Semorile, L., Tymczyszyn, E.E. (2018). Changes in the volatile profile of Pinot noir wines caused by Patagonian *Lactobacillus plantarum* and *Oenococcus oeni* strains. *Food Research International*, *106*, 22–28. https://doi.org/10.1016/j.foodres.2017.12.032
9. Brereton, R.G. (2003). Pattern recognition. Chapter 4. In R.G. Brereton (Ed.) *Chemometrics: Data Analysis for the Laboratory and Chemical Plant.* John Wiley & Sons, Chichester, pp. 183–269. https://doi.org/10.1002/0470863242.ch4
10. Callejon, R.M., Clavijo, A., Ortigueira, P., Troncoso, A.M., Paneque, P., Morales, M.L. (2010). Volatile and sensory profile of organic red wines produced by different selected autochthonous and commercial *Saccharomyces cerevisiae* strains. *Analytica Chimica Acta, 660*(1–2), 68–75. https://doi.org/10.1016/j.aca.2009.09.040
11. Cañas, P.M.I., Pérez-Martín, F., Romero, E.G., Prieto, S.S., Herreros, M.D.L.L.P. (2012). Influence of inoculation time of an autochthonous selected malolactic bacterium on volatile and sensory profile of Tempranillo and Merlot wines. *International Journal of Food Microbiology*, *156*(3), 245–254. https://doi.org/10.1016/j.ijfoodmicro.2012.03.033
12. Cioch-Skoneczny, M., Grabowski, M., Satora, P., Skoneczny, S., Klimczak, K. (2021). The use of yeast mixed cultures for deacidification and improvement of the composition of cold climate grape wines. *Molecules*, *26*(9), art. no. 2628. https://doi.org/10.3390/molecules26092628
13. Costello, P.J., Francis, I.L., Bartowsky, E.J. (2012). Variations in the effect of malolactic fermentation on the chemical and sensory properties of Cabernet Sauvignon wine: Interactive influences of *Oenococcus oeni* strain and wine matrix composition. *Australian Journal of Grape and Wine Research, 18*(3), 287–301. https://doi.org/10.1111/j.1755-0238.2012.00196.x
14. Diez-Ozaeta, I., Lavilla, M., Amárita, F. (2021). Wine aroma profile modification by *Oenococcus oeni* strains from Rioja Alavesa region: selection of potential malolactic starters. *International Journal of Food Microbiology*, *356*, art. no. 109324. https://doi.org/10.1016/j.ijfoodmicro.2021.109324
15. Duarte, W.F., Dias, D.R., Oliveira, J.M., Teixeira, J.A., De Almeida e Silva, J.B., Schwan, R.F. (2010). Characterization of different fruit wines made from cacao, cupuassu, gabiroba, jaboticaba and umbu. *LWT – Food Science and Technology, 43*(10), 1564–1572. https://doi.org/10.1016/j.lwt.2010.03.010
16. Englezos, V., Rantsiou, K., Cravero, F., Torchio, F., Giacosa, S., Ortiz-Julien, A., Gerbi, V., Rolle, L. Cocolin, L. (2018). Volatile profiles and chromatic characteristics of red wines produced

with *Starmerella bacillaris* and *Saccharomyces cerevisiae*. *Food Research International*, *109*, 298–309. https://doi.org/10.1016/j.foodres.2018.04.027

17. Ferreiro-González, M., Ruiz-Rodríguez, A., Barbero, G.F., Ayuso, J., Álvarez, J.A., Palma, M., Barroso, C.G. (2019). FT-IR, Vis spectroscopy, color and multivariate analysis for the control of ageing processes in distinctive Spanish wines. *Food Chemistry, 277*, 6–11. https://doi.org/10.1016/j.foodchem.2018.10.087
18. Gammacurta, M., Marchand, S., Albertin, W., Moine, V., de Revel, G. (2014). Impact of yeast strain on ester levels and fruity aroma persistence during aging of Bordeaux red wines. *Journal of Agricultural and Food Chemistry, 62*(23), 5378–5389. https://doi.org/10.1021/jf500707e
19. Gammacurta, M., Marchand, S., Moine, V., de Revel, G. (2017). Influence of different yeast/lactic acid bacteria combinations on the aromatic profile of red Bordeaux wine. *Journal of the Science of Food and Agriculture, 97*(12), 4046–4057. https://doi.org/10.1002/jsfa.8272
20. Geană, E.I., Ciucure, C.T., Apetrei, C., Artem, V. (2019). Application of spectroscopic UV-Vis and FT-IR screening techniques coupled with multivariate statistical analysis for red wine authentication: Varietal and vintage year discrimination. *Molecules, 24*(22), art. no. 4166. https://doi.org/10.3390/molecules24224166
21. Hu, X.Z., Liu, S.Q., Li, X.H., Wang, C.X., Ni, X.L., Liu, X., Wang, Y, Liu, Y., Xu, C.H. (2019). Geographical origin traceability of Cabernet Sauvignon wines based on infrared fingerprint technology combined with chemometrics. *Scientific Reports, 9*, art. no. 8256. https://doi.org/10.1038/s41598-019-44521-8
22. Jørgensen, U., Hansen, M., Christensen, L.P., Jensen, K., Kaack, K. (2000). Olfactory and quantitative analysis of aroma compounds in elder flower (*Sambucus nigra* L.) drink processed from five cultivars. *Journal of Agricultural and Food Chemistry, 48*(6), 2376–2383. https://doi.org/10.1021/jf000005f
23. Lasik-Kurdyś, M., Majcher, M., Nowak, J. (2018). Effects of different techniques of malolactic fermentation induction on diacetyl metabolism and biosynthesis of selected aromatic esters in cool-climate grape wines. *Molecules, 23*(10), art. no. 2549. https://doi.org/10.3390/molecules23102549
24. Lasik-Kurdyś, M., Gumienna, M., Nowak, J. (2017). Influence of malolactic bacteria inoculation scenarios on the efficiency of the vinification process and the quality of grape wine from the Central European region. *European Food Research and Technology*, *243*, 2163–2173. https://doi.org/10.1007/s00217-017-2919-x
25. Liu, J., Arneborg, N., Toldam-Andersen, T.B., Petersen, M.A., Bredie, W.L. (2017). Effect of sequential fermentations and grape cultivars on volatile compounds and sensory profiles of Danish wines. *Journal of the Science of Food and Agriculture, 97*(11), 3594–3602. https://doi.org/10.1002/jsfa.8218
26. López, R., López-Alfaro, I., Gutiérrez, A.R., Tenorio, C., Garijo, P., González-Arenzana, L., Santamaría, P. (2011). Malolactic fermentation of Tempranillo wine: contribution of the lactic acid bacteria inoculation to sensory quality and chemical composition. *International Journal of Food Science & Technology, 46*(11), 2373–2381. https://doi.org/10.1111/j.1365-2621.2011.02759.x
27. Malherbe, S., Tredoux, A.G., Nieuwoudt, H.H., du Toit, M. (2012). Comparative metabolic profiling to investigate the contribution of *O. oeni* MLF starter cultures to red wine composition. *Journal of Industrial Microbiology & Biotechnology, 39*(3), 477–494. https://doi.org/10.1007/s10295-011-1050-4
28. Mallouchos, A., Loukatos, P., Bekatorou, A., Koutinas, A., Komaitis, M. (2007). Ambient and low temperature winemaking by immobilized cells on brewer's spent grains: Effect on volatile composition. *Food Chemistry, 104*(3), 918–927. https://doi.org/10.1016/j.foodchem.2006.12.047
29. Martelo-Vidal, M.J., Domínguez-Agis, F., Vázquez, M. (2013). Ultraviolet/visible/near-infrared spectral analysis and chemometric tools for the discrimination of wines between subzones inside a controlled designation of origin: A case study of Rías Baixas. *Australian Journal of Grape and Wine Research, 19*(1), 62–67. https://doi.org/10.1111/ajgw.12003
30. Mendes, B., Gonçalves, J., Câmara, J.S. (2012). Effectiveness of high-throughput miniaturized sorbent- and solid phase microextraction techniques combined with gas chromatography-mass spectrometry analysis for a rapid screening of volatile and semi-volatile composition of wines – a comparative study. *Talanta, 88*, 79–94. https://doi.org/10.1016/j.talanta.2011.10.010
31. Ruocco, S., Perenzoni, D., Angeli, A., Stefanini, M., Rühl, E., Patz, C.D., Mattivi, F., Rauhut, D., Vrhovsek, U. (2019). Metabolite profiling of wines made from disease-tolerant varieties. *European Food Research and Technology, 245*(9), 2039–2052. https://doi.org/10.1007/s00217-019-03314-z
32. Shimoda, M., Shigematsu, H., Shiratsuchi, H., Osajima, Y. (1995). Comparison of the odor concentrates by SDE and adsorptive column method from green tea infusion. *Journal of Agricultural and Food Chemistry, 43*(6), 1616–1620. https://doi.org/10.1021/jf00054a037
33. Song, S., Tanga, Q., Hayat, K., Karangwa, E., Zhang, X., Xiao, Z. (2014). Effect of enzymatic hydrolysis with subsequent mild thermal oxidation of tallow on precursor formation and sensory profiles of beef flavours assessed by partial least squares regression. *Meat Science, 96*(3), 1191–1200. https://doi.org/10.1016/j.meatsci.2013.11.008
34. Stój, A., Czernecki, T., Domagała, D., Targoński, Z. (2017a). Comparative characterization of volatile profiles of French, Italian, Spanish, and Polish red wines using headspace solid-phase microextraction/gas chromatography-mass spectrometry. *International Journal of Food Properties, 20*(sup1), S830–S845. https://doi.org/10.1080/10942912.2017.1315590
35. Stój, A., Czernecki, T., Domagala, D., Targoński, Z. (2017b). Application of volatile compound analysis for distinguishing between red wines from Poland and from other European countries. *South African Journal of Enology and Viticulture, 38*(2), 245–263. https://doi.org/10.21548/38-2-2079
36. Stój, A. (2020a). Influence of yeast and lactic acid bacteria on the content of volatile compounds and other oenological parameters of wines. *Postępy Mikrobiologii – Advancements of Microbiology, 59*(2), 167–178 (in Polish; English abstract). https://doi.org/10.21307/PM-2020.59.2.013
37. Stój, A., Kapusta, I., Domagała, D. (2020b). Classification of red wines produced from Zweigelt and Rondo grape varieties based on the analysis of phenolic compounds by UPLC-PDA-MS/MS. *Molecules, 25*(6), art. no. 1342. https://doi.org/10.3390/molecules25061342

38. Sumby, K.M., Jiranek, V., Grbin, P.R. (2013). Ester synthesis and hydrolysis in an aqueous environment, and strain specific changes during malolactic fermentation in wine with *Oenococcus oeni*. *Food Chemistry*, *141*(3), 1673–1680. https://doi.org/10.1016/j.foodchem.2013.03.087
39. Styger, G., Prior, B., Bauer, F.F. (2011). Wine flavor and aroma. *Journal of Industrial Microbiology & Biotechnology, 38*(9), 1145–1159. https://doi.org/10.1007/s10295-011-1018-4
40. Tarantilis, P.A., Troianou, V.E., Pappas, C.S., Kotseridis, Y.S., Polissiou, M.G. (2008). Differentiation of Greek red wines on the basis of grape variety using attenuated total reflectance Fourier transform infrared spectroscopy. *Food Chemistry, 111*(1), 192–196. https://doi.org/10.1016/j.foodchem.2008.03.020
41. Tempère, S., Marchal, A., Barbe, J.C., Bely, M., Masneuf-Pomarede, I., Marullo, P., Albertin, W. (2018). The complexity of wine: clarifying the role of microorganisms. *Applied Microbiology and Biotechnology, 102*(9), 3995–4007. https://doi.org/10.1007/s00253-018-8914-8
42. Tristezza, M., di Feo, L., Tufariello, M., Grieco, F., Capozzi, V., Spano, G., Mita, G. (2016). Simultaneous inoculation of yeasts and lactic acid bacteria: Effects on fermentation dynamics and chemical composition of Negroamaro wine. *LWT – Food Science and Technology*, *66*, 406–412. https://doi.org/10.1016/j.lwt.2015.10.064
43. Tufariello, M., Chiriatti, M.A., Grieco, F., Perrotta, C., Capone, S., Rampino, P., Tristezza, M., Mita, G., Grieco, F. (2014). Influence of autochthonous *Saccharomyces cerevisiae* strains on volatile profile of Negroamaro wines. *LWT – Food Science and Technology, 58*(1), 35–48. https://doi.org/10.1016/j.lwt.2014.03.016
44. Versari, A., Laurie, V.F., Ricci, A., Laghi, L., Parpinello, G.P. (2014). Progress in authentication, typification and traceability of grapes and wines by chemometric approaches. *Food Research International, 60*, 2–18. https://doi.org/10.1016/j.foodres.2014.02.007
45. Vilanova, M., Cortés, S., Santiago, J.L., Martínez, C., Fernández, E. (2007). Aromatic compounds in wines produced during fermentation: effect of three red cultivars. *International Journal of Food Properties, 10*(4), 867–875. https://doi.org/10.1080/10942910601161615
46. Welke, J.E., Manfroi, V., Zanus, M., Lazzarotto, M., Zini, C.A. (2012). Characterization of the volatile profile of Brazilian Merlot wines through comprehensive two dimensional gas chromatography time-of-flight mass spectrometric detection. *Journal of Chromatography A, 1226*, 124–139. https://doi.org/10.1016/j.chroma.2012.01.002
47. Wojdyło, A., Samoticha, J., Nowicka, P., Chmielewska, J. (2018). Characterisation of (poly)phenolic constituents of two interspecific red hybrids of Rondo and Regent (*Vitis vinifera*) by LC-PDA-ESI-MS QTof. *Food Chemistry, 239*, 94–101. https://doi.org/10.1016/j.foodchem.2017.06.077
48. Xu, C.J., Liang, Y.Z., Chau, F.T., Vander Heyden, Y. (2006). Pretreatments of chromatographic fingerprints for quality control of herbal medicines. *Journal of Chromatography A, 1134*(1–2), 253–259. https://doi.org/10.1016/j.chroma.2006.08.060
49. Zhu, F., Du, B., Li, J. (2016). Aroma compounds in wine. In A. Morata, I. Loira (Eds.), *Grape and Wine Biotechnology*, Books on Demand GmbH, Norderstedt, Germany, pp. 273–283. https://doi.org/10.5772/65102

Pol. J. Food Nutr. Sci., 2022, Vol. 72, No. 1, pp. 57–67
On-line ISSN: 2083-6007
Print ISSN: 1230-0322
DOI: 10.31883/pjfns/145704
http://journal.pan.olsztyn.pl

Original article
Section: Food Technology

Pear Juice Clarification Using Polygalacturonase from *Beauveria bassiana*: Effects on Rheological, Antioxidant and Quality Properties

Ayodeji Amobonye[1], *Prashant Bhagwat*[1], *Faith Matiza Ruzengwe*[1,2], *Suren Singh*[1], *Santhosh Pillai*[1]*

[1]*Department of Biotechnology and Food Science, Faculty of Applied Sciences, Durban University of Technology, PO Box 1334, Durban, 4000, South Africa*
[2]*Department of Food Science and Technology, Chinhoyi University of Technology, P. Bag 7724, Chinhoyi, Zimbabwe*

Key words: antioxidant, *Beauveria bassiana*, juice clarification, enzyme, pear juice, polygalacturonase, rheology

Although pear is one of the most preferred fruits globally due to its high nutrient content, its juice products have not received equal consumer acceptability due to their undesirable haziness and turbidity. However, enzymatic treatment of juice has been noted to improve the overall acceptability of juices better than traditional decantation, filtration, and heating methods, which are either expensive or detrimental to the product quality. In this study, pear juice was effectively clarified using partially purified polygalacturonase from an entomopathogenic fungal endophyte *Beauveria bassiana* SAN01. The optimization of the juice clarification process led to 137% improvement in clarification compared to control, under optimal conditions of 39.37 U/mL enzyme load, 36.87°C temperature and 2.75 h treatment time. Results also showed that the polygalacturonase treatment resulted in a significant decrease in viscosity and an increase in the pseudoplasticity of the pear juice as the rheological data of the juice was observed to fit adequately into the power law model (R^2>0.9). Furthermore, the enzyme-assisted juice clarification was found to reduce browning index (-14.34%) and turbidity (-19.72%) while increasing the reducing sugar content (9.55%). Unlike some conventional juice treatments, the polygalacturonase treatment preserved the antioxidant potential and the total phenolic contents of the pear juice as no significant changes were observed after the treatment. This study thus demonstrates the efficacy of a fungal polygalacturonase in improving pear juice quality as well as the potential applicability of *B. bassiana* enzymes in the food industry.

INTRODUCTION

Enzymes have continued to gain prominence in food processing over traditional chemical- and mechanical-based methods, as they are eco-friendly and have been shown to increase food nutritional value, with lesser energy input requirement [Kumar *et al.*, 2016]. Various carbohydrases have since been produced commercially for their applications in fruit juice processing, as the potential of novel enzyme sources in enhancing customer desirability is continually being investigated. These biocatalysts are used to improve the clarity of fruit products such as juices, as consumer preference for well-clarified fruit juices devoid of opalescence is gaining more popularity [Sharma *et al.*, 2017]. Furthermore, clarification of juice is critical as haze- and sediment-forming substances diminish fruit juice quality during storage [Dıblan & Özkan, 2021]. Pectinolytic enzymes, including pectinesterases, polygalacturonases, pectin lyases, and protopectinases, have been the most exploited enzymes in this regard [Ramadan, 2019]. This is because the turbidity of fruit products is mainly caused by pectin, the primary plant polysaccharide in fruit products; hence, the pectinolytic enzymes hydrolyze pectic substances, promoting the flocculation of suspended particles and enhancing clarification [Karmakar & De, 2019].

However, the presence of other polysaccharides including cellulose, hemicellulose, starch as well as other compounds, such as lignin, oxidized phenolics, polyphenols, proteins, tannins, and metals, have also been implicated in the turbidity and cloudiness of different juices [Narnoliya *et al.*, 2020; Ogando *et al.*, 2019]. Hence, eliminating these components from fruit juices before packaging or serving to consumers is critical [Narnoliya *et al.*, 2020]. Additionally, the action of pectinase on fruit juices releases sugars that enhance the sweetness of the products, minimizing the addition of extra sweeteners. However, besides improving the physical attributes of fruit juices, the maintenance or improvement of their nutritional content is just as important during juice processing. The major nutritional benefit of fruit juices is attributed to their vitamins and antioxidants; however, different processing methods have shown detrimental effects on these constituents, particularly a reduction in their contents. For example, heat processing has been shown to reduce the vitamin

* Corresponding Author:
E-mail: santhoshk@dut.ac.za (S. Pillai)

Submitted: 7 November 2021
Accepted: 11 January 2022
Published on-line: 4 February 2022

contents of juice [Ordóñez-Santos & Martínez-Girón, 2020], while UV-radiation to decrease the antioxidant properties [Islam *et al.*, 2016]. However, despite different studies on the enzymatic clarification of fruit juices, the effects of these treatments on their nutritional contents have not been well demonstrated.

Pear is considered one of the most widely consumed fruits worldwide, and its popularity has been attributed to its high fiber, minerals, vitamins, and antioxidants [Salta *et al.*, 2010]. However, despite these remarkable qualities, especially the high nutrient content, it has been observed that pear juices are not as desirable as other fruit juices, especially apple and orange juices. This relatively low consumer acceptance of pear juice has been partly attributed to its haziness and insipid flavor, hence, the need for a more effective processing technology to meet consumer's preferences [Xie *et al.*, 2007].

Beauveria bassiana, though more widely known as an entomopathogenic fungal endophyte [Thaochan *et al.*, 2021], has also been shown to secrete different industrially important metabolites and enzymes including amylase, cellulase, chitinase, lipase and protease [Amobonye *et al.*, 2020]. The potential of the fungus to produce these biological macromolecules and its established safety for human use have thus prompted the application of many of its enzymes in chemical biotransformation [Shankar & Laxman, 2015]. We have previously demonstrated the potentials of partially purified *B. bassiana* endoglucanase and xylanase cocktail in biomass saccharification [Amobonye *et al.*, 2021b] as well as the potential of purified xylanase in wastepaper deinking [Amobonye *et al.*, 2021a]. Hence, this study investigated the enzymatic clarification of pear juice using partially purified polygalacturonase from *B. bassiana* SAN01. In this regard, the quality of pear juice was enhanced by statistically optimizing the enzymatic treatment using the central composite design of response surface methodology. Subsequently, the effects of the treatment on the rheological properties, color, total soluble solids, turbidity, and reducing sugar levels of the juice were evaluated. Furthermore, the total phenolic and flavonoid contents and antioxidant activities of the juice were selected as indicators of its functional quality after treatment. To the best of our knowledge, this is the first scientific attempt at clarifying pear juice after the extraction process using a microbial enzyme, as well as optimizing the process *via* a statistical approach.

MATERIALS AND METHODS

Chemicals and reagents

The wheat bran used in the study was obtained locally in Durban, South Africa. Activated charcoal, Folin-Ciocalteu reagent, gallic acid and 3,5-dinitrosalicylic acid (DNS) were purchased from Sigma-Aldrich (Saint Louis, MO, USA). All other chemicals and reagents used were of analytical grade and were obtained from validated suppliers.

Microorganism and enzyme production

The polygalacturonase used for the clarification of pear juice was produced from *B. bassiana* SAN01, which was isolated locally in its endophytic state from onion leaves [Amobonye *et al.*, 2021b]. The enzyme production was carried out under submerged fermentation conditions in a shaking incubator (120 rpm) using 1 mL of inoculum (1×10^7 spores/mL). The fermentation conditions include an initial media pH of 6.0, incubation temperature of 30.42°C and wheat bran concentration of 47.2 g/L. The polygalacturonase activity was measured using 1% orange peel pectin, while the reducing sugars released were determined by the DNS method according to Bailey *et al.* [1992]. One unit (U) of polygalacturonase activity is defined as the amount of enzyme liberating 1 μmol of galacturonic acid per min, under standard assay conditions (40°C, 50 mM phosphate buffer, pH 5.5).

Partial purification and decolorization of the enzyme

The crude enzyme was partially purified by ammonium sulphate precipitation (60%) for 24 h at 4°C and centrifuged at 10,000×*g* for 20 min at 4°C using a refrigerated centrifuge (Eppendorf 5810R, Hamburg, Germany). The precipitate was reconstituted in citrate buffer (50 mM, pH 5.5) and desalted by dialysis. Subsequently, the precipitated protein was decolorized using activated charcoal to obtain a clear enzyme. In this regard, 1% activated charcoal was added to the enzyme solution and incubated at 4°C for 30 min with gentle stirring. The mixture was then centrifuged at 5,000×*g* for 10 min to recover a clear supernatant [Kareem *et al.*, 2011]. Finally, the enzyme was concentrated by ultrafiltration using 10 kDa membrane centrifugal filter (Millipore Corp., Billerica, MA, USA) and passed through sterile syringe filters (0.2 mm) (Millipore Corp.) to remove microbial contaminants and other suspended solids.

Juice processing

Pears (Forelle varieties) weighing ~170 g were purchased from a local shop in Durban, South Africa. The fruits were washed thoroughly with distilled water, deseeded manually, chopped, and extracted using a juicer. The extract was rapidly strained through a stainless-steel sieve (3 mm pore diameter) for the separation of the suspended matter. Subsequently, the extract was vacuum filtered using Whatman® Grade 3 filter paper, transferred to clean Schott bottles and pasteurized in a water bath (Memmert WB 22, Memmert GmbH + Co. KG, Schwabach, Germany) at 95°C for 1 min [Petruzzi *et al.*, 2017].

Enzyme-assisted pear juice clarification

The Design Expert 11.0 (Stat-Ease, Minneapolis, USA) software was employed for the statistical optimization of the enzyme-assisted clarification of pear juice [Amobonye *et al.*, 2021b]. For each treatment, 50 mL of pear juice was subjected to different enzyme treatment conditions (Table 1). The three process parameters selected for the optimization of enzyme treatments by central composite design (CCD) as well as their ranges were identified from previous studies [Saxena *et al.*, 2014] and also based on preliminary experiments in our laboratory. These include the enzyme load, incubation time and temperature. Incubation was performed in a circulating water bath (IncuMax WB10C Water Bath, Amerex Instruments, Inc., Concord, CA, United States) with continuous agitation (50 rpm) while keeping the juice at its natural pH (pH 3.9). The partially purified polygalacturonase (40 U/mL)

TABLE 1. Coded and uncoded variables of the response surface design for the clarification of pear juice.

Independent variables	Units	Levels				
		-1.68	-1	0	+1	+1.68
Enzyme load (A)	U/mL	20	24.22	30	35.77	40
Temperature (B)	°C	30	34.23	40	45.78	50
Time (C)	h	1	1.42	2	2.58	3

was used in the optimization process and the enzyme treatment was terminated by heating the juice at 90°C for 1 min. The experimental design in the coded levels of process variables is summarized in Table 1. The optimization design was made of 15 combinations including 5 replicates of the center point and juice clarity was determined as the response.

Rheological properties of pear juice

Rheological properties of the juice samples were evaluated according to Domingues *et al.* [2011], using a rheometer (MCR102, Anton Paar GmbH, Graz, Austria), fitted with a parallel plate (50 mm diameter, 1.5 mm gap). The rheometer was equipped with a Peltier system (TEZ-15P-C) with a temperature accuracy of 0.01°C. For the steady flow studies, 2 mL of juice samples were placed between the plates. The shear stress (Pa) and viscosity were observed linearly increasing from 1 s^{-1} shear rate to 300 s^{-1}; the data points were collected and analyzed using US200 Universal Software (Paar Physica, Anton Paar GmbH). The shear rate range used in this study is in line with many food processing applications such as pumping, grinding, in-pipe flow, mixing and stirring [Deshmukh *et al.*, 2015].

Evaluation of fruit juice characteristics

Juice clarity

The change in percent transmittance (Δ% T) was considered a measure of the juice clarity [Zhao *et al.*, 2019]. Initially, the absorbance of the juice samples was recorded at 660 nm with a UV–VIS spectrophotometer (Model UV-1201, Shimadzu Corp., Kyoto, Japan) with distilled water and heat-inactivated enzyme serving as the blank and the control respectively. Subsequently, the change in percent transmittance (Δ% T) was calculated according to the formula given below.

$$\text{Juice clarity } (\Delta\%\ T) = \frac{(\%T_s - \%T_b)\times 100}{\%T_c - \%T_b} \quad (1)$$

where: $\%T_s$ – percent transmittance of test sample; $\%T_b$ – percent transmittance of blank; $\%T_c$ – percent transmittance of control.

Browning index and turbidity determination

To determine the browning index, 5 mL of juice sample was mixed with 5 mL of 95% ethanol and centrifuged at 4,000×*g* for 10 min. The supernatant obtained was passed through a 0.45 μm membrane filter, and the absorbance was measured at 420 nm [Uçan *et al.*, 2016]. The turbidity of the juice was determined using a Turbidometer (Oxoid, Basingstoke, UK) and reported as nephelometric turbidity units (NTU) using hexamethylenetetramine solution as a standard [Pradhan *et al.*, 2020].

Reducing sugars, total dissolved solids and titratable acidity

Reducing sugars released after the enzymatic treatment of pear juice were determined using the DNS method [Bailey *et al.*, 1992]. Total soluble solids were measured using a digital refractometer with automatic temperature compensation (Atago Co., Ltd, Tokyo, Japan) and expressed as °Brix (%). The pH of the juice was measured using a benchtop pH-meter (Hanna Instruments, Woonsocket, RI, USA), while the titratable acidity was estimated by titrating 10 mL of diluted juice (1:10; juice: distilled water) with 0.1 N NaOH solution, using phenolphthalein as an indicator, and the acidity value was expressed in citric acid (0.0064 acid factor) equivalents [Santana *et al.*, 2021].

Color measurement

The color parameters (CIE L^* a^* b^*) of the raw and treated juice samples were measured using a ColorFlex EZ Spectrophotometer (Hunter Associates Laboratory Inc., Reston, VA, USA), where L value indicates lightness while a^* denotes the red/green value ((+): red; (−): green) and b^* the yellow/blue value ((+): yellow; (−): blue). Furthermore, the chroma (C^*) of the samples was calculated according to the formula (2) [Uçan *et al.*, 2016].

$$C^* = \sqrt{(a^*)^2 + (b^*)^2} \quad (2)$$

Analysis of antioxidant activities and phenolic contents

DPPH radical scavenging activity

Reaction mixtures containing the sample (100 mL) and DPPH• (3.9 mL, 50 μM) in methanol were incubated in a water bath at 37°C for 30 min. The absorbance was measured at 517 nm using a Thermo Scientific GENESYS UV-Vis Spectrophotometer (Thermo Scientific, Waltham, MA, USA) and the DPPH• scavenging activity was calculated by the equation (3):

$$\text{DPPH radical scavenging activity } (\%) = \\ = [(Abs_0 - Abs_1)/Abs_0]\times 100 \quad (3)$$

where: Abs_0 and Abs_1 are the absorbance values of control (without juice) and test samples, respectively [Wang *et al.*, 2019].

Total phenolic content

The total phenolic content of juices was analyzed according to a modified method using Folin-Ciocalteu reagent. Each sample (0.1 mL) was mixed with 0.75 mL of diluted Folin-Ciocalteu reagent (10% *v/v*) and incubated for 5 min at room temperature and 0.75 mL of 2% sodium carbonate solution was added. After incubation for 15 min at room temperature, the absorbance of the solution was read at 750 nm. Gallic acid was used as the standard, and total phenolic content was expressed as mg gallic acid equivalents (GAE) per L of juice [Romero-González *et al.*, 2020].

Total flavonoid content

The total flavonoid content (TFC) of juices was estimated spectrophotometrically based on the aluminium chloride

colorimetric method [Cheng *et al.*, 2016]. Juice samples (0.5 mL) were added to 4.5 mL of an aluminium chloride reagent consisting of 10% aluminium chloride (0.1 mL), 1 M potassium acetate (0.1 mL), 95% ethanol (1.5 mL) and distilled water (2.8 mL). The absorbance of the reaction mixture was measured at 415 nm after incubation at room temperature for 30 min. The TFC in each juice sample was calculated based on a standard calibration curve of quercetin and expressed as mg quercetin equivalents (QE) per L of juice. The aluminium chloride reagent mixture alone, without the addition of the sample, was used as a blank.

Ferric reducing antioxidant power (FRAP)

The FRAP assay was performed using a modified Wang *et al.* [2019] method. Briefly, a FRAP reagent was prepared from 300 mM acetate and glacial acetic acid buffer (pH 3.6), 20 mM ferric chloride and 10 mM 4,6-tripryridyl-s-triazine (TPTZ) made up in 40 mM HCl. All three solutions were mixed in the ratio 10:1:1, *v/v/v*. The FRAP assay was performed by incubating 1 mL of dH_2O, 25 μL of juice and 1 mL of the FRAP reagent at 37°C. The absorbance readings at time zero and after 40 min were recorded at 593 nm [Benzie & Strain, 1996]. Ferrous sulphate was used as the standard, and the FRAP was expressed in μmol of Fe (II) per mL of juice.

Statistical analysis

All the data presented are the mean ± standard deviation of triplicate values. The variation between groups was evaluated using the Duncan test and one-way analysis of variance (ANOVA) of the IBM SPSS v26 software package (IBM Corp., Armonk, NY, USA). A significance level of 5% was used in all the analyses.

RESULTS AND DISCUSSION

Optimization of enzyme-assisted pear juice treatment

The efficacy of the *B. bassiana* SAN01 polygalacturonase in the clarification of pear juice was evaluated by response surface methodology (RSM) using a CCD design while measuring the juice clarity under different conditions as the response (Table 2). In the design of 15 experimental runs, pear juice clarity varied considerably from 25.46% and 100% with changing process conditions (Table 2). These results showed that the pear juice clarity was significantly improved by optimizing the enzyme load, incubation temperature and incubation period. In addition, close agreements were observed between all the experimental and predicted values in this study. It is posited that the polygalacturonase hydrolyzed the pectin into different monomers and oligomers, creating protein-sugar complexes which aggregated into larger particles and settled, resulting in improved clarity. Data from this study is corroborated by similar findings from previous investigations [Ahmed & Sohail, 2020; Sorrivas *et al.*, 2006].

The reliability of the model was confirmed from the F-value (41.06) and *p*-values as observed from the ANOVA (Table 3). The model, as well as some of the terms (A, B, C and AC), were found to be significant, judging from their *p*-values. However, exceptions were noticed in AB and BC with *p*-value greater than 0.05, which suggests that the interactive effects

TABLE 2. Central composite design (CCD) optimization of pear juice clarification and the response of the dependent variables.

	Level			Clarity (%)*	
	A**	B	C	Actual	Predicted
1	+1.68	0	0	74.87	77.72
2	0	-1.68	0	38.48	41.28
3	0	+1.68	0	61.95	64.75
4	0	0	-1.68	32.51	36.41
5	0	0	+1.68	65.72	69.62
6	+1	-1	+1	100.00	99.46
7	0	0	0	56.12	53.02
8	-1.68	0	0	25.46	28.31
9	0	0	0	58.06	53.02
10	-1	-1	-1	39.22	38.68
11	0	0	0	51.19	53.02
12	+1	+1	-1	36.79	36.25
13	0	0	0	59.15	53.02
14	-1	+1	+1	38.22	37.68
15	0	0	0	57.53	53.02

*Average of triplicate determinations. **Details of codes A, B & C are given in Table 1.

of the variables are not consequential. The model showed a high R^2 value of 0.9685, which demonstrates that the model can account for ~97% of the total variation and represent significant correlations among the selected variables.

The interactions between the selected factors affecting the optimized clarification of pear juice were also represented in contour and response surface plots (Figure 1). The interaction between AB was moderately significant (*p*-value 0.0726), with increasing the dose of enzyme, a simultaneous increase in juice clarification was observed where 20 U/mL showed 28%, while 40 U/mL showed 78% juice clarification, keeping time at zero level (2 h). While with increasing temperature, the juice clarification moderately increased, showing 41% clarification at 30°C and 65% at 50°C, suggesting the inefficiency of the enzyme to work both at low and high temperature regimes (Figure 1a). The interaction between AC was most significant (*p*-value <0.0001), where both incubation time and enzyme load were found to interact considerably (Figure 1b). However, at an extreme lower enzyme dosage of 20 U/mL and incubation time of 1 h, the juice clarification was not effective. In contrast, a sharp increase in juice clarification was observed (39–100%) with a steady rise in both the factors, comprising enzyme load (24–36 U/mL) and incubation time (1.4–2.6 h), while keeping the temperature at 34°C. The interaction among BC was found to be statistically insignificant (*p*-value 0.8473), suggesting little interactions between incubation time and incubation temperature (Figure 1c), which is mainly because of the level of enzyme dosage which was studied at zero level (30 U/mL). It further

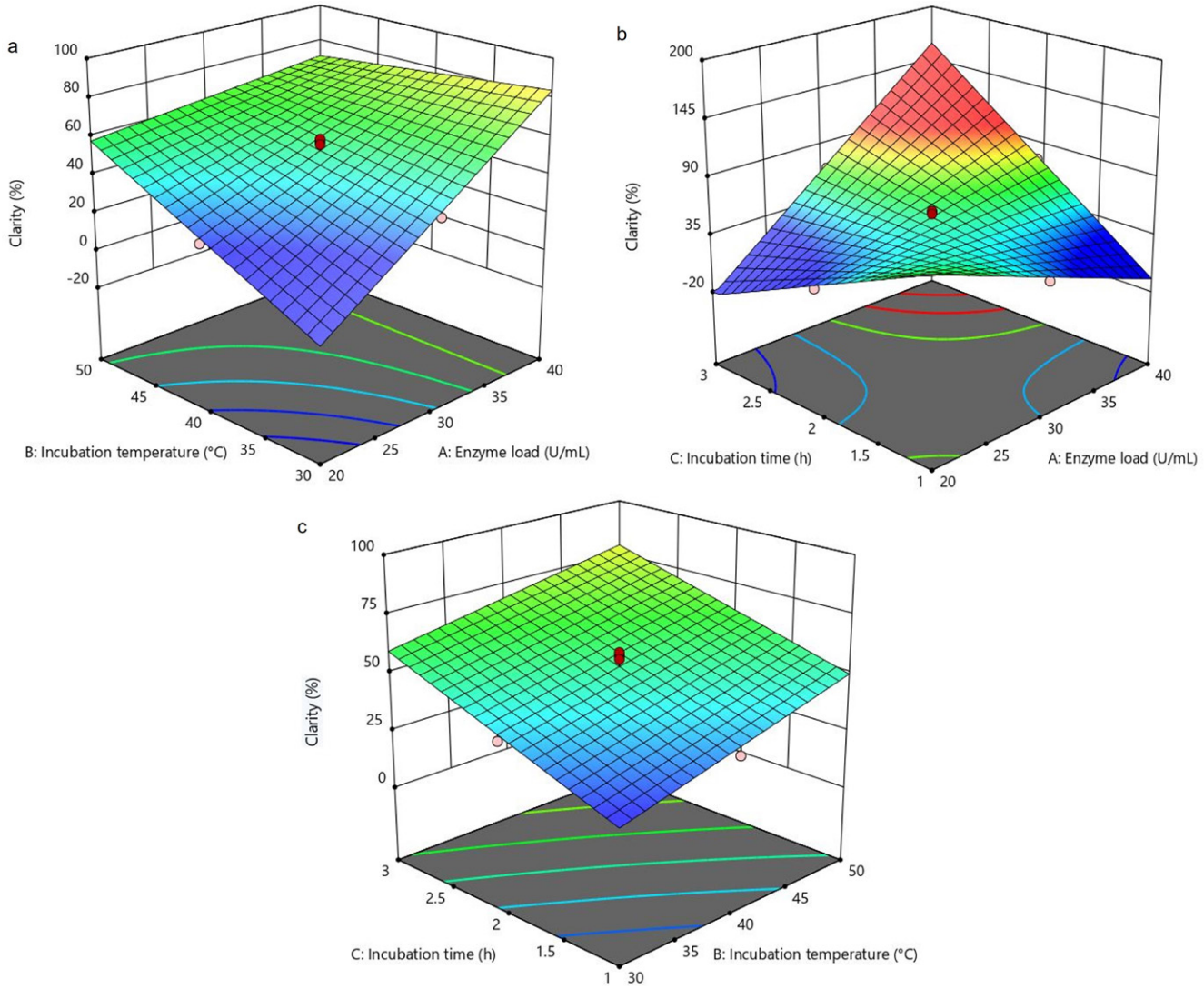

FIGURE 1. Response surface plots showing the interactions between the variables for enzymatic clarification of pear juice: (a) 3D plots of enzyme load – incubation temperature interaction; (b) 3D plots of enzyme load – incubation time interaction; (c) 3D plots of incubation time – incubation temperature interaction.

substantiates enzyme dose as the most critical factor, corroborated by its lowest *p*-value (<0.0001) (Table 3).

Validation of the experimental model

The adequacy of the model was further validated by conducting the enzyme treatment using derived optimal conditions. The conditions predicted for optimum pear juice clarification were enzyme load (39.37 U/mL), incubation temperature (36.87°C) and time (2 h 45 min) with a desirability of 0.927. As suggested by the model, the predicted value of maximum clarification, 140.65%, was in close agreement with the experimental value of 137±7.1%. Hence, the proximity between the predicted and experimental values points to the adequate prediction of the generated model. Thus, by applying the CCD designs, a 1.37-fold increase in clarity relative to the control was recorded.

Effect of enzyme treatment on pear juice rheology

The relationship between the shear stress and shear rate of the raw and enzyme-treated pear juice is shown

TABLE 3. Results of the analysis of variance (ANOVA) of quadratic models for pear juice clarification.

Source	Sum of Squares	df	Mean Square	F-value	*p*-Value*
Model	4926.40	6	821.07	41.06	< 0.0001
A**	1220.67	1	1220.67	61.05	< 0.0001
B	275.42	1	275.42	13.77	0.0059
C	551.45	1	551.45	27.58	0.0008
AB	85.41	1	85.41	4.27	0.0726
AC	1250.65	1	1250.65	62.54	< 0.0001
BC	0.7909	1	0.7909	0.0396	0.8473
Residual	121.15	8	20.00		
Lack of Fit	38.82	4	30.29	3.12	0.1481

R^2=0.9685, adjusted R^2=0.945, predicted R^2=0.9061, adequate precision (AP)=23.291.
*Significant at p<0.05. **Details of codes A, B & C are given in Table 1.

in Figure 2a. The rheograms of the raw and enzyme-clarified juice showed a monotonical increase in the shear stress with increasing shear rate. Subsequently, the Ostwald-de Waele model or power law equation was used to describe the relationships between the two variables as the recorded rate of increase of the shear stress was not directly linear to the shear rate increase [Sanchez *et al.*, 2009; Tavares *et al.*, 2007]:

$$\sigma = k \times \gamma^n \quad (4)$$

where: σ is the shear stress (Pa), k is the consistency coefficient (Pa×s^n), γ is the shear rate (s^{-1}) and n is the flow behavior index (-).

It was observed that flow behaviors of the raw and enzyme-treated juice samples fitted well within the power law model as shown by the $R^2>0.9$ (Table 4). Flow behavior index $n<1$ shows pseudoplasticity whilst $n=1$ shows Newtonian flow behavior. In this study, an increase in pseudoplasticity/shear thinning was observed after enzymatic treatment of the juice. In addition, the consistency coefficient, k, showed that the polygalacturonase treatment of pear juice decreased viscosity at any given shear rate (Table 4).

Similarly, a decrease in the viscosity values was observed in both samples with the increase in the shear rate (Figure 2b), and the treated juice was observed to be less viscous than

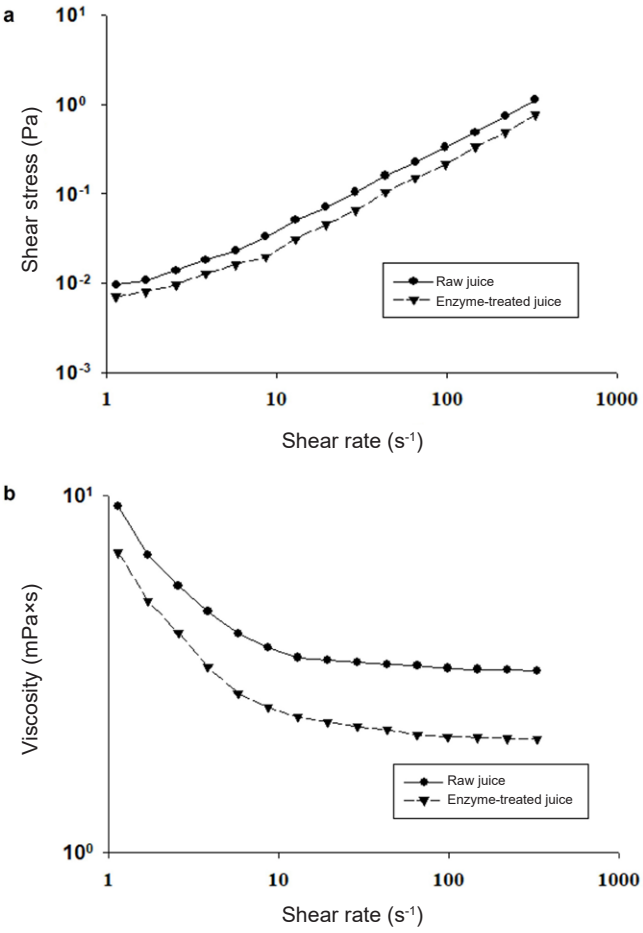

FIGURE 2. Effect of enzyme treatment on the (a) shear stress and (b) viscosity profile as a function of shear rate of pear juice.

TABLE 4. Power-law model coefficients of raw and enzyme-treated pear juice.

	k (Pa×s^n)	n	R^2
Raw juice	0.0061±0.0002	0.89±0.03	0.9977
Enzyme-treated juice	0.0047±0.0001	0.87±0.03	0.9962

Results expressed as mean ± standard deviation; k: consistency coefficient, n: flow behavior index, R^2: coefficient of determination.

the raw juice. Thus, it could be inferred that the observed decrease in the viscosity after enzymatic treatment is due to the hydrolytic action of the enzyme on the pectic materials present in the juice. This hydrolytic action of the enzyme results in reduced water holding capacity of the juice and subsequent release of free water into the system, reducing juice viscosity [Sharma *et al.*, 2017]. Similar flow behaviors have also been highlighted in previous clarification studies of various juices including apricot, banana, and sapodilla [Sharma *et al.*, 2017].

In practical terms, a reduction in the viscosity of fruit juice is considered vital as it prevents problems such as fouling of membrane surfaces encountered during the subsequent filtration process which often reduce juice quality and increase production cost. Furthermore, the reduction in viscosity and cluster formation resulting from the enzymatic clarification of juices further facilitates separation through centrifugation and filtration. Ultimately, these result in the final juice product exhibiting greater clarity, more concentrated flavor and color [Abdullah *et al.*, 2007; Sharma *et al.*, 2017]. In addition, many consumers have also shown preferences for juice products with relatively lower viscosity [Salehi, 2020].

Effect of enzyme treatment on pear juice quality

The color of food products is a major determining factor in customer preference. It has been observed that many consumers prefer brighter or lighter juices, hence, the color and the clarity of beverages are usually considered as standard quality indicators [Gonzalez Viejo *et al.*, 2019]. Browning, both enzymatic and non-enzymatic, has been noted for its detrimental effects on the nutritional and sensory appeal of fruit products. For example, in pear juice, the color has been noted to be one of the reasons for its non-preference by consumers [Xie *et al.*, 2007]. Furthermore, dark-colored fruit products are usually associated with deterioration, hence, a reduction in the dark color is desirable [Beveridge & Wrolstad, 1997; Singh *et al.*, 2021]. In this study, a reduction in browning (~14%) of pear juice was observed after the treatment with the fungal polygalacturonase (Table 5), indicating its effectives in improving the pear juice quality. The beneficial effect of polygalacturonase treatment is also demonstrated by the ~10% increase in reducing sugar content after processing (Table 5). This expected increase in reducing sugar content, which has also been observed in previous studies on juice clarification [Adedeji & Ezekiel, 2020; Yang *et al.*, 2019], is a result of the hydrolytic action of the glycosyl hydrolase on the pectin present in the raw juice. Furthermore, the increment in reducing sugar content is expected to enhance the sweetness and flavor of the juice products, thus, limiting the need for extra sweeteners during further processing.

TABLE 5. Effect of enzyme treatment on pear juice properties.

	Raw juice	Enzyme--treated juice	Percent change
Browning index	0.26±0.01	0.22±0.01	-14.34*
Color L^*	14.23±0.34	17.53±0.41	23.19*
a^*	-1.23±0.04	-0.83±0.04	32.52*
b^*	3.71±0.11	6.27±0.26	69.00*
C^*	3.91±0.14	6.33±0.31	61.89*
pH	3.93±0.04	3.79±0.03	-3.56
Reducing sugar content (mg/mL)	75.5±2.3	82.6±2.7	9.55*
Titratable acidity (g/100 mL)	0.28±0.01	0.27±0.01	-3.57
Total dissolved solids (Brix %)	8.90±0.1	9.2±0.2	3.37
Turbidity (NTU)	1411±74	1132±35	-19.72*

Results expressed as mean ± standard deviation (n=3). *Significant at p<0.05.

TABLE 6. Effect of enzyme treatment on pear juice antioxidant properties.

	Raw juice	Enzyme--treated juice	Percent change
DPPH· scavenging activity (%)	66.0±2.2	68.2±3.0	3.23
Total phenolic content (mg GAE/L)	318.0±12.3	313.0±7.3	-1.57
Total flavonoid content (mg QE/L)	118.6±3.4	136.8±4.7	15.35*
FRAP (μmol of Fe (II)/mL)	133.1±5.0	132.7±6.7	-0.34

Results expressed as mean ± standard deviation (n=3); GAE: gallic acid equivalents, QE: quercetin equivalents, FRAP: ferric reducing antioxidant power. *Significant at p<0.05.

It is also probable that the increased reducing sugar content observed in this study could be inhibitory to polyphenol oxidase and consequently resulted in reducing browning. Reducing sugars have been previously noted in this regard to inhibit the activity of polyphenol oxidase [Moon *et al.*, 2020; Nicoli *et al.*, 1991], an enzyme that has been implicated in enzymatic browning [Jiang *et al.*, 2016].

A significant improvement in the clarity of the juice was also inferred from the color change observed subsequent to the enzyme treatment as demonstrated by the ~23% increase in L^* value (Table 5). The increase in L^* value was also observed in a recent study on the application of pectinase in extracting juices from pears [Gani *et al.*, 2021]. Furthermore, there was an increase in the redness and yellowness of the enzyme-treated juice compared to the control, as deduced from the positive changes in the a^* and b^* values. Likewise, the increase in the color intensity and the brightness of the processed juice was also shown by the significant increase in the chroma value (61.89%) (Table 5).

Turbidity has been shown as a quality discriminant in fruit juice processing affecting food product stability [Salehi, 2020; Sharma *et al.*, 2017]. Turbidity in fruit juices results from unhydrolyzed complex carbohydrates, hence the hydrolysis of pectin has been identified as a significant step in this regard [Sorrivas *et al.*, 2006]. The efficacy of the *B. bassiana* polygalacturonase in the juice clarification process was highlighted by a ~20% reduction in its turbidity (Table 5). A similar trend in turbidity was also observed in the clarification of apple, grape and peach juices using polygalacturonase from *Coriolus versicolor* and *Penicillium notatum* [Amin *et al.*, 2017]. The reduction in turbidity and viscosity observed in this study after enzymatic treatment is also complemented by the observed increase in reducing sugar content. This could be comparable with a finding from Yang *et al.* [2019] where a linear relationship existed between complex sugars (substrates) clearance, and the reducing sugars (products) released.

The pH, titratable acidity, and total dissolved solids (Brix %) have been identified as important factors in the quality control of fruit juices, especially regarding storage stability [Adedeji & Ezekiel, 2020]. Minor fluctuations were observed between the pH of the control and the treated juice as only a 3.56% change was recorded (Table 5). Similar trends were observed for titratable acidity and total dissolved solids in previous enzymatic treatments of banana and strawberry juices, where the pH, titratable acidity and total dissolved solids were barely affected [Barman *et al.*, 2015; Sandri & Silveira, 2018]. The observed reduction in the pH and increase in titratable acidity is believed to be due to the release of galacturonic acid which is the hydrolytic product of pectin while the rise in Brix (%) could be due to the enzyme-facilitated degradation of the complex carbohydrate polymers in the juices [Bora *et al.*, 2017; Kyamuhangire *et al.*, 2002].

Effect of *B. bassiana* polygalacturonase on antioxidant properties and phenolic contents

The increase in juice consumption has been ascribed to the reported health benefits of their antioxidants [Ern *et al.*, 2016]; hence, it is crucial to determine the effect of the enzymatic treatment on the antioxidant properties of fruit juices. Studies have shown the detrimental effects of various treatment processes, such as thermal, mechanical and irradiation, on the desirable antioxidant benefits of fruits and their products [Al-juhaimi *et al.*, 2018]. Though polygalacturonase treatment has been shown in a few studies to have negative effects on the DPPH radical scavenging activity of fruit juices, a slight increase in the scavenging activity (of 3.32%) was observed for pear juice after the polygalacturonase treatment (Table 6). Hence, it is hypothesized that the polygalacturonase enzyme was involved in the hydrolysis of the different linkages and complexes made between pear juice antioxidants and its pectin [Ribas-Agustí *et al.*, 2018].

Phenolics including flavonoids contribute the most to the antioxidant activities of fruits and their products. In this study, the total phenolic contents were not significantly affected after enzyme clarification; however, there was a significant increase (15.25%) in the total flavonoid content (Table 6). Pear juices have been shown to be very rich in phenolic compounds, including arbutin, chlorogenic acid, epicatechin, quercetin 3–glucoside, quercetin 3–galactoside and quercetin 3–rutinoside [Schieber *et al.*, 2001]. It is posited that

the hydrolytic action of the enzyme could release these compounds bound to the cell wall as well as cleave the internal glycosidic bonds of flavonoids into their aglycone moieties, thus, causing a significant increase in total flavonoids, and consequently an increase in the antioxidant activity, as shown previously by Mandalari *et al.* [2006]. Furthermore, it has also been noted that the enhancement of total antioxidative activity might be due to an increase in flavonoid aglycones [Gu *et al.*, 2019]. The FRAP assay is regarded as one of the best tests for determining the antioxidant capabilities of fruit juices [Sethi *et al.*, 2020]. The antioxidant activities, as measured by the FRAP method, were shown to be preserved in pear juice following *B. bassiana* polygalacturonase treatment as no significant change was observed. This recorded preservation of FRAP in processed juice relative to the untreated juice could be corroborated with previous studies such as in the enzyme-assisted processing of Indian plum juice [Koley *et al.*, 2011].

CONCLUSIONS

Despite the popularity of the pear fruit, very little focus has been placed on its juice as a commercial product unlike other popular fruits, such as apples, oranges and pineapples. As earlier highlighted, this might partly be due to the undesirable cloudiness post-extraction. According to available literature, there are no research focused on the clarification of extracted pear juice, and particularly, no attempt has been made using microbial enzymes in that process. Thus, this study effectively utilized RSM to establish the optimum parameters for pear juice clarification using *B. bassiana* polygalacturonase. The optimal clarification conditions were validated using the conditions derived from the CCD model. The analysis of the quality characteristics and some biochemical properties has revealed that the polygalacturonase treatment had no detrimental effect on the most-desired physical and antioxidant properties of the juice. It was further observed that the enzyme-assisted treatment significantly enhanced many of the characteristics of the product, which are in line with customer and industrial preferences. Hence, results from this study have demonstrated, for the first time, the practical application of a novel fungal enzyme in improving some organoleptic properties of pear juice, especially the visual appeal. Like most fungi, *B. bassiana* has been shown to be acidophilic, thus, it is most probable that the polygalacturonase from this study will perform optimally at the acidic pH range, which is most suitable for its application in the juice and wine industries. However, further investigation into the enzyme's biochemical characteristics, its stability, and the effects of different immobilization methods on its activity will enhance its probability of being considered a commercial enzyme. Thus, in addition to the already established safety of the fungus and its products, findings from this study further underscore its applicability in many industrial processes, particularly in juice processing. Therefore, *B. bassiana* could be considered an important candidate for food processing enzymes, in addition to its well-known use in the agricultural industry.

RESEARCH FUNDING

This work was supported by the National Research Foundation of South Africa under grant numbers [UID 105447 and UID 114227].

CONFLICT OF INTERESTS

The authors declare that they have no known competing financial interests or personal relationships that could have influenced the work reported in this paper.

ORCID IDs

A. Ayodeji https://orcid.org/0000-0002-3220-5858
P. Bhagwat https://orcid.org/0000-0001-5790-7824
S. Pillai https://orcid.org/0000-0003-3474-1555
F.M. Ruzengwe https://orcid.org/0000-0001-8589-7475
S. Singh https://orcid.org/0000-0003-1064-6297

REFERENCES

1. Abdullah, A.L., Sulaiman, N., Aroua, M., Noor, M.M.M. (2007). Response surface optimization of conditions for clarification of carambola fruit juice using a commercial enzyme. *Journal of Food Engineering*, *81*(1), 65–71. https://doi.org/10.1016/j.jfoodeng.2006.10.013
2. Adedeji, O.E., Ezekiel, O.O. (2020). Chemical composition and physicochemical properties of mango juice extracted using polygalacturonase produced by *Aspergillus awamori* CICC 2040 on pretreated orange peel. *LWT – Food Science and Technology*, *132*, art. no. 109891. https://doi.org/10.1016/j.lwt.2020.109891
3. Ahmed, A., Sohail, M. (2020). Characterization of pectinase from *Geotrichum candidum* AA15 and its potential application in orange juice clarification. *Journal of King Saud University-Science*, *32*(1), 955–961. https://doi.org/10.1016/j.jksus.2019.07.002
4. Al-juhaimi, F., Ghafoor, K., Özcan, M.M., Jahurul, M., Babiker, E.E., Jinap, S., Sahena, F., Sharifudin, M., Zaidul, I. (2018). Effect of various food processing and handling methods on preservation of natural antioxidants in fruits and vegetables. *Journal of Food Science and Technology*, *55*(10), 3872–3880. https://doi.org/10.1007/s13197-018-3370-0
5. Amin, F., Bhatti, H.N., Bilal, M., Asgher, M. (2017). Multiple parameter optimizations for enhanced biosynthesis of exo-polygalacturonase enzyme and its application in fruit juice clarification. *International Journal of Food Engineering*, *13*(2), art. no. 20160256. https://doi.org/10.1515/ijfe-2016-0256
6. Amobonye, A., Bhagwat, P., Pandey, A., Singh, S., Pillai, S. (2020). Biotechnological potential of *Beauveria bassiana* as a source of novel biocatalysts and metabolites. *Critical Reviews in Biotechnology*, *40*(7), 1019–1034. https://doi.org/10.1080/07388551.2020.1805403
7. Amobonye, A., Bhagwat, P., Singh, S., Pillai, S. (2021a). *Beauveria bassiana* xylanase: characterization and wastepaper deinking

potential of a novel glycosyl hydrolase from an endophytic fungal entomopathogen. *Journal of Fungi*, *7*(8), art. no. 668. https://doi.org/10.3390/jof7080668

8. Amobonye, A., Bhagwat, P., Singh, S., Pillai, S. (2021b). Enhanced xylanase and endoglucanase production from *Beauveria bassiana* SAN01, an entomopathogenic fungal endophyte. *Fungal Biology*, *125*(1), 39–48. https://doi.org/10.1016/j.funbio.2020.10.003
9. Bailey, M.J., Biely, P., Poutanen, K. (1992). Interlaboratory testing of methods for assay of xylanase activity. *Journal of Biotechnology*, *23*(3), 257–270. https://doi.org/10.1016/0168-1656(92)90074-J
10. Barman, S., Sit, N., Badwaik, L.S., Deka, S.C. (2015). Pectinase production by *Aspergillus niger* using banana (*Musa balbisiana*) peel as substrate and its effect on clarification of banana juice. *Journal of Food Science and Technology*, *52*(6), 3579–3589. https://doi.org/10.1007/s13197-014-1413-
11. Benzie, I.F., Strain, J.J. (1996). The ferric reducing ability of plasma (FRAP) as a measure of "antioxidant power": the FRAP assay. *Analytical Biochemistry*, *239*(1), 70–76. https://doi.org/10.1006/abio.1996.0292
12. Beveridge, T., Wrolstad, R.E. (1997). Haze and cloud in apple juices. *Critical Reviews in Food Science and Nutrition*, *37*(1), 75–91. https://doi.org/10.1080/10408399709527768
13. Bora, S.J., Handique, J., Sit, N. (2017). Effect of ultrasound and enzymatic pre-treatment on yield and properties of banana juice. *Ultrasonics Sonochemistry*, *37*, 445–451. https://doi.org/10.1016/j.ultsonch.2017.01.039
14. Cheng, S.H., Khoo, H., Ismail, A., Abdul-Hamid, A., Barakatun-Nisak, M. (2016). Influence of extraction solvents on *Cosmos caudatus* leaf antioxidant properties. *Iranian Journal of Science and Technology, Transactions A: Science*, *40*(1), 51–58. https://doi.org/10.1007/s40995-016-0007-x
15. Deshmukh, P.S., Manjunatha, S.S., Raju, P.S. (2015). Rheological behaviour of enzyme clarified sapota (*Achras sapota* L) juice at different concentration and temperatures. *Journal of Food Science and Technology*, *52*(4), 1896–1910. https://doi.org/10.1007/s13197-013-1222-5
16. Dıblan, S., Özkan, M. (2021). Effects of various clarification treatments on anthocyanins, color, phenolics and antioxidant activity of red grape juice. *Food Chemistry*, *352*, art. no. 129321. https://doi.org/10.1016/j.foodchem.2021.129321
17. Domingues, R.C., Junior, S.B., Silva, R.B., Madrona, G.S., Cardoso, V.L., Reis, M.H. (2011). Evaluation of enzymatic pretreatment of passion fruit juice. *Chemical Engineering Transactions*, *24*, 517–522.
18. Ern, K., Aron, H.A.H., Eng, C. (2016). Comparison of total phenolic contents (tpc) and antioxidant activities of fresh fruit juices, commercial 100% fruit juices and fruit drinks *Sains Malaysiana*, *45*(9), 1319–1327.
19. Gani, G., Naik, H., Jan, N., Bashir, O., Hussain, S.Z., Rather, A., Reshi, M., Amin, T. (2021). Physicochemical and antioxidant properties of pear juice prepared through pectinase enzyme-assisted extraction from William Bartlett variety. *Journal of Food Measurement and Characterization*, *15*(1), 743–757. https://doi.org/10.1007/s11694-020-00676-x
20. Gonzalez Viejo, C., Torrico, D.D., Dunshea, F.R., Fuentes, S. (2019). Emerging technologies based on artificial intelligence to assess the quality and consumer preference of beverages. *Beverages*, *5*(4), art. no. 62. https://doi.org/10.3390/beverages5040062
21. Gu, Q., Duan, G., Yu, X. (2019). Bioconversion of flavonoid glycosides from *Hippophae rhamnoides* leaves into flavonoid aglycones by *Eurotium amstelodami*. *Microorganisms*, *7*(5), art. no. 122. https://doi.org/10.3390/microorganisms7050122
22. Islam, M.S., Patras, A., Pokharel, B., Wu, Y., Vergne, M.J., Shade, L., Xiao, H., Sasges, M. (2016). UV-C irradiation as an alternative disinfection technique: Study of its effect on polyphenols and antioxidant activity of apple juice. *Innovative Food Science and Emerging Technologies*, *34*, 344–351. https://doi.org/10.1016/j.ifset.2016.02.009
23. Jiang, G.H., Kim, Y.M., Nam, S.H., Yim, S.H., Eun, J.B. (2016). Enzymatic browning inhibition and antioxidant activity of pear juice from a new cultivar of asian pear (*Pyrus pyrifolia* Nakai cv. Sinhwa) with different concentrations of ascorbic acid. *Food Science and Biotechnology*, *25*(1), 153–158. https://doi.org/10.1007/s10068-016-0023-9
24. Kareem, S., Akpan, I., Popoola, T., Sanni, L. (2011). Activated charcoal – a potential material in glucoamylase recovery. *Enzyme Research*, *2011*, art. no. 483943. https://doi.org/10.4061/2011/483943
25. Karmakar, S., De, S. (2019). Pectin removal and clarification of juices. Chapter 5, In: Ch.M. Galanakis (Ed.), *Separation of Functional Molecules in Food by Membrane Technology*, Elsevier, Academic Press, pp. 155–194. https://doi.org/10.1016/B978-0-12-815056-6.00005-X
26. Koley, T.K., Walia, S., Nath, P., Awasthi, O., Kaur, C. (2011). Nutraceutical composition of *Zizyphus mauritiana* Lamk (Indian ber): effect of enzyme-assisted processing. *International Journal of Food Sciences and Nutrition*, *62*(3), 276–279. https://doi.org/10.3109/09637486.2010.526930
27. Kumar, K., Arumugam, N., Permaul, K., Singh, S. (2016). Thermostable enzymes and their industrial applications. Chapter 5, In: P. Shukla (Ed.), *Microbial Biotechnology Interdisciplinary Approach*, 1st ed., CRC Press, Boca Raton, USA, pp. 115–162. https://doi.org/10.1201/9781315367880
28. Kyamuhangire, W., Myhre, H., Sørensen, H.T., Pehrson, R. (2002). Yield, characteristics and composition of banana juice extracted by the enzymatic and mechanical methods. *Journal of the Science of Food and Agriculture*, *82*(4), 478–482. https://doi.org/10.1002/jsfa.1052
29. Mandalari, G., Bennett, R.N., Kirby, A.R., Lo Curto, R.B., Bisignano, G., Waldron, K.W., Faulds, C.B. (2006). Enzymatic hydrolysis of flavonoids and pectic oligosaccharides from bergamot (*Citrus bergamia* Risso) peel. *Journal of Agricultural and Food Chemistry*, *54*(21), 8307–8313. https://doi.org/10.1021/jf0615799
30. Moon, K.M., Kwon, E.B., Lee, B., Kim, C.Y. (2020). Recent trends in controlling the enzymatic browning of fruit and vegetable products. *Molecules*, *25*(12), art. no. 2754. https://doi.org/10.3390/molecules25122754
31. Narnoliya, L.K., Jadaun, J.S., Chownk, M., Singh, S.P. (2020). Enzymatic systems for the development of juice clarification strategies. Chapter 18, In: S.P. Singh, A. Pandey, R.R. Singhania, Ch. Larroche, Z. Li (Eds.), *Biomass, Biofuels, Biochemi-*

cals – Advances in Enzyme Catalysis and Technologies, Elsevier, pp. 397–412. https://doi.org/10.1016/B978-0-12-819820-9.00018-1

32. Nicoli, M.C., Elizalde, B.E., Pitotti, A., Lerici, C.R. (1991). Effect of sugars and maillard reaction products on polyphenol oxidase and peroxidase activity in food. *Journal of Food Biochemistry*, *15*(3), 169–184. https://doi.org/10.1111/j.1745-4514.1991.tb00153.x
33. Ogando, F.I.B., de Aguiar, C.L., Viotto, J.V.N., Heredia, F.J., Hernanz, D. (2019). Removal of phenolic, turbidity and color in sugarcane juice by electrocoagulation as a sulfur-free process. *Food Research International*, *122*, 643–652. https://doi.org/10.1016/j.foodres.2019.01.039
34. Ordóñez-Santos, L.E., Martínez-Girón, J. (2020). Thermal degradation kinetics of carotenoids, vitamin C and provitamin A in tree tomato juice. *International Journal of Food Science and Technology*, *55*(1), 201–210. https://doi.org/10.1111/ijfs.14263
35. Petruzzi, L., Campaniello, D., Speranza, B., Corbo, M.R., Sinigaglia, M., Bevilacqua, A. (2017). Thermal treatments for fruit and vegetable juices and beverages: A literature overview. *Comprehensive Reviews in Food Science and Food Safety*, *16*(4), 668–691. https://doi.org/10.1111/1541-4337.12270
36. Pradhan, D., Abdullah, S., Pradhan, R.C. (2020). Optimization of pectinase assisted extraction of chironji (*Buchanania lanzan*) fruit juice using response surface methodology and artificial neural network. *International Journal of Fruit Science*, *20*(Suppl. 2), S318-S336. https://doi.org/10.1080/15538362.2020.1734895
37. Ramadan, M.F. (2019). Enzymes in fruit juice processing. Chapter 4, In: M. Kuddus (Ed.), *Enzymes in Food Biotechnology – Production, Applications, and Future Prospects*, Elsevier, Academic Press, pp. 45–59. https://doi.org/10.1016/B978-0-12-813280-7.00004-9
38. Salta, J., Martins, A., Santos, R.G., Neng, N.R., Nogueira, J.M., Justino, J., Rauter, A.P. (2010). Phenolic composition and antioxidant activity of Rocha pear and other pear cultivars–a comparative study. *Journal of Functional Foods*, *2*(2), 153–157. https://doi.org/10.1016/j.jff.2010.02.002
39. Ribas-Agustí, A., Martín-Belloso, O., Soliva-Fortuny, R., Elez-Martínez, P. (2018). Food processing strategies to enhance phenolic compounds bioaccessibility and bioavailability in plant-based foods. *Critical Reviews in Food Science and Nutrition*, *58*(15), 2531–2548. https://doi.org/10.1080/10408398.2017.1331200
40. Romero-González, J., Ah-Hen, K.S., Lemus-Mondaca, R., Muñoz-Fariña, O. (2020). Total phenolics, anthocyanin profile and antioxidant activity of maqui, Aristotelia chilensis (Mol.) Stuntz, berries extract in freeze-dried polysaccharides microcapsules. *Food Chemistry*, *313*, art. no. 126115. https://doi.org/10.1016/j.foodchem.2019.126115
41. Salehi, F. (2020). Physicochemical characteristics and rheological behaviour of some fruit juices and their concentrates. *Journal of Food Measurement and Characterization, 14*, 2472–2488. https://doi.org/10.1007/s11694-020-00495-0
42. Sanchez, C., Blanco, D., Oria, R., Sánchez-Gimeno, A.C. (2009). White guava fruit and purees: textural and rheological properties and effect of the temperature. *Journal of Texture Studies*, *40*(3), 334–345. https://doi.org/10.1111/j.1745-4603.2009.00185.x
43. Sandri, I.G., Silveira, M.M.d. (2018). Production and application of pectinases from *Aspergillus niger* obtained in solid state cultivation. *Beverages*, *4*(3), art. no. 48. https://doi.org/10.3390/beverages4030048
44. Santana, M.L., Bispo, J.A.C., de Sena, A.R., Teshima, E., de Brito, A.R., Costa, F.S., Franco, M., de Assis, S.A. (2021). Clarification of tangerine juice using cellulases from *Pseudoyma* sp. *Journal of Food Science and Technology-Mysore*, *58*(1), 44–51. https://doi.org/10.1007/s13197-020-04511-5
45. Saxena, D., Sabikhi, L., Chakraborty, S.K., Singh, D. (2014). Process optimization for enzyme aided clarification of watermelon juice. *Journal of Food Science and Technology, 51*(10), 2490–2498. https://doi.org/10.1007/s13197-012-0720-1
46. Schieber, A., Keller, P., Carle, R. (2001). Determination of phenolic acids and flavonoids of apple and pear by high-performance liquid chromatography. *Journal of Chromatography A*, *910*(2), 265–273. https://doi.org/10.1016/S0021-9673(00)01217-6
47. Sethi, S., Joshi, A., Arora, B., Bhowmik, A., Sharma, R., Kumar, P. (2020). Significance of FRAP, DPPH, and CUPRAC assays for antioxidant activity determination in apple fruit extracts. *European Food Research and Technology*, *246*(3), 591–598. https://doi.org/10.1007/s00217-020-03432-z
48. Shankar, S., Laxman, R.S. (2015). Biophysicochemical characterization of an alkaline protease from Beauveria sp. MTCC 5184 with multiple applications. *Applied Biochemistry and Biotechnology*, *175*(1), 589–602. https://doi.org/10.1007/s12010-014-1314-3
49. Sharma, H.P., Patel, H., Sugandha, (2017). Enzymatic added extraction and clarification of fruit juices – a review. *Critical Reviews in Food Science and Nutrition*, *57*(6), 1215–1227. https://doi.org/10.1080/10408398.2014.977434
50. Singh, V., Jawandha, S., Gill, P. (2021). Effect of exogenous putrescine treatment on internal browning and colour retention of pear fruit. *Journal of Food Measurement and Characterization*, *15*, 905–913. https://doi.org/10.1007/s11694-020-00696-7
51. Sorrivas, V., Genovese, D., Lozano, J. (2006). Effect of pectinolytic and amylolytic enzymes on apple juice turbidity. *Journal of Food Processing and Preservation*, *30*(2), 118–133. https://doi.org/10.1111/j.1745-4549.2006.00054.x
52. Tavares, D.T., Alcantara, M.R., Tadini, C.C., Telis-Romero, J. (2007). Rheological properties of frozen concentrated orange juice (FCOJ) as a function of concentration and subzero temperatures. *International Journal of Food Properties*, *10*(4), 829–839. https://doi.org/10.1080/10942910601118805
53. Thaochan, N., Ngampongsai, A., Prabhakar, C.S., Hu, Q. (2021). *Beauveria bassiana* PSUB01 simultaneously displays biocontrol activity against *Lipaphis erysimi* (Kalt.)(Hemiptera: Aphididae) and promotes plant growth in Chinese kale under hydroponic growing conditions. *Biocontrol Science and Technology*, *31*(10), 997–1015. https://doi.org/10.1080/09583157.2021.1917512

54. Uçan, F., Ağçam, E., Akyildiz, A. (2016). Bioactive compounds and quality parameters of natural cloudy lemon juices. *Journal of Food Science and Technology*, *53*(3), 1465–1474. https://doi.org/10.1007/s13197-015-2155-y
55. Wang, J., Vanga, S.K., Raghavan, V. (2019). High-intensity ultrasound processing of kiwifruit juice: Effects on the ascorbic acid, total phenolics, flavonoids and antioxidant capacity. *LWT – Food Science and Technology*, *107*, 299–307. https://doi.org/10.1016/j.lwt.2019.03.024
56. Xie, D., Zhong, H.-Y., Mo, J., Li, Z.-H., Cui, T., Yi, C.-P. (2007). Nutritional and medicinal quality of pear juice: Next hotspot?. *Food*, *1*(1), 41–48.
57. Yang, S.Q., Dai, X.Y., Wei, X.Y., Zhu, Q., Zhou, T. (2019). Co-immobilization of pectinase and glucoamylase onto sodium aliginate/graphene oxide composite beads and its application in the preparation of pumpkin–hawthorn juice. *Journal of Food Biochemistry*, *43*(3), art. no. e12741. https://doi.org/10.1111/jfbc.12741
58. Zhao, D., Wang, Y., Na, J., Ping, W., Ge, J. (2019). The response surface optimization of β-mannanase produced by *Lactobacillus casei* HDS-01 and its potential in juice clarification. *Preparative Biochemistry and Biotechnology*, *49*(2), 202–207. https://doi.org/10.1080/10826068.2019.1566151

Pol. J. Food Nutr. Sci., 2022, Vol. 72, No. 1, pp. 69–78
On-line ISSN: 2083-6007
Print ISSN: 1230-0322
DOI: 10.31883/pjfns/146175
http://journal.pan.olsztyn.pl

Original article
Section: Food Technology

Drying Kinetics, Physicochemical Properties and Sensory Quality of the Instant Foxtail Millet as Affected by Drying Methods

*Yingqiang Wang**, *Hongxia Zhao*, *Xi Song*, *Wenjie Zhang*, *Feng Yang*

College of Agriculture and Forestry, Longdong University, 745000, Qingyang, China

Key words: instant foxtail millet, drying kinetics, physicochemical properties, sensory quality

The instant foxtail millet was prepared using microwave vacuum drying (MVD), microwave-hot air drying (MHAD), hot air drying (HAD) and traditional roasting (TR). Their effects on drying kinetics, physicochemical properties as well as sensory quality were evaluated and compared. Results showed that the total drying time varied with the drying method used and was about 160, 100, 260, and 45 min for MVD, MHAD, HAD and TR, respectively. The effective moisture diffusion coefficients (D_{eff}) were 6.57×10^{-9} m^2/s, 9.80×10^{-9} m^2/s, 4.14×10^{-9} m^2/s and 6.20×10^{-9} m^2/s for MVD, MHAD, HAD and TR, respectively. Drying resulted in a significant decrease in L^* and an increase in a^* and b^* of the color of products. MVD, MHAD and HAD products had a comparable rehydration ratio and cooking time. Scanning electron microscopy and rehydration process revealed that MHAD and MVD samples had a similar structure with the HAD sample. Drying caused a loss of 6.5–54.9% in the total phenolic content and a loss of 38.4–62.2% in total yellow pigment content. MVD millet displayed the highest total phenolic content (142.56 mg GAE/100 g dry matter) and yellow pigment content (9.56 mg CE/kg dry matter). In sensory evaluation, MHAD, HAD and MVD samples had comparable scores and were all accepted by the panelists, either in dry or rehydrated form. MHAD and MVD can be used as an alternative to hot air drying or traditional roasting in the production of the instant millet due to shorter drying time and better product quality.

INTRODUCTION

Foxtail millet (*Setaria italica L.*) belongs to the small-seeded subsistence cereal crop in the family Poaceae [Pradeep & Sreerama, 2015]. It has excellent drought resistance and is extensively cultivated in the arid and semi-arid areas of the world [Sharma & Niranjan, 2018]. Foxtail millet grains are rich in a variety of essential nutritive compounds, which are comparable to that of major cereals such as wheat and rice [Saleh *et al*., 2013]. It is reported that the protein content in millet grains is equal or even superior to that in wheat, rice, maize and sorghum grains [FAO, 2005]. Foxtail millets also contain phytochemicals and micronutrients such as phenolic compounds and carotenoids. The total yellow pigment content in millet grains was found to be 17.32–3.46 mg/kg and higher than that in maize, wheat and sorghum [Li *et al*., 2021]. Total phenolic and total flavonoid content was 72.70 mg/100 g and 87.63 mg/100 g, respectively [Pradeep & Sreerama, 2015; Zhang *et al*., 2017]. It became a staple food source for humans before the rise of wheat and rice foxtail millet and played an increasingly important role in enhancing nutritional and food security [Wang *et al.*, 2017]. Sharma & Niranjan [2018] and Saleh *et al.* [2013] gave an insight into the nutritional quality, health benefits and processing utilization in their review articles publicized in recent several years. They highlighted that the foxtail millet remained an under-utilized state as an excellent food source.

The traditional methods used for cooking the foxtail millet in China include roasting and boiling [Bi *et al.*, 2019]. Boiling is the primary method of cooking and the boiled foxtail millet porridge was widely eaten in daily diet by Chinese or in traditional meals as a nourishing gruel or soup for pregnant and nursing women for food therapy [Sharma & Niranjan, 2018]. Besides these, the foxtail millet was also processed into a handful of foods such as yellow wine prepared by fermentation, popping meals, instant millet powder prepared by roasting or extrusion expansion and so on. However, there are some obvious problems such as fewer processing categories, low processing rate as well as missing of instant processing products conforming to traditional consumption habits, which are restricting its consumption in China. Processing them using traditional as well as contemporary methods for preparation of value-added and convenience products would certainly diversify their food uses [Pradeep & Sreerama, 2015]. Instant rice or quick cooking rice is defined as the processed dried whole grain, which belongs to granular α-rice products prepared by gelatinization and dehydration and could be ready for eating after rehydrating for a few

* Corresponding Author:
E-mail: sxxds2008@163.com (Y. Wang)

Submitted: 26 November 2021
Accepted: 27 January 2022
Published on-line: 18 February 2022

minutes in hot water [Sripinyowanich & Noomhorm, 2013; Wang *et al*., 2017]. Such a kind of product provides a convenient way to consume rice for modern people and is increasing in popularity [Hsu *et al*., 2015]. To obtain the instant rice, the freshly cooked rice must be dehydrated to a certain moisture content, practically 6–12 g/100 g dry matter, so the drying operation is one of the critical steps in the preparation of instant rice [Luangmalawat *et al*., 2008]. There are many drying techniques to dehydrate foods including the instant rice. Hot-air drying is the most widely used drying method due to its little capital, simple equipment and low energy input, but it also generates the dried food product with a low quality due to long time and high process temperature [Luangmalawat *et al*., 2008; Rewthong *et al.*, 2011; Ritudomphol & Luangsakul, 2019; Shingare & Thorat, 2013; Sripinyowanich & Noomhorm, 2013]. Freeze drying under vacuum conditions is the best water removal method for all kinds of foods, while it requires long drying time that would lead to high energy consumption and high capital investment. Therefore, freeze drying is applied only with the high added-value products [Lenaerts *et al*., 2018; Lin *et al*., 1998].

Microwave-assisted drying is a more rapid method of moisture removal based on microwave heating substitution for convective or conduction heat transfer [Zhang *et al*., 2006]. The advantages of microwave-assisted drying include shorter drying time, reduced energy consumption, improved product quality and flexibility in producing a wide variety of dried products [Lin *et al*., 1998; Zhang *et al*., 2006]. The application of microwave energy with hot air drying of the cooked rice could reduce the drying time by 25%–50% as compared to the conventional drying [Jiao *et al*., 2014; Palamanit *et al*., 2020]. Sripinyowanich & Noomhorm [2013] dried the cooked rice using the microwave vibro-fluidized bed and the vibro--fluidized bed and found that the microwave vibro-fluidized bed drying had the highest drying rate and the shortest drying time as well as the lowest energy. The research of Lenaerts *et al*. [2018] showed that the microwave drying with or without vacuum can be a proper alternative to freeze drying for mealworms because microwave dried mealworms had no differences with the freeze dried ones in the proximate composition and displayed a lower oxidation status of the fat. The microwave-assisted convective dried instant rice had lower true densities and faster rehydration rate than air-dried samples due to a porous structure of the microwave-dried samples [Jiao *et al*., 2014; Le & Jittanit, 2015, 2012]. Although the use of microwave energy in food drying has a huge advantage in shortening drying time and improving energy efficiency, too rapid moisture transport under microwave heating conditions can cause quality damage or undesirable changes in the food texture due to "puffing" in some cases. However, this might or might not be a limitation, depending on the desired quality attributes of the final product [Zhang *et al*., 2006]. Microwave-related drying has been applied widely to dehydrate fruits and vegetables and is not common in grains and cereals drying [Wang *et al*., 2017].

Up to date, most research on instant grains is mainly focused on hot air drying of the instant rice and the effect of pretreatment prior to drying on quality. Limited studies are available concerning the effects of different drying methods on quality of the instant millet, like foxtail millet. Therefore, the objective of this study was to compare the effects of four drying methods (microwave vacuum drying (MVD), microwave-hot air drying (MHAD), hot air drying (HAD) and traditional roasting (TR)) on the physicochemical properties, and sensory quality of the instant foxtail millet to provide more information for its value-added processing.

MATERIALS AND METHODS

Materials

Freshly hulled raw foxtail millet was purchased from a local supermarket (Qingyang, Gansu, China) and stored in a cool and dry place after arrival to lab for further use. All chemical reagents used were of analytical grade.

Cooking of the millet

The cleaned raw millet was soaked in plenty of tap water for 3 h at room temperature. After soaking, the steeping water was drained off from the millet and the obtained millet was added into the tap water at a 3:1 (*w/v*) ratio of millet to water and steamed at high pressure (121°C, 0.12 MPa) for 40 min. After cooking, the gelatinized millet granules were spread out on the plate and cooled to room temperature. The resulting cooked millet was used for MVD, MHAD and HAD. The cleaned raw millet was directly applied to TR.

Drying of the cooked millet and raw millet roasting

Microwave-vacuum drying (MVD): a batch of 300 g cooked millet was dried in a lab-scale microwave-vacuum dryer (ORW1.2S-5Z, Orient Microwave Co., Ltd., Nanjing, China). The samples to be dried were arranged in a single layer of 5 mm on a tray and the microwave-vacuum dryer was operated at 5 kPa (absolute pressure) and the power intensity for each drying test was 2.5 W/g (original mass of 300 g the cooked sample). The temperature of the material to be dried was monitored through an infrared temperature sensor and controlled at 60°C using an automatic on–off controller to avoid local charring.

Microwave hot air drying (MHAD): a batch of 300 g cooked millet was dried in a lab-scale microwave convection dryer (ORW 1.0S-3000R, Orient Microwave Co., Ltd.,). The samples to be dried were arranged in a single layer of 5 mm on a tray. The power intensity of 1.25 W/g was used. The temperature of the material to be dried was monitored through an infrared temperature sensor and controlled at 60°C. Hot air with a temperature of 60°C was fed into the dryer chamber and crossed the material surface at 0.5 m/s velocity.

Hot air drying (HAD): a batch of 300 g cooked millet was dried in an electricity heat drum wind drying oven (DHG-9420A, Yiheng Instrument Co., Ltd., Shanghai, China). The samples to be dried were arranged in a single layer of 5 mm on a tray. During the period of drying, hot air with a temperature of 60°C circulated in the box at 0.5 m/s velocity.

Traditional roasting (TR): about 300 g of raw foxtail millet grains were spread on a tray as a single layer of thickness of 5 mm and dried and roasted at the selected temperature of 150°C. The electricity heat drum wind drying oven mentioned above was applied.

During the drying and roasting process, moisture loss of the samples was recorded at a regular interval using a digital balance (JH2102, Shanghai Precision & Scientific Instrument Co., Ltd., Shanghai, China) with 0.01 g precision. The samples were dehydrated until a moisture content of less than 7 g/100 g was reached. Each drying experiment was conducted in triplicate. After the drying process was completed, the dried products were cooled down to room temperature and then kept in sealed polyethylene bags in desiccators with a silica gel-self indicator.

Drying characterization evaluation

Calculation of moisture ratio and drying rate

During drying process, drying rate was determined as follows:

$$Drying\ rate = \frac{X_t - X_{t+\Delta t}}{\Delta t} \quad (1)$$

where: X_t, $X_{t+\Delta t}$ is moisture content (kg water/kg dry matter) at time t and $t+\Delta t$, respectively, Δt is time interval (min).

The change of moisture content in time was defined as a dimensionless parameter and expressed as the following equation:

$$MR = \frac{X - X_e}{X_0 - X_e} \quad (2)$$

where: MR is the dimensionless moisture ratio, X, X_0 and X_e stand for the initial moisture content, the moisture content at drying time t and the equilibrium moisture content, respectively. All results were expressed per dry basis (kg water/kg dry matter). The Eq. 2 can be simplified to:

$$MR = \frac{X}{X_0} \quad (3)$$

because the value of dynamic equilibrium moisture content X_e was very small as in comparison with X_0 and X [Kaya *et al*., 2007].

Calculation of moisture diffusivity

Drying process was proven to occur mostly in the falling rate period, and moisture transfer during drying was controlled by internal diffusion. Fick's second diffusion law (Eq. 4) had been widely used to describe the drying process in the falling rate period for most biological materials [Schoessler *et al*., 2012].

$$\frac{\partial X}{\partial t} = \Delta[D_{eff}(\nabla X)] \quad (4)$$

where: D_{eff} is the effective moisture diffusion coefficient (m^2/s), which was a mass diffusion property of the product.

Assuming unidirectional and constant moisture diffusion, negligible shrinkage and temperature change during drying, analytical solutions of Eq. 4 for an infinite slab geometry are expressed as Eq. 5:

$$\frac{X - X_e}{X_0 - X_e} = \frac{8}{\pi^2}\sum_{n=0}^{\infty}\frac{1}{(2n+1)^2} \times \exp\left(-\frac{(2n+1)^2\pi^2 \times D_{eff}}{4L^2} \times t\right) \quad (5)$$

where: L is the thickness of the sample slices (m).

For long drying periods, the first term of the series solution in Eq. 5 can be used as stated in Eq. 6.

$$MR = \frac{8}{\pi^2}\exp\left(-\frac{\pi^2 \times D_{eff}}{4L^2} \times t\right) \quad (6)$$

Eq. 6 can be simplified to a straight-line equation as follows:

$$lnMR = \ln\left(\frac{8}{\pi^2}\right) - \frac{\pi^2 \times D_{eff}}{4L^2} \times t \quad (7)$$

Plotting experimental drying data in terms of ln*MR versus* time, a straight line can be obtained. D_{eff} was calculated according to the slop of the straight line.

Analysis of physicochemical and sensory properties

Moisture content

The moisture content of the raw and cooked samples was determined by the oven method at 105°C [AOAC, 1997] and expressed per dry basis. Every experiment was repeated three times.

Color parameters

A chromaticity instrument (CR-400, Konica Minolta Co., Tokyo, Japan) calibrated using a white standard board was used to measure the color of the millet sample surface. Readings were expressed in CIE1976 $L^*a^*b^*$ scale, where L^* measures lightness, with 100 being very white and 0 being dark; the a^* value measures green (–) to red (+) and b^* represents blueness (–) to yellowness (+). Each sample was tested in five different locations. Total color difference (ΔE), hue angle ($h°$) and chroma (C^*) were also calculated according to the following equations [Chong *et al.*, 2008]:

$$\Delta E = \sqrt{(\Delta L^*)^2 + (\Delta a^*)^2 + (\Delta b^*)^2} \quad (8)$$

$$h^\circ = \text{arctg}(b^*/a^*) \quad (9)$$

$$C^* = \sqrt{(a^*)^2 + (b^*)^2} \quad (10)$$

where: ΔL^*, Δa^*, Δb^* are the difference value of L^*, a^* and b^* between the raw millet and the dried ones, respectively. The hue angle ($h°$) expresses the color nuance; the values are defined as follows: red-purple: 0°, yellow: 90°, bluish-green: 180°, blue: 270°. The C^* expresses chromaticity and denotes the purity or the saturation of the color.

Rehydration ratio and cooking time

Rehydration ratio of the dried instant millets was measured according to the method described by Wang L. *et al*. [2013]. In brief, 5 g of the dried sample was immersed in 100 mL of distilled water at room temperature. Samples were drained and weighed at an interval of 30 min for 300 min. After taking out of the water, the excess water was removed using a dry blotting paper, and then the weight was measured. Rehydration ratio was calculated according to the mass ratio of the rehydrated and original dried sample at a point. Every experiment was conducted in triplicate and the results were expressed as the mean values.

Cooking time was defined as the time which the millet grains required to be fully rehydrated in boiling water. After full rehydration, the center of the millet grains became completely softened and the white core in its center position was justly lost. Cooking time was determined according to the method descried by Wang L. *et al*. [2013]. About 10 g of dried instant millet was put into 100 mL of boiling water for a while, during which the millet grains were taken out and observed, and the time lapsed was recorded till full rehydration.

Microstructure

Scanning electron microscope (EVO 15, Carl Zeiss AG, Oberkochen, Germany) was used to analyze the microstructure of the raw and dried millets. The specimen fragments were glued to the holder, sputter-coated with gold and examined for the inner structure and photographed at an accelerating voltage of 2 kV. The gold-coated samples were viewed under the microscope and a ×500 magnification was used in all microscopic observations.

Total yellow pigment content

Total yellow pigment content in the raw and dried millet was determined using the method described by Shen *et al*. [2015]. Ground sample (2 g) was added to a 50 mL centrifuge tube, and combined with 20 mL of water-saturated *n*-butanol. After closing the stopper, the tube was mixed to fully wet the sample. The centrifuge tube was placed on a reciprocating shaker for 3 h. Subsequently, the tube was allowed to stand for 10 min and then centrifuged at 4,000×*g* (TDL-40B centrifuge, Anting, Shanghai, China) for 10 min. The supernatants were collected and adjusted to 25 mL using the water-saturated *n*-butanol, then filtered through 0.45 mm filters. Water-saturated *n*-butanol blank was used as a control. The absorbance of sample extracts was measured at 450 nm with a 751 UV--VIS spectrophotometer (Shanghai Analytical Instrument Factory, Shanghai, China). β-Carotene (Sigma Chemical Co., St. Louis, MO, USA) (0–5 μg/mL) was used as a standard for the calibration curve. The tests were performed in triplicate. Total yellow pigment content was expressed as mg β-carotene equivalent (CE) per kg of dry matter.

Total phenolic content

Total phenolic content in the raw and dried millet was determined with the Folin-Ciocalteau reagent [Singleton *et al*., 1999]. In brief, 3 g of the ground sample was extracted subsequently by a methanol:water solution acidified with HCl (50:50 *v/v*, pH 2, 25 mL/g sample) and an acetone:water solution (70:30 *v/v*, 25 mL/g sample) with continuous stirring at room temperature for 60 min. The extracts were filtered through a Whatman No.1 filter paper, then the supernatants were combined and centrifuged at 3,000×*g* for 15 min (TDL--40B centrifuge). The obtained supernatant of 0.5 mL was mixed with 0.5 mL of the Folin-Ciocalteu reagent in a 25 mL glass-stopped tube. After 3 min, 10 mL of a sodium carbonate solution (75 g/L) were added and mixed. Additional distilled water (14 mL was added up to make a final volume of 25 mL) was added and then the sample was mixed thoroughly by inverting the tubes several times. After 1 h, the absorbance at 750 nm was recorded with a 751 UV–VIS spectrophotometer. Gallic acid (Sigma Chemical Co., 0–100 mg/L) was used as a standard for the calibration curve. The tests were performed in triplicate. Total phenolic content was expressed as mg gallic acid equivalent (GAE) per g of dry matter.

Sensory evaluation

Sensory evaluation of the dried and rehydrated samples was carried out separately to obtain preliminary information on consumer preference and eating quality of the dried millet. For the dried millet, ten untrained panelists (between 24 and 50 years old) were asked to rate their liking of the samples in terms of appearance, color, odor, tactility, mouthfeel, taste and overall acceptability on a 1 to 9 hedonic scale: 1 – dislike extremely, 5 – neither like nor dislike, 9 – like extremely [Lin *et al*., 1998]. The panelists were also asked to make comments and recommendations in regard to each sensory attribute. The rehydrated samples were made to the instant millet porridge and the instant millet beverage to evaluate their eating quality. These panelists gave a score on the overall acceptability of the product. A score of 5 or below was considered the limit of acceptability for all sensory attributes tested. To prepare the instant millet porridge, the dried little millet was poured into hot water and boiled for 6–8 min at the 1:10 (*w/v*) ratio of millet to water. The instant millet beverage was prepared by crushing the dried sample followed by brewing with hot water, which consisted of 15 g of millet flour, 5 g of sucrose and 200 mL of hot water. The sensory evaluation was performed in triplicate.

Statistical analysis

All data obtained in this study were analyzed statistically. The results were expressed as means ± standard deviation (SD). Differences among mean values were estimated by analysis of variance (ANOVA) with the application of Duncan's multiple range tests using SPSS 17.0.1 software (SPSS Inc., Chicago, IL, USA). Mean values were considered significantly different when $p<0.05$.

RESULTS AND DISCUSSIONS

Characteristics of millet drying

The initial moisture content of the cooked millets prior to MVD, MHAD and HAD was found to be 1.23 kg water/kg dry matter while the one of the raw millets before TR was found to be 0.14 kg water/kg dry matter. Figure 1a presents the variation of moisture content with drying time under the four different drying conditions. The moisture content sharply decreased at the initial drying stage and subsequently slowly reduced as MVD, MHAD and HAD proceeded. On the other hand, the curve of moisture content *vs.* time had a gentle incline for TR. These differences may have been due to great differences in initial moisture content of the samples. The total drying time reached the desired moisture content of 0.07 kg water/kg dry matter was about 160, 100, 260, and 45 min for MVD, MHAD, HAD and TR, respectively. TR drying time of the instant little millets was the shortest while the HAD one was the longest. Compared with HAD, both MHAD and MVD could reduce the drying time of the instant millets by 38.5–61.5% due to microwave fast heating capacity. Comparable findings were reported while drying instant

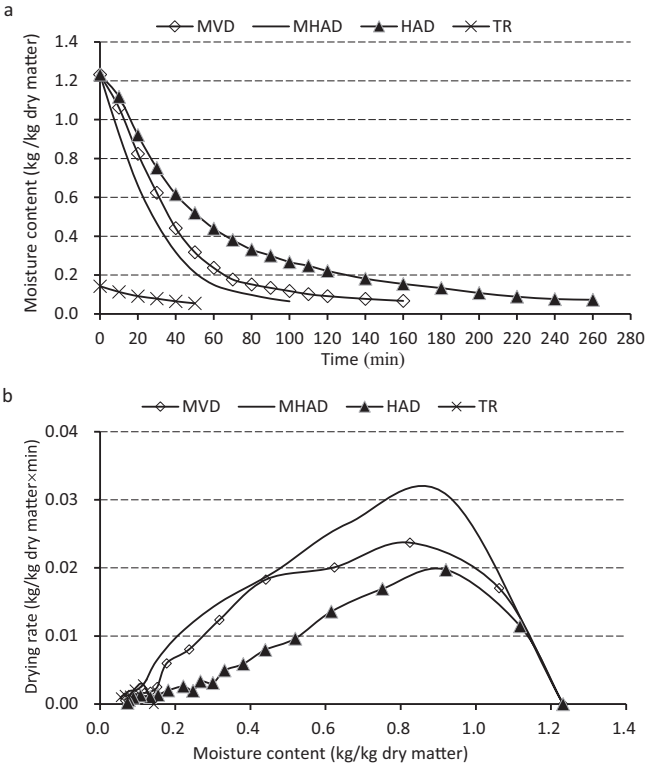

FIGURE 1. Drying curves (a) and drying rate curves (b) of the instant foxtail millet with different drying methods. MVD: microwave-vacuum drying, MHAD: microwave-hot air drying, HAD: hot air drying, TR: traditional roasting.

rice [Jiao *et al.*, 2014; Palamanit *et al.*, 2020]. The mentioned authors found that the incorporation of microwave power with hot air drying helped to reduce the drying time by 25–50% in comparison with the conventional hot air drying.

Drying rate, a function of drying time and moisture content, was a fundamental parameter that was computed from the drying data by estimating geometric derivation occurring in each consecutive time interval, and was expressed as kg water/(kg dry matter×min). Figure 1b depicts the variation of drying rate with moisture content in the millet under the four drying conditions. Drying method had a strong influence on drying rate curve. HAD and MVD underwent a warm-up, raising speed period at the beginning, followed by a falling rate period for a long time while MHAD only underwent a falling rate period due to the difference in moisture movement capacity and heat transfer. The moisture movement behavior including diffusion and vaporization during drying of food depended on the drying conditions and the characteristic of the material to be dried [Zogzas *et al.*, 1996]. A falling rate drying signified that the drying process was controlled by the inner water diffusion [Schoessler *et al.*, 2012; Wang *et al.*, 2019b].

The graph of experimental values of ln*MR* of the millet against drying time was plotted for each drying method, and the D_{eff} of the millet was calculated according to Eq. 7 and presented in Table 1. The coefficients of determination (R^2) of linear regression for ln*MR* against time presented values greater than 0.95, which indicated a good linear relationship between ln*MR* and time. The D_{eff} was in the range from 6.57×10^{-9} m^2/s to 9.80×10^{-9} m^2/s, with the highest value

TABLE 1. Effective moisture diffusion coefficient (D_{eff}) of the instant foxtail millet obtained with different drying methods.

Drying method	R^2	D_{eff} ($\times10^{-9}$ m^2/s)
MVD	0.9563	6.57±0.85^b
MHAD	0.9839	9.80±0.67^a
HAD	0.9313	4.14±0.12^c
TR	0.9888	6.20±0.34^b

Data are presented as mean ± standard deviation (n=3) and means within a column with different letters are significantly different at $p<0.05$. MVD: microwave-vacuum drying, MHAD: microwave-hot air drying, HAD: hot air drying, TR: traditional roasting, R^2: coefficient of determination of linear regression.

determined for MHAD followed by MVD. The lowest D_{eff} was found for HAD. The values of D_{eff} obtained from this study were in the range typical for food materials drying (from 10^{-12} to 10^{-8} m^2/s) [Zogzas *et al.*, 1996]. The effective moisture diffusivity was associated with the drying conditions and the nature of the material to be dried (material thickness, initial moisture content, moisture state as well as the cell disruption induced by different pre-treatments) [Chong *et al.*, 2008; Wang *et al.*, 2019b; Zogzas *et al.*, 1996].

Physical properties of raw and dried instant millet

Color parameters

Color of food is an important attribute which influences consumer acceptability. The raw foxtail millet presented a pale yellow due to the presence of crude starch and yellow pigment. The color parameters including L^*, a^*, b^*, C*, ΔE and h^o of both the raw and the dried instant millet were determined and the results were listed in Table 2. Drying operation resulted in a significant ($p<0.05$) decrease in the L^* value and a significant ($p<0.05$) increase in a^*, b^*, and C^* values of the dried millets in comparison with the raw sample. Lower L^* indicated more dark color while higher a^* and b^* value signifies lighter red color and lower blue color, respectively. This indicates that the final dried millet became darker and appeared light brown. Similar results were found in the fluidized bed drying of finger millets and roasted pigmented wheat [Dhua *et al.*, 2021; Shingare & Thorat, 2013].

The a^* and b^* and C^* value in TR products were significantly ($p<0.05$) lower than that of the three dried products after cooking (Table 2). In turn, there were no significant ($p\geq0.05$) differences between a^* and b^* and C^* values of the MHAD and MVD and HAD products. The MHAD and MVD products had also a comparable value of the L^*, but it was significantly ($p<0.05$) higher than that found for the HAD product. The TR product had a minimum value of ΔE while a maximum value of ΔE was observed in HAD product, which indicates that the color of TR product is closest to the original color of the raw millet.

The hue angle (h^o) for both the raw and all the dried samples was in the range of 73.5–82.8^o (Table 2), which was located in a color nuance between red-purple to yellow and tended to be yellow. The raw and TR products were more

TABLE 2. Color parameters of the raw and instant foxtail millet obtained with different drying methods.

Treatment	L^*	a^*	b^*	C^*	h^o	ΔE
Raw	71.10±2.21^a	3.29±0.26^c	25.90±1.09^c	26.11±1.22^c	82.80±2.34^a	
MVD	56.03±1.32^c	9.04±0.89^a	32.17±1.43^a	33.42±1.65^a	74.34±2.33^c	16.32±1.12^b
MHAD	55.75±1.23^c	9.56±0.67^a	32.19±1.07^a	33.58±1.98^a	73.50±1.34^c	16.60±1.09^b
HAD	50.61±0.98^d	9.21±0.98^a	33.22±1.55^a	34.47±2.34^a	74.54±2.34^c	21.76±1.34^a
TR	65.14±2.34^b	6.46±0.46^b	28.58±1.67^b	29.30±1.78^b	77.30±3.24^b	7.03±0.56^c

Data are presented as mean ± standard deviation (n=3) and means within a column with different letters are significantly different at p<0.05. MVD: microwave-vacuum drying, MHAD: microwave-hot air drying, HAD: hot air drying, TR: traditional roasting.

yellow than the dried products after cooking. The differences in color values of the products might be related to structural changes of starch granule, browning reaction including Maillard reaction and caramelization favored by heat as well as change in yellow pigment concentration during processing and these multiple factors are responsible for color changes [Dhua *et al*., 2021; Shingare & Thorat, 2013].

Rehydration characteristics and cooking time

Most dehydrated products need to be rehydrated prior to use; rapid and complete rehydration when immersed in water is desirable. Additionally, rehydration is a measure of damage to the material caused during drying [Wang *et al*., 2019a]. Figure 2a presents the variation of the rehydration ratio *vs.* time for the four dried millets during rehydration at room temperature for 300 min. In all cases, the rehydration ratio tended to reach a relative stabilization state at a decreasing rate. The rehydration curves for MVD, MHAD and HAD products overlapped each other and presented a similar rehydrated behavior. It was indicated that microwave heating caused no damage to the structure of the cooked millet during drying and the dried millet products maintained the typical structure in the non-polypass gelatinized starch products like instant rice [Luangmalawat *et al*., 2008; Palamanit *et al*., 2020], vermicelli and rice flour noodles [Xing *et al*., 2015]. TR product had a faster rate but a lower rehydration ratio than the other three products due to millet cracking caused by high temperature. The rehydration ratios of MVD, MHAD, HAD and TR instant little millet were 2.67, 2.61, 2.65 and 1.82 at 300 min, respectively. There were also no significant (p≥0.05) differences observed in the dried products after cooking.

Figure 2b presents the cooking time of the instant foxtail millet with different drying methods. Cooking time for the MVD, MHAD, HAD and TR millet was 352 s, 348 s, 349 s and 559 s, respectively. It was indicated that the millet porridge could be prepared in a short time from these instant millet products. MVD, MHAD and HAD products had a comparable (p≥0.05) cooking time and their cooking time was significantly (p<0.05) shorter than that of the TR millet.

Microstructure of the instant millet

In order to understand the structure changes in the instant millets caused by the drying methods, the microstructures of the raw and dried millet were observed using scanning electron microscopy and were shown in Figure 3. It can be seen that both the raw millet and TR product had a similar and rough inner structure, where the crude starch granule with a crystal structure was embed in the fragment of the millet grain. In the MVD, HAD and MHAD products, the fragment of the millet grain appeared a fine, smooth and dense surface due to recrystallization of gelatinized starch. There were no obvious differences observed among them. A porous and obviously expanded structure easily developed in microwave-related drying of many food materials such as restructured fish and starch gel product [Wang Y. *et al.,* 2012; 2013] and fruit slices [Lin *et al*., 1998; Zhang *et al*., 2006] was not found in this study. Probably a viscoelastic gel structure that can trap water vapor and higher microwave power density applied can expand more readily under microwave volumetric heating. Similar microstructure observed in the dried millets after cooking led to insignificant differences in the rehydration curve of the rehydrated millet as mentioned in the previous section. This result

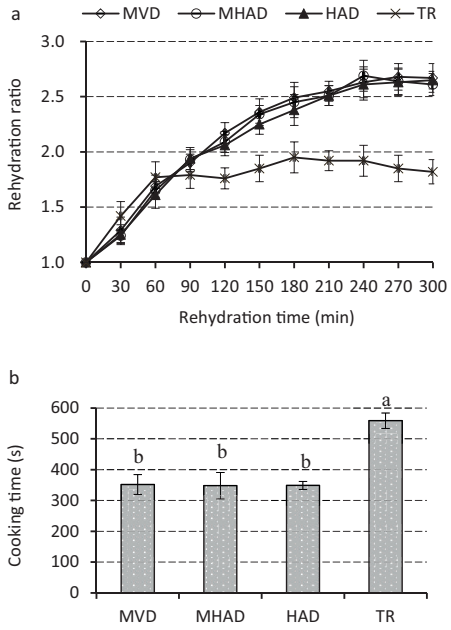

FIGURE 2. Rehydration curves (a) and cooking time (b) of the instant foxtail millet obtained with different drying methods. Data are presented as bars with mean ± standard deviation (n=3) and means with different letters are significantly different at p<0.05. MVD: microwave-vacuum drying, MHAD: microwave-hot air drying, HAD: hot air drying, TR: traditional roasting.

was in agreement with the findings of Luangmalawat *et al.* [2008] and Palamanit *et al.* [2020]. They found that drying temperature and application of microwave power in hot air drying did not affect the rehydration ratio and microstructure of the instant rice.

Total phenolic and yellow pigment contents of raw and dried instant millet

Phenolics and yellow pigments are the most important phytochemicals present in foxtail millet grains, which play an important role in imparting antioxidant property to the grains [Sharma & Niranjan, 2018]. The main component of millet yellow pigment is natural carotenoids which are believed to impart yellow color to the foxtail millet grains except for healthy effect [Shen *et al*., 2015]. Figure 4 shows total phenolic and yellow pigment contents in the raw millet and the instant millet dried using different methods. Total phenolic and yellow pigment contents in the raw millet were 152.45 mg GAE/100 g dry matter and 15.51 mg CE/kg dry matter, respectively. In the dried millets, total phenolic content ranged from 142.56 mg GAE/100 g dry matter to 68.77 mg GAE/100 g dry matter while yellow pigment content was in the range of 9.56 mg CE/kg dry matter to 5.86 mg CE/kg dry matter. Drying caused a loss of 6.5–54.9% in the total phenolic content and a loss of 38.4–62.2% in total yellow pigment content and there were significant ($p<0.05$) differences among dried millets. MVD dried millet displayed the highest total phenolic and yellow pigment contents due to the oxygen-free condition and shorter drying time, followed by the MHAD and HAD; both the total phenolic and yellow pigment contents of the TR sample were the lowest because of roasting at high temperature. This result indicated that MVD and MHAD was more beneficial to the retention of phenolics and yellow pigments in the millet than the other drying method.

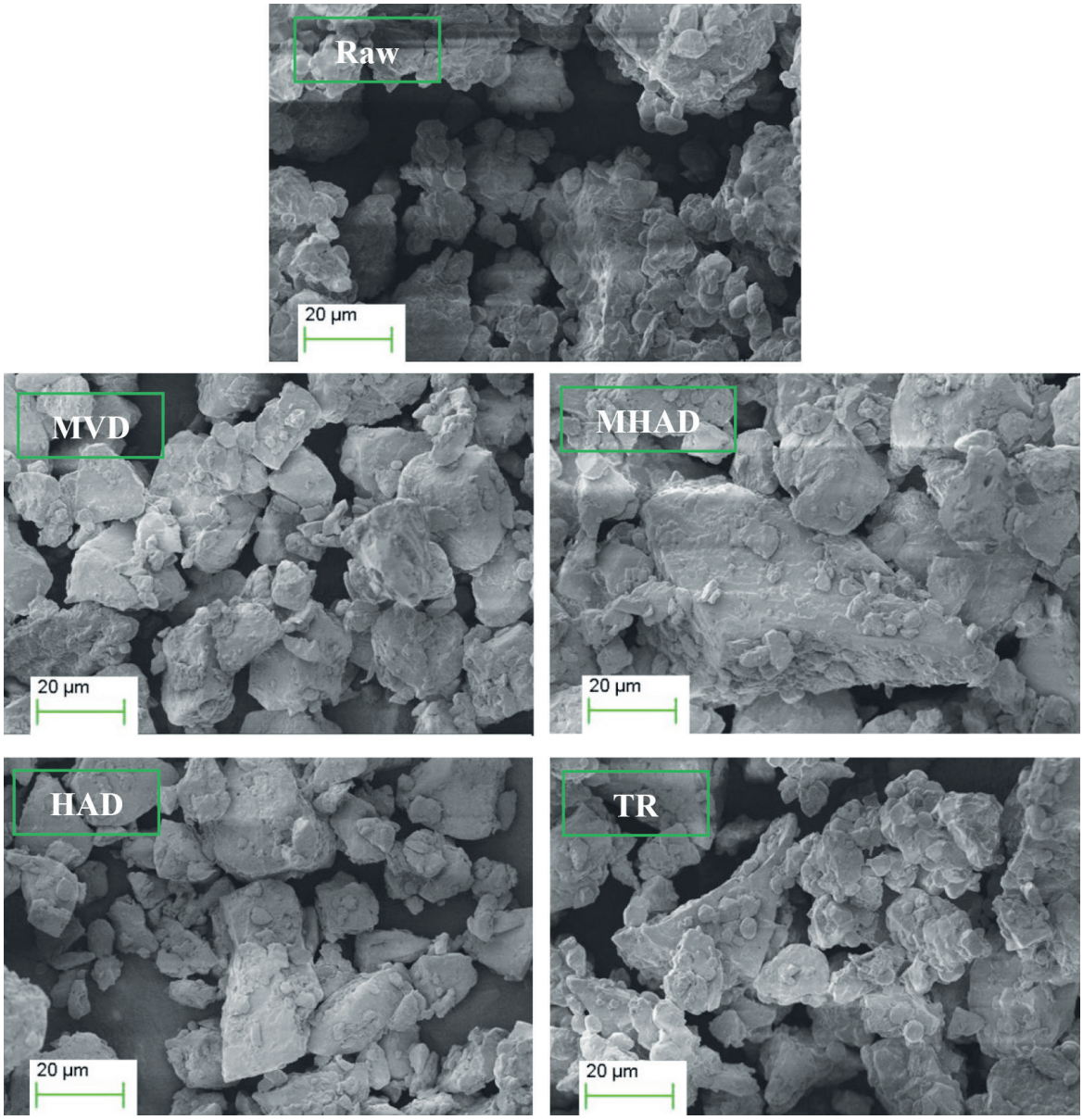

FIGURE 3. Scanning electron micrographs of the raw and instant foxtail millet obtained with different drying methods. MVD: microwave-vacuum drying, MHAD: microwave-hot air drying, HAD: hot air drying, TR: traditional roasting.

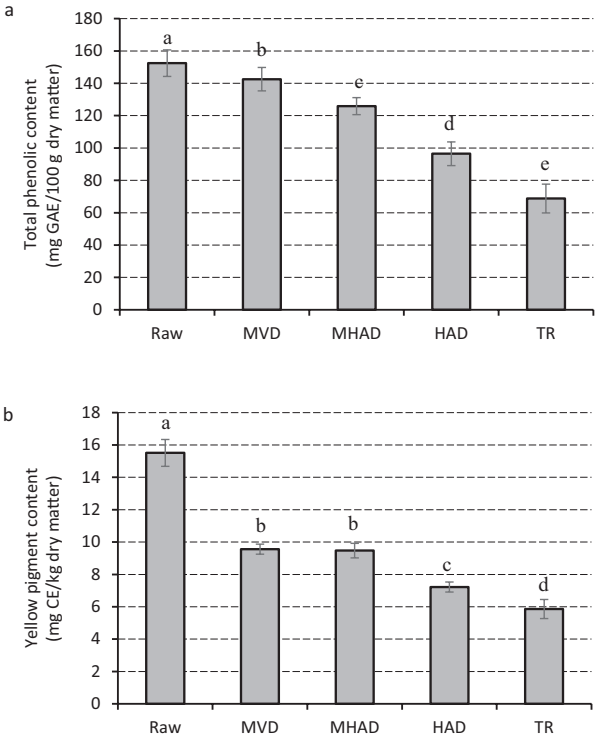

FIGURE 4. Total phenolic content (a) and total yellow pigment content (b) of the raw and instant foxtail millet obtained with different drying methods. Data are presented as bars with mean ± standard deviation (n=3) and means with different letters are significantly different at p<0.05. MVD: microwave-vacuum drying, MHAD: microwave-hot air drying, HAD: hot air drying, TR: traditional roasting, GAE: gallic acid equivalent, CE: β-carotene equivalent.

Phenolics and yellow pigments in food systems are sensitive to heat, and deterioration reactions easily occur during the thermal process like cooking and drying. The loss of total phenolic content due to drying was found for microwave-dried green peas [Chahbani *et al.*, 2018], steam- and microwave-treated small millets [Hithamani & Srinivasan, 2014] and microwave-roasted pigmented wheat [Dhua *et al*., 2021]. Carotenoid degradation reactions, including isomerization and oxidation, are known to occur easily during a thermal process [Shen *et al.*, 2015]. These reactions caused also the instability and loss of the carotenoids of foxtail millet during cooking and drying. Shen *et al*. [2015] found that the atmospheric-pressure cooking and high-pressure cooking resulted in an around 10–20% and 60%, respectively, loss of total yellow pigment contents in the foxtail millet.

Sensory score of the dried instant millet and rehydrated products

Table 3 lists the results of sensory evaluation for both the dried and rehydrated millet products. In dry form, the MHAD, HAD and MVD samples showed no significant (p≥0.05) differences in sensory evaluation and were all characterized by a transparent, hard and granular appearance, a more yellow color and a full-bodied millet fragrance while the TR sample had a crispy mouthfeel, pale color, globular appearance and roasted aroma. The former three products presented a light sweet taste and were superior to the TR one. The popcorn-like and smoky odors were noted for roasted foxtail millet, and the development of pyrazines contributed to the odor. Each sensory attribute for all the dried samples except mouthfeels was scored above 5 and was ranked as liked very much or slightly liked by the panelists. As for overall acceptability, they were all accepted by the panelists as a commodity although TR product had a lower score than the others.

With regard to eating quality after rehydration, the MHAD, HAD and MVD samples were scored above 7 as porridge and were all accepted by the panelists while TR one was scored below 4 and was not accepted by the panelists. When eating as beverage, all the instant millets were scored above 7 and were all accepted by the panelists. Moreover, the panelists preferred the TR sample to the other three samples due to the presence of roasted aroma.

CONCLUSION

Based on results of the present investigation, we concluded that the drying methods have profound effect on the drying kinetics and quality of the dried instant foxtail millet. As compared with the conventional HAD and TR, microwave-assisted drying including MVD and MHAD had shorter drying time and higher drying rate, which could reduce the drying time of the instant little millets by 38.5–61.5%. Moreover, MVD and MHAD samples possessed higher total phenolic and yellow pigment contents as well as excellent physical and sensory indexes. MVD and MHAD are suitable for drying the instant millet, and the instant millet obtained could be used as the food to make quick-cooking porridge or beverage.

TABLE 3. Results of sensory evaluation of the instant foxtail millet obtained with different drying methods and products from instant foxtail millets.

Drying methods	Color	Odor	Appearance	Tactility	Mouthfeel	Taste	Overall acceptability	Eating quality	
								Porridge	Beverage
MVD	8.2±0.4^{a}	8.5±0.1^{a}	8.3±0.2^{a}	7.3±0.4^{b}	2.0±0.2^{b}	7.3±0.2^{a}	8.3±0.2^{a}	7.4±0.1^{a}	7.2±0.2^{b}
MHAD	8.1±0.2^{a}	8.3±0.4^{a}	8.2±0.1^{a}	7.1±0.3^{b}	1.9±0.3^{b}	7.2±0.1^{a}	8.2±0.1^{a}	7.8±0.3^{a}	7.5±0.3^{b}
HAD	8.3±0.3^{a}	8.1±0.2^{a}	8.3±0.3^{a}	7.2±0.6^{b}	2.1±0.2^{b}	7.3±0.3^{a}	8.3±0.3^{a}	7.1±0.2^{a}	7.1±0.2^{b}
TR	7.5±0.2^{b}	8.8±0.3^{a}	8.0±0.5^{a}	8.6±0.2^{a}	5.5±0.1^{a}	5.5±0.5^{b}	7.0±0.5^{b}	3.9±0.2^{b}	8.5±0.2^{a}

Data are presented as mean ± standard deviation (n=3) and means within a column with different letters are significantly different at p<0.05. MVD: microwave-vacuum drying, MHAD: microwave-hot air drying, HAD: hot air drying, TR: traditional roasting.

RESEARCH FUNDING

The authors gratefully acknowledged the financial supports provided by the National Natural Science Foundation of China (No.31460398 and No.32060544) and the Scientific Research Starting Foundation for Doctor (No.2014XYBY1) and Youth Science and Technology Innovation Project (No. XYZK1707) of Longdong University.

DECLARATION OF CONFLICTING INTERESTS

The authors declare no potential conflicts of interest with respect to the research, authorship, and/or publication of this article.

ORCID IDs

Y. Wang https://orcid.org/0000-0002-7186-2367
H. Zhao https://orcid.org/0000-0001-6523-3233

REFERENCES

1. AOAC. 1997. Official Methods of Analysis of the Association of Official Analytical Chemists. 16th ed. Washington, DC.
2. Bi, S., Wang, A., Wang, Y., Xu, X., Luo, D., Shen, Q., Wu, J. (2019). Effect of cooking on aroma profiles of Chinese foxtail millet (*Setaria italica*) and correlation with sensory quality. *Food Chemistry*, *289*(15), 680–692. https://doi.org/10.1016/j.foodchem.2019.03.108
3. Chahbani, A., Fakhfakh, N., Balti, M.A., Mabrouk, M., El-Hatmi, H., Zourai, N., Kechaou, N. (2018). Microwave drying effects on drying kinetics, bioactive compounds and antioxidant activity of green peas (*Pisum sativum L.*). *Food Bioscience*, *25*, 32–38. https://doi.org/10.1016/j.fbio.2018.07.004
4. Chong, C.H., Law, C.L., Cloke, M., Hii, C.L., Abdullah, L.C., Daud, W.R. W. (2008). Drying kinetics and product quality of dried Chempedak. *Journal of Food Engineering, 88*(4), 522–527. https://doi.org/10.1016/j.jfoodeng.2008.03.013
5. Dhua, S., Kheto, A., Sharanagat, V.S., Singh, L., Kumar, K., Nema, P.K. (2021). Quality characteristics of sand, pan and microwave roasted pigmented wheat (*Triticum aestivum*). *Food Chemistry*, *365*, art. no. 130372. https://doi.org/10.1016/j.foodchem.2021.130372
6. FAO (2005). Sorghum and millets in human nutrition. *FAO Food and Nutrition Series, No.68. Rome*, p. 277.
7. Hithamani, G., Srinivasan, K. (2014). Effect of domestic processing on the polyphenol content and bioaccessibility in finger millet (*Eleusine coracana*) and pearl millet (*Pennisetum glaucum*). *Food Chemistry*, *164*, 55–62. https://doi.org/10.1016/j.foodchem.2014.04.107
8. Hsu, R.J.C., Chen, H.J., Lu, S., Chiang, W.C. (2015). Effects of cooking, retrogradation and drying on starch digestibility in instant rice making. *Journal of Cereal Science*, *65*, 154–161. https://doi.org/10.1016/j.jcs.2015.05.015
9. Jiao, A., Xu, X., Jin, Z. (2014). Modelling of dehydration–rehydration of instant rice in combined microwave-hot air drying. *Food and Bioproducts Processing*, *92*(3), 259–265. https://doi.org/10.1016/j.fbp.2013.08.002
10. Kaya, A., Aydin, O., Demirtas, C., Akgün, M. (2007). An experimental study on the drying kinetics of quince. *Desalination*, *212*(1–3), 328–343. https://doi.org/10.1016/j.desal.2006.10.017
11. Le, T.Q., Jittanit, W. (2012). Drying characteristics of cooked jasmine brown rice and true densities of dried products. *Kasetsart Journal (Natural Science)*, 46, 256–271.
12. Le, T.Q., Jittanit, W. (2015). Optimization of operating process parameters for instant brown rice production with microwave--followed by convective hot air drying. *Journal of Stored Products Research*, *61*, 1–8. https://doi.org/10.1016/j.jspr.2015.01.004
13. Lenaerts, S., Borght, M.V.D., Callens, A., Van Campenhout, L. (2018). Suitability of microwave drying for mealworms (*Tenebrio molitor*) as alternative to freeze drying: Impact on nutritional quality and color. *Food Chemistry*, 254, 129–136. https://doi.org/10.1016/j.foodchem.2018.02.006
14. Li, S., Zhao, W., Liu, S., Li, P., Zhang, A., Zhang, J., Wang, Y., Liu, Y., Liu, J. (2021). Characterization of nutritional properties and aroma compounds in different colored kernel varieties of foxtail millet (*Setaria italica*). *Journal of Cereal Science*, 100, art. no. 103248. https://doi.org/10.1016/j.jcs.2021.103248.
15. Lin, T.M., Durance, T.D., Scaman, C.H. (1998). Characterization of vacuum microwave, air and freeze dried carrot slices. *Food Research International*, *31*(2), 111–117. https://doi.org/10.1016/S0963-9969(98)00070-2
16. Luangmalawat, P., Prachayawatakorn, S., Nathakaranakule, A., Soponronnarit, S. (2008). Effect of temperature on drying characteristic and quality of cooked rice. *LWT – Food Science and Technology*, *41*(4), 716–723. https://doi.org/10.1016/j.lwt.2007.04.010
17. Palamanit, A., Sugira, A.M., Soponronnarit, S., Prachayawarakorn, S., Tungtrakul, P., Kalkan, F., Raghavan, V. (2020). Study on quality attributes and drying kinetics of instant parboiled rice fortified with turmeric using hot air and microwave-assisted hot air drying. *Drying Technology*, *38*(4), 420–433. https://doi.org/10.1080/07373937.2019.1579735
18. Pradeep, P.M., Sreerama, Y.N. (2015).Impact of processing on the phenolic profiles of small millets: Evaluation of their antioxidant and enzyme inhibitory properties associated with hyperglycemia. *Food Chemistry*, *169*, 455–463. https://doi.org/10.1016/j.foodchem.2014.08.010
19. Rewthong, O., Soponronnarit, S., Taechapairoj, C., Tungtrakul, P., Prachayawarakorn, S. (2011). Effects of cooking, drying, and pretreatment methods on texture and starch digestibility of instant rice. *Journal of Food Engineering*, *103*(3), 258–264. https://doi.org/10.1016/j.jfoodeng.2010.10.022
20. Ritudomphol, O., Luangsakul, N. (2019). Optimization of processing condition of instant rice to lower the glycemic index. *Journal of Food Science*, *84*(1), 101–110. https://doi.org/10.1111/1750-3841.14406
21. Saleh, A.S.M., Zhang, Q., Chen, J., Shen, Q. (2013). Millet grains: nutritional quality, processing, and potential health benefits. *Comprehensive Reviews in Food Science & Food Safety*, *12*(3), 281–295. https://doi.org/10.1111/1541-4337.12012
22. Schoessler, K., Jaeger, H., Knorr, D. (2012). Effect of continuous and intermittent ultrasound on drying time and effective diffusiv-

ity during convective drying of apple and red bell pepper. *Journal of Food Engineering*, *108*(1), 103–110. https://doi.org/10.1016/j.jfoodeng.2011.07.018

23. Sharma, N., Niranjan, K. (2018). Foxtail millet: properties, processing, health benefits, and uses. *Food Reviews International*, *34*(4), 329–363. https://doi.org/10.1080/87559129.2017.1290103
24. Shen, R., Yang, S.P., Zhao, G.H., Shen, Q., Diao, X.M. (2015). Identification of carotenoids in foxtail millet (*Setaria italica*) and the effects of cooking methods on carotenoid content. *Journal of Cereal Science*, *61*, 86–93. https://doi.org/10.1016/j.jcs.2014.10.009
25. Shingare, S.P., Thorat, B.N. (2013). Effect of drying temperature and pretreatment on protein content and color changes during fluidized bed drying of finger millets (Ragi, *Eleusine coracana*) sprouts. *Drying Technology*, *31*(5), 507–518. https://doi.org/10.1080/07373937.2012.744033
26. Singleton, V.L., Orthofer, R., Ramuela-Raventos, R.M. (1999). Analysis of total phenols and other oxidation substrates and antioxidants by means of Folin-Ciocalteu reagent. *Oxidants and Antioxidants, 299*(1), 152–178. https://doi.org/10.1016/S0076-6879(99)99017-1
27. Sripinyowanich, J., Noomhorm, A. (2013). Effects of freezing pretreatment, microwave assisted vibro-fluidized bed drying and drying temperature on instant rice production and quality. *Journal of Food Processing and Preservation*, *37*(4), 314–324. https://doi.org/10.1111/j.1745-4549.2011.00651.x
28. Wang, Q., Li, S., Han, X., Ni, Y., Zhao, D., Hao, J. (2019a). Quality evaluation and drying kinetics of shitake mushrooms dried by hot air, infrared and intermittent microwave-assisted drying methods. *LWT – Food Science and Technology*, *107*, 236–242. https://doi.org/10.1016/j.lwt.2019.03.020
29. Wang, Y., Zhao, H., Deng, H., Song, X., Zhang, W., Wu, S., Wang, J. (2019b). Influence of pretreatments on microwave vacuum drying kinetics, physicochemical properties and sensory quality of apple slices. *Polish Journal of Food and Nutrition Sciences*, *69*(3), 297–306. https://doi.org/10.31883/pjfns/110734
30. Wang, R.C., Chen, C., Guo, S.T. (2017). Effects of drying methods on starch crystallinity of gelatinized foxtail millet (α-millet) and its eating quality. *Journal of Food Engineering, 207*, 81–89. https://doi.org/10.1016/j.jfoodeng.2017.03.018
31. Wang, L., Zhang, G., Bao, G., Zhang, L. (2013). Study on rehydration of instant millet gruel by microwave and hot air combined drying. *Cereal and Feed Industry, 12*(6), 25–28.
32. Wang, Y., Zhang, M., Mujumdar, A.S. (2013). Effect of cassava starch gel, fish gel and mixed gels and thermal treatment on structure development and various quality parameters in microwave vacuum-dried gel slices. *Food Hydrocolloids*, *33*(1), 26–37. https://doi.org/10.1016/j.foodhyd.2013.02.005
33. Wang, Y., Zhang, M., Mujumdar, A.S., Mothibe, K.J. (2012). Quality changes of dehydrated restructured fish product from silver carp as affected by drying methods. *Food and Bioprocess Technology, 6*(7), 1664–1680. https://doi.org/10.1007/s11947-012-0812-y
34. Xing, L.J., Mu, T.H., Zhang, M., Yu, S.X., Chen, J.W., Yang, H.Y. (2015). Effects of different low-temperature and drying treatment on the properties of purple sweet potato starch noodle. *Food Science and Technology*, *40*(3), 15–121.
35. Zogzas, N.P., Maroulis, Z.B., Marinos-Kouris, D. (1996). Moisture diffusivity data compilation in foodstuffs. *Drying Technology*, *14*(10), 2225–2253. https://doi.org/10.1080/07373939608917205
36. Zhang, M., Tang, J.M., Mujumdar, A.S., Wang, S. (2006). Trends in microwave-related drying of fruits and vegetables. *Trends in Food Science & Technology*, *17*(10), 524–534. https://doi.org/10.1016/j.tifs.2006.04.011
37. Zhang, L., Li, J., Han, F., Ding, Z., Fan, L. (2017). Effects of different processing methods on the antioxidant activity of 6 cultivars of foxtail millet. *Journal of Food Quality*, *2017*(SI), art. no. 8372854. https://doi.org/10.1155/2017/8372854

Pol. J. Food Nutr. Sci., 2022, Vol. 72, No. 1, pp. 79–89
On-line ISSN: 2083-6007
Print ISSN: 1230-0322
DOI: 10.31883/pjfns/146317
http://journal.pan.olsztyn.pl

Original article
Section: Food Quality and Functionality

Antioxidant Activity of Hybrid Sturgeon (*Huso dauricus* × *Acipenser schrenckii*) Protein Hydrolysate Prepared Using Bromelain, Its Fractions and Purified Peptides

Anwar Noman[1,2], Yuxia Wang[1], Chao Zhang[1], Sherif M. Abed[3]*

[1]Key Laboratory of Fermentation Resource and Application in Sichuan Higher Education, Faculty of Agriculture, Forestry and Food Engineering, Yibin University, Yibin, 644000, Sichuan, China
[2]Department of Agricultural Engineering, Faculty of Agriculture, Foods and Environment, Sana'a University, Sana'a, Yemen
[3]Food and Dairy Science and Technology Department, Faculty of Environmental Agricultural Science, Arish University, North Sinai, Egypt

Key words: hybrid sturgeon, enzymatic hydrolysis, hydrolysis optimization, bromelain, degree of hydrolysis, radical scavenging activity, peptide purification

Protein hydrolysates could be a natural and safer source of antioxidant peptides. The purpose of this study was to optimize the hydrolysis of *Huso dauricus* × *Acipenser schrenckii* sturgeon proteins using bromelain and purify antioxidant peptides from hydrolysate. The degree of hydrolysis of 18.69% was obtained under the optimal conditions and hydrolysate had 94.76% solubility, 902 nm particle size and high antioxidant activity. The IC_{50} for DPPH$^{\bullet}$ and ABTS$^{\bullet+}$ scavenging activity were 3.14 and 3.81 mg/mL, respectively. The fraction of hydrolysate with a molecular weight of <1 kDa exhibited the highest antiradical activity against DPPH$^{\bullet}$ with IC_{50} of 2.10 mg/mL. In turn, the IC_{50} of the most active fraction after the Sephadex G-15 separation was 1.77 mg/mL. The reverse phase high performance liquid chromatography (RP-HPLC) was used to purify the peptides from this fraction. The peptide with histidine, leucine and glycine (MW of 0.2955 kDa) exhibited the highest antioxidant activity (IC_{50} of 1.33 mg/mL). The obtained fractions and peptides with antioxidant activity could be used as natural substitutes for synthetic antioxidants, especially in food and pharmaceuticals.

INTRODUCTION

Sturgeons are freshwater fishes with a high protein content in the meat ranging from 15 g/100 g to 21 g/100 g [Abraha *et al*., 2018]. The main areas of sturgeon distribution are considered to be the estuaries of large rivers of Eurasia and North America [Billard & Lecointre, 2000]. Sturgeon aquaculture is developed in China, which is well-known for its raising large scale commercial breeding with a production of 79,638 tons (~77% of the global production) of sturgeon species in 2017 [Bronzi *et al*., 2019]. Hybrid sturgeons are characterized by fast growth and high disease resistance [Luo *et al*., 2015]. Among the hybrid sturgeon species, the *Huso dauricus* × *Acipenser schrenckii* is the most abundant [Jin *et al*., 2020].

Free radicals are highly unstable molecules, which easily react with unsaturated lipids and carbohydrate polymers leading to various damages to food as a result of the oxidation process [Jang *et al.,* 2016]. Additionally, free radicals can cause a variety of serious diseases including cancer, diabetes mellitus, tissue inflammation, neurodegenerative diseases and aging [Zhang *et al*., 2021]. To reduce or prevent free radical-induced food oxidation, synthetic antioxidants such as propyl gallate, butylated hydroxyanisole, butylated hydroxytoluene, and tert-butylhydroquinone are required; however, due to their negative effects, the search for safe natural sources has increased [Samaranayaka & Li-Chan, 2011]. Tan *et al.* [2018] found that the peptides produced by the enzymatic hydrolysis process have antioxidant and antimicrobial properties. They can perform other physiological functions in the human body, such as antihypertensive and antithrombotic activities, in addition to their effective activity against lipid peroxidation and free radicals [Chi *et al.,* 2014; Zhang *et al.,* 2019]. The properties of hydrolysates and peptides resulting from enzymolysis make them potentially useful in the prevention, treatment, and amelioration of several diseases, in addition to extending the shelf life of food products [Famuwagun *et al.,* 2020].

Recently, many studies have found that enzymatic protein hydrolysates from different fish parts had good functional characteristics and high antioxidant activities [Elavarasan & Shamasundar, 2016; Latorres *et al*., 2018; Wang

* Corresponding Author:
E-mail: wangyx5166@163.com (Y. Wang)

Submitted: 11 October 2021
Accepted: 1 February 2022
Published on-line: 1 March 2022

Z. *et al*., 2021]. The proper selection of enzymolysis conditions, as well as the monitoring the progress of this process, may result in a production of protein hydrolysates with exceptional sensory quality as well as desired functional and biological properties [Marson *et al*., 2019]. The antioxidant activity of peptides (3 to 20 amino acid residues) released during hydrolysis is associated to their molecular weights and amino acid profiles [Chalamaiah *et al*., 2015]. These peptides can be released from fish proteins through *in vitro* enzymatic hydrolysis, but also by *in vivo* digestion, or bacterial fermentation [Chi *et al*., 2015a]. Several studies depend on protein hydrolysis to isolate antioxidant peptides using ultrafiltration and chromatography techniques from fish hydrolysates such as pacific herring [Wang *et al.,* 2019], skipjack tuna [Zhang *et al.,* 2019] and bluefin leatherjacket [Chi *et al*., 2015b].

The objective of the current study was to find optimal hydrolysis conditions of hybrid sturgeon (*Huso dauricus* × *Acipenser schrenckii*) protein using bromelain and to purify antioxidant peptides from hydrolysate by its step-by-step fractionation using ultrafiltration membranes, gel filtration chromatography, and reverse-phase high-performance liquid chromatography (RP-HPLC).

MATERIALS AND METHODS

Chemicals and reagents

Bromelain (EC 3.4.22.33, 600 U/mg) was purchased from Beijing Solarbio Sciences and Technology Co., Ltd. (Beijing, China). 1,1-Diphenyl-2-picrylhydrazyl (DPPH) radical was obtained from Bomei Biotechnology Co., Ltd (Hefei, China), and 2,2-azino-bis(3-ehtylbenzothiazoline-6-sulfonic acid) (ABTS) was purchased from Sigma Chemical Co. (Shanghai, China). Standard amino acids (aspartic acid, histidine, glutamic acid, serine, glycine, threonine, alanine, arginine, tyrosine, cystine, valine, methionine, phenylalanine, isoleucine, leucine, lysine and proline) were purchased from Sigma Chemical Co. (Shanghai, China). All of the chemicals and reagents used in this study were of analytical grade and high purity.

Fish muscle preparation

Hybrid sturgeon *Huso dauricus* × *Acipenser schrenckii* was used as experimental material. The live fish farmed in Leshan City, Sichuan Province, China were obtained from aquatic products company branch in Yibin city, Sichuan, China. The fishes (length of ~80 cm and a weight of ~2 kg) were immediately transported to the laboratory in a water basin, slaughtered, and the viscera were then removed. The hybrid sturgeon muscles (15.25±0.83 g protein/100 g muscles) were separated from the by-products (head, fins, skin, tail, fat and membranes). Following that, the muscles were minced with a blender for 2 min, packaged in polyethylene bags, frozen, and stored at –18°C until use. The prepared muscles were thawed overnight in a refrigerator at 4°C before being subjected to the enzymatic hydrolysis procedure.

Hydrolysates production

To optimize the conditions of hydrolysis of hybrid sturgeon muscle proteins, the single-factor experimental design was applied. The parameters affecting the enzymatic hydrolysis were the sample-to-buffer ratio, *i.e.* solid/liquid (S/L; 1:1, 1:2, and 1:3, *w/v*) with constant other parameters (E/S 1:100, pH 6.0, temperature 40°C and time 3 h), enzyme/substrate ratio (E/S; 0.5:100, 1:100, 2:100, 3:100 and 4:100, *w/w*) with constant other parameters (optimal S/L 1:1, pH 6.0, temperature 40°C and time 3 h), pH (5.0, 5.5, 6.0, 6.5, 7.0, and 7.5) with constant other parameters (optimal S/L 1:1, optimal E/S 1:100, temperature 40°C and time 3 h), and reaction temperature (30, 35, 40, 45, 50, 55, and 60°C) with constant other parameters (optimal S/L 1:1, optimal E/S 1:100, optimal pH 6.5, and time 3 h). To assess the impact of those parameters, the degree of hydrolysis (DH) was used as a response parameter. Finally, the hydrolysis were carried out under optimal conditions of S/L, E/S, pH and temperature for 1, 3, 6, and 9 h to determine the optimal incubation time.

The reactions were conducted in jacketed glass vessels (200 mL) heated in a circular water bath. According to the required pH, the minced muscles (100 g) were mixed with acetic acid or sodium phosphate buffer (25 mM). The bromelain was dissolved in the same buffer, and then added at required temperature. The pH was monitored during the reaction time and adjusted with NaOH or HCL (1 N). After the designated time of hydrolysis, the mixture was incubated in a water bath at 90°C for 15 min to inhibit any further enzymatic reactions [Ovissipour *et al.*, 2013], followed by a centrifugation step for 10 min at 12,000×*g* and 4°C (TGL-18 centrifuge, Sichuan Shuke Instrument Co., Ltd., Chengdu, China). The supernatant was freeze-dried for 48 h at -55°C with a vacuum of 0.25 mbar (BioSafer-18A freeze--dryer, Safer Co., Ltd., Nanjing, China). The lyophilized protein hydrolysates obtained using bromelain (BH) were stored at -20°C in airtight containers until they were used for final product analysis.

Degree of hydrolysis determination

DH was measured as the ratio of α-amino nitrogen (AN) content to total nitrogen (TN) content in the tested samples. The formal titration procedure proposed by Taylor [1957] with modifications was applied to determine the AN content. The homogeneous hydrolysate mixture (1.5 g) obtained from the enzymolysis process was carefully taken, and the weight was increased to 50 g by adding distilled water. The pH of the hydrolysate solution was adjusted to 7.0 using 0.1 N of NaOH solution, then 10 mL of formaldehyde 38% (*v/v*) was added, and the resultant mixture was left at 25±2°C for 5 min. Finally, the titration process was continued to a pH of 8.5 using the same NaOH solution. The following equation was used to calculate the AN content:

$$\mathrm{AN} = \frac{V \times C \times 14.007}{\mathrm{W} \times 1000} \times 100 \quad (1)$$

where: V is the volume of NaOH (mL), C is the concentration of NaOH, and W is the hydrolysate weight (g).

The DH was calculated according Equation (2) after TN determination using the macro-Kjeldahl procedure [method 955.04; AOAC, 1998].

$$\mathrm{DH}\ (\%) = \frac{\mathrm{AN}}{\mathrm{TN}} \times 100 \quad (2)$$

Amino acid composition analysis

The determination of the amino acid profile of hybrid sturgeon lyophilized protein hydrolysate and purified peptide was carried out according to the method of Noman *et al*. [2020a]. Briefly, 100 mg of BH, and 5 mg of purified peptide, which was collected during repeated batches of the purification process by RP-HPLC, were separately hydrolyzed for 22 h at 120°C under a nitrogen atmosphere using 8 mL of 6 N HCl solution. After cooling the mixtures to room temperature (25±2°C), 4.8 mL of 10 N NaOH was added. The volume of the mixtures was adjusted to 25 mL by adding distilled water, filtered through two layers of No.40 filter paper, and then centrifuged at 11,200×*g* for 10 min. Finally, the Agilent 1100 HPLC system (Agilent Ltd., Palo Alto, CA, USA) was utilized to separate amino acids. The pre-prepared samples (1 μL) were injected into a Zorbax 80 A, C-18 column (250×4.0 mm, 5 μm particle size; Agilent, USA), at a flow rate of 1 mL/min heated to 40°C. The UV detector was set at 338 nm. The solutions of the mobile phases A and B were prepared. The mobile phase A was sodium acetate (7.35 mM)/triethylamine/tetrahydrofuran with a mixing ratio of 500:0.12:2.5 (*v/v/v*) adjusted to pH 7.5 using acetic acid, whilst the mobile phase B was sodium acetate (7.35 mM)/methanol/acetonitrile (1:2:2, *v/v/v*) at pH 7.2. The utilized mobile phase gradient was as follows: 0 min, 8% B; 17 min, 50% B; 20.1 min, 100% B; 24 min, 0% B. Amino acids were identified based on the comparison of the retention time of an amino acid standard. External standard quantitative method was used to quantify the amino acid contents of BH and peptide, and the results were expressed as g per 100 g of hydrolysate or total amino acids (TAA) of peptide, respectively.

Particle size distribution

A laser particle size analyzer (Brookhaven, Holtsville, NY, USA) was used to determine the particle size of BH. Briefly, the solution of hydrolysate (10 μg/mL) was diluted with deionized water, and then 3 mL of the resulting solution was placed in the measurement cell. The measurement was taken after 2 min of equilibration of sample solutions at 25°C. The particle size of the product was presented in nm.

Protein hydrolysate solubility

The solubility of BH was estimated following the method of García-Moreno *et al*. [2017] with some modifications. BH (100 mg) was mixed with 40 mL of deionized water, and the pH was adjusted with NaOH and HCL (0.1 N) solutions to 2, 4, 6, 8, and 10. The mixtures were mixed at high speed for 5 min before being centrifuged for 5 min at 1,790×*g*. Finally, 20 mL of the supernatant was collected and dried for 4 h at 110°C. The following equation was used to calculate the hydrolysate solubility (%):

$$\text{Hydrolysate solubility (\%)} = \left[\frac{W_2 \times 2}{W_1}\right] \times 100 \quad (3)$$

where: W_1 is the weight of the dissolved BH sample and W_2 is the weight of the dried supernatant.

DPPH radical scavenging activity

The DPPH$^{\bullet}$ scavenging activity of BH, its fractions and purified peptides was estimated according to the method mentioned by Adjimani & Asare [2015] with modifications. In short, 2 mL of BH solution, 1 mL of ultrafiltration fraction, 500 μL of gel filtration fraction or 200 μL of purified peptide solution (1, 2, 3, 4, and 5 mg/mL) was added to 2 mL of DPPH$^{\bullet}$ solution in 95% ethanol (0.1 mM). These mixtures were vortexed and held for 15 min in the absence of light at 25±2°C. The absorbance of final solutions (A_{sample}) and control samples ($A_{control}$) at 517 nm was measured using a UV--spectrophotometer (Mapada Instruments Co., Ltd., Shanghai, China). Instead of the sample solution, distilled water was used in the control sample. The following formula was used to calculate the DPPH$^{\bullet}$ scavenging activity:

$$\text{DPPH radical scavenging activity \%} = \frac{A_{control} - A_{sample}}{A_{control}} \times 100 \quad (4)$$

Next, the IC_{50} of BH, its fractions and peptide, defined as the sample concentration sufficient to inhibit 50% of DPPH radical was calculated using Excel 2010 (Microsoft, Redmond, WA, USA). A lower IC_{50} indicates a higher DPPH radical scavenging activity of the sample.

ABTS radical cation scavenging activity

The ABTS$^{\bullet+}$ scavenging activity of BH was determined according to Latorres *et al*. [2018] with some modifications. ABTS solution (7.4 mM) and potassium persulfate (2.6 mM) were mixed in equal quantities for 16 h at 25°C in the dark to make a stock solution. The absorbance of 1 mL of work solution was adjusted to 0.70±0.02 at 734 nm by mixing with 50 mL of ethanol (98%). Exactly, 200 μL from each BH concentration (1, 2, 3, 4 and 5 mg/mL) was mixed with 3.5 mL of ABTS$^{\bullet+}$ working solution and left at room temperature for 10 min in the absence of light. To prepare the control sample in this procedure, distilled water was utilized in place of the protein hydrolysate. The absorbance of solutions with BT (A_{sample}) and control ($A_{control}$) was measured precisely at 734 nm and the ABTS$^{\bullet+}$ scavenging activity was calculated using the following formula:

$$\text{ABTS (\%)} = \left[1 - \left(\frac{A_{sample}}{A_{control}}\right)\right] \times 100 \quad (5)$$

The IC_{50}, defined as the BH concentration sufficient to scavenge 50% of ABTS$^{\bullet+}$, was calculated.

Ultrafiltration of hydrolysate

The BH was fractionated using an ultrafiltration unit (Millipore Minitan system, Millipore, Bedford, MA, USA) with three different molecular weight cut-off (MWCO, 1, 2 and 3 kDa) membranes. The hydrolysate was dissolved in deionized water (50 mg/mL) and four fractions were separated and collected (F1, <1 kDa), (F2, 1–2 kDa), (F3, 2–3 kDa) and (F4, >3 kDa). The fractions were lyophilized and the antioxidant activity was estimated using the DPPH assay.

Separation of peptides by gel filtration chromatography

Gel filtration was used to separate the peptides of fraction with the highest antioxidant activity (MW <1 kDa). Briefly, fraction (60 mg) was dissolved in deionized water at

a concentration of 30 mg/mL and loaded onto a Sephadex G-15 column (2.6×80 cm). The peptides were eluted from the column with deionized water at a flow rate of 1.0 mL/min, aliquots of 3 mL of the eluate were collected and monitored by measuring the absorbance at 280 nm [Chi *et al*., 2015a] using a spectrophotometer (Mapada Instruments Co., Ltd., Shanghai, China). Six fractions were separated and freeze-dried. Hence, the fraction with the highest antioxidant activity (F4) was subjected to the following procedure.

Purification of peptide by RP-HPLC

The HPLC system (Agilent 1260, Santa Clara, CA, USA) was used to purify the peptides from F4 fraction resulting from gel filtration according to the method of Zhang *et al*. [2017] with minor modifications. Briefly, 10 mg of the fraction were diluted in 1 mL of 0.1% (*v/v*) trifluoroacetic acid (TFA), and 20 μL of the resultant solution was injected into a Zorbax SB, C-18 column (4.6 mm×250 mm, 5 μm particle size, Agilent). The mobile phase A was 0.1% (*v/v*) TFA and B was 30% (*v/v*) acetonitrile containing 0.1% (*v/v*) TFA under a flow rate of 0.8 mL/min using a gradient of 0–9 min, 0% B; 10–20 min, 10% B; 20.5–31.5 min, 20% B; 32–41 min, 40% B; and 41.5–43 min, 50% B. The eluate was detected at 280 nm, and six peptides (P1-P6) were isolated, collected and lyophilized.

Molecular weight determination of purified peptide

Gel permeation chromatography was applied using the HPLC system (Waters 1525, Milford, MA, USA) to determine the molecular weight of purified peptide (P2) according to the procedure described by Kong *et al*. [2008]. The TSK gel 2000SW$_{XL}$ column (300×7.8 mm) (Tosoh, Tokyo, Japan) was equilibrated with acetonitrile:water (40:60, *v/v*) with TFA (0.1%, *v/v*). The peptides were eluted at an isocratic flow rate of 0.5 mL/min. Detection was at 220 nm and column was heated to 30°C.

Statistical analysis

All chemical experiments were carried out in triplicate, and the average with the standard deviation was recorded. The results obtained were subjected to one-way analysis of variance (ANOVA) to establish the statistical differences. Fisher's least significant difference test was used to evaluate significant differences between mean values using SPSS version 20.0.0 (SPSS IBM, Chicago, IL, USA) at $p<0.05$.

RESULTS AND DISCUSSION

Optimization of the hydrolysis

DH is a useful parameter for measuring the efficiency of the hydrolysis process [Zheng *et al*., 2019]. It is dependent on enzyme and substrate concentrations, temperature, pH value, and reaction time [Villamil *et al*., 2017]. Therefore, the differences in its values may be due to one or more of factors, including enzyme specificity and the experimental conditions used, those influence the enzymatic hydrolysis mechanism [Ktari *et al*., 2013]. Generally, DH is a valuable tool for monitoring the hydrolytic reaction, allowing end-users to obtain protein hydrolysates with distinct peptide profiles, and thus with different functional and biological properties [Ang & Ismail-Fitry, 2019]. In the current study, the effect of conditions of hydrolysis using bromelain was tested to reach the maximum DH (Figure 1). The highest DH of 12.17% was reached for the S/L ratio of 1:1 (*w/v*). The DH was significantly ($p<0.05$) reduced when the portion of liquid in the reaction mixture was increased (Figure 1A). The obtained maximal S/L ratio was consistent with previous results which indicated that the same 1:1 (*w/v*) ratio was optimal for hydrolysis of fish proteins using Alcalase or papain [Bhaskar *et al*., 2008; Noman *et al*., 2018]. As a result, this ratio was chosen for future experiments. The effect of the E/S ratio on the DH was investigated at 0.5:100, 1:100, 2:100, 3:100, and 4:100 (*w/w*) as shown in Figure 1B. When the bromelain concentration was increased from 0.5:100 to 1:100 (*w/w*), the DH increased significantly ($p<0.05$) from 11.47 to 14.93%, respectively. However, by further increasing the concentration to 2:100 and 3:100, there was no significant ($p<0.05$) increase in DH. Whereas, DH decreased to 14.16% as the E/S ratio was increased to 4:100. This may be attributed to enzyme aggregation, which prevents proteins from interacting with the enzymes' catalytic sites. Hence, the reaction rate is saturating and the enzymolysis process is inhibited [Gao *et al*., 2020]. As a result, in our study, 1:100 (*w/w*) was selected to be the optimal E/S ratio.

The effect of pH on DH was measured over a range of six levels from 5.0 to 7.5 (Figure 1C). The DH increased from 9.79 to 16.06% by increasing the pH from 5.0 to 6.5. Increasing the pH to 7.0 and 7.5 reduced the DH insignificantly ($p\geq0.05$) to 15.78 and 15.59%, respectively. According to the result of DH, the pH 6.5 was chosen in this stage of optimizing the hydrolysis conditions. Do Evangelho *et al*. [2017] mentioned that some differences in the DH could be attributed to the pH value. The deamination process of glutamine to glutamic acid and asparagine to aspartic acid may occur by acid hydrolysis rather than enzymatic hydrolysis. Therefore, authors observed that the acidic medium led to an increase in the DH. The optimal pH may change based on substrate, and enzyme concentration used in the reaction. However, pH may cause denaturation of the enzyme protein structure or a change in the ionic character of the substrates used in the reaction, both of which reduce the substrates' ability to bind to the enzyme [Salwanee *et al*., 2013]. In our study, the effects of seven temperatures ranging from 30 to 60°C were investigated, and the results revealed that the maximum DH was obtained at 45°C and 50°C (Figure 1D). There was a significant decrease of DH for hydrolyses obtained at temperatures above 50°C. The reduction in DH may be due to the thermal denaturation, which renders the enzyme inactive and reduces its ability to severe the peptide bonds under high-temperature conditions [Gao *et al*., 2020; Guérard *et al*., 2002]. The 45°C was chosen for future experiments.

Finally, the enzymolysis was carried out for various durations under the obtained optimal conditions, and the impact of reaction time on the DH was evaluated within the time range of 1–9 h, as shown in Figure 1E. During the first hour, more than 60% of the hydrolysis occurred. This indicated that the maximum number of peptide bonds were broken during this time period. There was a significant increase ($p<0.05$) of DH when the time was increased from 1 h (12.15%) to 6 h (18.69%). Nevertheless, increasing the hydrolysis time to

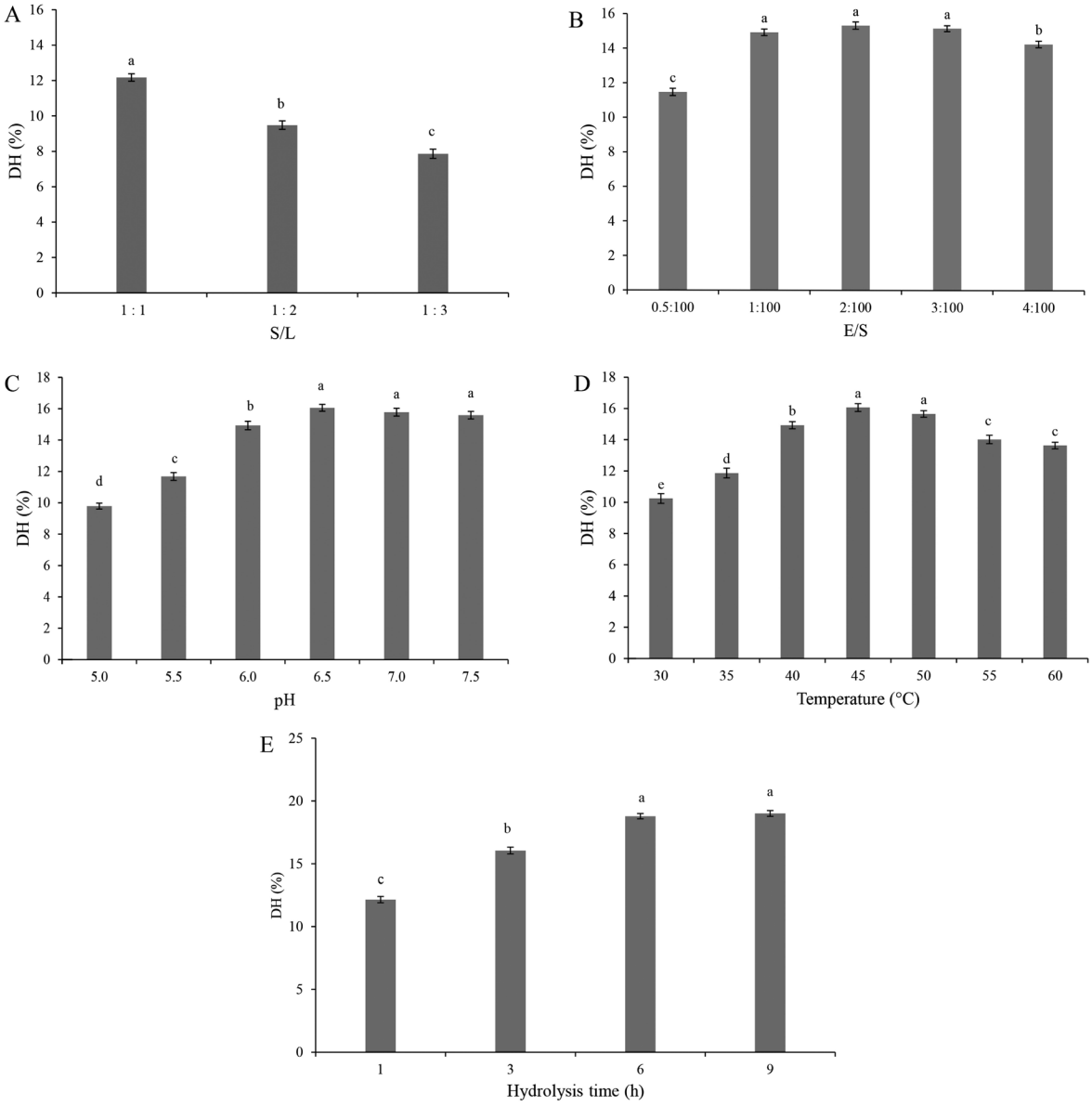

FIGURE 1. The degree of hydrolysis (DH) of hybrid sturgeon (*Huso dauricus* × *Acipenser schrenckii*) proteins using bromelain at different conditions of (A) solid to liquid ratio (S/L); (B) enzyme to substrate ratio (E/S); (C) temperature; (D) pH and (E) reaction time. Different letters above bars indicate significant differences at $p<0.05$. Data are expressed as mean ± standard deviation of triplicate determinations.

9 h did not result in a significant increase of DH, thus 6 h was chosen as appropriate reaction time for obtaining protein hydrolysate. The DH under optimal conditions (18.69%) was close to results obtained for hydrolyses of Chinese sturgeon (*Acipenser sinensis*) muscles using Alcalase [Noman *et al*., 2019], and monkfish (*Lophius litulon*) muscle using trypsin [Chi *et al*., 2014], which were 19.1% and 19.83%, respectively. However, the DH in our study was higher than that obtained for the hydrolysis of tilapia (*Oreochromis niloticus*) frame using pepsin, trypsin, Flavourzyme, Neutrase and papain, which ranged from 5.3% to 15.1% [Fan *et al*., 2012].

Amino acid profile of hydrolysate

The amino acid profile of the optimized hybrid sturgeon hydrolysate is displayed in Table 1. The arginine, lysine, leucine, and valine were the most abundant among essential amino acids, while proline, valine and leucine accounted for nearly 54% of hydrophobic amino acids. In our study (Table 1), the content of total hydrophobic amino acids was higher than that obtained by Ghanbari *et al*. [2015] for sea cucumber (*Actinopyga lecanora*) hydrolysates prepared with several enzymes and by Saidi *et al.* [2014] for tuna dark muscle by-product protein hydrolysate. On the other hand, the amino acid profile of BH showed that there were significant contents of histidine, tyrosine, and phenylalanine, which together with high contents of leucine and valine (Table 1), could be related to antioxidant activities of protein hydrolysate of hybrid sturgeon. Bahari *et al*. [2020] reported that the presence of the mentioned amino acids in the peptide sequences enhanced their antiradical activity.

Generally, glutamine and asparagine accounted for about 25% of the total amino acids in the obtained hydrolysate

TABLE 1. Amino acid composition of optimized hybrid sturgeon protein hydrolysate obtained using bromelain.

	Amino acids	Content (g/100 g hydrolysate)
Essential amino acid	Histidine	2.27±0.10
	Threonine	2.47±0.22
	Arginine	11.35±0.10
	Tyrosine*	2.17±0.11
	Valine*	5.70±0.14
	Methionine*	2.57±0.13
	Phenylalanine*	2.38±0.06
	Isoleucine*	3.11±0.10
	Leucine*	5.45±0.11
	Lysine	7.16±0.14
Non-essential amino acids	Asparagine	9.20±0.21
	Glutamine	16.83±0.12
	Serine	2.56±0.10
	Glycine*	3.49±0.25
	Alanine*	2.23±0.10
	Cystine*	1.65±0.06
	Proline*	9.46±0.30
Total	TAAs	90.05±1.01
	TEAAs	44.63±0.61
	TN-EAAs	45.42±0.46
	THAAs	38.21±0.51

Results are expressed as mean ± standard deviation (n=3); TAAs: total amino acids; TEAAs: total essential amino acids; TN-EAAs: total non-essential amino acids; THAAs: total hydrophobic amino acids.
*Hydrophobic amino acid.

(Table 1), which was consistent with the content of these amino acids in sea cucumber *Isostichopus badionotus* hydrolysate [Pérez-Vega *et al*., 2013], and was close to the results reported for rohu roe (*Labeo rohita*) protein hydrolysates [Chalamaiah *et al*., 2013]. Hybrid sturgeon hydrolysate prepared using bromelain proved to be a good source of lysine with a content of 7.16 g/100 g (Table 1). Consequently, BH could be beneficial in diet formulations to alleviate protein malnutrition caused by lysine deficiency, which is limited in cereals and their products [Chalamaiah *et al*., 2013].

Particle size of hydrolysate

The particle size of BH was 902±61 nm. This result was within the particle size range (100–1500 nm) of swamp eel (*Monopterus albus*) protein hydrolysate obtained by Priatni *et al*. [2020]. The particle size distribution is affected by temperature and hydrolysis time. Noman *et al*. [2020b] reported that after 6 h of hydrolysis at 70°C the particle size was higher than after incubation at 55°C due to the high temperature-induced formation of aggregates. On the other hand, Wang Y.-Y. *et al*. [2021] found that the smaller particle size was related to higher DH, due to the increasing number of small peptides or amino acids in hydrolysates with increasingly higher DH.

Solubility of hydrolysates

Solubility affects a number of other functional properties of proteins, thus increasing solubility makes protein hydrolysate a potential source suitable for application in different food systems. Figure 2A depicts the solubility of BH at various pH, and it was found that the BH exhibited a higher solubility at pH 8, representing 94.76%, followed by pH 10 (92.15%) and pH 2 (90.45%) with a significant difference (p<0.05), while the minimum solubility was at the pH 4 (83.17%). These results are in line with previous studies [Latorres *et al*., 2018; Naqash & Nazeer, 2013], which found that the protein hydrolysate solubility was affected by pH values. Solubility of sturgeon proteins increases as the pH moves away from their isoelectric points (pH 4.5–5.5) because the net charge of the original proteins is reduced at that range. Thus, protein-protein interactions increase, and the protein-water interactions decrease [Noman *et al*., 2019]. On the other hand, increased solubility as a result of enzymatic hydrolysis may be attributed to an increase in smaller peptides content and charged groups such as $-NH_3^+$ and $-COO^-$, which reinforce protein-water interactions and cause more electrostatic repulsion between peptides in the solution [Eberhardt *et al*., 2019].

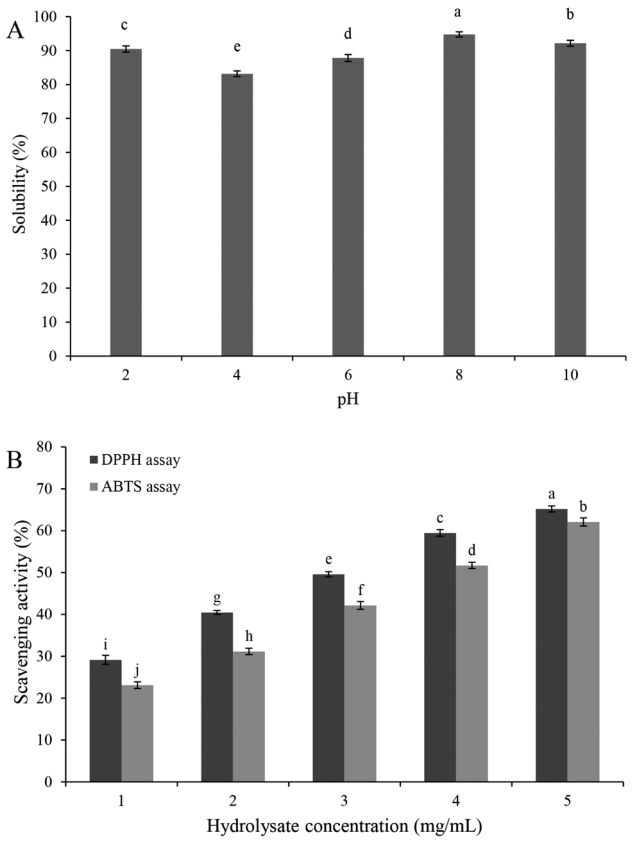

FIGURE 2. The solubility (A) and antioxidant activity (B) of hybrid sturgeon (*Huso dauricus* × *Acipenser schrenckii*) hydrolysate obtained using bromelain. Different letters above bars indicate significant differences at p<0.05. Data are expressed as mean ± standard deviation.

Antioxidant activities of BH

The DPPH radical scavenging activity of hybrid sturgeon protein hydrolysate is displayed in Figure 2B. It was shown that the antiradical activity against DPPH of BH increased significantly ($p<0.05$) from 29.15% to 65.17% as hydrolysate concentration increased from 1 to 5 mg/mL and IC_{50} was 3.14 mg/mL. The results of this study are consistent with previous studies that found an increase in antioxidant activity as protein hydrolysate concentration increased [De Quadros *et al*., 2019; Galla *et al*., 2012]. The DPPH radical scavenging activity of BH at 5 mg/mL exceeded that of shrimp protein hydrolysates prepared using Alcalase and Protamex [Latorres *et al*., 2018], and *Pseudosciaena crocea* protein hydrolysates obtained using neutral protease [Zhang *et al*., 2017] at the same concentration. The IC_{50} of BH in DPPH assay was lower than that of salmon by-product hydrolysates prepared using Alcalase, Flavorzyme, Neutrase, Protamex and trypsin, which ranged from 3.62 to 4.95 mg/mL, while it was higher than that of the hydrolysate obtained using pepsin, which was 1.63 mg/mL [Ahn *et al*., 2014]. The release of bioactive peptides during the hydrolysis depends on enzyme specificity [Famuwagun *et al*., 2020]. In turn, the DH strongly correlates with the bioactivities of peptides generated during the hydrolysis because it affects the amino acid composition, in addition to the sizes and structures of these peptides [Jang *et al*., 2016]. The hydrophobic amino acids are remarkably responsible for the antioxidant activities of enzymatically-hydrolyzed protein [Ghanbari *et al*., 2015]. Among them, leucine, valine, methionine, and alanine as well as aromatic amino acids, such as tyrosine, histidine, and phenylalanine play a key role in peptide activity in the DPPH assay [Bahari *et al*., 2020]. Analysis of the amino acid profile of BH indicated the presence of these amino acids with significant contents, as shown in Table 1. The type of assay employed to assess antioxidant activity can affect the results, thus, two or more systems acting with different radicals are necessary to evaluate the radical scavenging activities of the selected antioxidants [Centenaro *et al*., 2011]. Figure 2B displays the ability of BH with different concentrations (1–5 mg/mL) to scavenge the $ABTS^{\bullet+}$. The results showed that the antiradical activity of BH against $ABTS^{\bullet+}$ ranged from 23.09% at 1 mg/mL to 62.07% at 5 mg/mL with IC_{50} of 3.81 mg/mL. Concentration-dependent activity in the ABTS assay was consistent with previous results, which found that increased fish protein hydrolysate concentrations resulted in increased antioxidant activity [Chalamaiah *et al*., 2013; Tian *et al*., 2020]. Latorres *et al*. [2018] reported that the ability of protein hydrolysate to scavenge the $ABTS^{\bullet+}$ was associated with the size of the peptide chain and the enzyme specificity to break the peptide bonds during the enzymolysis. The amino acid composition, particularly the essential and hydrophobic amino acids, may explain differences in the activities of protein hydrolysates from different sources. Histidine, methionine, cysteine, phenylalanine, and tyrosine, may lead to improved $ABTS^{\bullet+}$ scavenging activity [Chalamaiah *et al*., 2015].

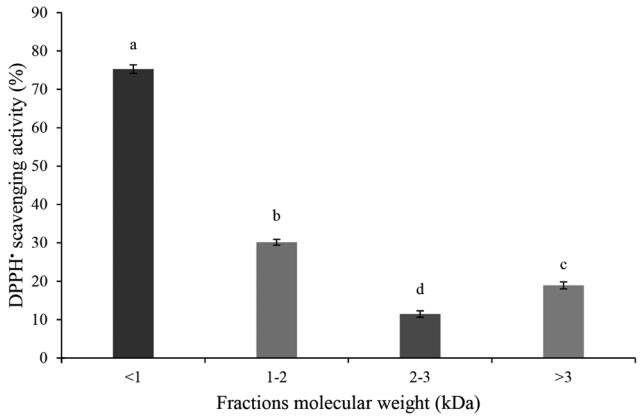

FIGURE 3. $DPPH^{\bullet}$ scavenging activity of membrane ultrafiltration fractions of hybrid sturgeon (*Huso dauricus* × *Acipenser schrenckii*) hydrolysate obtained using bromelain. Different letters above bars indicate significant differences at $p<0.05$. Data are expressed as mean ± standard deviation.

Antioxidant activities of fractions and peptides

Hydrolysate fractions obtained using ultrafiltration

Ultrafiltration membranes are used to separate molecules dissolved in a solution depending on the molecular weight. In the case of protein hydrolysates, ultrafiltration is often used to extract fractions with specific biological properties [Chi *et al*., 2014]. Figure 3 shows the DPPH radical scavenging activity of the peptide fractions separated from BH by ultrafiltration. The results indicate that the peptide fractions had varying antioxidant activities against $DPPH^{\bullet}$. The fraction of MW <1 kDa exhibited the highest antioxidant activity (75.28% and IC_{50} of 2.10 mg/mL) with significant differences compared to the other fractions at the same concentrations. This result may be attributed to the content of peptides and amino acids in this fraction that are more active as antioxidants. This finding is consistent with previous studies indicating that low molecular weight peptides were more active as antioxidants due to their ability to scavenge free radicals [Zhang *et al*., 2019]. According to Zaky *et al*. [2020], the fractions with small molecular weights resulting from the separation process contained peptides, which act as electron donors and can easily interact with free radicals to turn them into more stable products. On the other hand, not only the MW of the peptides, but also their amino acid content and sequences affect the antioxidant activity [Zou *et al*., 2016]. According to the result of this experiment, the MW <1 kDa fraction was subjected to further purification.

Gel filtration chromatography fractions

Gel filtration has been extensively used to separate enzymatically-hydrolyzed protein peptides and is an efficient procedure for isolating bioactive molecules with varying molecular weights [Hong *et al*., 2014]. As shown in Figure 4A, the fraction of MW <1 kDa was separated into six fractions (F1, F2, F3, F4, F5 and F6) using Sephadex G-15. Among these fractions, F4 fraction showed the highest DPPH radical scavenging activity ($p<0.05$), which was 79.37% (Figure 4B) with IC_{50} of 1.77 mg/mL. The activity of F4 may be attributed to the presence of peptides that could easily scavenge DPPH radicals.

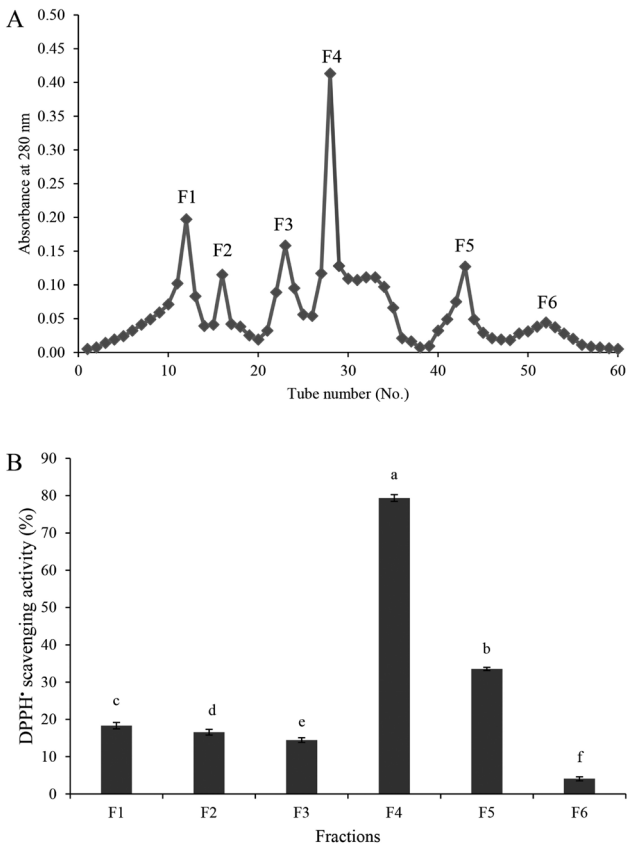

FIGURE 4. Hybrid sturgeon hydrolysate fraction with molecular weight <1 kDa separated by gel filtration chromatography on Sephadex G-15 (A) and DPPH• scavenging activity of the separated F1-F6 fractions (B). Different letters above bars indicate significant differences at $p<0.05$. Data are expressed as mean ± standard deviation.

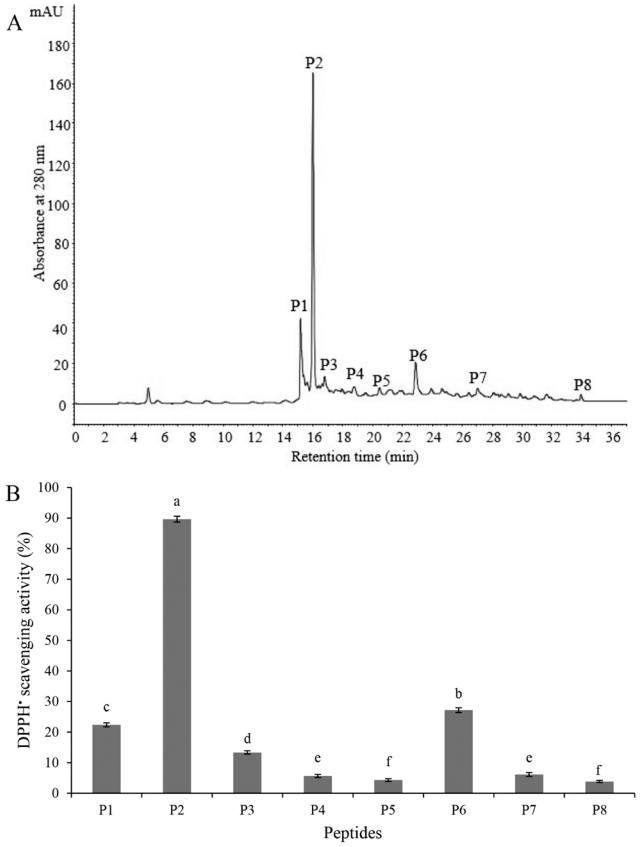

FIGURE 5. RP-HLPC chromatogram of the fraction F4 obtained using Sephadex G-15 gel filtration (A) and DPPH• scavenging activity of the separated P1-P8 peptides (B). Different letters above bars indicate significant differences at $p<0.05$. Data are expressed as mean ± standard deviation.

Peptides purified using RP-HPLC

The F4 fraction obtained by Sephadex G-15 gel filtration that displayed the highest DPPH radical scavenging activity was separated further using RP-HPLC on a Zorbax SB, C-18 column. The chromatogram shows eight peaks corresponding to the P1-P8 peptides (Figure 5A). The peak corresponding to P2 peptide was the highest. All isolated peptides were collected separately to determine DPPH radical scavenging activity. Results of the DPPH assay are shown in Figure 5B. The P2 peptide showed a superior antioxidant activity (89.65% with IC_{50} of 1.33 mg/mL) compared to the other isolated peptides. This peptide contained histidine (28.54±0.96% TAA), leucine (16.10±1.03% TAA), and glycine (55.37±1.14% TAA), and had a molecular weight of 0.2955 kDa. According literature data [Ahn *et al*., 2014], these amino acids, especially histidine and leucine, may be responsible for the antioxidant activity of the purified peptide. The purification process of peptide leads to an increase in hydrogen at *N*-terminals, which are capable of donating hydrogen atoms and scavenging free radicals [Halim *et al*., 2018]. On the other hand, Jang *et al*. [2016] reported that the histidine-containing peptides displayed strong radical scavenging activity due to the imidazole ring's ability to chelate and trap lipid radicals.

CONCLUSIONS

In this study, the enzymatic hydrolysis conditions were optimized to obtain a protein hydrolysate from hybrid sturgeon (*Huso dauricus* × *Acipenser schrenckii*) using bromelain. A S/L ratio of 1:1, an E/S ratio of 1:100, a pH of 6.5, a temperature of 45°C, and a hydrolysis time of 6 h were the optimum conditions for protein hydrolysis. The bromelain hydrolysate (BH) contained 44.63 g/100 g essential amino acids and 38.21 g/100 g hydrophobic amino acids. According to the current findings, BH fraction with a MW <1 kDa provided high DPPH• and $ABTS^{•+}$ scavenging activities. The antioxidant activity of the peptides from BH could be attributed to their small size and amino acid composition. The obtained antioxidant peptide, which consisted of three amino acids and had an MW of 0.2955 kDa, exhibited a good antiradical activity against DPPH•. The current study provided valuable information for improving BH production and purifying its peptides, which could be used as a natural antioxidant peptide source for food preservation and as bioactive food components. However, further work should be conducted to determine the other potential activities and health benefits of BH, and its peptides by simulating the digestion conditions and applying animal models.

RESEARCH FUNDING

This work supported by Key Laboratory of Solid-state Fermentation Resource Utilization of Sichuan Province (2015GTY001), and the Scientific Research Fund of Sichuan Provincial Education Department (18TD0041).

CONFLICT OF INTEREST

The authors declare no conflict of interest.

ORCID IDs

S.M. Abed https://orcid.org/0000-0002-1866-6367
A. Noman https://orcid.org/0000-0002-1096-6277

REFERENCES

1. Abraha, B., Mahmud, A., Admassu, H., Habte-Tsion, H.-M., Xia, W., Yang, F. (2018). Production of biscuit from Chinese sturgeon fish fillet powder (*Acipeneser sinensis*): A snack food for children. *Journal of Aquatic Food Product Technology*, *27*(10), 1048–1062. https://doi.org/10.1080/10498850.2018.1533906
2. Adjimani, J.P., Asare, P. (2015). Antioxidant and free radical scavenging activity of iron chelators. *Toxicology Reports*, *2*, 721–728. https://doi.org/10.1016/j.toxrep.2015.04.005
3. Ahn, C.-B., Kim, J.-G., Je, J.-Y. (2014). Purification and antioxidant properties of octapeptide from salmon byproduct protein hydrolysate by gastrointestinal digestion. *Food Chemistry*, *147*, 78–83. https://doi.org/10.1016/j.foodchem.2013.09.136
4. Ang, S.-S., Ismail-Fitry, M.R. (2019). Production of different mushroom protein hydrolysates as potential flavourings in chicken soup using stem bromelain hydrolysis. *Food Technology and Biotechnology*, *57*(4), 472–480. https://doi.org/10.17113/ftb.57.04.19.6294
5. AOAC. (1998). *Official Methods of Analysis of AOAC International,* 16th ed., 4th rev. ed., AOAC International.
6. Bahari, A.N., Saari, N., Salim, N., Ashari, S.E. (2020). Response factorial design analysis on papain-generated hydrolysates from *Actinopyga lecanora* for determination of antioxidant and antityrosinase activities. *Molecules*, *25*(11), art. no. 2663. https://doi.org/10.3390/molecules25112663
7. Bhaskar, N., Benila, T., Radha, C., Lalitha, R.G. (2008). Optimization of enzymatic hydrolysis of visceral waste proteins of Catla (*Catla catla*) for preparing protein hydrolysate using a commercial protease. *Bioresource Technology*, *99*(2), 335–343. https://doi.org/10.1016/j.biortech.2006.12.015
8. Billard, R., Lecointre, G. (2000). Biology and conservation of sturgeon and paddlefish. *Reviews in Fish Biology and Fisheries*, *10* (4), 355–392. https://doi.org/10.1023/A:1012231526151
9. Bronzi, P., Chebanov, M., Michaels, J.T., Wei, Q., Rosenthal, H., Gessner, J. (2019). Sturgeon meat and caviar production: Global update 2017. *Journal of Applied Ichthyology*, *35*(1), 257–266. https://doi.org/10.1111/jai.13870
10. Centenaro, G.S., Centenaro, M.S., Hernandez, C.P. (2011). Antioxidant activity of protein hydrolysates of fish and chicken bones. *Advance Journal of Food Science and Technology 3*(4), 280–288.
11. Chalamaiah, M., Jyothirmayi, T., Bhaskarachary, K., Vajreswari, A., Hemalatha, R., Kumar, B.D. (2013). Chemical composition, molecular mass distribution and antioxidant capacity of rohu (*Labeo rohita*) roe (egg) protein hydrolysates prepared by gastrointestinal proteases. *Food Research International*, *52*(1), 221–229. https://doi.org/10.1016/j.foodres.2013.03.020
12. Chalamaiah, M., Jyothirmayi, T., Diwan, P.V., Kumar, B.D. (2015). Antioxidant activity and functional properties of enzymatic protein hydrolysates from common carp (*Cyprinus carpio*) roe (egg). *Journal of Food Science and Technology*, *52*(9), 5817–5825. https://doi.org/10.1007/s13197-015-1714-6
13. Chi, C.-F., Wang, B., Deng, Y.-Y., Wang, Y.-M., Deng, S.-G., Ma, J.-Y. (2014). Isolation and characterization of three antioxidant pentapeptides from protein hydrolysate of monkfish (*Lophius litulon*) muscle. *Food Research International*, *55*, 222–228. https://doi.org/10.1016/j.foodres.2013.11.018
14. Chi, C.-F., Wang, B., Wang, Y.-M., Zhang, B., Deng, S.-G. (2015a). Isolation and characterization of three antioxidant peptides from protein hydrolysate of bluefin leatherjacket (*Navodon septentrionalis*) heads. *Journal of Functional Foods*, *12*, 1–10 https://doi.org/10.1016/j.jff.2014.10.027
15. Chi, C.-F., Wang, B., Hu, F.-Y., Wang, Y.-M., Zhang, B., Deng, S.-G., Wu, C.-W. (2015b). Purification and identification of three novel antioxidant peptides from protein hydrolysate of bluefin leatherjacket (*Navodon septentrionalis*) skin. *Food Research International*, *73*, 124–129. https://doi.org/10.1016/j.foodres.2014.08.038
16. De Quadros, C.D.C., Lima, K.O., Bueno, C.H.L., Fogaça, F.H.d. S., Da Rocha, M., Prentice, C. (2019). Evaluation of the antioxidant and antimicrobial activity of protein hydrolysates and peptide fractions derived from *Colossoma macropomum* and their effect on ground beef lipid oxidation. *Journal of Aquatic Food Product Technology*, *28*(6), 677–688. https://doi.org/10.1080/10498850.2019.1628152
17. Do Evangelho, J.A., Vanier, N.L., Pinto, V.Z., De Berrios, J.J., Dias, A.R.G., Da Rosa Zavareze, E. (2017). Black bean (*Phaseolus vulgaris* L.) protein hydrolysates: Physicochemical and functional properties. *Food Chemistry*, *214*, 460–467. https://doi.org/10.1016/j.foodchem.2016.07.046
18. Eberhardt, A., López, E.C., Ceruti, R.J., Marino, F., Mammarella, E.J., Manzo, R.M., Sihufe, G.A. (2019). Influence of the degree of hydrolysis on the bioactive properties of whey protein hydrolysates using Alcalase®. *International Journal of Dairy Technology*, *72*(4), 573–584. https://doi.org/10.1111/1471-0307.12606
19. Elavarasan, K., Shamasundar, B.A. (2016). Effect of oven drying and freeze drying on the antioxidant and functional properties of protein hydrolysates derived from freshwater fish (*Cirrhinus mrigala*) using papain enzyme. *Journal of Food Science and Technology*, *53*(2), 1303–1311. https://doi.org/10.1007/s13197-015-2084-9
20. Famuwagun, A.A., Alashi, A.M., Gbadamosi, S.O., Taiwo, K.A., Oyedele, D.J., Adobooye, O., Aluko, R.E. (2020). *In vitro* characterization of fluted pumpkin leaf protein hydrolysates and ultrafiltration of peptide fractions: Antioxidant and enzyme-inhibitory properties. *Polish Journal of Food and Nutrition Sciences*, *70*(4), 429–443. https://doi.org/10.31883/pjfns/130401

21. Fan, J., He, J., Zhuang, Y., Sun, L. (2012). Purification and identification of antioxidant peptides from enzymatic hydrolysates of tilapia (*Oreochromis niloticus*) frame protein. *Molecules*, *17*(11), 12836–12850. https://doi.org/10.3390/molecules171112836
22. Galla, N.R., Pamidighantam, P.R., Akula, S., Karakala, B. (2012). Functional properties and in vitro antioxidant activity of roe protein hydrolysates of *Channa striatus* and *Labeo rohita*. *Food Chemistry*, *135*(3), 1479–1484. https://doi.org/10.1016/j.foodchem.2012.05.098
23. Gao, R., Shen, Y., Shu, W., Bai, F., Jin, W., Wang, J., Yuan, L. (2020). Optimization of enzymatic conditions of sturgeon muscles and their anti-inflammatory potential. *Journal of Food Quality*, *2020*, art. no. 9698134. https://doi.org/10.1155/2020/9698134
24. García-Moreno, P.J., Pérez-Gálvez, R., Espejo-Carpio, F.J., Ruiz-Quesada, C., Pérez-Morilla, A.I., Martínez-Agustín, O., Guadix, A., Guadix, E.M. (2017). Functional, bioactive and antigenicity properties of blue whiting protein hydrolysates: Effect of enzymatic treatment and degree of hydrolysis. *Journal of the Science of Food and Agriculture*, *97*(1), 299–308. https://doi.org/10.1002/jsfa.7731
25. Ghanbari, R., Zarei, M., Ebrahimpour, A., Abdul-Hamid, A., Ismail, A., Saari, N. (2015). Angiotensin-I converting enzyme (ACE) inhibitory and anti-oxidant activities of sea cucumber (*Actinopyga lecanora*) hydrolysates. *International Journal of Molecular Sciences*, *16*(12), 28870–28885. https://doi.org/10.3390/ijms161226140
26. Guérard, F., Guimas, L., Binet, A. (2002). Production of tuna waste hydrolysates by a commercial neutral protease preparation. *Journal of Molecular Catalysis B: Enzymatic*, *19*, 489–498. https://doi.org/10.1016/S1381-1177(02)00203-5
27. Halim, N.R.A., Azlan, A., Yusof, H.M., Sarbon, N.M. (2018). Antioxidant and anticancer activities of enzymatic eel (*Monopterus* sp.) protein hydrolysate as influenced by different molecular weight. *Biocatalysis and Agricultural Biotechnology*, *16*, 10–16. https://doi.org/10.1016/j.bcab.2018.06.006
28. Hong, J., Chen, T.-T., Hu, P., Yang, J., Wang, S.-Y. (2014). Purification and characterization of an antioxidant peptide (GSQ) from Chinese leek (*Allium tuberosum* Rottler) seeds. *Journal of Functional Foods*, *10*, 144–153. https://doi.org/10.1016/j.jff.2014.05.014
29. Jang, H.L., Liceaga, A.M., Yoon, K.Y. (2016). Purification, characterisation and stability of an antioxidant peptide derived from sandfish (*Arctoscopus japonicus*) protein hydrolysates. *Journal of Functional Foods*, *20*, 433–442. https://doi.org/10.1016/j.jff.2015.11.020
30. Jin, J., Chu, Z., Chen, X., Liang, X. (2020). Responses of hybrid sturgeon (*Huso dauricus*♀ × *Acipenser schrenckii*♂) to oral administration of phosphorus. *Aquaculture Research*, *51*(4), 1428–1436. https://doi.org/10.1111/are.14488
31. Kong, X., Guo, M., Hua, Y., Cao, D., Zhang, C. (2008). Enzymatic preparation of immunomodulating hydrolysates from soy proteins. *Bioresource Technology*, *99* (18), 8873–8879. https://doi.org/10.1016/j.biortech.2008.04.056
32. Ktari, N., Fakhfakh, N., Balti, R., Ben Khaled, H., Nasri, M., Bougatef, A. (2013). Effect of degree of hydrolysis and protease type on the antioxidant activity of protein hydrolysates from cuttlefish (*Sepia officinalis*) by-products. *Journal of Aquatic Food Product Technology*, *22*(5), 436–448. https://doi.org/10.1080/10498850.2012.658961
33. Latorres, J., Rios, D., Saggiomo, G., Wasielesky, W., Prentice-Hernandez, C. (2018). Functional and antioxidant properties of protein hydrolysates obtained from white shrimp (*Litopenaeus vannamei*). *Journal of Food Science and Technology*, *55*(2), 721–729. https://doi.org/10.1007/s13197-017-2983-z
34. Luo, L., Li, T., Xing, W., Xue, M., Ma, Z., Jiang, N., Li, W. (2015). Effects of feeding rates and feeding frequency on the growth performances of juvenile hybrid sturgeon, *Acipenser schrenckii* Brandt♀ × *A. baeri* Brandt♂. *Aquaculture*, *448*, 229–233. https://doi.org/10.1016/j.aquaculture.2015.06.005
35. Marson, G.V., Da Costa Machado, M.T., De Castro, R.J.S., Hubinger, M.D. (2019). Sequential hydrolysis of spent brewer's yeast improved its physico-chemical characteristics and antioxidant properties: A strategy to transform waste into added-value biomolecules. *Process Biochemistry*, *84*, 91–102. https://doi.org/10.1016/j.procbio.2019.06.018
36. Naqash, S.Y., Nazeer, R. (2013). Antioxidant and functional properties of protein hydrolysates from pink perch (*Nemipterus japonicus*) muscle. *Journal of Food Science and Technology*, *50*(5), 972–978. https://doi.org/10.1007/s13197-011-0416-y
37. Noman, A., Qixing, J., Xu, Y., Abed, S.M., Obadi, M., Ali, A.H., AL-Bukhaiti, W.Q., Xia, W. (2020a). Effects of ultrasonic, microwave, and combined ultrasonic-microwave pretreatments on the enzymatic hydrolysis process and protein hydrolysate properties obtained from Chinese sturgeon (*Acipenser sinensis*). *Journal of Food Biochemistry*, *44*(8), art. no. e13292. https://doi.org/10.1111/jfbc.13292
38. Noman, A., Ali, A.H., AL-Bukhaiti, W.Q., Mahdi, A.A., Xia, W. (2020b). Structural and physicochemical characteristics of lyophilized Chinese sturgeon protein hydrolysates prepared by using two different enzymes. *Journal of Food Science*, *85*(10), 3313–3322. https://doi.org/10.1111/1750-3841.15345
39. Noman, A., Qixing, J., Xu, Y., Ali, A.H., Al-Bukhaiti, W.Q., Abed, S.M., Xia, W. (2019). Influence of degree of hydrolysis on chemical composition, functional properties, and antioxidant activities of Chinese sturgeon (*Acipenser sinensis*) hydrolysates obtained by using alcalase 2.4 L. *Journal of Aquatic Food Product Technology*, *28*(6), 583–597. https://doi.org/10.1080/10498850.2019.1626523
40. Noman, A., Xu, Y., AL-Bukhaiti, W.Q., Abed, S.M., Ali, A.H., Ramadhan, A.H., Xia, W. (2018). Influence of enzymatic hydrolysis conditions on the degree of hydrolysis and functional properties of protein hydrolysate obtained from Chinese sturgeon (*Acipenser sinensis*) by using papain enzyme. *Process Biochemistry*, *67*, 19–28. https://doi.org/10.1016/j.procbio.2018.01.009
41. Ovissipour, M., Rasco, B., Shiroodi, S.G., Modanlow, M., Gholami, S., Nemati, M. (2013). Antioxidant activity of protein hydrolysates from whole anchovy sprat (*Clupeonella engrauliformis*) prepared using endogenous enzymes and commercial proteases. *Journal of the Science of Food and Agriculture*, *93*(7), 1718–1726. https://doi.org/10.1002/jsfa.5957

42. Pérez-Vega, J.A., Olivera-Castillo, L., Gómez-Ruiz, J.Á., Hernández-Ledesma, B. (2013). Release of multifunctional peptides by gastrointestinal digestion of sea cucumber (*Isostichopus badionotus*). *Journal of Functional Foods*, *5*(2), 869–877. https://doi.org/10.1016/j.jff.2013.01.036
43. Priatni, S., Harimadi, K., Buana, E., Kosasih, W., Rohmatussolihat, R. (2020). Production and characterization of spray-dried swamp eel (*Monopterus albus*) protein hydrolysate prepared by papain. *Sains Malaysiana*, *49*(3), 545–552. https://doi.org/10.17576/jsm-2020-4903-09
44. Saidi, S., Deratani, A., Belleville, M.-P., Amar, R.B. (2014). Production and fractionation of tuna by-product protein hydrolysate by ultrafiltration and nanofiltration: Impact on interesting peptides fractions and nutritional properties. *Food Research International*, *65, Part C,* 453–461. https://doi.org/10.1016/j.foodres.2014.04.026
45. Salwanee S., Aida, W.M.W., Mamot, S., Maskat, M.Y., Ibrahim, S. (2013). Effects of enzyme concentration, temperature, pH and time on the degree of hydrolysis of protein extract from viscera of tuna (*Euthynnus affinis*) by using alcalase. *Sains Malaysiana*, *42*(3), 279–287.
46. Samaranayaka, A.G., Li-Chan, E.C. (2011). Food-derived peptidic antioxidants: A review of their production, assessment, and potential applications. *Journal of Functional Foods*, *3*(4), 229–254. https://doi.org/10.1016/j.jff.2011.05.006
47. Tan, X., Qi, L., Fan, F., Guo, Z., Wang, Z., Song, W., Du, M. (2018). Analysis of volatile compounds and nutritional properties of enzymatic hydrolysate of protein from cod bone. *Food Chemistry*, *264*, 350–357. https://doi.org/10.1016/j.foodchem.2018.05.034
48. Taylor, W. (1957). Formol titration: an evaluation of its various modifications. *Analyst*, *82*(976), 488–498. https://doi.org/10.1039/an9578200488
49. Tian, X., Zheng, J., Xu, B., Ye, J., Yang, Z., Yuan, F. (2020). Optimization of extraction of bioactive peptides from monkfish (*Lophius litulon*) and characterization of their role in H_2O_2-induced lesion. *Marine Drugs*, *18*(9), art. no. 468. https://doi.org/10.3390/md18090468
50. Villamil, O., Váquiro, H., Solanilla, J.F. (2017). Fish viscera protein hydrolysates: Production, potential applications and functional and bioactive properties. *Food Chemistry*, *224*, 160–171. https://doi.org/10.1016/j.foodchem.2016.12.057
51. Wang, X., Yu, H., Xing, R., Liu, S., Chen, X., Li, P. (2019). Preparation and identification of antioxidative peptides from pacific herring (*Clupea pallasii*) protein. *Molecules*, *24* (10), art. no. 1946. https://doi.org/10.3390/molecules24101946
52. Wang, Y.-Y., Wang, C.-Y., Wang, S.-T., Li, Y.-Q., Mo, H.-Z., He, J.-X. (2021). Physicochemical properties and antioxidant activities of tree peony (*Paeonia suffruticosa* Andr.) seed protein hydrolysates obtained with different proteases. *Food Chemistry*, *345*, art. no. 128765. https://doi.org/10.1016/j.foodchem.2020.128765
53. Wang, Z., Liu, X., Xie, H., Liu, Z., Rakariyatham, K., Yu, C., Shahidi, F., Zhou, D. (2021). Antioxidant activity and functional properties of Alcalase-hydrolyzed scallop protein hydrolysate and its role in the inhibition of cytotoxicity *in vitro*. *Food Chemistry*, *344,* art. no. 128566. https://doi.org/10.1016/j.foodchem.2020.128566
54. Zaky, A.A., Liu, Y., Han, P., Ma, A., Jia, Y. (2020). Effect of flavorzyme digestion on the antioxidant capacities of ultra-filtrated rice bran protein hydrolysates. *Journal of Food Processing and Preservation*, *44* (8), art. no. e14551. https://doi.org/10.1111/jfpp.14551
55. Zhang, F., Qu, J., Thakur, K., Zhang, J.-G., Mocan, A., Wei, Z.-J. (2019). Purification and identification of an antioxidative peptide from peony (*Paeonia suffruticosa* Andr.) seed dreg. *Food Chemistry*, *285*, 266–274. https://doi.org/10.1016/j.foodchem.2019.01.168
56. Zhang, L., Zhao, G.-X., Zhao, Y.-Q., Qiu, Y.-T., Chi, C.-F., Wang, B. (2019). Identification and active evaluation of antioxidant peptides from protein hydrolysates of skipjack tuna (*Katsuwonus pelamis*) head. *Antioxidants*, *8*(8), art. no. 318. https://doi.org/10.3390/antiox8080318
57. Zhang, N., Zhang, C., Chen, Y., Zheng, B. (2017). Purification and characterization of antioxidant peptides of *Pseudosciaena crocea* protein hydrolysates. *Molecules*, *22*(1), art. no. 57. https://doi.org/10.3390/molecules22010057
58. Zhang, Y., Wang, J., Zhu, Z., Li, X., Sun, S., Wang, W., Sadiq, F.A. (2021). Identification and characterization of two novel antioxidant peptides from silkworm pupae protein hydrolysates. *European Food Research and Technology*, *247*(2), 343–352. https://doi.org/10.1007/s00217-020-03626-5
59. Zheng, Z., Li, J., Li, J., Sun, H., Liu, Y. (2019). Physicochemical and antioxidative characteristics of black bean protein hydrolysates obtained from different enzymes. *Food Hydrocolloids*, *97*, art. no. 105222. https://doi.org/10.1016/j.foodhyd.2019.105222
60. Zou, T.-B., He, T.-P., Li, H.-B., Tang, H.-W., Xia, E.-Q. (2016). The structure-activity relationship of the antioxidant peptides from natural proteins. *Molecules*, *21*(1), art. no. 72. https://doi.org/10.3390/molecules21010072

Pol. J. Food Nutr. Sci., 2022, Vol. 72, No. 1, pp. 91–100
On-line ISSN: 2083-6007
Print ISSN: 1230-0322
DOI: 10.31883/pjfns/146640
http://journal.pan.olsztyn.pl

Original article
Section: Food Technology

Fractional Factorial Design and Desirability Function-Based Approach in Spice Paprika Processing Technology to Improve Extractable Colour Stability

Arnold Koncsek[1], Lajos Szokol[1], Vivien Krizsa[1], Hussein G. Daood[2], Lajos Helyes[2], Antal Véha[3], Balázs P. Szabó[3]*

[1]*Rubin Spice Paprika Processing Szeged Ltd., 173. Szerb Str., Szeged-Szőreg H-6771, Hungary*
[2]*Horticultural Science Department, Hungarian University of Agriculture and Life Sciences, 1 Páter Károly Str., Gödöllő H-2100, Hungary*
[3]*University of Szeged, Faculty of Engineering, 5–7 Moszkvai Av., Szeged H-6725, Hungary*

Key words: spice-paprika, extractable colour, experimental design, accelerated shelf-life test

The storage-stability of extractable colour in paprika powder is strongly influenced by the processing steps. The purpose of this research work was to decrease the degradation rate of extractable colour of paprika powders to 3–4 ASTA units/month and increase the shelf-life. Fractional factorial experimental design and desirability function-based approach was applied to moderate the adverse effect of the key-importance processing steps on colour agent content. Photochemical-accelerated shelf-life test was used for the empirically-based quality improvement. Post-harvest ripening, drying, sorting (seed content), milling and additives (paprika seed oil, tocopherol extract) were identified as important for the degradation rate of extractable colour. The colour stability was very sensitive to the milling and drying intensity, while proper setup of other processing steps compensated the adverse effect of drying and milling parameters. The supplementation with cold-pressed spice paprika seed oil was demonstrated as a natural way of colour stabilization. At the highest desirability value (0.986) the rate constant of accelerated colour stability test (k) and shelf-life time ($\theta_{S[100ASTA]}$) were -0.494 ASTA units/day and 2326 days, respectively. Alternative factor level settings enabled taking into account processing-tradition and efficiency expectation. In these cases, desirability values and the predicted shelf-life were 0.5–0.8 and 712–918 days, respectively. Validation study showed that the real observed rate constant and shelf-life values met the predicted values and their 95% confidence interval.

INTRODUCTON

The Hungarian red spice paprika (*Capsicum annuum* L.) powder is a highly appreciated product by consumers, professional chefs and food industry for its traditions and unique characteristics as spice. Red paprika was brought to Hungary at the end of 1500's [Moór & Somogyi, 2017]. Growers and researchers have bred paprika cultivars that were most suitable for the local agricultural conditions and for the production of unique quality ground paprika. Empirically-based processing tradition has been developed by several generations of growers keeping in mind the gentle-handling of the raw material and developing the characteristics of milled paprika. The red spice paprika has become one of the most profitable agricultural products in Hungary after 1880 [Obermayer, 1934].

Spice paprika contains several valuable phytochemicals such as water- and fat-soluble antioxidants: phenolic compounds, capsaicinoids and carotenoids [Martí *et al.*, 2011]. Epidemiological data have indicated possible roles of these phytochemicals in the prevention of numerous chronic diseases, including certain types of cancer, cardiovascular disease, stroke, and atherosclerosis [Chopan & Littenberg, 2017; Hamed *et al.*, 2019; Spiller *et al.*, 2008].

During maturation, the fruit undergoes visual colour transformation due to the biosynthesis of carotenoids and the transformation of chloroplasts to chromoplasts [Martí *et al.*, 2009]. The deep red colour of ripe pepper fruits is due to the high content of fat-soluble carotenoid-type pigment [Márkus *et al.*, 1999]. More than 50 carotenoid-type compounds were identified in red pepper, mainly esterified with fatty acids in a form of mono- and di-esters [Daood *et al.*, 2006; Giuffrida *et al.*, 2013; Márkus *et al.*, 1999]. Carotenoids are fairly stable in their natural environment, but become sensitive to light, temperature, enzymes, metals or oxygen as the structure of pod tissue and cells injures during post-harvest handling and processing [Perez-Galvez *et al.*, 2009; Schieber & Carle, 2005]. The colour stability of spice paprika was substantially influenced by the degree of carotenoid-esterification, the level of antioxidants, such as ascorbic acid and tocopherols, formed during the ripening of pods [Daood *et al.*, 2006; Márkus *et al.*, 1999].

* Corresponding Author:
Tel.: 00-36-70-3335964;
E-mail: labor@rubinpaprika.hu (A. Koncsek)

Submitted: 27 October 2021
Accepted: 8 February 2022
Published on-line: 1 March 2022

In the industrial and commercial practice, the extractable colour determined by the American Spice Trade Association (ASTA) method and expressed as ASTA colour value is indicative of quality of spice paprika powder, which is easy to measure (photometric method) and representative throughout the product shelf-life [ASTA, 1997]. The degradation rate of extractable colour is a suitable indicator for evaluating the effect of processing factors.

The industrial mass production has pushed the experience of traditional gentle processing into the background. Long-term experience of present research group showed that the degradation rate of extractable colour is 6–8 ASTA units/month with the generally applied industrial processing of spice paprika. This means that the shelf-life is 360–400 days, calculated for 100 ASTA units of final colour value, as the minimum requirement of 1st grade paprika powder [ISO 7540:2006].

Numerous research works are available in literature focusing on the optimization of a selected single processing step [Daood *et al.*, 1996, 2006; Hamed *et al.*, 2019; Ibrahim *et al.*, 1997; İnanç *et al.*, 2010; Karam *et al.*, 2016; Koncsek *et al.*, 2019; Márkus *et al.*, 1999; Singh & Goswami, 1999]. However, the processing of spice paprika is a complex technology. Simultaneous and comprehensive optimization of industrial operations was required, taking into consideration the sensitivity of the valuable components in spice paprika. The objective of this research work was to decrease the degradation rate of extractable colour to 3–4 ASTA units/month in red spice paprika powders and increase the shelf-life. During the fresh spice paprika processing, the improper post-harvest ripening, heat stress (drying and milling) and mechanical stress (surface increase due to milling) enhance the process of the colour degradation [Daood *et al.*, 2006; Márkus *et al.*, 1999]. The research team assumed that the adverse effects of key-importance processing steps on colour agent content can be moderated with the help of fractional factorial experimental design and desirability function-based approach. Three varieties of cultivated fresh spice paprika were involved in the investigations. Variety, post-harvest ripening methods, intensity of drying and milling, sorting (seed content), and using of additives (paprika seed oil and tocopherol extract) were simultaneously and comprehensively investigated.

MATERIALS AND METHODS

Raw materials

The spice paprika varieties were cultivated on the fields of the Gorzsa Agricultural PLC (Hodmezovasarhely, Hungary), within the traditional Szegedi Spice Paprika production area. In the present study, varieties Meteorit, Fesztival and Mihalyteleki were used. The ripe (deep red) pods were hand-harvested in the 2017 and 2018 season.

Processing and experimental design

Seven processing variables (variety, post-harvest ripening, drying, sorting, milling, paprika seed oil and tocopherol extract as additives), as quantitative and qualitative factors, were investigated in the fractional factorial design at 3 levels, thus the experiment consisted of 81 runs (Table 1). The variables were decided earlier in preliminary studies at Rubin Spice Paprika Processing Ltd. (Szeged, Hungary). The pilot factory technology is shown in Figure 1.

According to the traditional Hungarian processing principles, the hand-harvested fresh pods were stored for 1.5 weeks to reach post-harvest technological ripeness. The thermal dehydration was done in an industrial drying unit (Hans Binder HGI/18F, Marzling, Germany, 1986), with washing equipment, manual sorting, chopper and drying tunnel.

The seeds were separated with the help of an industrial sorting sieving machine (Index Ltd., Kalocsa, Hungary, 1995). A screw oil press machine (OKB-1 models, 150 kg/h capacity, 7.5 kW power, Seed-Imex Ltd., Kisbér, Hungary) was used for the cold-pressing of spice paprika seed oil. The oil was cleaned through a 1.0 mm screen and then by gravitational sedimentation.

The dry spice paprika lots were processed in a milling system (Constructed by Zöldacél kft., Szeged, Hungary; id. no.: 001/2017, 35 kW) including a pin mill followed by an in-line sieve that allowed fine particles (<450 μm) in a mixer. The coarse particles were sent back from the screen to the grinder. The paprika powders were mechanically homogenized with additives (tocopherol and/or cold pressed seed oil) in the mixer.

The processing was repeated with the 2018 season's crop in order to validate the optimized processing parameters.

Accelerated colour stability test

The colour stability of paprika powder samples was analysed by the photochemical-accelerated method as described previously by Koncsek *et al*. [2016]. Samples of 15 g for each (in triplicate) were spread in Petri dishes to maintain the equal laying thickness (approx. 5 mm) and exposed to illumination of 6,000 lux in a light chamber. The samples were mixed daily. The chamber (420×1,040×500 mm) was equipped with two fluorescent lamps (Oshram Biolux T8 daylight, 30 W, colour temperature: 6,500 K) and light intensity adjusting unit. The light intensity was monitored by a digital Voltcraft MS-1300 light meter (Conrad, Berlin, Germany).

The extractable colour of paprika samples was measured according to the ASTA 20.1 method [ASTA, 1997] at the beginning of the experiment and after 7, 14 and 28 days, and expressed as ASTA colour value which was calculated according to the following formula:

$$ASTA\ colour\ value = \frac{Absorbance\ of\ sample \times 16.4 \times Factor}{Weight\ of\ sample\ (g)} \quad (1)$$

where: factor is 0.315 per absorbance of the standard colour solution.

Data analysis

The extractable colour loss was evaluated with chemical kinetics principles. The photochemical-accelerated degradation followed apparent zero order reaction model [Koncsek *et al.*, 2016]:

$$[C] = -k \times t + [C_0] \quad (2)$$

where: k is the apparent reaction rate constant, C is the extractable colour (ASTA colour value), and C_0 is the initial extractable colour (initial ASTA colour value).

TABLE 1. Variables of spice paprika processing experiment design (fractional factorial design at 3 levels).

Factors	Setup	Coded level	Details
Variety (x_1)	Meteorit	-1	
	Fesztival	0	
	Mihalyteleki	1	
Post-harvest ripening (x_2)	Outdoors, spread	-1	200 mm layer
	Outdoors, heap	0	600 mm heap
	Protected area	1	300 mm layer
Drying (x_3)	Slow, 330 kg/h	-1	Initial zone: 69–76°C Middle zone: 43–55°C Final zone: 25–30°C
	Moderate, 416 kg/h	0	Initial zone: 75–85°C Middle zone: 55–65°C Final zone: 29–36°C
	Intensive, 500 kg/h	1	Initial zone: 95–105°C Middle zone: 72–80°C Final zone: 35–40°C
Seed content (sorting) (x_4)	3%	-1	Without seeds: ~3%
	10.5%	0	Medium seed content: 9–12%
	20.5%	1	Total seed content: 19–22%
Milling (x_5)	Slow, 110 kg/h	-1	Stationary pin number: 63 Rotating pins: 86
	Moderate, 140 kg/h	0	Stationary pin number: 84 Rotating pins: 115
	Intensive, 170 kg/h	1	Stationary pin number: 105 Rotating pins: 145
Paprika seed oil (x_6)	0%	-1	
	3%	0	
	6%	1	
Tocopherol additive (x_7)	0%	-1	
	0.1%	0	
	0.2%	1	

Half-life time ($t_{1/2}$) is described by Eq. 3:

$$t_{1/2} = \frac{[C_0]}{2k} \tag{3}$$

The relationship between the illumination level and reaction time was expressed by a power function and the shelf-life to a specified ASTA colour value was estimated with empirically developed formula [Koncsek *et al.*, 2016]:

$$\theta_{S[100ASTA]} = \frac{[C] - [C_0]}{-k \times I^b} \tag{4}$$

where: $\theta_{S[100\ ASTA]}$ is predicted shelf-life to 100 ASTA colour value, I is illumination level, and b is the slope of shelf-life plot functions (-0.286). The bias of model was taken into consideration in the calculation.

Microsoft Excel (Microsoft, Redmond, WA, USA) and Statistica 8.0 (StatSoft Inc., Tulsa, OK, USA, 2007) softwares were used for the fractional factorial design analysis and kinetics computations. Shapiro-Wilk test was used for checking the normal distribution. Box-Cox transformation was used for stabilizing variance and improving the data analysis. In all analyses, a 5% significance level was considered.

Desirability function-based approach was used for optimizing processing parameters. This approach converts an optimization problem with multiple quality characteristics into a single dimensionless response optimization problem. Response variables (Y_i) are transformed into desirability values d_i ($0 \leq d_i \leq 1$). If the product characteristic is in an unacceptable range, the desirability value (D) is 0 and if the product characteristic is at the optimum, the value is 1 [Pal & Gauri, 2018]. The equations describe this approach:

$$d_i = \begin{cases} 0 & Y_i < Low_i \\ \left(\frac{Y_i - Low_i}{High_i - Low_i}\right)^w & Low_i < Y_i < High_i \\ 1 & Y_i > High_i \end{cases} \tag{5}$$

$$d_i = \begin{cases} 1 & Y_i < Low_i \\ \left(\frac{Y_i - Low_i}{High_i - Low_i}\right)^w & Low_i < Y_i < High_i \\ 0 & Y_i > High_i \end{cases} \tag{6}$$

$$D = \left(\prod_{i=1}^{n} d_i^{r_i}\right)^{1/\sum r_i} \tag{7}$$

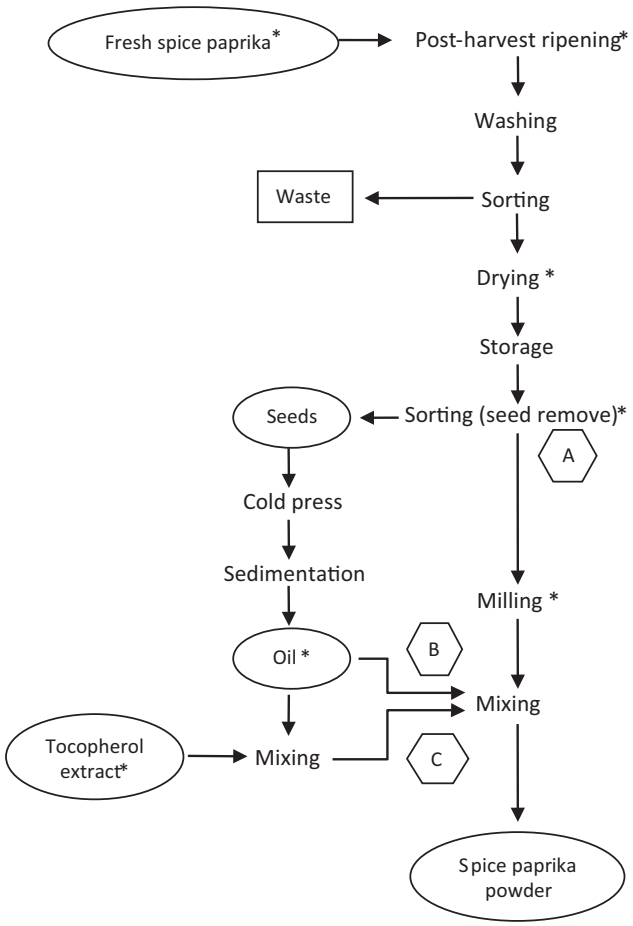

FIGURE 1. Flow chart of spice paprika processing technology in the pilot factory (*investigated factors, "A" – Processing without additives, "B" – Processing combined with cold pressed spice paprika seeds oil, "C" – Processing combined with tocopherol additive).

RESULTS AND DISCUSSION

The initial extractable colour (C_0) of paprika powder samples is shown in Figure 2 as ASTA colour values. The powder of Meteorit variety without seed sorting had the lowest colour values (145–157 ASTA units) that showed no significant increase in the protected storage condition. For this variety, the outdoors storage and semi-protected arrangement (in 600 mm heap) means satisfactory conditions to reach technological ripeness. The extractable colour values of Fesztival and Mihalyteleki paprika were 162 and 194 ASTA units in the protected storage area, while colour values were 10–18 ASTA units lower in the unprotected areas. In the case of Fesztival and Mihalyteleki paprika, the "*de novo*" extractable colour accumulation was remarkably aided by protected storage. The protected condition was set up in well-ventilated and dark warehouse. Thin layer arrangement of batches increased the adverse effects of environment (light, temperature fluctuation) on extractable colour synthesis. As shown by other authors, sun-drying (exposure to light) caused a remarkable decrease in the contents of carotenoids and antioxidants [Daood *et al.*, 2014; Topuz & Ozdemir, 2003]. The importance of balanced and moderate storage temperature has been confirmed by Márkus *et al.* [1999] and Acedo [2010],

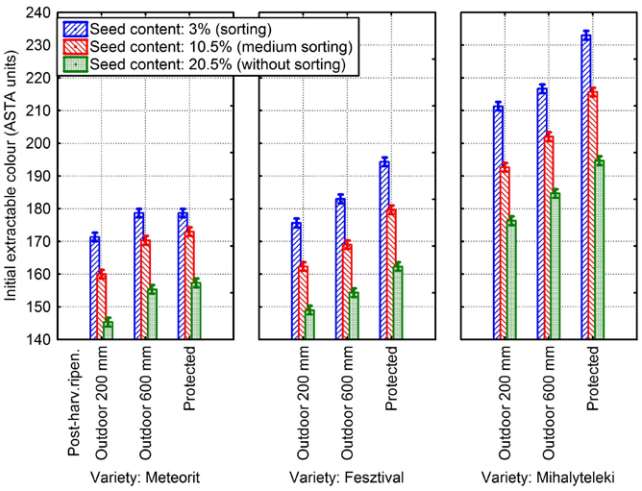

FIGURE 2. Effect of variety, post-harvest ripening methods and sorting (seed content) on the initial extractable colour values (ASTA units) of spice paprika powder.

because storage at 20 to 23°C improved the development of red colour in partially ripe paprika. In accordance with a study of Pola *et al.* [2020], the present results suggested that different *Capsicum* varieties have a diversity of post ripening demands (time, light or dark and temperature) to reach the best carotenoid accumulation.

The seeds do not contain carotenoids, thus total-seed-containing paprika powders had lower initial extractable colour, than sorted samples (Figure 2). Depending on post-ripening procedure, the available highest colour values were 171–178 ASTA units in Meteorit, 175–194 ASTA units in Fesztival and 211–233 ASTA units in Mihalyteleki paprika, when the seed content was only around 3%. The decrease of content or removal of seeds gave better initial quality of paprika powder and its effect on the colour stability was investigated with the help of kinetic parameters.

The pigment degradation kinetic parameters (initial extractable colour, C_0 and rate constant, k) and the estimated shelf-life time ($\theta_{S[100ASTA]}$) were calculated for 81 runs (factor combinations). The outcome of simple linear regression, fitting the regression line (R^2, adjusted $R^2>0.9$), results of F test ($p<0.05$) and residual analysis, confirmed the zero-order kinetic model. The estimated shelf-life was calculated for 100 ASTA units of final colour value, as the minimum requirement of 1st grade paprika powder [ISO 7540:2006]. The rate constant and the estimated shelf-life of accelerated colour stability test showed wide range differences (k=-3.208–0.453 ASTA units/day, $\theta_{S[100ASTA]}$=260–2240 days, all data is not shown), indicating the importance of processing factor setups on colour stability.

Figure 3 and Figure 4 shows the normal probability plot of the standardized effects and Pareto plot to evaluate the significance of each factor and its interactions on k and $\theta_{S[100ASTA]}$. The standardized effects are ranked, and then plotted against the expected normal probability. The effects that are negligible are normally distributed, with mean zero and variance σ2 and tend to fall along a straight line [Montgomery, 2013]. The significant real effects are separated in the upper

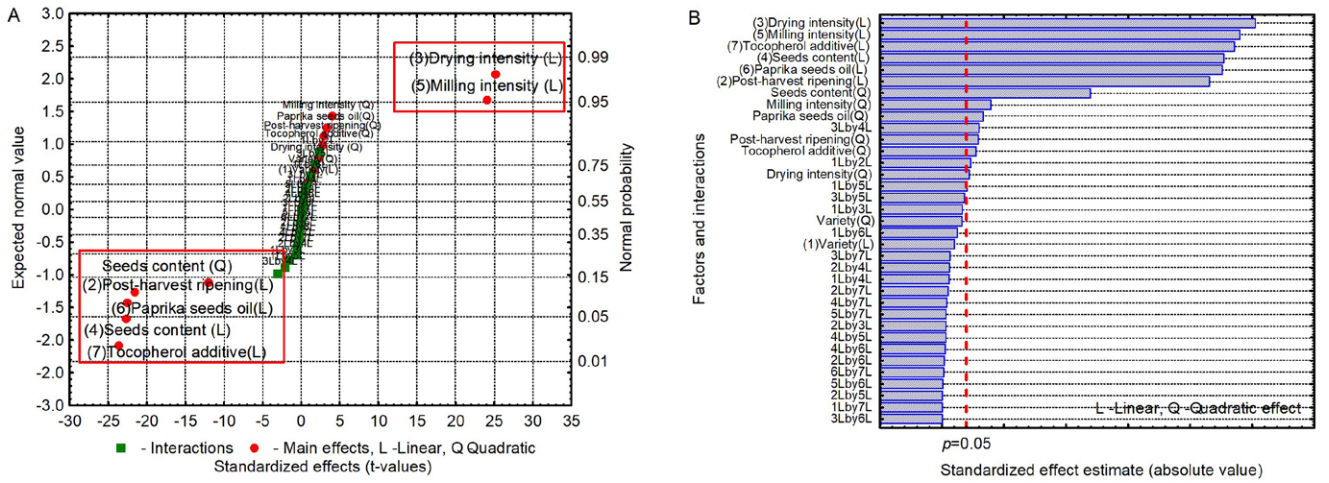

FIGURE 3. Normal probability plot (A) and Pareto chart of the standardized effects (B) on the (transformed) degradation rate constant (k) of extractable colour in spice paprika powder. (Red frames indicate the processing variables that were identified as important for degradation rate constant).

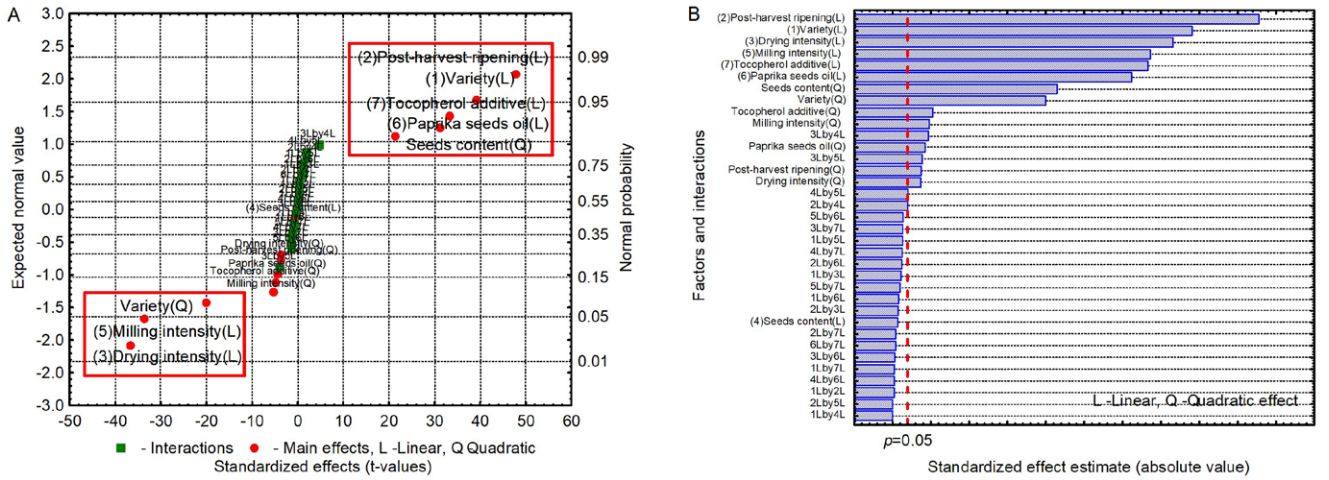

FIGURE 4. Normal probability plot (A) and Pareto chart of the standardized effects (B) on estimated shelf-life time ($\theta_{S[100ASTA]}$) of spice paprika powder. (Red frames indicate the processing variables that were identified as important for shelf-life).

right-hand and lower left-hand corner of the plots (Figure 3A and Figure 4A).

All processing variables, as main effects, were identified as important for rate constant. Positive position of variables (drying and milling) means that a change from a low to a high level increased the degradation rate of extractable colour (Figure 3A). The Pareto chart with high absolute standardized effects of these factors indicated their remarkable influence on the degradation rate of extractable colour (Figure 3B). High factor levels of other processing steps (*e.g.* seed content, supplementation with spice paprika seed oil or tocopherol) suggested the compensation opportunity against the adverse effect of drying and milling parameters.

Besides processing factors, the variety was significant for the shelf-life response variable. Drying and milling intensity negatively affected the shelf-life (Figure 4A). This preliminary analysis indicated that the proper setup of parameters contributes to the extended stability of products. The plot shows that the colour stability is very sensitive to the milling and drying intensity if the parameters were at high levels. Variety factor appeared in positive and negative position in the normal probability plot as linear and quadratic variables of model. This suggested that this qualitative variable represents complex properties. The shelf-life estimation formula indicated that the calculated time values depended on the initial extractable colour of paprika powders. This clearly appeared in the Pareto chart (Figure 4B), since standardized effects of variety and post-ripening control factors were the largest among the other factors. Earlier studies have found intensive esterification of capsanthin, capsorubin and other xanthophylls with fatty acids during the post-harvest ripening [Márkus *et al.*, 1999]. These conversions promoted the stabilization of carotenoids during the further processing and storage of spice paprika, providing stability against thermo, photo and enzymatic oxidation reactions [Arimboor *et al.*, 2015].

The effect of processing variables on rate constant of accelerated colour stability test is shown graphically in Figure 5. These marginal means plots averaged the means across the settings and combinations of settings of the factors.

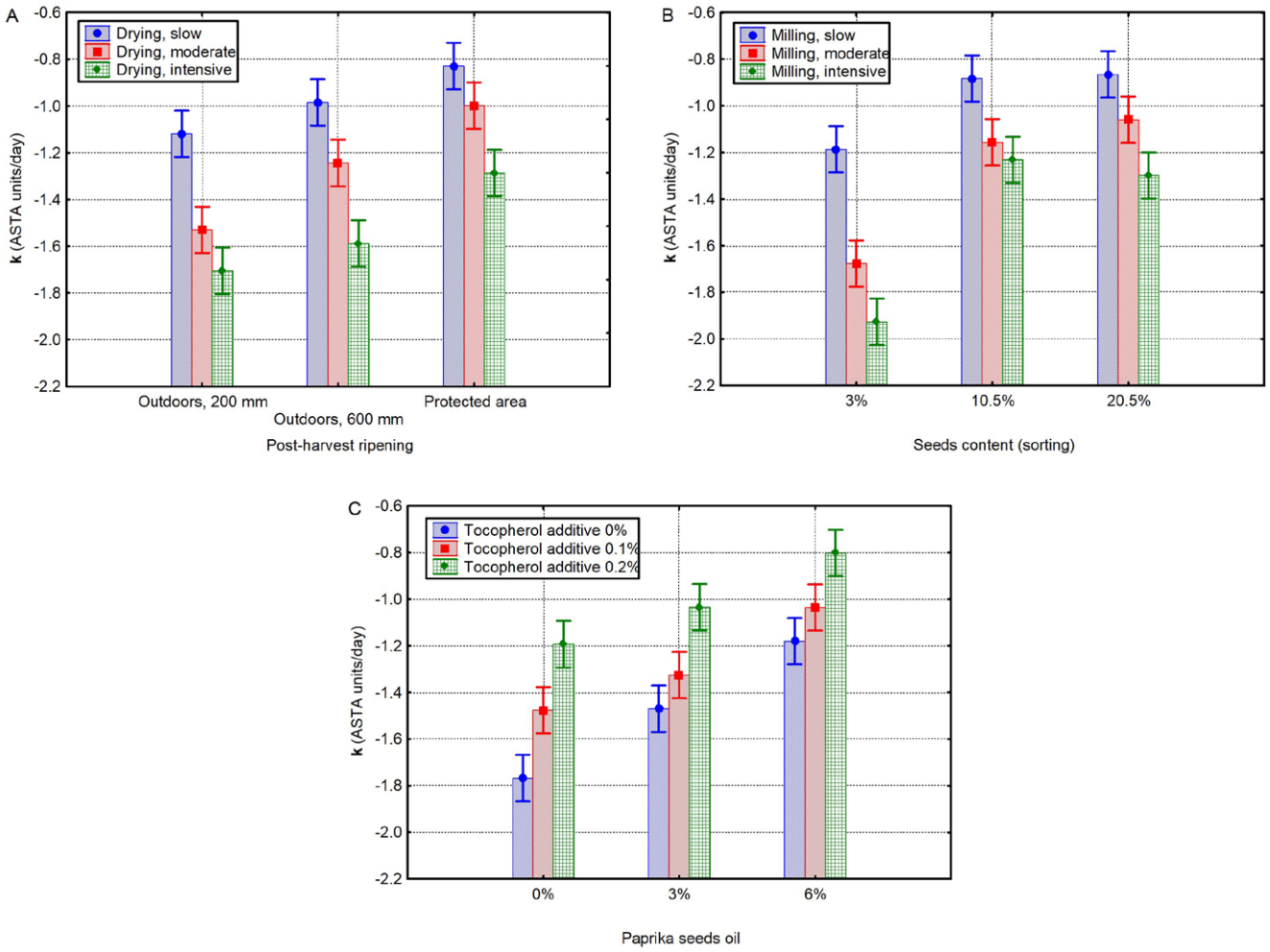

FIGURE 5. The effect of processing variables on the degradation rate constant (k) of extractable colour in spice paprika powder. Plot A – processing in drying factory, Plot B – processing in milling factory, Plot C – processing combined with additives.

The indicated confidence limits were computed based on the respective estimates of the standard errors.

Outdoors post-ripening is a generally applied method in the case of industrial volumes. Thin layer (200 mm) storage was not advised because remarkable damages were observed in pods and higher degradation rate of extractable colour with rate constants of -1.705 and -1.530 ASTA units/day for intensive and moderate dried samples, respectively (Figure 5A), indicating weaker colour stability in the final product. However, the slow drying significantly compensated the adverse effect of thin layer outdoors post-ripening (k=-1.119 ASTA units/day). Storage in 600 mm heaps and protected area combined with moderate or slow drying intensity revealed significantly lower degradation rate of extractable colour (k ranged from -0.828 to -0.998 ASTA units/day). Post-ripening in 600 mm heaps protected the deep layers from the external conditions. Protected post-ripening was most advantageous on colour retention, and seemed to compensate the adverse effect of intensive drying. This method is less usable in industrial volumes because of remarkable place-demand, but useful in craft-like processing tradition. These findings were consistent with several previous studies. Ibrahim *et al.* [1997] have identified two stages in carotenoid content change during light-exposed and protected (in dark) natural drying of spice paprika. The first stage was a biosynthetic and the second was degradative with more adverse effect of light-exposure than darkness. The retention of phytochemicals (ascorbic acid and tocopherols), that play important role in carotenoid stability, has been found to be significantly worse in naturally dried paprika than in thermally-dried paprika [Daood *et al.*, 1996, 2014].

Exposure of spice paprika to higher temperature (intensive drying) resulted in substantial deterioration of extractable colour during the accelerated storage-stability experiment (Figure 5A). The marginal means of rate constants were 1.5–1.6 and 1.1–1.3 times lower, as compared with slow drying and moderate drying, respectively. Many authors have reported the colour deterioration as proportional with the temperature and time of hot-air drying technology, which might be due to Maillard reactions and heat sensitivity of carotenoids and other antioxidants [Daood *et al.*, 2006; Karam *et al.*, 2016].

Reduction of the seed content to 3% accelerated the extractable colour degradation, especially with more intensive milling (Figure 5B). The marginal means of rate constants (-1.187 ASTA·units/day) were 1.3–1.4 times lower

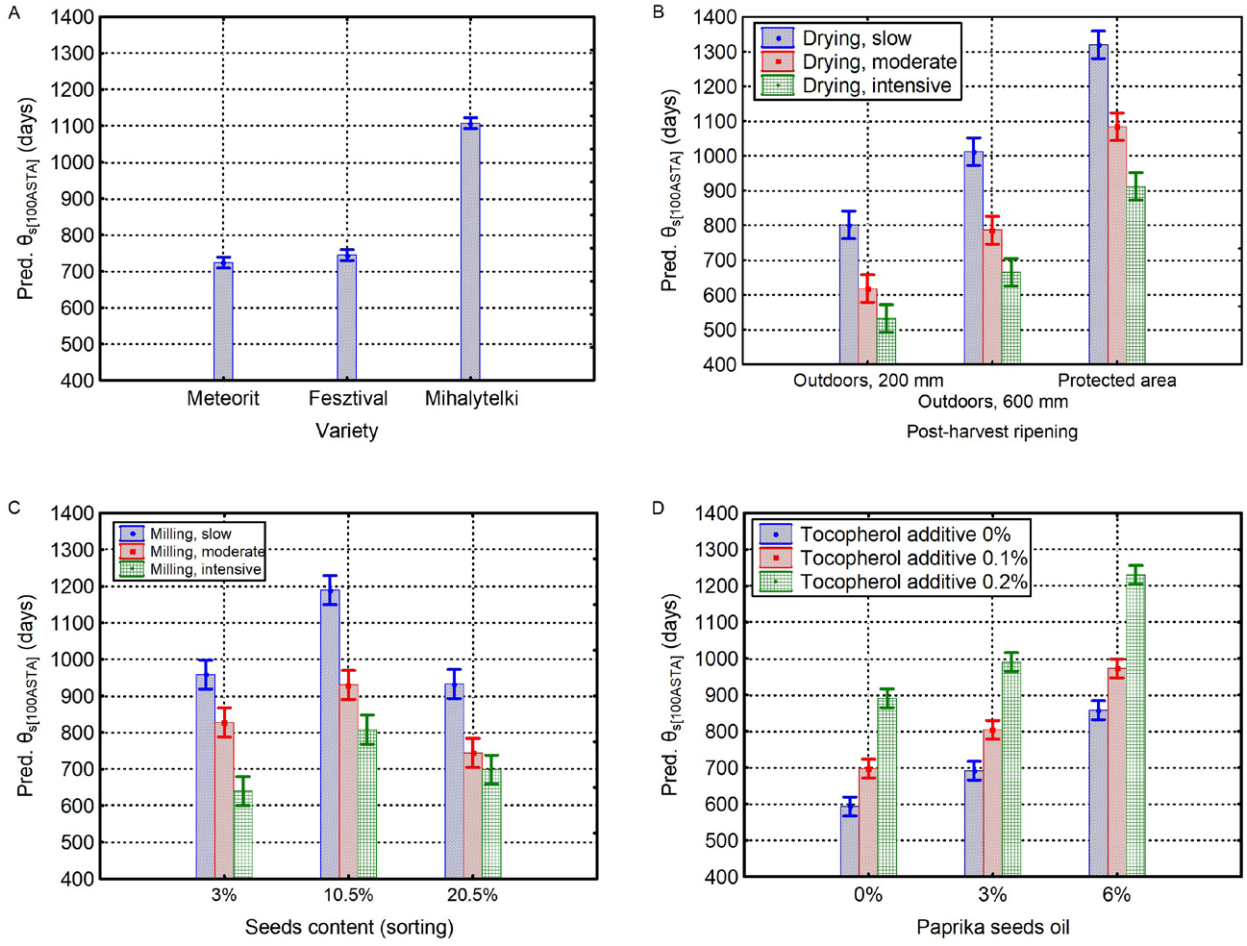

FIGURE 6. The effect of processing variables on estimated shelf-life time ($\theta_{S[100ASTA]}$) of spice paprika powder. Plot A – variety, Plot B – processing in drying factory, Plot C –processing in milling factory, Plot D – processing combined with additives.

in the slow- and moderate-intensity milled seed-less samples, than in their medium seed-content and non-sorted alternatives (-0.874 ASTA units/day). Studies have demonstrated that the oil and γ-tocopherol derived from seeds are essential elements in the carotenoid stability of paprika powder [Daood *et al.*, 1996; Koncsek *et al.*, 2016]. There were no significant differences between the effects of medium and total seed content on the rate constant. Omitting of sorting might be a reasonable decision to decrease degradation rate of extractable colour.

The slow and moderate milling intensity was found to be favourable, resulting in slower degradation rate than intensive milling (Figure 5A). Conventional grinding can rise the temperature over 90°C due to the friction-induced heat, causing important losses of aroma, nutrients and flavour components, as well as considerable quality degradation [Karam *et al.*, 2016; Singh & Goswani, 1999]. However, heat and mechanical forces played an important role in the quality of traditional spice paprika powders. During grinding, the heat enabled to release the oil from the seeds, which interacted with the pigment in the pericarp particles to produce intense red colour [Berke & Shieh, 2001; Szegedi paprika, 2010].

The supplementation with cold-pressed spice paprika seed oil and tocopherol extract decreased the degradation rate of extractable colour of paprika powder (Figure 5C and Figure 5D). The spice paprika seed oil was less effective (k=-1.180–1.147 ASTA units/day) than the combination of oil and tocopherol additive (k=-0.801–1.034 ASTA units/day). However, at higher dose (6%), the oil was close to the efficacy of the 0.2% tocopherol additive (k=-1.193 ASTA units/day). The supplementation with oil is a natural way of quality stabilization using the original compounds of spice paprika. Earlier studies have shown successful application of high-oleic sunflower seed [Pérez-Gálvez *et al.*, 2000], soybean oil [İnanç *et al.*, 2010], δ-tocopherol [Osuna-Garcia *et al.*, 1997] and rosemary extract [Koncsek *et al.*, 2019] as additives to moderate the carotenoid degradation in paprika powders or products. The principles of the processing technology, laid down in the related legislative regulations, restricted the presence of non-paprika origin components in the traditional Hungarian spice paprika powder marketed in retail.

The effects of processing variables on estimated shelf-life time ($\theta_{S[100ASTA]}$) are shown graphically in Figure 6. The variety-effect plot shows that Mihalyteleki variety with the highest initial extractable colour (203 ASTA units) revealed the best marginal mean of estimated shelf-life time (1107 days). This can be attributed to the zero-order degradation kinetics

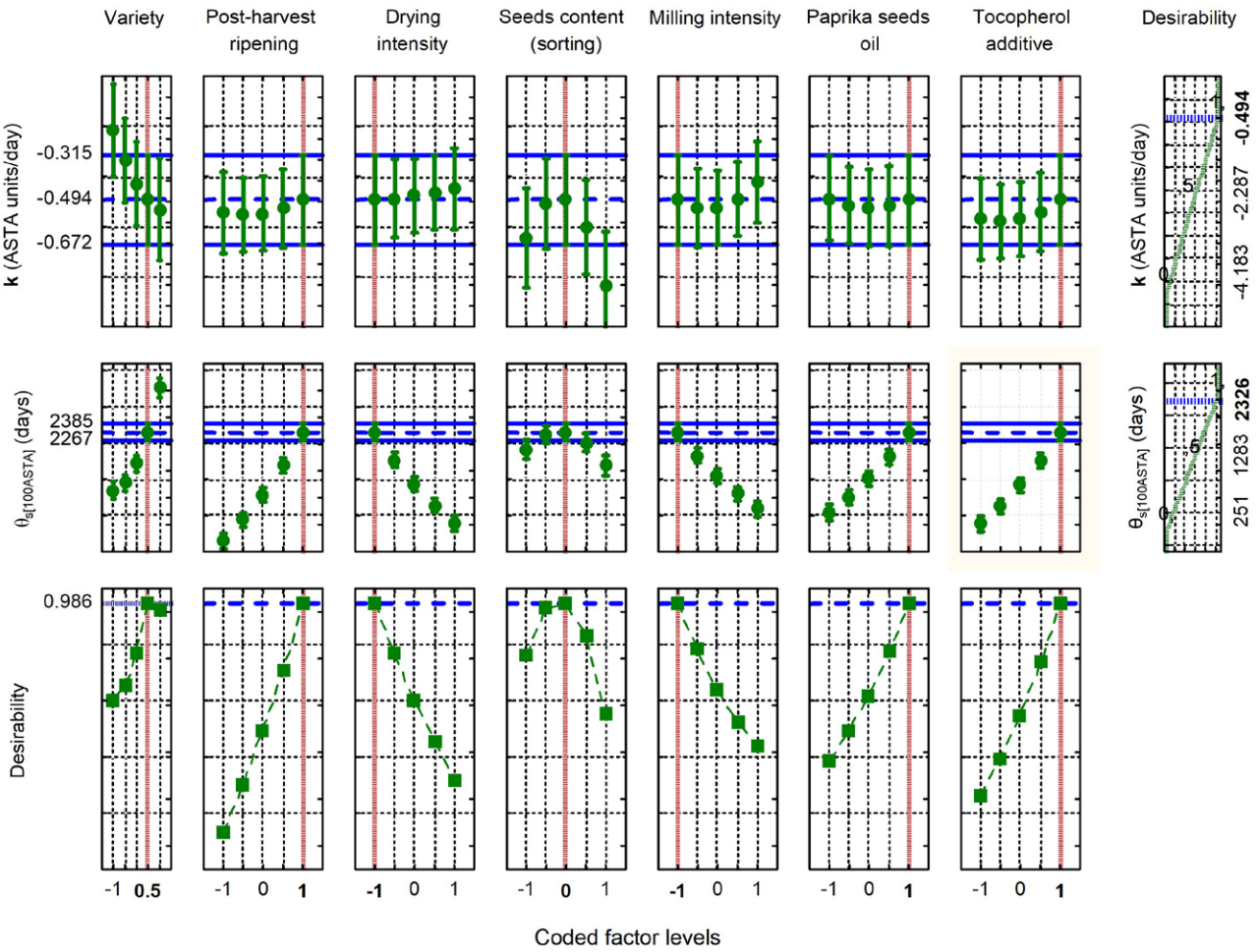

FIGURE 7. Desirability function-based approach for spice paprika processing at the highest desirability level. (Red vertical dashed lines – the best processing factor settings, blue horizontal dashed lines – the highest available shelf-life and lowest degradation rate constant, green points – shelf-life and degradation rate constant values, continous blue lines – 95%-level confidence prediction).

of carotenoids, because in this model the degradation time depends on the initial concentration of the useful component [Koncsek *et al.*, 2016; Peleg, 2017].

Both reduction of the seed content to 3% and omitting of seed sorting shortened the estimated shelf-life time (Figure 6C). As mentioned above, the seeds do not contain carotenoids and thus total-seed-containing paprika powders had a lower initial extractable colour value (164±16 ASTA units), compared to the medium-sorted samples. This lower initial extractable colour decreased the $\theta_{S[100ASTA]}$ (698–937 days). Higher initial ASTA colour values were available with help of total seed content removal (193±20 ASTA units), than with medium sorting (180±18 ASTA units); however, significantly longer shelf-life was not achieved (639–958 days). This confirmed that the products were deprived of useful compounds of seeds, which play important protective role against the oxidative degradation of carotenoids. The paprika seed oil and tocopherol additives decreased the degradation rate of extractable colour, thus improving the estimated shelf-life time up to 1,230 days marginal mean (Figure 6D).

The desirability function approach enabled the inspection of predicted dependent variables at different combinations of levels of independent variables. Figure 7 shows the searching result for the predictor (processing) variables that produce the highest desirability value (0.986). This was available with the following factor settings: high extractable colour of paprika variety, protected post-harvest ripening, slow drying and milling intensity (330 kg/h and 110 kg/h), medium seed content (10.5%) and supplementation with spice paprika seed oil (6%) and tocopherol extract (0.2%). The predicted values of rate constant of accelerated storage-stability test and shelf-life time were -0.494 ASTA units/day and 2,326 days, respectively. The predicted shelf-life extremely exceeded the preliminary goal of the present study (two years). This meant an opportunity for modified factor level settings that resulted in lower desirability values, but enabled taking into account some important expectations or practical considerations.

Table 2 shows some alternative factor level settings with satisfactory dependent variables, meanwhile the intensity of processing was increased and the tocopherol additive was omitted. The processing was repeated with No. 1, 2 and 3 settings, using 2018 season's spice paprika crop. The observed shelf-life values (with their 95% confidence intervals) were 926 days (894–958 days), 772 days (745–798 days) and 631 days (610–653 days) for No 1, 2 and 3 settings, respectively. These results showed that the real observed values

TABLE 2. Desirability function-based prediction of colour degradation rate constant and shelf-life of spice paprika powder products, based on alternative factor-level settings.

No.	Variety (x_1)	Post-harvest ripening (x_2)	Drying (x_3)	Seed content (x_4)	Milling (x_5)	Paprika seed oil (x_6)	Tocopherol additive (x_7)	Desirability (D)	k (ASTA units/day)*	$\theta_{s[100ASTA]}$ (days)*
0.	Mihalyteleki	Protected	Slow (330 kg/h)	Medium (10.5%)	Slow (110 kg/h)	6%	0.2%	0.986	-0.494 (-0.672–0.315)	2326 (2267–2385)
1.	Fesztival	Outdoors, heap	Moderate (416 kg/h)	Medium (10.5%)	Moderate (140 kg/h)	3%	0.2%	0.802	-0.972 (-1.069–0.874)	918 (885–950)
2.	Fesztival	Outdoors, heap	Moderate (416 kg/h)	Medium (10.5%)	Moderate (140 kg/h)	3%	0%	0.589	-1.420 (-1.518–1.322)	712 (680–744)
3.	Meteorit	Outdoors, heap	Moderate (416 kg/h)	Medium (10.5%)	Moderate (140 kg/h)	3%	0%	0.505	-1.381 (-1.489–1.274)	617 (581–652)

*Mean and minimum-maximum predicted values. k – degradation rate constant of extractable colour, $\theta_{s[100ASTA]}$ – estimated shelf-life, calculated for 100 ASTA units.

of dependent variables met the predicted values and their 95% confidence intervals (Table 2).

CONCLUSIONS

This study demonstrated that the desirability profiler, based on extended set of experimental data, is a useful tool for empirically-based quality improvement in spice paprika processing. The model is suitable to take into account the changing conditions and some important expectations, for example productivity, additive-free requirements *etc*.

Post-harvest ripening, drying, sorting (seed content modification), milling and additives (paprika seed oil and/or tocopherol extract) were identified as important for the degradation rate constant of extractable colour of paprika powders. Post-harvest ripening is crucial in the biosynthesis of stable carotenoids. The results suggested that different *Capsicum* varieties have a diversity of post ripening demands (time, light or dark and temperature) to reach the best extractable colour accumulation. The extractable colour stability was very sensitive to the milling and drying intensity, while proper setup of other processing steps (*e.g.* seed content, supplementation with spice paprika seed oil or tocopherol) can compensate the adverse effect of drying and milling parameters. The study proved that processing steps have an additive impact on the storage stability of extractable colour of spice paprika powder. The presented technology with moderate intensity of processing steps and moderate treatments were found to be appropriate to maintain the achieved extended shelf-life.

The results revealed that the planned fractional factorial experimental design methods, extended to entire processing line, lead to better optimal solution for colour stability improvement than the investigation of some selected processing steps.

RESEARCH FUNDING

This work was supported by GINOP-2.1.7-15-2016-01670 project at the Rubin Spice Paprika Processing Szeged Ltd. (Hungary, traditional spice paprika production area of Szeged).

CONFLICT OF INTERESTS

The authors declare that there is no conflict of interest.

ORCID IDs

H.G. Daood https://orcid.org/0000-0001-6004-7650
L. Helyes https://orcid.org/0000-0001-7365-8653
A. Koncsek https://orcid.org/0000-0001-7532-7401
B.P. Szabó https://orcid.org/0000-0001-5950-3858

REFERENCES

1. Acedo, A.L. (2010). International cooperator's guide of post -harvest technology for fresh chili pepper in Cambodia, Laos, and Vietnam. *International Cooperator's Guide. AVRDC World Vegetable Center, 10–735*, 1–6.
2. Arimboor, R., Natarajan, R.B., Menon, K.R., Chandrasekhar, L.P., Moorkoth, V. (2015). Red pepper (*Capsicum annuum*) carotenoids as a source of natural food colors: Analysis and stability—a review. *Journal of Food Science and Technology, 52,* 1258–1271. https://doi.org/10.1007/s13197-014-1260-7
3. ASTA (AMERICAN SPICE TRADE ASSOCIATION) (1997). Extractable colour in capsicums and their oleoresins. Method no. 20.1. *Official Analytical Methods of the American Spice Trade Association,* 4th ed., pp. 89–104.
4. Berke, T.G., Shieh, S.C. (2001) Capsicum, chillies, paprika, bird's eye chilli. In K.V. Peter (Ed.), *Handbook of Herbs and Spices*. Published in North and South America by CRC Press LLC, pp. 111–121. https://doi.org/10.1533/9781855736450.111
5. Chopan, M., Littenberg, B. (2017). The association of hot red chili pepper consumption and mortality: A large population-based cohort study. *PLoS ONE*, *12*(1), art. no. e0169876. https://doi.org/10.1371/journal.pone.0169876
6. Daood, H.G., Kapitany, J., Biacs, P.A., Albrecht, K. (2006). Drying temperature, endogenous antioxidants and capsaicinoids affect carotenoid stability in paprika (red pepper spice). *Journal of the Science of Food and Agriculture, 86*(14), 2450–2457 https://doi.org/10.1002/jsfa.2639
7. Daood, H.G., Palotás, G., Palotás, G., Somogyi, G., Pék, Z., Helyes, L. (2014). Carotenoid and antioxidant content of ground paprika from indoor-cultivated traditional varieties and new hybrids of spice red peppers. *Food Research International, 65,* Part B, 231–237. https://doi.org/10.1016/j.foodres.2014.04.048

8. Daood, H.G., Vinkler, M., Markus, F., Hebshi, E.A., Biacs, P.A. (1996). Antioxidant vitamin content of spice red pepper (paprika) as affected by technological and varietal factors. *Food Chemistry, 55*(4), 365–372. https://doi.org/10.1016/0308-8146(95)00136-0
9. Giuffrida D., Dugo, P., Torre, G., Bignardi, C., Cavazza, A., Corradini, C., Dugo, G. (2013) Characterization of 12 *Capsicum* varieties by evaluation of their carotenoid profile and pungency determination. *Food Chemistry, 140*(4), 794–802. https://doi.org/10.1016/j.foodchem.2012.09.060
10. Hamed, M., Kalita, D., Bartolo, M.E., Jayanty, S. (2019). Capsaicinoids, polyphenols and antioxidant activities of *Capsicum annuum*: Comparative study of the effect of ripening stage and cooking methods. *Antioxidants, 8*(9), art. no. 364. https://doi.org/10.3390/antiox8090364
11. Ibrahim, H.M.A, Ragab, G.H., Moharram, H.A. (1997). Paprika color quality: Effect of air and natural drying treatments. *Grasas y Aceites, 48*(4), 200–206. https://doi.org/10.3989/gya.1997.v48.i4.790
12. İnanç, L.A., Demirci, M., Alpaslan, M. (2010). Effects of vegetable oils on the quality parameters of red pepper during storage. *Journal of Tekirdag Agricultural Faculty, 7(1)*, 39–47.
13. ISO 7540:2006 Ground paprika (*Capsicum annuum* L.) specification.
14. Karam, M.C., Petit, J., Zimmer, D., Djantou, E.B., Scher, J. (2016). Effects of drying and grinding in production of fruit and vegetable powders: A review. *Journal of Food Engineering, 188,* 32–49. https://doi.org/10.1016/j.jfoodeng.2016.05.001
15. Koncsek, A., Daood, H.G., Horváth Zs.H., Fekete, M., Véha, A., Helyes, L. (2019). Improvement of antioxidant content and color stability in spice paprika powder by rosemary extract supplementation. *Journal of Food Processing and Preservation, 43*(8), art. no. 14000. https://doi.org/10.1111/jfpp.14000
16. Koncsek, A., Kruppai, L., Helyes, L., Bori, Zs., Daood, H.G. (2016). Storage stability of carotenoids in paprika from conventional, organic and frost-damaged spice red peppers as influenced by illumination and antioxidant supplementation. *Journal of Food Processing and Preservation, 40*(3), 453–462. https://doi.org/10.1111/jfpp.12623
17. Márkus, F., Daood, H.G., Kapitany, J., Biacs, P.A. (1999). Change in the carotenoid and antioxidant content of spice red pepper (paprika) as a function of ripening and some technological factors. *Journal of Agricultural and Food Chemistry, 47*(1), 100–107. https://doi.org/10.1021/jf980485z
18. Martí, M.C., Camejo, D., Olmos, E., Sandalio, L.M., Fernández- García, N., Jiménez, A., Sevilla, F. (2009). Characterization and changes in the antioxidant system of chloroplasts and chromoplasts isolated from green and mature pepper fruits. *Plant Biology, 11*(4), 613–624. https://doi.org/10.1111/j.1438-8677.2008.00149.x
19. Martí, M.C., Camejo, D., Vallejo, F., Romojano, F., Bacarizo, S., Palma, J.M., Sevilla, F., Jiménez, A. (2011). Influence of fruit ripening stage and harvest period on the antioxidant content of sweet pepper cultivars. *Plant Foods and Human Nutrition 66,* 416–423. https://doi.org/10.1007/s11130-011-0249-x
20. Montgomery, D.C. (2013). Design and Analysis of Experiments (8th ed.). John Wiley & Sons, Inc. ISBN 978–1118–14692–7, p. 257.
21. Moór, J., Somogyi, N. (2017). History of spice paprika research in Hungary. In Gyuricza, Cs., Somogyi, N. and Radó G. (Eds.), *The Spice Paprika Research in Hungary is 100 Years Old.* NAIK, ISBN: 978–615–5784–02–8, 7–16 (in Hungarian).
22. Obermayer, E. (1934). Commodity knowledge of Hungarian Paprika. Reprinted in: Gyuricza, Cs., Somogyi, N., Radó G. (Eds.), (2017), *The Spice Paprika Research in Hungary is 100 Years Old.* NAIK, ISBN: 978–615–5784–02–8, 29–34 (in Hungarian).
23. Osuna-Garcia, J.A., Wall, M.M., Waddell, C.A. (1997). Natural antioxidants for preventing color loss in stored paprika. *Journal of Food Science, 62*(5), 1017–1021. https://doi.org/10.1111/j.1365-2621.1997.tb15027.x
24. Pal, S., Gauri, S.K. (2018). A desirability functions-based approach for simultaneous optimization of quantitative and ordinal response variables in industrial processes. *International Journal of Engineering, Science and Technology, 10*(1), 76–87. https://doi.org/10.4314/ijest.v10i1.6
25. Peleg, M., Normand, M.D., Corradini, M.G. (2017). A new look at kinetics in relation to food storage. *Annual Review of Food Science and Technology, 8,* 1–19. https://doi.org/10.1146/annurev-food-030216-025915
26. Pérez-Gálvez, A., Garrido-Fernández, J., Mínguez-Mosquera, M.I. (2000). Effect of high-oleic sunflower seed on the carotenoid stability of ground pepper. *Journal of Agricultural and Food Chemistry, 77*(1), 79–83. https://doi.org/10.1007/s11746-000-0012-x
27. Perez-Galvez, A., Hornero-Mendez, D., Minguez-Mosquera, M.I. (2009). Stability of paprika without supplementary antioxidants during storage under industrial controlled conditions. *Journal of Agricultural and Food Chemistry, 57*(11), 4718–4723. https://doi.org/10.1021/jf804058m
28. Pola, W., Sugaya, S., Photchanachai, S. (2020). Influence of postharvest temperatures on carotenoid biosynthesis and phytochemicals in mature green chili (*Capsicum annuum* L.). *Antioxidants, 9*(3), art. no. 203. https://doi.org/10.3390/antiox9030203
29. Schieber, A., Carle, R. (2005). Occurrence of carotenoid *cis*-isomers in food: Technological, analytical, and nutritional implications. *Trends in Food Science & Technology, 16*(9), 416–422. https://doi.org/10.1016/j.tifs.2005.03.018
30. Singh, K.K., Goswami, T.K. (1999). Design of a cryogenic grinding system for spices. *Journal of Food Engineering, 39*(4), 359–368. https://doi.org/10.1016/S0260-8774(98)00172-1
31. Spiller, F., Alves, M.K., Vieria, S., Carvalho, T.A., Leite, C.E., Lunardelli, A., Poloni, J.A., Cunha, F.Q., de Oliveira, J.R. (2008). Anti-inflammatory effects of red pepper (*Capsicum baccatum*) on carrageenan and antigen-induced inflammation. *Journal of Pharmacy and Pharmacology, 60*(4), 473–478. https://doi.org/10.1211/jpp.60.4.0010
32. Szegedipaprika (2010). HU/PDO/0005/0395 [http://ec.europa.eu/agriculture/quality/door/registeredName.html?denominationId=2111]. Accessed November 10, 2020.
33. Topuz, A., Ozdemir, F. (2003). Influences of γ-irradiation and storage on the carotenoids of sun-dried and dehydrated paprika. *Journal of Agricultural and Food Chemistry, 51*(17), 4972–4977. https://doi.org/10.1021/jf034177z

Pol. J. Food Nutr. Sci., 2022, Vol. 72, No. 1, pp. 101–108
On-line ISSN: 2083-6007
Print ISSN: 1230-0322
DOI: 10.31883/pjfns/146562
http://journal.pan.olsztyn.pl

Original article
Section: Food Quality and Functionality

Antioxidative Capacity of Soyfoods and Soy Active Compounds

Wanida T. Chitisankul[1], Kazuko Shimada[2], Chigen Tsukamoto[3]*

[1]Nutrition and Health, Institute of Food Research and Product Development, Kasetsart University, 50 Ngamwongwan Rd., Chatuchak, Bangkok, 10900, Thailand
[2]Faculty of Health Science, Hiroshima Shudo University, 1-1-1 Ozukahigashi, Asaminami-ku, Hiroshima, 731-3195, Japan
[3]Faculty Agriculture, Iwate University, 3-18-8 Ueda, Morioka, Iwate, 020-8550, Japan

Key words: soybean, ORAC, isoflavone, peroxyl radical scavenging, soy saponin

Soyfood isoflavones and soyasaponins are effective compounds in terms of their health-promoting properties. Their chemical structure plays an important role in their antioxidative activity. Thus, six isoflavones and four soyasaponins that are targeted in soyfood were evaluated for their peroxyl radical scavenging capacities by the hydrophilic-oxygen radical absorbance capacity (H-ORAC) method. The antioxidant capacity of non-fermented and fermented soyfoods was also determined by the same method. The results revealed that isoflavones showed higher peroxyl radical scavenging capacities than soyasaponin, with their activities found to depend on their chemical structure. The aglycone isoflavones promoted higher H-ORAC values than glycoside and malonyl glycoside isoflavones, respectively. On the other hand, DDMP saponin promoted a higher H-ORAC value than its derived compound, group B saponin, and the aglycone soyasaponin. In the case of soyfoods, fermented soyfoods had higher antioxidative capacity that the non-fermented ones, especially the long-term fermented products. Soybean-koji miso presented the highest H-ORAC value, followed by natto, soy sauce, and tempeh. Moreover, lightness (L^*) of miso and soy sauce showed a negative correlation with H-ORAC value probably due to browning substances which might derive from the amino-carbonyl reaction. Considering the high antioxidant capacity of fermented soyfoods, it might relate to aglycone isoflavones which promote strong radical scavenging capacity. Thus, fermented soyfoods, especially miso and natto, could be considered as health-promoting foods.

INTRODUCTION

A peroxyl radical was reported as a cause of non-communicable diseases, such as cardiovascular disease, cancer, and neurological disease [Pizzino *et al*., 2017]. As its excess *in vivo* and lifestyle diseases, such as arteriosclerosis, are related, food that includes antioxidative components is strongly recommended to be consumed for these diseases prevention. Soybean is a familiar plant-based protein food component to people in Japan and Southeast Asia which additionally promotes the antioxidative effect due to its functional ingredients, such as isoflavones [Han *et al*., 2009; Kim *et al*., 2022], saponins [Yoshiki *et al.*, 2001; Yoshiki & Okubo, 1995], tocopherols [Carrera & Seguin, 2016], anthocyanins [Kähkönen & Heinonen, 2003; Zilic *et al*., 2019], and proanthocyanins [Xu *et al*., 2017]. However, rather than consuming soybeans as fresh, almost all of them are consumed as processed products. These soyfoods, *e.g.* miso [Matsuo & Hitomi, 2007], soy sauce [Long *et al*., 2000], natto [Ping *et al*., 2012], and tempeh [Chang *et al*., 2009; Kameda *et al*., 2018], have also been reported as a source of natural antioxidants. The thermal processes, as well as pressurization and fermentation are used to obtain soyfoods. They could induce degradation and/or conversion of soybean native active ingredients and, in consequence, affect their functionalities [Chitisankul *et al.*, 2015; 2021; Khosravi & Razavi, 2021; Ping *et al*., 2012].

The antioxidant properties of foods and food ingredients have been measured by various methods, including the hydrophilic-oxygen radical absorbance capacity (H--ORAC) assay [Ou *et al.*, 2001], which is an *in vitro* method for determining the antioxidative capacity by measuring peroxyl radical-scavenging activity of water-soluble substances [Zhong & Shahidi, 2015]. Isoflavones [Han *et al*., 2009; Kim *et al.*, 2022], 2,3-dihydro-2,5-dihydroxy-6-methyl-4*H*-pyran-4-one (DDMP) saponins [Yoshiki *et al*., 2001; Yoshiki & Okubo, 1995], peptides [Sanjukta & Rai, 2016; Tonolo *et al*., 2020], and browning substances [Ando *et al*., 2003] are the main water-soluble antioxidants which could be extracted by the aqueous ethanol solution from soybeans and processed soybean foods. The isoflavones contained in soybeans undergo demalonylation and further aglycone conversion by cooking and processing [Toda *et al*., 2000].

* Corresponding Author:
E-mail: wanida.te@ku.ac.th (W.T. Chitisankul)

Submitted: 14 August 2021
Accepted: 8 February 2022
Published on-line: 4 March 2022

Their antioxidative activity was evaluated by the low-density lipoprotein (LDL) oxidation method and it had been shown that aglycone isoflavones promote higher antioxidative activity than glycosides [Lee *et al*., 2005]. On the other hand, the antioxidative activity of isoflavones was evaluated by the ABTS method [Ruiz-Larrea *et al*., 1997] and the liposome oxidation method [Arora *et al*., 1998], which showed no significant differences between the properties of glycoside isoflavones and their aglycones. In addition, DDMP saponins were reported to promote antioxidative capacity [Yoshiki *et al*., 2001; Yoshiki & Okubo, 1995]. But it also was reported that DDMP saponin can be degraded by heating, fermenting, and aging [Chitisankul *et al.*, 2015; Omizu *et al*., 2011]. However, there is no report about an evaluation of the antioxidant capacity of individual isoflavones, soyasaponins, and their derived compounds by the same methodology including several processed soybeans. Therefore, this research aimed to evaluate the peroxyl radical scavenging capacities of isoflavones, soyasaponin, and several soyfood samples by the H-ORAC assay.

MATERIAL AND METHODS

Samples and reagents

Soyfoods were purchased from food supermarkets in Morioka (Iwate, Japan). The samples included non-fermented soyfoods (NFS) and fermented soyfoods (FS) as shown in Table 1. The 11 samples of six kinds of NFS included steamed soybean, young soybean, soymilk, soy beverage, tofu, and fried tofu. The nine samples of four kinds of FS included natto, tempeh, miso, and soy sauce.

All standard reagents were of HPLC grade. They included six isoflavone standard reagents: malonyldaidzin, malonylgenistin, daidzin, genistin, daidzein, and genistein (Wako Pure Chemical Industries, Ltd., Osaka, Japan); and soyasaponin standard reagents: soyasapogenol A and soyasapogenol B (Koshiro Company Ltd., Osaka, Japan). The 2,2-azobis (2-amidinopropane) dihydrochloride (AAPH) (Wako Pure Chemical Industries, Ltd., Osaka, Japan), fluorescein sodium salt (Sigma Aldrich, Tokyo, Japan), and 6-hydroxy-2,5,7,8-tetramethylchroman-2-carboxylic acid (Trolox) (Tokyo Chemical Industry Co., Ltd., Tokyo, Japan) were analytical grade reagents.

Isoflavone and saponin preparation

Six isoflavones and soyasaponins, soyasapogenol A and soyasapogenol B, were dissolved and mixed well in a 70% (*v/v*) aqueous ethanol solution by vortexing or ultrasonication with the final concentration of 500 μM or 1 mM solution, respectively. DDMP saponin βg was extracted and purified from soybean hypocotyl [Chitisankul *et al*., 2015]. Purified DDMP saponin βg and group B saponin Bb were analyzed using HPLC [Chitisankul *et al.*, 2019], and the purity of the purified saponin was 95% or higher. The purified DDMP saponin solution was composed of 852.1 μM saponin βg and the group B saponin solution was composed of 1118 μM saponin Bb.

Sample preparation

Liquid soyfoods were directly extracted by 10-fold volume (*w/v*) of a 70% (*v/v*) aqueous ethanol solution.

TABLE 1. Code, name, and description of soyfoods including non-fermented (NF) and fermented (F) products.

Code	Sample name	Sample description
NF1	Steamed soybean	Steamed whole seeds
NF2	Edamame	Heated and frozen green (young) soybean
NF3	Soymilk	Regular type soymilk
NF4	Soymilk w/o LOX	Soymilk from lipoxygenase enzyme deficient soybean
NF5	Modified soymilk	Blended soymilk
NF6	Soybean beverage	Beverage from whole soybean (including okara)
NF7	Black soybean beverage	Beverage from whole black soybean (including okara)
NF8	Momen tofu	Regular type tofu
NF9	Silken tofu	Very soft tofu
NF10	Abura-age	Twice-fried tofu, deep fried thin sliced tofu
NF11	Nama-age	Deep fried tofu
F1	Natto	Regular type natto
F2	Black soybean natto	Black soybean natto
F3	Tempe	Fermented soybean with *Rhizopus* spp.
F4	Rice miso, sweet – white	Rice-koji miso: sweet-white type
F5	Rice miso, light yellow	Rice-koji miso: light yellow type
F6	Barley miso	Barley-koji miso
F7	Soy miso	Soybean-koji miso
F8	Dark soy sauce	Dark soy sauce
F9	Light soy sauce	Light soy sauce

The sample solution was homogenized (15,500 rpm, 1 min, Polytron homogenizer, Jakarta, Indonesia) and left to stand for 1 h with every 10 min vortex mixing. The supernatant was obtained by centrifugation at 27,000×*g* and 15°C for 15 min (Kubota 7780 centrifuge, Tokyo, Japan) as a crude extract, and then filtered with a 0.45 μm membrane filter. For all tofu samples, the outer part was cut off with a ceramic knife, then the samples were fined in a mortar. Steamed soybean, edamame, natto, tempeh, and miso were crushed with a mallet and then fined in a mortar. Each solid soyfood sample was extracted in the same manner as liquid samples. The crude extracts were kept in the opaque bottles at -20°C until analysis.

Color measurement

For miso and soy sauce, CIE-L^* (lightness), a^* (green to red color), b^* (blue to yellow color) were measured using a colorimeter (color meter Z-300A, Nippon Denshoku Industries Co., Ltd., Tokyo, Japan). Miso was packed in a Petri dish, the lid was put on, and the reflectance was measured. In addition, soy sauce was placed in a glass cell and permeation was measured. Miso was triplicate measured per sample, and soy sauce was measured once per sample.

Peroxyl radical scavenging capability evaluation

Hydrophilic-oxygen radical absorbance capacity (H--ORAC) assay was used to measure peroxyl radical scavenging capability [Ou *et al*., 2001]. The standard and sample solution were diluted with phosphate buffer (75 mM, pH 7.0), then the Trolox standard solution of 6.25 μM to 100 μM was used as a standard curve. The H-ORAC values of isoflavone and soyasaponin were reported as mol Trolox equivalent (TE)/mol and those of the processed soybean food as mmol Trolox equivalent (TE)/100 g sample. A fluorescence plate reader (Bio-Tek FL600, Bio-Tek Instruments, Inc., Winooski, VT, USA) was used for measurements.

Statistical analysis

Analysis of variance (ANOVA) of the experimental data was performed and the least significant difference was evaluated by Tukey's test at a 95% confidence interval. The correlation coefficient (r) of the experimental data was analyzed. All analyses were repeated in triplicate.

RESULTS AND DISCUSSION

Peroxyl radical scavenging capacity of isoflavones and soyasaponins

The peroxyl radical scavenging capacity of isoflavones and soyasaponins had been shown as H-ORAC values (mol TE/mol) in Figure 1. Isoflavones presented higher antioxidative capacity than soyasaponins. The chemical structure of active ingredients promoted different activities. For isoflavones, high H-ORAC values presented in the order of aglycone form then glycoside form, and malonyl glycoside form. Daidzein had the highest antioxidant ability, with the H-ORAC value reaching 9.94±0.45 mol TE/mol, followed by genistein, genistin, daidzin, and malonyl glycoside isoflavone, respectively. The result was supported by a previous report which revealed that the antioxidative activity of aglycones (daidzein, genistein) was higher than that of glycosides (daidzin, genistin) depending on the method of measuring the lag time of LDL oxidation (lag time assay) [Lee *et al*., 2005]. Recently, Kim *et al.* [2022] also found that the $ABTS^{\bullet+}$ scavenging activity and ferric-reducing antioxidant power (FRAP) of soy isoflavones as aglycone were higher than those of their glycosides, and malonyl glycoside derivatives had the lowest activity. Isoflavones are generally found as glycoside forms in natural sources, but their bioavailability is lower compared to aglycones [Kim *et al*., 2022; Setchell *et al*., 2002]. However, the glycoside isoflavone would be converted to aglycone by gut microflora [Bultosa, 2016].

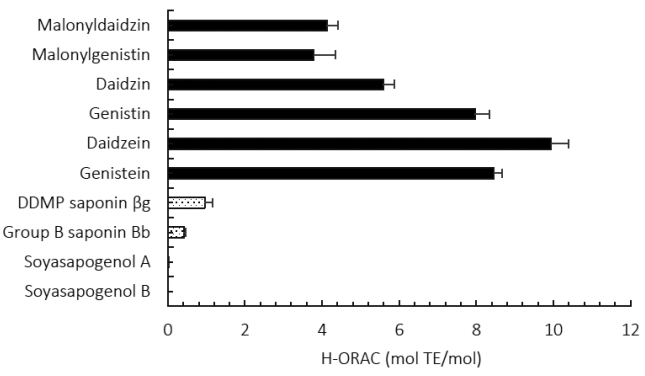

FIGURE 1. Hydrophilic-oxygen radical absorbance capacity (H-ORAC) of isoflavones and saponins.

On the other hand, high H-ORAC values of soyasaponins are presented in the order of DDMP glycoside (DDMP saponin βg) then glycoside (group B saponin Bb), and aglycone (soyasapogenol A, soyasapogenol B) (Figure 1). According to this statement, it clearly shows that the changing chemical structure affects the antioxidant activity of the compound. The degradation of DDMP saponin resulted in antioxidant activity reduction, which was agreeable with other reports [Yoshiki *et al*., 2001; Yoshiki & Okubo, 1995]. The reports also revealed that the DDMP site is involved in superoxide scavenging ability [Yoshiki *et al*., 2001; Yoshiki & Okubo, 1995], thus group B saponin Bb which lacks the DDMP site will not present scavenging activity. Following the evaluation of soyasaponin peroxyl radical scavenging activity in this research, DDMP saponin βg presented strong peroxyl radical scavenging activity while group B saponin Bb presented low peroxyl radical scavenging activity. These results suggest that DDMP saponin βg can scavenge both peroxyl radicals and superoxide. Although, group B saponin Bb cannot scavenge superoxide [Yoshiki *et al*., 2001; Yoshiki & Okubo, 1995], it can eliminate peroxyl radical. On the other hand, the aglycone saponins: soyasapogenol A and soyasapogenol B, showed no scavenging activity against peroxyl radicals (Figure 1). From the above findings, it was speculated that the peroxyl radical scavenging ability was related to the DDMP site and sugar chain portion of soyasaponin. Nevertheless, DDMP saponin could be naturally found in fresh soybean or low processed soybean products which might vary depending on soybean variety and processing treatment [Chitisankul *et al*., 2019, 2021].

Peroxyl radical scavenging capacity of non-fermented soyfoods

The nutraceutical property due to the antioxidative capacity of 11 non-fermented soyfoods (NFS) differed and depended on the type of products (Figure 2), namely to their processing treatments. The NFS products could be categorized into three major groups: (1) steamed soybean (NF1) and frozen boiled edamame (NF2) as low-processed products, (2) soymilk or soy beverages (NF3-NF7), and (3) tofu (NF8-NF11). Only heat processes were applied to obtain the products of the first group whilst several treatments such soaking, extraction, and heating were required to produce other NFS. Among all NFSs, the steamed soybean showed the highest H-ORAC value (2.35±0.31 mmol TE/100 g). However, H-ORAC of the second low-processed product – edamame (young soybean seed), was much lower. It could be assumed that the difference was due to the content of the main antioxidative compounds, isoflavones, and soyasaponins. Indeed, it was reported that contents of daidzein and genistein in soybean were at 0.25––1.23 mg/g and 0.33–1.17 mg/g, respectively [Wu *et al*., 2004]. On the other hand, edamame contained daidzein and genistein in the amounts of 0.11–0.55 mg/g and 0.16–0.62 mg/g, respectively [Wu *et al*., 2004]. Moreover, as reported in the previous

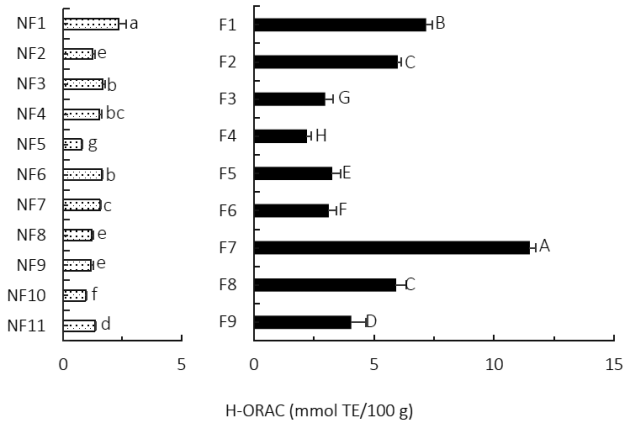

FIGURE 2. Hydrophilic-oxygen radical absorbance capacity (H-ORAC) of non-fermented (NF) and fermented (F) soyfoods. Details on the samples NF1–N11 and F1–F9 are provided in Table 1. Different letters present significant differences between samples ($p<0.05$), lowercase letter for non-fermented soyfoods and uppercase letter for fermented soyfoods.

research, edamame contained much less soyasaponins than mature soybeans, and more active DDMP saponins were degraded to group B saponin during heating [Chitisankul *et al*., 2021]. Thus, the different antioxidant capacities of these low-processed samples might not be related to the food process but varied depending on the maturity of soybean.

For soymilk and soy beverages, four of five samples showed non-significant differences in H-ORAC values and only H-ORAC of modified soymilk (NF5) was significantly ($p<0.05$) lower (Figure 2). Soy solid content of soymilk and soy beverages might play a significant role in their functional properties. On the report of product labeling, solid contents of regular (non-modified) soymilk (NF3), lipoxygenase-deficient soymilk (prepared from a soybean variety 'Kinusayaka' deficient in all of 3 lipoxygenase isozymes) (NF 4) and soy beverage (NF6) were 9 to 14 g/100 g or more, whereas the modified soymilk (NF5) contained about 7 g/100 g. Therefore, it could be considered that soy solid content might play an important role in antioxidative capacity in soymilk and soy beverages. In turn, black soybean beverage (NF7) was expected to be a rich antioxidative compound source. The previous study revealed that black soybean, in addition to isoflavones and saponins, contained significant amounts of anthocyanins and proanthocyanidins [Xu *et al*., 2017; Zilic *et al*., 2019] and showed significantly higher antioxidative capacity than regular soybean [Chitisankul *et al*., 2019]. However, anthocyanins are unstable water-soluble components that could be degraded by enzymatic reaction and thermal treatment [Slavu(Ursu) *et al*., 2020]. The thermal treatment is generally required to preserve and process food for safety purposes. The traditional soymilk process might require thermal treatment at 99°C while steam-infusion treatment might facilitate a higher temperature of about 99–154°C [Johnson *et al*., 1981]. In the last group of NFS samples, tofu products showed the lowest peroxyl radical scavenging capacity, especially abura-age, twice-fried tofu (NF10) (Figure 2). There was no significant difference in H-ORAC between momen tofu (NF8) and silken tofu (NF9), with their H-ORAC values being lower than that of nama-age, fried tofu (NF11).

In summary, there was a significant difference in H-ORAC values among each group of NFS soyfoods. It was considered that the slight difference found was mainly due to the difference in the isoflavone and saponin contents and the respective compositions caused by the difference in the food processing treatment such as thermal process, extraction, and coagulation. This indicates that the bioactive compounds may change upon food processing and that each food product requires a different treatment process. The chemical structures of active compounds such as isoflavones and soyasaponins have an important role in nutraceutical property in soyfood as mentioned above. Malonyl glycoside, which is the main component of soybean isoflavone, is unstable to heat and derived from malonyl glycoside to glycoside and further to aglycone upon thermal treatment [Kasuga *et al*., 2006; Toda *et al*., 2000]. DDMP saponin can be degraded to group B saponin by thermal treatment and group E saponins by lipoxygenase-induced radical reaction during grinding [Chitisankul *et al*., 2015]. It was considered that the non-fermented soybean foods had different antioxidative capacities due to their isoflavone and DDMP saponin compositions, depending on the processing treatment during the manufacturing process.

Peroxyl radical scavenging capacity of fermented soybean food

Fermented soyfoods (FS) could be categorized into four groups; natto (F1 and F2), tempeh (F3), miso (F4-F7), and soy sauce (F8 and F9). Among all FS samples, soy miso showed the highest H-ORAC value followed by natto, soy sauce, other types of miso (F5 and F6), and tempeh, respectively (Figure 2). In the comparison of NF and FS samples, all FS products had higher H-ORAC values than NFS samples. The H-ORAC value of FS samples ranged from 2.21±0.19 to 11.53±0.41 mmol TE/100 g while whole soybean seed (NF1) had 2.35 mmol TE/100 g.

High antioxidative capacity of black soybean natto was expected because, as mentioned above, the seed coat of black soybean is rich in anthocyanins. Moreover, the previous research revealed that the H-ORAC value of black soybean was 5,870±115 μmol TE/100 g while that of soybean was 4,369±418 μmol TE/100 g [Chitisankul *et al*., 2019]. However, the previous research also reported that isoflavone content of soybean was higher than that of black soybean [Chitisankul *et al*., 2019]. Thus, it could be considered that isoflavones make a significant contribution to the peroxyl radical scavenging capacity instead of anthocyanins in natto. In addition, the H-ORAC value of natto was 3-fold higher compared to steamed soybean. Therefore, it clearly showed that the fermented process of natto could induce nutraceutical properties as enhancing antioxidant capacity. The biotransformation of isoflavones plays an important role to enhance those functionalities. The consistent reports explained the glycoside conjugates of isoflavones could be converted to isoflavone aglycones by β-glucosidase of *Bacillus subtilis* during fermentation [Dajanta *et al*., 2009; Khosravi & Razavi, 2021; Ping *et al*., 2012]. Hence, the enhanced antioxidative capacity of regular soybean natto compared to black soybean natto might be due to three reasons: regular soybean had a higher isoflavone content, aglycone isoflavones presented

stronger antioxidative capacity than anthocyanins, and degradation of water-soluble anthocyanins during natto production resulted in functionality losses. Moreover, it was found that natto had a higher antioxidant capacity than steamed soybeans (Figure 2). The browning substances derived from the amino-carbonyl reaction [Ando *et al*., 2003] and antioxidant peptides released from proteins during fermentation [Sanjukta & Rai, 2016; Tonolo *et al*., 2020] could additionally contribute to the antioxidant potential of natto.

Although soy-miso (F7) showed the highest antioxidant activity, other kinds of miso (F4-F6) presented much lower peroxyl radical scavenging capacity especially the sweet-white type of rice miso (F4) with H-ORAC value of 2.21±0.19 mmol TE/100 g (Figure 2). In the consent report, the antioxidant properties of different kinds of miso were evaluated by determining 2,2-diphenyl-1-picrylhydrazyl (DPPH) radical and superoxide scavenging activities [Matsuo & Hitomi, 2007]. The soy-miso presented the highest antioxidative capacity following dark-yellow rice miso, light yellow rice miso, and sweet-white rice miso. And barley miso showed similar property with dark-yellow rice miso. Moreover, it was reported that the DPPH radical scavenging ability and the superoxide scavenging activity were strongly positively correlated with the total isoflavone content and aglycone content, respectively [Matsuo & Hitomi, 2007]. During *Aspergillus* spp. fermentation in miso, the β-glucosidase was produced and activated to hydrolyze glycoside isoflavone to aglycone type isoflavones [Yamabe *et al*., 2007; Yan *et al*., 2016]. Furthermore, during the malting process in soy miso, aglycones (daidzein and genistein) could be converted to *o*-dihydroxy -isoflavones (ODI) while rice miso and barley miso do not contain ODI [Esaki *et al*., 2001b]. It was reported that ODI also contribute to the antioxidant properties of miso, since the higher the amount of ODI, the higher the antioxidant capacity [Esaki *et al*., 2001a]. Additionally, the lower lightness (*L**) of the miso sample was revealed as related to higher antioxidative capacity. It was speculated that the browning substance derived from the amino-carbonyl reaction during fermentation and aging could contribute to the peroxyl radical scavenging activity of miso. For soy sauce, the H-ORAC value of dark-colored soy sauce (F8) was higher than that of light-yellow soy sauce (F9) (Figure 2). Similarly to miso, soy sauce undergoes fermentation and aging which result in aglycone isoflavone production; but there was a low total isoflavone content in soy sauce [Toda *et al*., 2000]. Although the aglycone isoflavones were formed during the soy sauce production, they were detected as remaining in soy sauce cake, a by-product [Esaki *et al*., 2004]. However, a positive correlation was found between the ODI content of soy sauce and its antioxidative capacity, and it was reported that ODI also contributed to the antioxidative capacity of soy sauce [Esaki *et al*., 2002]. According to this evaluation, it is considered that the peroxyl radical scavenging activity of soy sauce, which was recognized by the ORAC value, is related to the browning substance derived from the amino-carbonyl reaction and ODI. Tempeh (F3) had a similar H-ORAC value as rice miso and barley miso, but lower than that of natto (Figure 2). β-Glucosidase produced by *Rhizopus filamentous* fungi, which is used for tempeh fermentation, hydrolyzes isoflavone glycosides into aglycones [Kameda *et al*., 2018]. It was suggested that the isoflavone aglycone produced during fermentation might contribute to the antioxidant properties of tempeh [Murakami *et al*., 1984].

TABLE 2. Color parameters of miso and soy sauces.

Soybean foods	*L**	*a**	*b**
Rice miso: sweet-white type	65.33±0.03^{a}	4.35±0.05^{d}	35.37±0.03^{c}
Rice miso: light yellow type	48.82±0.04^{b}	9.33±0.08^{a}	41.96±0.02^{a}
Barley miso	44.86±0.08^{c}	6.86±0.01^{b}	35.68±0.08^{b}
Soy miso	10.90±0.09^{d}	5.73±0.26^{c}	8.24±0.26^{d}
Dark soy sauce	14.16	29.92	23.38
Light soy sauce	43.64	36.73	72.23

Values for miso are expressed as mean ± standard deviation (n=3); for soy sauce value n=1. Different letters in column presented significant differences (p<0.05); *L**, lightness; *a**, redness; *b**, yellowness.

Color of fermented soybean food *vs*. peroxyl radical scavenging capacity

The color parameters of long-term fermented soyfood samples, miso, and soy sauce were measured and *L**, *a**, and *b** values are shown in Table 2. The relationship of color parameters with antioxidative capacity was also evaluated. The *L** value of miso decreased in order of sweet-white rice miso, light yellow rice miso, barley miso, and soy miso, the darkest miso. The *a** value of light yellow rice miso was slightly higher than that of the other four miso samples. There was no significant difference in the *b** value among miso samples, except soy-miso which showed the lowest yellowness. On the other hand, dark soy sauce showed lower *L**, *a**, and *b** values than light soy sauce. After *L**, *a**, *b** value measurement, the correlations between these values and peroxyl radical scavenging capacity were found for miso and soy sauce. The results revealed that there were no significant correlations of H-ORAC values with *a** and *b** values. On the other hand, a strong negative correlation (r=-0.9747, p=0.0048) was found between the *L** and H-ORAC values of miso samples and soy sauce, excluding soy miso (Figure 3). Therefore, the low *L** value, darkness

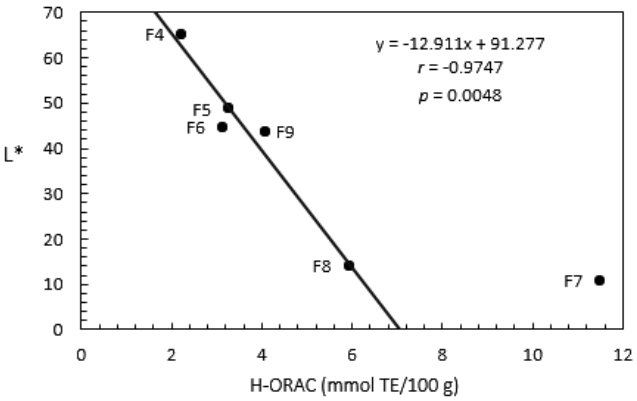

FIGURE 3 . Correlation between lightness (*L**) and hydrophilic-oxygen radical absorbance capacity (H-ORAC) of long-term fermented soyfoods; miso (F4–F7) and soy sauces (F8–F9). For code of samples see Table 1. The correlation coefficient (r) and significance level (p) were calculated excluding soy miso (F7).

of soy sauce or miso, might be an index of browning reagent contents, the amino-carbonyl reaction product which induced a higher H-ORAC value. The result was supported by other consistent reports. The correlations of L^* value with both DPPH radical and superoxide scavenging activities of various miso paste samples were negative [Matsuo & Hitomi, 2007]. In our study, soybean miso presented a significantly higher H-ORAC value than the expected H-ORAC value based on the L^* value (Figure 3). It could be explained that soybean miso had a higher ratio of soybean content than other kinds of miso, and the soybean miso production might be different too. Therefore, the strong peroxyl radical scavenging capacity of soybean miso might be due to the high content of isoflavones, saponins, ODI [Esaki *et al*., 2001a,b], and antioxidative peptides released from proteins [Sanjukta & Rai, 2016].

CONCLUSIONS

Since the H-ORAC method is an *in vitro* method for measuring antioxidant capacity, its results might not directly reflect the antioxidative capacity *in vivo*, but it can be a simple primary screening tool for antioxidant capacity measurments in many soyfoods. Fermented soybean could promote higher antioxidant properties compared to non-fermented soyfood due to peroxyl radical scavenging capacity. The chemical structure of bioactive compounds in soybean plays an important role in the antioxidant properties of soyfood products. The technological processes could cause transformations of those healthy functional compounds and thus enhance or diminish the antioxidative capacity. The experiment demonstrated that derived isoflavone as aglycone could promote higher antioxidative activity while derived soyasaponins, such as group A and group B saponins, showed lower activity than DDMP--saponin. According to the H-ORAC value of soyfood sample, fermented soyfood presented the highest antioxidant capacity which was due to a high aglycone isoflavone content. Furthermore, it was also considered that peptides and free amino acids produced by aging also contributed to the antioxidant capacity of fermented soybean foods. Among all processed soyfood samples, the soy-miso sample had the highest H-ORAC value followed by natto samples. Eventually, considering the serving size and antioxidant capacity, natto is the most effective product compared to miso or soy sauce having a high salt content. However, long-term fermented soyfood should still be in the focus of interest to researchers as health promoting food. There is a lack of data on their minor bioactive components such as antioxidant peptides and ODI. Thus, these minor components should be considered for further study.

RESEARCH FUNDING

This research was partly supported by "JSPS RONPAKU (Dissertation Ph.D.) Program 2012 (Grant ID No. THA – 11206)" and "Kasetsart University Research and Development Institute".

CONFLICT OF INTERESTS

Authors declare no conflict of interests.

ORCID IDs

W.T. Chitisankul https://orcid.org/0000-0003-2556-7698
Ch. Tsukamoto https://orcid.org/0000-0002-6437-2140

REFERENCES

1. Ando, M., Harada, K., Kitao, S., Kobayashi, M., Tamura, Y. (2003). Relationship between peroxyl radical scavenging capability measured by the chemiluminescence method and an aminocarbonyl reaction product in soy sauce. *International Journal of Molecular Medicine*, *12*(6), 923–928. https://doi.org/10.3892/ijmm.12.6.923
2. Arora, A., Nair, M.G., Strasburg, G.M. (1998). Antioxidant activities of isoflavones and their biological metabolites in a liposomal system. *Archives of Biochemistry and Biophysics*, *356*(2), 133–141. https://doi.org/10.1006/abbi.1998.0783
3. Bultosa, G. (2016). Functional foods: Overview. In C. Wrigley, H. Corke, K. Seetharaman, J. Faubion (Eds.), *Encyclopedia of Food Grains* (Second Edition), Academic Press, Oxford, pp. 1–10. https://doi.org/10.1016/B978-0-12-394437-5.00071-1
4. Carrera, C.S., Seguin, P. (2016). Factors affecting tocopherol concentrations in soybean seeds. *Journal of Agricultural and Food Chemistry, 64*(50), 9465–9474. https://doi.org/10.1021/acs.jafc.6b03902
5. Chang, C.-T., Hsu, C.-K., Chou, S.-T., Chen, Y.-C., Huang, F.-S., Chung, Y.-C. (2009). Effect of fermentation time on the antioxidant activities of tempeh prepared from fermented soybean using *Rhizopus oligosporus*. *International Journal of Food Science & Technology, 44*(4), 799–806. https://doi.org/10.1111/j.1365-2621.2009.01907.x
6. Chitisankul, W.T., Itabashi, M., Son, H., Takahashi, Y., Ito, A., Varanyanond, W., Tsukamoto, C. (2021). Soyasaponin composition complexities in soyfoods relating nutraceutical properties and undesirable taste characteristics. *LWT – Food Science and Technology, 146*, art. no. 111337. https://doi.org/10.1016/j.lwt.2021.111337
7. Chitisankul, W.T., Murakami, M., Tsukamoto, C., Shimada, K. (2019). Effects of long-term soaking on nutraceutical and taste characteristic components in Thai soybeans. *LWT – Food Science and Technology, 115*, art no. 108432. https://doi.org/10.1016/j.lwt.2019.108432
8. Chitisankul, W.T., Shimada, K., Omizu, Y., Uemoto, Y., Varanyanond, W., Tsukamoto, C. (2015). Mechanism of DDMP-saponin degradation and maltol production in soymilk preparation. *LWT – Food Science and Technology, 64*(1), 197–204. https://doi.org/10.1016/j.lwt.2015.05.023
9. Dajanta, K., Chukeatirote, E., Apichartsrangkoon, A., Frazier, R. (2009). Enhanced aglycone production of fermented soybean products by *Bacillus species*. *Acta Biologica Szegediensis, 53*, 93–98.
10. Esaki, H., Kawakishi, S., Inoue, T., Osawa, T. (2001a). Potent antioxidative *o*-dihydroxyisoflavones in soybean pastes and their antioxidative activities. *Nippon Shokuhin Kagaku Kogaku Kaishi, 48*(1), 51–57. https://doi.org/10.3136/nskkk.48.51

11. Esaki, H., Osawa, T., Kawakishi, S. (2002). Potent antioxidative *o*-dihydroxyisoflavones in soy sauces and their antioxidative activities. *Nippon Shokuhin Kagaku Kogaku Kaishi, 49*(7), 476–483. https://doi.org/10.3136/nskkk.49.476
12. Esaki, H., Watanabe, R., Hishikawa, N., Osawa, T., Kawakishi, S. (2004). Utility of isoflavone preparations from soy sauce cake as antioxidant materials. *Nippon Shokuhin Kagaku Kogaku Kaishi, 51*(1), 47–53. https://doi.org/10.3136/nskkk.51.47
13. Esaki, H., Watanabe, R., Masuda, H., Osawa, T., Kawakishi, S. (2001b). Formations and changes of *o*-dihydroxyisoflavones during production of soybean pastes. *Nippon Shokuhin Kagaku Kogaku Kaishi, 48*(3), 189–195. https://doi.org/10.3136/nskkk.48.189
14. Han, R.-M., Tian, Y.-X., Liu, Y., Chen, C.-H., Ai, X.-C., Zhang, J.-P., Skibsted, L.H. (2009). Comparison of flavonoids and isoflavonoids as antioxidants. *Journal of Agricultural and Food Chemistry, 57*(9), 3780–3785. https://doi.org/10.1021/jf803850p
15. Johnson, L.A., Deyoe, C.W., Hoover, W.J. (1981). Yield and quality of soymilk processed by steam-infusion cooking. *Journal of Food Science, 46*(1), 239–248. https://doi.org/10.1111/j.1365-2621.1981.tb14572.x
16. Kähkönen, M.P., Heinonen, M. (2003). Antioxidant activity of anthocyanins and their aglycons. *Journal of Agricultural and Food Chemistry, 51*(3), 628–633. https://doi.org/10.1021/jf025551i
17. Kameda, T., Aoki, H., Yanaka, N., Kumrungsee, T., Kato, N. (2018). Production of isoflavone aglycone-enriched tempeh with *Rhizopus stolonnifer*. *Food Science and Technology Research, 24*(3), 493–499. https://doi.org/10.3136/fstr.24.493
18. Kasuga, A., Ogiwara, E., Aoyagi, Y., Kimura, H. (2006). Changes in isoflavone content of soybeans during heating process. *Nippon Shokuhin Kagaku Kogaku Kaishi, 53*(7), 365–372. https://doi.org/10.3136/nskkk.53.365
19. Khosravi, A., Razavi, S.H. (2021). Therapeutic effects of polyphenols in fermented soybean and black soybean products. *Journal of Functional Foods, 81*, art. no. 104467. https://doi.org/10.1016/j.jff.2021.104467
20. Kim, M.S., Jung, Y.S., Jang, D., Cho, C.H., Lee, S.-H., Han, N.S., Kim, D-O. (2022). Antioxidant capacity of 12 major soybean isoflavones and their bioavailability under simulated digestion and in human intestinal Caco-2 cells. *Food Chemistry, 374,* art. no. 131493. https://doi.org/10.1016/j.foodchem.2021.131493
21. Lee, C.H., Yang, L., Xu, J.Z., Yeung, S.Y.V., Huang, Y., Chen, Z.-Y. (2005). Relative antioxidant activity of soybean isoflavones and their glycosides. *Food Chemistry, 90*(4), 735–741. https://doi.org/10.1016/j.foodchem.2004.04.034
22. Long, L.H., Kwee, D.C.T., Halliwell, B. (2000). The antioxidant activities of seasonings used in Asian cooking. Powerful antioxidant activity of dark soy sauce revealed using the ABTS assay. *Free Radical Research, 32*(2), 181–186. https://doi.org/10.1080/10715760000300181
23. Matsuo, M., Hitomi, E. (2007). Changes in antioxidant activity of miso by variety, cooking and added spices. *Nippon Shokuhin Kagaku Kogaku Kaishi, 54*(11), 503–508. https://doi.org/10.3136/nskkk.54.503
24. Murakami, H., Asakawa, T., Terao, J., Matsushita, S. (1984). Antioxidative stability of tempeh and liberation of isoflavones by fermentation. *Agricultural and Biological Chemistry, 48*(12), 2971–2975. https://doi.org/10.1080/00021369.1984.10866635
25. Omizu, Y., Tsukamoto, C., Chettri, R., Tamang, J.P. (2011). Determination of saponin contents in raw soybean and fermented soybean foods of India. *Journal of Scientific & Industrial Research, 70,* 533–538.
26. Ou, B., Hampsch-Woodill, M., Prior, R. (2001). Development and validation of an improved oxygen radical absorbance capacity assay using fluorescein as the fluorescent probe. *Journal of Agricultural and Food Chemistry, 49*(10), 4619–4626. https://doi.org/10.1021/jf010586o
27. Ping, S.P., Shih, S.C., Rong, C.T., King, W.Q. (2012). Effect of isoflavone aglycone content and antioxidation activity in natto by various cultures of *Bacillus Subtilis* during the fermentation period. *Journal of Nutrition & Food Sciences, 2*(7), art. no. 1000153. https://doi.org/10.4172/2155-9600.1000153
28. Pizzino, G., Irrera, N., Cucinotta, M., Pallio, G., Mannino, F., Arcoraci, V., Squadrito, F., Altavilla, D., Bitto, A. (2017). Oxidative stress: Harms and benefits for human health. *Oxidative Medicine and Cellular Longevity, 2017*, art. no. 8416763. https://doi.org/10.1155/2017/8416763
29. Ruiz-Larrea, M.B., Mohan, A.R., Paganga, G., Miller, N.J., Bolwell, G.P., Rice-Evans, C.A. (1997). Antioxidant activity of phytoestrogenic isoflavones. *Free Radical Research, 26*(1), 63–70. https://doi.org/10.3109/10715769709097785
30. Sanjukta, S., Rai, A.K. (2016). Production of bioactive peptides during soybean fermentation and their potential health benefits. *Trends in Food Science & Technology, 50*, 1–10. https://doi.org/10.1016/j.tifs.2016.01.010
31. Setchell, K., Brown, N., Zimmer-Nechemias, L., Brashear, W., Wolfe, B., Kirschner, A., Heubi, J. (2002). Evidence for lack of absorption of soy isoflavone glycosides in humans, supporting the crucial role of intestinal metabolism for bioavailability. *The American Journal of Clinical Nutrition, 76*(2), 447–453. https://doi.org/10.1093/ajcn/76.2.447
32. Slavu(Ursu), M., Aprodu, I., Milea, S.A., Enachi, E., Râpeanu, G., Bahrim, G.E., Stanciuc, N. (2020). Thermal degradation kinetics of anthocyanins extracted from purple maize flour extract and the effect of heating on selected biological functionality. *Foods, 9*(11), art. no. 1593. https://doi.org/10.3390/foods9111593
33. Toda, T., Sakamoto, A., Takayanagi, T., Yokotsuka, K. (2000). Changes in isoflavone compositions of soybean foods during cooking process. *Food Science and Technology Research, 6*(4), 314–319. https://doi.org/10.3136/fstr.6.314
34. Tonolo, F., Moretto, L., Grinzato, A., Fiorese, F., Folda, A., Scalcon, V., Ferro, S., Arrigoni, G., Bellamio, M., Feller, E., Bindoli, A., Marin, O., Rigobello, M.P. (2020). Fermented soy-derived bioactive peptides selected by a molecular docking approach show antioxidant properties involving the Keap1/Nrf2 pathway. *Antioxidants, 9*(12), art. no. 1306. https://doi.org/10.3390/antiox9121306
35. Wu, Q., Wang, M., Sciarappa, W.J., Simon, J.E. (2004). LC/UV/ESI-MS analysis of isoflavones in edamame and tofu soybeans. *Journal of Agricultural Food Chemistry, 52*(10), 2763–2769. https://doi.org/10.1021/jf035053p

36. Xu, J.L., Shin, J.-S., Park, S.K., Kang, S., Jeong, S.-C., Moon, J.-K., Choi, Y. (2017). Differences in the metabolic profiles and antioxidant activities of wild and cultivated black soybeans evaluated by correlation analysis. *Food Research International, 100*(Part 2), 166–174. https://doi.org/10.1016/j.foodres.2017.08.026
37. Yamabe, S., Kobayashi-Hattori, K., Kaneko, K., Endo, H., Takita, T. (2007). Effect of soybean varieties on the content and composition of isoflavone in rice-koji miso. *Food Chemistry, 100*(1), 369–374. https://doi.org/10.1016/j.foodchem.2005.09.061
38. Yan, F.-Y., Xia, W., Zhang, X.-X., Chen, S., Nie, X.-Z., Qian, L.-C. (2016). Characterization of β-glucosidase from *Aspergillus terreus* and its application in the hydrolysis of soybean isoflavones. *Journal of Zhejiang University Science B, 17*(6), 455–464. https://doi.org/10.1631/jzus.B1500317
39. Yoshiki, Y., Okubo, K. (1995). Active oxygen scavenging activity of DDMP (2,3-Dihydro-2,5-dihydroxy-6-methyl-4*H*-pyran-4-one) saponin in soybean seed. *Bioscience, Biotechnology, and Biochemistry, 59*(8), 1556–1557. https://doi.org/10.1271/bbb.59.1556
40. Yoshiki, Y., Kahara, T., Okubo, K., Sakabe, T., Yamasaki, T. (2001). Superoxide- and 1,1-diphenyl-2-picrylhydrazyl radical-scavenging activities of soyasaponin βg related to gallic acid. *Bioscience, Biotechnology, and Biochemistry, 65*(10), 2162–2165. https://doi.org/10.1271/bbb.65.2162
41. Zhong, Y., Shahidi, F. (2015). Methods for the assessment of antioxidant activity in foods. In F. Shahidi (Ed.), *Handbook of Antioxidants for Food Preservation*, Woodhead Publishing, Cambridge, pp. 287–333.
42. Zilic, S., Dodig, D., Vancetovic, J., Grcic, N., Peric, V., Titan, P., Maksimovic, V. (2019). Composition of anthocyanins in colored grains and the relationship of their non-acylated and acylated derivatives. *Polish Journal of Food and Nutrition Sciences, 69*(2), 137–146. https://doi.org/10.31883/pjfns-2019-105100

http://journal.pan.olsztyn.pl Pol. J. Food Nutr. Sci., 2022, Vol. 72, No. 1, pp. 109–110

71 VOLUME'S REVIEWERS

The Editors gratefully thank the following reviewers for their valuable help in reviewing manuscripts published in this volume and other papers reviewed between 1st January 2021 and 31st December 2021.

Alvez E., Federal University of Lavras, Lavras, Brazil
Alzamora S.M., University of Buenos Aires, Buenos Aires, Argentina
Amarowicz R., Institute of Animal Reproduction and Food Research of the Polish Academy of Sciences, Olsztyn, Poland
Anwar A., National Research Centre, Dokki, Cairo, Egypt
Aoki N., National Institute of Crop Science, Tsukuba, Japan
Arslan I., Zonguldak Bülent Ecevit University, Zonguldak, Turkey

Beneduce L., University of Foggia, Foggia, Italy
Bordonaro M., Geisinger Commonwealth School of Medicine, Denville, PA, USA
Brückner-Gühmann M., Technical University of Berlin, Berlin, Germany

Cabral A., Federal University of Rio Grande do Norte, Rio Grande do Norte, Brazil
Calder P.C., University of Southampton, Southampton, UK
Cesoniene L., Vytautas Magnus University, Kaunas, Lithuania
Chalamaiah M., University of Alberta, Edmonton, Canada
Colombino E., University of Torino, Torino, Italy
Cvetković D., University of Niš, Niš, Serbia
Czubiński J., Poznań University of Life Sciences, Poznań, Poland

Dankowska A., Poznań University of Economics, Poznań, Poland
de Castilhos M.B., São Paulo State University, São Paulo, Brazil
Denev P.N., Institute of Organic Chemistry with Centre of Phytochemistry, Bulgarian Academy of Sciences, Plovidiv, Bulgaria
Dib J.R., National Scientific and Technical Research Council, San Miguel de Tucumán, Argentina
Drabińska N., Institute of Animal Reproduction and Food Research of the Polish Academy of Sciences, Olsztyn, Poland
du Plessis H., Agricultural Research Council, ARC Infruitec-Nietvoorbij, Stellenbosch, South Africa
Dudkiewicz A., Jan Długosz University in Częstochowa, Częstochowa, Poland

Fardin-Kia A.R., U.S. Department of Health and Human Services, Food and Drug Administration (FDA), Washington, DC, USA
Fecka I., Wrocław Medical University, Wrocław, Poland
Feng Ch.H., RIKEN: Sendai, Miyagi, Japan
Fotschki B., Institute of Animal Reproduction and Food Research of the Polish Academy of Sciences, Olsztyn, Poland
Frezza C., La Sapienza, University of Rome, Rome, Italy
Fu I., Southwest University, Chongqing, China

Gabriele M., Istituto di Biologia e Biotecnologia Agraria, IBBA-CNR, Milano, Italy
García-Sifuentes C., Centro de Investigación en Alimentación y Desarrollo A.C. (CIAD), Hermosillo, Mexico
Gardikis K., APIVITA, Athens, Greece
Gayathri D., Davangere University, Karnataka, India
Gerschenson L., Buenos Aires University, Buenos Aires, Argentina
Giménez-Bastida J., Food Science and Technology, CEBAS-CSIC, Murcia, Spain
Gugołek A., University of Warmia and Mazury in Olsztyn, Olsztyn, Poland
Gülseren İ., Istanbul Sabahattin Zaim University, Istanbul, Turkey

Janiak M., Institute of Animal Reproduction and Food Research of the Polish Academy of Sciences, Olsztyn, Poland
Jozinović A., Josip Juraj Strossmayer University of Osijek, Osijek, Croatia

Kara H., Cumhuriyet University, Sivas, Turkey
Karamać M., Institute of Animal Reproduction and Food Research of the Polish Academy of Sciences, Olsztyn, Poland
Karaś M., University of Life Sciences in Lublin, Poland
Keutgen A., Universität für Bodenkultur, Vienna, Austria
Kolniak-Ostek A., Wrocław University of Environmental and Life Sciences, Wrocław, Poland
Kopcewicz M., Institute of Animal Reproduction and Food Research of the Polish Academy of Sciences, Olsztyn, Poland
Kowalski S., University of Agriculture in Cracow, Cracow, Poland

Krauze M., Lublin University of Life Sciences, Lublin, Poland
Kruzselyi D., Plant Protection Institute Centre for Agricultural Research, Budapest, Hungary

Lesiow T., Wrocław University of Economics, Wrocław, Poland
Lima G., São Paulo State University, São Paulo, Brazil
Liu W., Henan University of Technology, Henan, China
Lo Scalzo R., CREA – Council for Agricultural Research and Economics, Roma, Italy
Lošák T., Mendel University in Brno, Brno, Czech Republic
Loypimai P., Bansomdejchaopaya Rajabhat University, Bangkok, Thailand

Madadlou A., Wageningen University and Research, Wageningen, The Netherlands
Martínez-Ávila G., Universidad Autónoma de Nuevo León, San Nicolás de los Garza, Mexico
Michalska-Ciechanowska A., Wrocław University of Environmental and Life Sciences, Wrocław, Poland
Mikulski D., Kazimierz Wielki University, Bydgoszcz, Poland
Miladinovic B., University of Niš, Niš, Serbia
Minnaar P., Agricultural Research Council, Infruitec--Nietvoorbij, Stellenbosch, South Africa
Muszyńska B., Collegium Medicum, Jagiellonian University, Cracow, Poland

Nowak E., Massey University, Palmerston North, New Zealand

Ogrodowczyk A., Institute of Animal Reproduction and Food Research of the Polish Academy of Sciences, Olsztyn, Poland

Paciulli M., University of Parma, Parma, Italy
Peteiro M., Centro Tecnológico de la Carne de Galicia, Ourense, Spain
Pelvan E., TUBITAK Marmara Research Center (MAM), Gebze, Turkey
Pereira P.R., Federal University of Rio de Janeiro, Rio de Janeiro, Brazil
Proestos Ch., National and Kapodistrian University of Athens, Athens, Attiki, Greece

Radojcin M., University of Novi Sad, Novi Sad, Serbia
Ramirez Ascheri J.L., EMBRAPA – Brazilian Agricultural Research Corporation, Ministry of Agriculture, Livestock and Food Supply, Brasilia, DF, Brazil
Ratcliffe N.M., University of the West of England, Bristol, UK
Rodríguez-Miranda J., Tecnológico Nacional de México/ Instituto Tecnológico de Tuxtepec, Tuxtepec, Oaxaca, Mexico
Rosa A., University of Cagliari, Cagliari, Italy

Sawicki T., University of Warmia and Mazury in Olsztyn, Olsztyn, Poland
Stajić S., University of Belgrade, Belgrade, Serbia
Staroszczyk H., Gdańsk University of Technology, Gdańsk, Poland
Starowicz M., Institute of Animal Reproduction and Food Research of the Polish Academy of Sciences, Olsztyn, Poland

Tao Y., Nanjing Agricultural University, Nanjing, China
Tomaszewska-Gras J., Poznań University of Life Sciences, Poznań, Poland
Tömösközi-Farkas R., Food Science Research Institute, Budapest, Hungary
Topalović A., University of Montenegro, Podgorica, Montenegro
Tsaballa A., Hellenic Agricultural Organization (ELGO)--Demeter, Greece
Turabi Yolaçaner E., Hacettepe University, Ankara, Turkey

Uzun Y., Van Yüzüncü Yıl University, Tuşba/Van, Turkey

Valík L., Slovak University of Technology in Bratislava, Bratislava, Slovak Republic
Vamanu E., University of Agronomic Sciences and Veterinary Medicine of Bucharest, Bucharest, Romania
Venditti A., La Sapienza, University of Rome, Rome, Italy
Vetter J., University of Veterinary Medicine, Budapest, Hungary

Walendzik K., Institute of Animal Reproduction and Food Research of the Polish Academy of Sciences, Olsztyn, Poland
Wierzbicka A., Warsaw University of Life Sciences, Warsaw, Poland
Wilson A.D., USDA, SRS – Southern Research Station, Stoneville, MS, USA
Wiśniewska J., Institute of Animal Reproduction and Food Research of the Polish Academy of Sciences, Olsztyn, Poland
Wronkowska M., Institute of Animal Reproduction and Food Research of the Polish Academy of Sciences, Olsztyn, Poland
Wybraniec S., Cracow University of Technology, Cracow, Poland

Yao W., Jiangnan University, Wuxi City, Jiangsu Province, P.R. China

Żary-Sikorska E., Bydgoszcz University of Science and Technology, Bydgoszcz, Poland

Pol. J. Food Nutr. Sci., 2021, Vol. 72, No. 1, pp. 111–113
http://journal.pan.olsztyn.pl

Instruction for Authors
Section: Editorial News

INSTRUCTIONS FOR AUTHORS

SUBMISSION. Original contributions relevant to food and nutrition sciences are accepted on the understanding that the material has not been, nor is being, considered for publication elsewhere. **All papers should be submitted and will be processed electronically via Editorial Manager system (available from PJFNS web site: http://journal.pan.olsztyn.pl). On submission, a corresponding author will be asked to provide: Cover letter; Files with Manuscripts, Tables, Figures/Photos; and Names of two potential reviewers (one from the author's homeland – but outside author's Institution, and the other from abroad).** All papers which have been qualified as relevant with the scope of our Journal are reviewed. All contributions, except the invited reviews are charged. Proofs will be sent to the corresponding author or to the first author and should be returned within one week since receipt. No new material may be inserted in the text at proof stage. It is the author's duty to proofread proofs for errors.

Authors should very carefully consider the preparation of papers to ensure that they communicate efficiently, because it permits the reader to gain the greatest return for the time invested in reading. Thus, we are more likely to accept those that are carefully designed and conform the instruction. Otherwise, papers will be rejected and removed from the on-line submission system.

SCOPE. The Polish Journal of Food and Nutrition Sciences publishes original, basic and applied papers, and reviews on fundamental and applied food research, preferably these based on a research hypothesis, in the following Sections:

Food Technology:
– Innovative technology of food development including biotechnological and microbiological aspects
– Effects of processing on food composition and nutritional value

Food Chemistry:
– Bioactive constituents of foods
– Chemistry relating to major and minor components of food
– Analytical methods

Food Quality and Functionality:
– Sensory methodologies
– Functional properties of food
– Food physics
– Quality, storage and safety of food

Nutritional Research Section:
– Nutritional studies relating to major and minor components of food (excluding works related to questionnaire surveys)

"News" section:
– Announcements of congresses
– Miscellanea

OUT OF THE SCOPE OF THE JOURNAL ARE:
– Works which do not have a substantial impact on food and nutrition sciences
– Works which are of only local significance i.e. concern indigenous foods, without wider applicability or exceptional nutritional or health related properties
– Works which comprise merely data collections, based on the use of routine analytical or bacteriological methods (i.e. standard methods, determination of mineral content or proximate analysis)
– Works concerning biological activities of foods but do not provide the chemical characteristics of compounds responsible for these properties
– Nutritional questionnaire surveys
– Works related to the characteristics of foods purchased at local markets
– Works related to food law
– Works emphasizing effects of farming / agricultural conditions / weather conditions on the quality of food constituents
– Works which address plants for non-food uses (i.e. plants exhibiting therapeutic and/or medicinal effects)

TYPES OF CONTRIBUTIONS. *Reviews:* (at least: 30 pages and 70 references) these are critical and conclusive accounts on trends in food and nutrition sciences; *Original papers:* (maximally: 30 pages and 40 references) these are reports of substantial research; *Reports on post and forthcoming scientific events, and letters to the Editor* (all up to three pages) are also invited (free of charge).

REVIEW PROCESS. All scientific contributions will be peer-reviewed on the criteria of originality and quality. Submitted manuscripts will be pre-evaluated by Editor-in-Chief and Statistical Editor (except for review articles), and when meeting PJFNS' scope and formal requirements, they will be sent to a section Editor who upon positive pre-evaluation will assign at least two reviewers from Advisory Board Members, reviewers suggested by the author or other experts in the field. Based on the reviews achieved, Section Editor and Editor-in-Chief will make a decision on whether a manuscript will be accepted for publication, sent back to the corresponding author for revision, or rejected. Once a manuscript is sent back to the corresponding author for revision, all points of the reviews should be answered or rebuttal should be provided in the Explanation letter. The revised manuscripts will be checked by Section Editor and by the original reviewers (if necessary), and a final decision will be made on acceptance or rejection by both Section Editor and Editor-in-Chief.

Polish Journal of Food and Nutrition Sciences uses CrossCheck's iThenticate software to detect instances of similarity in submitted manuscripts. In publishing only original research, PJFNS is committed to deterring plagiarism, including self-plagiarism. Your manuscript may be screened for similarity to published materials.

COPYRIGHT LICENSE AGREEMENT referring to Authorship Responsibility and Acknowledgement, Conflict of Interest and Financial Disclosure, Copyright Transfer, are required for all authors, i.e. *Authorship Responsibility and Acknowledgement*: Everyone who has made substantial intellectual contributions to the study on which the article is based (for example, to the research question, design, analysis, interpretation, and written description) should be an author. It is dishonest to omit mention of someone who has participated in writing the manuscript ("ghost authorship") and unfair to omit investigator who have had important engagement with other aspects of the work. All contributors who do not meet the criteria for authorship should be listed in an Acknowledgments section. Examples of those who might be acknowledged include a person who provided purely technical help, writing assistance, or a department chairperson who provided only general support. Any financial and material support should also be acknowledged. *Conflict of Interest and Financial Disclosure*: Authors are responsible for disclosing financial support from the industry or other conflicts of interest that might bias the interpretation of results. *Copyright License Agreement*: Authors agree that papers accepted become the copyright of the Institute of Animal Reproduction and Food Research of the Polish Academy of Sciences in Olsztyn, Poland, and may not be published elsewhere without the Editor's permission in writing.

A manuscript will not be published once the signed form has not been submitted to the Editor with the manuscript revised after positive reviews.

ETHICAL APPROVAL OF STUDIES AND INFORMED CONSENT. For all manuscripts reporting data from studies involving human participants or animals, formal approval by an appropriate institutional review board or ethics committee is required and should be described in the Methods section. For those investigators who do not have formal ethics review committees, the principles outlined in the Declaration of Helsinki should be followed. For investigations of humans, state in the Methods section the manner in which informed consent was obtained from the study participants (i.e., oral or written). Editors may request that authors provide documentation of the formal review and recommendation from the institutional review board or ethics committee responsible for oversight of the study.

UNAUTHORIZED USE AND COPYRIGHT AGREEMENT. Published manuscripts become the property of the Institute of Animal Reproduction and Food Research of the Polish Academy of Sciences (IAR&FR PAS) and may not be published elsewhere without written permission. Unauthorized use of the PJFNS name, logo, or any content for commercial purposes or to promote commercial goods and services (in any format, including print, video, audio, and digital) is not permitted by IAR&FR PAS.

MANUSCRIPTS. A manuscript in English must be single-sided, preferably in Times New Roman (12) with 1.5-point spacing, without numbers of lines. The Editor reserves the right to make literary corrections and to make suggestions to improve brevity. English is the official language. The English version of the paper will be checked by Language Editor. Unclear and unintelligible version will be sent to the author(s) for correction.

Every paper should be divided under the following headings in this order: a **Title** (possibly below 150 spaces), **Running title** (up to 50 spaces, submitted under the Title); the Names(s) of the author(s) in full. In paper with more than one author, the asterisk indicates the name of the author to whom correspondence and inquiries should be addressed, otherwise the first author is considered for the correspondence. Current full postal address of the indicated corresponding author or the first author must be given in a footnote on the title page; the Place(s) where the work was done including the institution name, city, country if not Poland. In papers originated from several institutions the names of the authors should be marked with respective superscripts; the **Key words** (up to 6 words or phrases) for the main topics of the paper; an **Abstract** (up to 250 words for regular papers and reviews and 100 words for Short Reports) summarizing briefly main results of the paper, no literature references; an **Introduction** giving essential background by saying why the research is important, how it relates to previous works and stating clearly the objectives at the end; **Materials and Methods** with sufficient experimental details permitting to repeat or extend the experiments. Literature references to the methods, sources of material, company names and location (city, country) for specific instruments must be given. Describe how the data were evaluated, including selection criteria used; **Results and Discussion** presented together (in one chapter). Results should be presented concisely and organized to supplement, but not repeat, data in tables and figures. Do not display the data in both tabular and graphic form. Use narrative form to present the data for which tables or figures are unnecessary. Discussion should cover the implications and consequences, not merely recapitulating the results, and it must be accomplished with concise **Conclusions**; **Acknowledgements** should be made to persons who do not fill the authorship criteria (see: Authorship forms); **Research funding** should include financial and material support; and **References** as shown below.

REFERENCES each must be listed alphabetically at the end of the paper (each should have an Arabic number in the list) in the form as follows: **Periodicals** – names and initials of all the authors, year of publication, title of the paper, journal title as in Chemical Abstracts, year of publication, volume, issue, inclusive page numbers; **Books** – names and initials of all the authors, names of editors, chapter title, year of publication, publishing company, place of publication, inclusive page numbers; **Patents** – the name of the application, the title, the country, patent number or application number, the year of publication.

For papers published in language other than English, manuscript title should be provided in English, whereas a note on the original language and English abstract should be given in parentheses at the end.

The reference list should only include peer-reviewed full-text works that have been published or accepted for publication. Citations of MSc/PhD theses and works unavailable to international Editors, Reviewers, and Readers should be limited as much as possible.

References in the text must be cited by name and year in square parentheses (e.g.: one author – [Tokarz, 1994]; two authors – [Słonimski & Campbell, 1987]; more than two authors – [Amarowicz *et al*., 1994]). If more than one paper is published in the same year by the same author or group of authors use [Tokarz, 1994a, b]. Unpublished work must only be cited where necessary and only in the text by giving the person's name.

Examples:

Article in a journal:

Słonimski, B.A., Campbell, L.D., Batista, E., Howard B. (2008). Gas chromatographic determination of indole glucosinolates. *Journal of Science and Food Agriculture*, *40*(5), 131–143.

Book:

Weber, W., Ashton, L., Milton, C. (2012). *Antioxidants – Friends or Foes?* 2nd edition. PBD Publishing, Birmingham, UK. pp. 218–223.

Chapter in a book:

Uden, C., Gambino, A., Lamar, K. (2016). Gas chromatography. In M. Queresi, W. Bolton (Eds.), *CRC Handbook of Chromatography*, CRC Press Inc., Boca Raton, Florida, USA, pp. 44–46.

ABBREVIATIONS AND UNITS. Abbreviations should only be used when long or unwieldy names occur frequently, and never in the title; they should be given at the first mention of the name. Metric SI units should be used. The capital letter L should be used for liters. Avoid the use of percentages (% g/g,% w/w; Mol-%; vol-%), ppm, ppb. Instead, the expression such as g/kg, g/L, mg/kg, mg/mL should be used. A space must be left between a number and a symbol (e.g. 50 mL not 50mL). A small x must be used as multiplication sign between numeric values (e.g. 5×10^2 g/mL). Statistics and measurements should be given in figures, except when the number begins a sentence. Chemical formulae and solutions must specify the form used. Chemical abbreviations, unless they are internationally known, Greek symbols and unusual symbols for the first time should be defined by name. Common species names should be followed by the Latin at the first mention, with contracting it to a single letter or word for subsequent use.

FIGURES should be submitted in separate files. Each must have an Arabic number and a caption. Captions of all Figures should be provided on a separate page "Figure Captions". Figures should be comprehensible without reference to the text. Self-explanatory legend to all figures should be provided under the heading "Legends to figures"; all abbreviations appearing on figures should be explained in figure footnotes. Three-dimensional graphs should only be used to illustrate real 3-D relationships. Start the scale of axes and bars or columns at zero, do not interrupt them or omit missing data on them. Figures must be cited in Arabic numbers in the text.

TABLES should be submitted in separate files. They should be as few in number and as simple as possible (like figures, they are expensive and space consuming), and include only essential data with appropriate statistical values. Each must have an Arabic number and a caption. Captions of all Tables should be provided on a separate page "Table Captions". Tables should be self-explanatory; all abbreviations appearing in tables should be explained in table footnotes. Tables must be cited in Arabic numbers in the text.

PAGE CHARGES. A standard publication fee has been established at the rate of 450 EUR + tax (if applicable) irrespective of the number of pages and tables/figures. For Polish Authors an equivalent fee was set at 1950 PLN + VAT. Payment instructions will be sent to Authors via e-mail with acceptance letter.

Information on publishing and subscription is available from:

Ms. Joanna Molga
Editorial Office of Pol. J. Food Nutr. Sci.
Institute of Animal Reproduction and Food Research
Tuwima 10 Str., 10–748 Olsztyn 5, Poland
phone (48 89) 523–46–70, fax (48 89) 523–46–70;
e-mail: pjfns@pan.olsztyn.pl; http://journal.pan.olsztyn.pl

Nutrition